INTEREST RATE DERIVATIVES **EXPLAINED**

VOLUME 2: TERM STRUCTURE AND VOLATILITY MODELLING

Jörg Kienitz
Peter Caspers

FINANCIAL
ENGINEERING
EXPLAINED

Financial Engineering Explained

Series editor

Wim Schoutens
Department of Mathematics
Katholieke Universiteit Leuven
Heverlee, Belgium

'This book is the perfect follow-up to Part 1. It is a lucid, modern and practical explanation of what has become a very complicated area of financial engineering. I thoroughly recommend it to both academics and practitioners in mathematical finance.'
—**David Taylor**, Associate Professor University of Cape Town and Director, African Collaboration for Quantitative Finance and Risk Research

'If you are a newcomer to the world of Interest Rate Exotics, want to catch up with up-to-date research, or need to find some practical way to compute XVAs, this is the book you are looking for. Dr. Jörg Kienitz and Mr. Peter Caspers managed to present cutting edge research in a very concise form. You will quickly gain intuition about IR and volatility models' behavior, what is the strategy to calibrate them to real market data and which numerical technique is most effective in application. Everything is supported with carefully selected bibliography to broaden your knowledge in the future. It is extremely difficult to explain complex topics in short and precise words, yet this book proves that it is possible.'
—**Wojciech Ślusarski**, FRM, CQF, Head of Market Risk Control, Bank Pekao SA, Warsaw, Poland

'The authors of this book are among the few exotic hybrids in this field: being at same time practitioners with a long term industry experience and academics with broad research interest. Consequently, they know how to cover a topic from its theory to application. In this book, Jörg Kienitz and Peter Caspers continue to discuss interest rate derivatives. On the product side the book covers a broad range of interest rate product, from plain swaps to exotic products like multi-callable or TARNS. Correspondingly, the model side ranges from standard short rate models to multi-curve term-structure models. The discussion of the model is accompanied with a discussion of the appropriate numerical techniques.'
—**Christian Fries**, Professor of Financial Mathematics, LMU, and Head of Model Development, DZ Bank

Financial Engineering Explained is a series of concise, practical guides to modern finance, focusing on key, technical areas of risk management and asset pricing. Written for practitioners, researchers and students, the series discusses a range of topics in a non-mathematical but highly intuitive way. Each self-contained volume is dedicated to a specific topic and offers a thorough introduction with all the necessary depth, but without too much technical ballast. Where applicable, theory is illustrated with real world examples, with special attention to the numerical implementation.

More information about this series at
http://www.springer.com/series/14984

Jörg Kienitz · Peter Caspers

Interest Rate Derivatives Explained: Volume 2

Term Structure and Volatility Modelling

palgrave
macmillan

Jörg Kienitz
Bonn
Germany

Peter Caspers
Erkelenz
Germany

Financial Engineering Explained
ISBN 978-1-137-36018-2 ISBN 978-1-137-36019-9 (eBook)
DOI 10.1057/978-1-137-36019-9

Library of Congress Control Number: 2017937922

© The Editor(s) (if applicable) and The Author(s) The author(s) has/have asserted their right(s) to be identified as the author(s) of this work in accordance with the Copyright, Designs and Patents Act 1988., 2017
This work is subject to copyright. All rights are solely and exclusively licensed by the Publisher, whether the whole or part of the material is concerned, specifically the rights of translation, reprinting, reuse of illustrations, recitation, broadcasting, reproduction on microfilms or in any other physical way, and transmission or information storage and retrieval, electronic adaptation, computer software, or by similar or dissimilar methodology now known or hereafter developed.
The use of general descriptive names, registered names, trademarks, service marks, etc. in this publication does not imply, even in the absence of a specific statement, that such names are exempt from the relevant protective laws and regulations and therefore free for general use.
The publisher, the authors and the editors are safe to assume that the advice and information in this book are believed to be true and accurate at the date of publication. Neither the publisher nor the authors or the editors give a warranty, express or implied, with respect to the material contained herein or for any errors or omissions that may have been made. The publisher remains neutral with regard to jurisdictional claims in published maps and institutional affiliations.

Cover image: © Rowan Moore

Printed on acid-free paper

This Palgrave Macmillan imprint is published by Springer Nature
The registered company is Macmillan Publishers Ltd.
The registered company address is: The Campus, 4 Crinan Street, London, N1 9XW, United Kingdom

To Amberley, Beatrice and Benoît
Jörg Kienitz

To Kirsten, David, Fiona, Kendra and Noel
Peter Caspers

Contents

Part I Products

1 Vanilla Bonds and Asset Swaps 3

2 Callability Features 15

3 Structured Finance 39

4 More Exotic Features and Basis Risk Hedging 45

5 Exposures 57

Part II Volatility

6 The Heston Model 73

7 The SABR Model 87

Part III Term Structure Models

8 Term Structure Models 125

9 Short Rate Models 139

10 A Gaussian Rates-Credit Pricing Framework 175

11 Instantaneous Forward Rate Models and the Heath–Jarrow–Morton Framework 183

12 The Libor Market Model 197

Appendix A: Numerical Techniques for Pricing and Exposure Modelling 221

Index 245

List of Figures

Fig. 2.1 Exercise region for 9th (the last, 2025-05-19) and the 5th (2021-05-18) exercise dates of a fixed rate bond, states in which the bond is exercised are taken from the Monte Carlo simulation used for pricing 20

Fig. 2.2 Exercise region for 10th exercise date (2020-11-28) of a floating rate bond; exercise states are taken from the Monte Carlo simulation used for pricing 32

Fig. 5.1 Exposure measures illustrated on a portfolio of interest rate swaps. We show several paths (*top*), a particular one (*mid*) and the values contributing to the exposure (*bottom*) 60

Fig. 5.2 Exposure measures (*top*) and the expected exposure (*bottom*) 61

Fig. 5.3 The effect on the exposure of adding trades to a given portfolio. We consider the case **a** (*top left*), **b** (*top right*), **c** (*bottom left*) and adding the trades from (**b**) and (**c**) (*bottom right*) 62

Fig. 5.4 Effect of the collateral on the exposure of a given Netting Set. While the graphs (*top left*), (*top right*) and (*bottom left*) illustrate this on a sampled path, the graph (*bottom right*) shows the averaged effect 62

Fig. 5.5 Exposure profiles of different interest rate swaps with maturity 25 years. The ATM pay/receive cases (*top-left* and *right*), ATM −1% pay/receive (*mid-left* and *right*) and ATM + 1% pay/receive (*bottom-left* and *right*) 64

Fig. 5.6 Exposure profiles of different interest rate swaps with maturity 10 years. The ATM case (*top*) and the cases of positive market value (*mid*) and a negative one (*bottom*) 65

Fig. 5.7 Sample paths of the value of a cross-currency swap without periodic reset 66

Fig. 5.8 Exposures of cross-currency swaps that are not periodically reset. Perspective EUR/USD (*top*) and USD/EUR (*bottom*) 66
Fig. 5.9 Scenarios generated to calculate the profile of a multi-callable swap. The swap (*top*), the Bermudan Swaption (*mid*) and the combination of both (*bottom*) 67
Fig. 5.10 Exposure profile of the swap resulting from physical settlement of the exercised swaption 68
Fig. 5.11 Exposure profiles of the constituting elements. The swap (*top*) and the option (*bottom*) 69
Fig. 5.12 Exposure profile of a multi-callable swap 70
Fig. 6.1 Effect of the model parameters on the Implied Volatility Curve for a fixed maturity. Spot Variance (*top*), long term variance (*mid*) and Mean Rerversion (*bottom*) 78
Fig. 6.2 Effect of the model parameters on the Implied Volatility Curve for a fixed maturity. Volatility of Variance (*top*) and Correlation (*bottom*) 79
Fig. 6.3 Effect of the model parameters on the Implied Volatility Surface. We consider the Spot Variance (*top*), long term variance (*mid*) and the Mean Reversion (*bottom*) 80
Fig. 6.4 Effect of the model parameters on the Implied Volatility Surface. Volatility of Variance (*top*) and Correlation (*bottom*) 81
Fig. 7.1 Negative values if the risk neutral density is calculated with the volatility from (7.4) as an input 90
Fig. 7.2 Implied Bachelier volatility—intuition for the parameters determining the SABR model for *top* to *bottom* we have σ_0, resp. α, β, ν, ρ and f_0 91
Fig. 7.3 Applying the dampening method to the SABR model for different values of the dampening parameter M 95
Fig. 7.4 Regression to determine CEV coefficient β 97
Fig. 7.5 Coordinate transformation for the equidistant grid to a more suited one 99
Fig. 7.6 Densities for the SABR (*top*) and the free boundary SABR (*bottom*) models 104
Fig. 7.7 Illustration of the pricing using the effective equation 106
Fig. 7.8 Log-Normal volatilities from Hagan formula, Andreasen–Huge method using log-normal and normal volatilities. The parameters are $\nu_0 = 0.0873$, $\beta = 0.7$, $\gamma = 0.47$, $\rho = -0.48$, $T = 10$ and $f = 0.0325$ 109
Fig. 7.9 Hagan approximate solution, raw solution and the refined solution for the SABR model are plotted for different values of β_ν 114

Fig. 7.10 ZABR implied Bachelier volatilities (*right*) for $\beta_v = 0, 0.5, 1, 1.5, 1.7$ and the parameters from $\sigma_0 = 0.0873$, $\beta = 0.7$, $\rho = -0.48$, $\gamma = 0.47$, $f = 0.0325$ and $T = 10$ 115
Fig. 7.11 Values of the function under the square root in the above equation. We have chosen different CEV coefficients (*top*) and different values for the correlation (*bottom*) 116
Fig. 7.12 Prices for European call options (*top*) and implied Bachelier volatilities for choosing different upper bounds in the integration formula (*bottom*) 117
Fig. 7.13 Intuition for the effect of the parameters on the implied Bachelier volatility for the Free SABR model from *top* to *bottom* σ_0, resp. α, β, ν, ρ and f_0 118
Fig. 7.14 Mixing of a normal and a Free boundary SABR model with zero correlation. We have varied the mixing parameter to toggle between the impact of a model 119
Fig. 8.1 Illustration of the modelling of short rates 127
Fig. 8.2 Illustration of the modelling of instantaneous forward rates 130
Fig. 8.3 Illustration of the modelling of market rates 130
Fig. 9.1 Simulated short rate paths for different spot rates. We let $r(0) = -0.01$ (*top*) and $r(0) = 0.01$. The other parameters are $\kappa = 0.2$, $\theta = 0.03$ and $\sigma = 0.02$ (*bottom*) 142
Fig. 9.2 Two simulated term structures for the Gaussian short rate model with $\kappa = 0.2$ (*top*) and $\kappa = 0.5$ (*bottom*), $\theta = 0.03$, $\sigma = 0.02$ and $r = 0.01$ 143
Fig. 9.3 Hedging Instruments for the calibration of the LGM model to Bermudan swaptions 154
Fig. 9.4 Calibration strategy I 155
Fig. 9.5 Calibration strategy II 155
Fig. 9.6 Calibration strategy III 155
Fig. 9.7 Calibration strategy IV 155
Fig. 9.8 Calibration strategy V 155
Fig. 9.9 Calibration Error for the strategies (**I–V**) 156
Fig. 9.10 Two simulated term structures for the CIR model with $\kappa = 0.2$ (*top*) and $\kappa = 0.5$ (*bottom*), $\theta = 0.02$, $\sigma = 0.02$ and $r = 0.01$ 159
Fig. 9.11 Implied Volatility for a short rate model extended by a stochastic basis component. We displayed different levels of correlation 171
Fig. 10.1 One Monte Carlo path for the interest rate model state x and the credit spread model state y in an LGM 2F model with volatilities $\alpha = 0.0050$, $\alpha_c = 0.0080$ and correlation $\rho = 0.5$ 180
Fig. 10.2 Ten Monte Carlo paths for the interest rate model state x, with a volatility of $\alpha = 0.0050$ 181
Fig. 11.1 Typical hump shape realized using the deterministic volatility for the Trolle and Schwartz model (parameters $N = 1$, $\alpha_{01} = 0.16$, $\alpha_{11} = 0.25$ and $\gamma_1 = 0.15$) 189

Fig. 11.2 Term structure generated using the Trolle and Schwartz model 191
Fig. 11.3 Pricing of interest rate options using the Cheyette model with unspanned stochastic volatility. The prices for zero coupon bonds (*top*), Caplets (*mid*) and Swaptions (*bottom*) are shown together with the error with a Monte Carlo simulation as the benchmark. Generated with codes implemented by G. Schumann for a MSc supervised by J. Kienitz, see Schumann (2016) 192
Fig. 11.4 We applied the approximation formulae to the pricing of Caplets and compared them to Monte Carlo simulations. $N = 1$ (*left*) and $N = 3$ (*right*). Generated with codes implemented by G. Schumann for a MSc supervised by J. Kienitz, see Schumann (2016) 192
Fig. 11.5 Application of three different numerical schemes for generating the sample path namely the Euler method, the Milstein method and the QE method. We have chosen three driving factors which are plotted (*left*) and the corresponding forward rates (*right*). Generated with codes implemented by G. Schumann for a MSc supervised by J. Kienitz, see Schumann (2016) 193
Fig. 11.6 Pricing of Zero Coupon Bond options (*top*), Swaption (*mid*) and a Cap (*bottom*) with a Milstein and a QE scheme. Generated with codes implemented byG. Schumann for a MSc supervised by J. Kienitz, see Schumann (2016) 194
Fig. 12.1 Base parameters: $a = 0.0134$, $b = 0.1908$, $c = 0.9746$ and $d = 0.0808$ 204
Fig. 12.2 Different possible shapes of the correlation structure (12.17) 207
Fig. 12.3 A possible parametrization of the correlation matrix for (12.19) 208
Fig. 12.4 Different possible shapes of the correlation structure. We have chosen the parameter sets given in Table 12.1 209
Fig. 12.5 Illustration of tenor structures and Forward Rates 212
Fig. A.1 Effect of dampening on a payoff for a call option $\log(S/K) = 0, 0.01, \ldots, 2$ and$\alpha = 0, 0.5, 1, 1.5, 2$ 223
Fig. A.2 Density via the forward method 229
Fig. A.3 Price via the backward method 229

List of Tables

Table 1.1 Fix rate bond schedule, with annual coupon payments @5%, Actual/Actual bond basis, unadjusted accrual dates (which leads to identical coupon amounts for each period) and payment dates adjusted with respect to the TARGET calendar and "Following" rolling convention 5

Table 1.2 Fix rate bond valuation as of 2016-05-23 (flat yield term structure @2% and Z-spread $\lambda = 3\%$) the risk free net present value $\mathrm{NPV}_{\mathrm{rf}}$ is the product of the amount and the discount factor, the final NPV is the product of this and the credit risk damping factor $e^{-\lambda T_i}$ 6

Table 1.3 Hedge swap versus Euribor 6M Actual/360, floating leg fixing, index estimation, accrual and payment dates, the index start and accrual start are identical here, as well as the accrual end and payment dates; in general all these dates are independent of each other though 9

Table 1.4 Hedge swap, fix leg valuation as of 2016-05-23 (discount curve for a collateralized swap is assumed to be flat @1.9%) 10

Table 1.5 Hedge swap versus Euribor 6M Actual/360, with zero margin, float leg valuation as of 2016-05-23 (discount curve is flat @1.9%, Euribor 6M forward curve is flat @2%) 10

Table 1.6 Asset Swap calculation, all values in EUR except fair margin, which is in basis points. The BPS is the NPV of 1bp payments on the float leg payment dates, the fair margin is then the difference between the nominal (discounted from the settlement date to today) and the NPV of Bond + Swap, divided by the BPS 11

Table 2.1 Exercise and settlement dates for a callable fix rate bond, the exercise decision has to be taken on the exercise date, while in case of an exercise the redemption amount is to be paid on the settlement date. Here, the exercise date is chosen to have a 5 business days notice period before the settlement date, which is the accrual start date of the first coupon period that is part of the exercise 18
Table 2.2 NPV of a callable fix rate bond and its Asset Swap (Euribor 6M + 315.6bp) for OAS = 3%, IR volatility 0.0050, CR volatility 0.0080, IR-CR correlation 50% 19
Table 2.3 NPV of a callable fix rate bond under different model parameter scenarios 21
Table 2.4 Calibration basket for a callable fixed rate bond, following the representative basket approach 24
Table 2.5 Calibrated model interest rate volatility, reversion is fixed at 0.0020 25
Table 2.6 Calibrated model interest rate volatility, with different reversion, now fixed at 0.0030 26
Table 2.7 NPV of a callable fix rate bond with calibrated interest rate volatility, both with and without recalibration under the reversion shift 26
Table 2.8 Fix rate amortizing bond schedule 27
Table 2.9 Asset swap of an amortizing fix rate bond, fixed leg schedule 27
Table 2.10 Asset swap of an amortizing fix rate bond (zero margin), floating leg schedule, Euribor 6M rates are estimated on a flat forward curve @2% 28
Table 2.11 Calibration basket for an amortizing bond, following the representative basket approach 28
Table 2.12 Euribor 6M floater schedule without the notional repayment at the end 30
Table 2.13 Euribro 6M Floater call schedule, the settlement dates are chosen to be equal to the accrual start date of the first period that is part of the exercise right, the exercise date has a 5 business days (TARGET) notice period 31
Table 2.14 NPV of a callable floater 31
Table 2.15 NPV of a floating rate bond under different IR-CR correlations 31
Table 2.16 NPV of a callable floating rate bond under different model parameter scenarios and IR and CR rate shifts 32
Table 2.17 Inverse floater schedule with a simulated series of fixings 33
Table 2.18 Fixed rate compounded zero bond schedule, the only physical payment occurs at maturity 34
Table 2.19 Fixed rate discounted zero bond schedule; the repayment at maturity is equal to the nominal of the bond 34
Table 2.20 Floating zero bond schedule with simulated fixings 35

Table 2.21 Asset swap for fixed rate compounded zero bond schedule, fixed leg 35
Table 2.22 Asset swap for fixed rate compounded zero bond schedule, floating leg (amount is estimated on a flat 2%) forward curve 36
Table 2.23 Zero fix compounded call schedule, the exercise amount is equal to the compounded nominal schedule, the exercise date is chosen to have a notice period of 5 business days (TARGET) before the settlement date 36
Table 2.24 Zero fix compounded calibration basket, following the representative basket approach 37
Table 3.1 NPV of a draw option, 1,000,000.00 EUR can be drawn yearly, after being drawn the notional is then yearly callable 42
Table 3.2 NPV of a PIK option, all coupons of the bond are eligible for deferral 43
Table 4.1 Example TaRN payments in Scenario 1, the investor receives high coupons, but the note is terminated after 5.5 years 46
Table 4.2 Example TaRN payments in Scenario 2, the investor receives low coupons, and the note runs until its original maturity 47
Table 4.3 Snowball note schedule with simulated fixings, the average coupon paid is 5.03% 49
Table 4.4 Single coupon period taken from a range accrual structure 50
Table 4.5 Range condition hit counting for each business day in the coupon period, with simulated fixings 51
Table 4.6 Volatility note schedule with simulated fixings for the reference 10y swap rate S 53
Table 12.1 Parameter sets for illustrating different shapes of the correlation matrix 210
Table A.1 Model parameters for the numerical tests of the QE scheme 240
Table A.2 Prices for European Call options using the Hestonmodel for strike $K = 70$, 100and 140 and the test cases 241
Table A.3 Relative differences of the Monte Carlo prices for different numbers of timesteps using the standard QE scheme and the semi-analytic prices 241

Goals of this Book and Global Overview

Introduction and Management Summary

The first volume of Interest Rate Derivatives Explained, Kienitz (2014b), is dedicated to introduce basic interest rate products and give an overview of the corresponding markets. There, we outlined day count conventions, defined different rates and considered products that can be priced using the current yield curves and volatility surfaces, respectively cubes. This included Interest Rate Swaps but also more involved products such as swaptions, caps and floors or constant maturity swaps and the corresponding options referencing to constant maturity swap rates such as CMS spread options.

In the current volume, we wish to extend the scope to modelling volatility and the term structure of interest rates. Such methods are important for the daily work of financial institutions since exposures need to be determined, path-dependent contracts even with early exercise features but also products including negative rates, deep in or out of the money options and alike need to be valued, processed and risk managed. Take a constant maturity swap for instance. In Interest Rate Derivatives Explained 1, Kienitz (2014b), we have assumed the entire volatility smile given. Then, a static replication argument was applied for pricing and risk management of such trades. In this volume, we wish to show how the volatility smile is build and we wish to propose methods that can be applied to a wide range of market scenarios and do not stuck as some standard models that cannot safely be applied or even do not work at all. For instance, take the SABR model, here either standard methods generate too high volatilities for ITM or OTM options, lead to arbitrage or simply the current observed rates do not fit into the models scope. We show

how to adjust models and suggest other numerical approaches that are applicable in challenges market scenarios.

Other trades and products need to address different issues. Consider path-dependence for instance. For a sound risk management, a financial institution has to be able to handle such features often embedded in interest rate trades. This can materialize as an exercise right in a bond or swap contract. Even standard products such as mortgages in Germany have built in callability features. A mortgage loan can be called off after ten years at any day with a notice period of half a year. Another aspect is accounting. With regard to applying IFRS rules, the instruments held by a financial institution may need to be accounted for by assigning a fair value. This of course can include exotic rate products.

We have structured the book in three parts. The first part of the book deals with interest rate products. We give important examples for products that cannot be priced only taking into account the current yield curves and a swaption volatility surface. The future evolution of the term structure is necessary to determine the price and to apply an efficient hedge and risk management. Products which we consider include path dependencies in many ways. One important feature we consider is callability. Bermudan swaptions are the most prominent representatives of this product class. Then, we describe how volatility is modelled. Even for European options, it is necessary to think about a sound volatility model since quotes are only available for some maturities and strikes. If the maturity or the strike of an option is not quoted, methods for inter- and extrapolation have to be considered. All strikes and maturities need to be available to apply the before-mentioned replication technique to price CMS Caps, CMS Floors, CMS Swaps or CMS Spread options. After summarizing the task of volatility modelling, we consider two popular models in detail, namely the Heston model and the SABR model. Furthermore, the models can also be used to enhance term structure models with a stochastic volatility component. This additional component helps to model observed market features and improves the quality of fitting observed option prices.

The third part is concerned with term structure models. Such models are used to evolve the current yield curve into the future. There exist several methodologies for achieving this goal. We give an overview of term structure models ranging from one factor short rates over infinite dimensional models for the instantaneous forward rate to high dimensional market models. Often the modeller has to achieve a trade off between model complexity, accuracy and numerical tractability. In fact the latter might soon become a bottle neck when we consider the current regulated markets where all kind of value adjustments, see Kienitz (2014b), have to be calculated for large and diverse

portfolios. The basis of such adjustments is the generation of the future exposure. This is done by simulating risk factors for given future times called view points. Therefore, the simulation of many thousands of scenarios is the market standard method. This together with the valuation of complex options including path dependencies is very challenging. It is not hard to guess that the computational workload for fulfilling this task is immense. But once the data are available, the adjustments and exposure measures are easy to determine.

The current volume has three parts and an appendix with all together 12 chapters. Each part is dedicated to a single topic starting with products, then considering volatility modelling and finally covering term structure models. The appendix gives information on the numerical techniques that need to be applied for implementing the models and methods considered in this book. Summarizing we have:

- Part I
  - Vanilla Bonds and Asset Swaps
  - Callability Features
  - Structured Finance
  - More Exotic Features and Basis Risk Hedging
  - Exposures
- Part II
  - The Heston Model
  - The SABR Model
- Part III
  - Term Structure Models
  - Short Rate Models
  - A Gaussian Rates-Credit Pricing Framework
  - Instantaneous Forward Rate Models and the Heath–Jarrow–Morton Framework
  - The Libor Market Model
- Appendix
  - Numerical Techniques for Pricing and Exposure Modelling

Now, let us summarize some hot topics that are considered in the main body of the book. Some of those even appear the first time in book format since they were recently published and are part for ongoing research.

First, we have a wide coverage of products including Bermudan style derivatives with the Bermudan swaption as the most important one. Other more exotic interest rate derivatives are also still in the trading and banking books of financial institutions. We cover TaRN, floating rate notes or range accruals. You find valuable information on these types of trades including examples on how they work and the coupon mechanism works.

Then, we consider the very important topic of exposures. As already outlined in Kienitz (2014b), this is a very hot topic at the moment. The exposure profile of trades and portfolios is the key to measure counterparty credit risk either for regulatory or for accounting purposes. Exposure measures and examples for many common interest rate derivatives are considered. This includes multi-callable swaps where a Bermudan swaption is embedded into a swap-type contract. All is illustrated with pictures and graphs.

We give a broad overview of volatility modelling which is a very important topic and there has been a great body of research. We point to the corresponding literature and cover two of the models commonly applied in interest rate markets, namely the Heston and the SABR models. The latter models appeared most prominent in the quantitative finance literature. Foremost we have to mention Hagan et al. (2015) and Antonov et al. (2015). We think the reader will appreciate that we included the new developments here with new approximation formulas, numerical schemes for achieving a no-arbitrage representation of the probability density and even methods to use the newly proposed Free Boundary SABR model. We do not know of any other book covering this together with the new market paradigms of negative rates and Bachelier volatilities.

When it comes to term structure modelling financial institutions can choose from a variety of different models. To this end, we outline the main approaches to term structure modelling including ways to account for a stochastic basis. After laying out the different approaches we consider some representatives of each model class, namely

- Short Rate models with a focus on the Gaussian Short Rate model class
- Cheyette models with unspanned stochastic volatility
- Libor Market models with many different correlation structures

The reader will appreciate that many of the concepts are illustrated using spreadsheets that can be downloaded, see Section "Code".

At the end of the book you find a round up of numerical methods that are necessary to apply the models in practice. This extents the exposition from volume 1 where we considered bootstrapping, yield curve calibration and interpolation techniques. In Appendix A, we outline the application of

transformation techniques which can be applied but are not only restricted to the Heston model. In fact many jump models and stochastic volatility models can be tackled with the described techniques. Then, we cover the PDE approach using finite difference approximations of continuous quantities in some detail. The method is often applied in financial mathematics and we use it in our exposition to implement the SABR model. Finally, one of the most important numerical methods called Monte Carlo simulation is described. This technique is more important than ever. This is due to the fact that exposure for large portfolios that depend on a large number of risk factors has to be considered. Monte Carlo methods are the only tractable way of achieving this.

Code

Some of the methods and models are illustrated using spreadsheets. For instance, the different parsimonious approaches to model volatility and correlation in the context of Libor Market models or some flavours of using approximation formulae for the SABR model are illustrated in this way. All the examples are for pedagogical use only. The sheets cannot be used for sound modelling the interest rate markets but can serve as the basis for creating proprietary implementations and generating ideas.

The material for this book and for the first volume are available via www.jkienitz.de. There you also find additional material and further illustrations on quantitative finance, mathematical modelling and related topics.

Many publicly available software libraries have term structure models already implemented. We especially mention QuantLib (www.quantlib.org) and ORE (www.opensourcerisk.org).

Further Reading

This book can of course not give all the nitty gritty details and cannot provide a full account of all products, models and numerical techniques. To this end, we put together a list of relevant literature the reader might consult after reading this book. We decided to give hints on further reading with respect to the three parts of the book. For the appendix on numerical methods, we place the references for further reading directly below the last section of that chapter.

We also suggest further to the given references to do a search on the well-known preprint services including SSRN, ResearchGate or arXiv.

Part I

For the first part, we refer to Andersen and Piterbarg (2010a) and Andersen and Piterbarg (2010c). Many of the products discussed in this first part are also analysed and further explained in these books. Another standard reference is the compendium Brigo and Mercurio (2006). Also many products are considered there and many closed form solutions for derivatives products as well as intuition, hedging issues and further ideas are covered in a well written and clear manner. If you are looking for an account on recent advances in exposure modelling for rates consider to read Lichters et al. (2015). Many approaches such as the CSA Floor at 0 or tackling derivatives in the multi curve framework are reviewed and described in detail.

Some further books on valuation which are relevant for the first part are Henrad (2014) and Kenyon and Stamm (2012). They cover the changes the interest rate markets have undergone after August 2007 and how derivatives and options are tackled in this new era. Finally, we mention Kienitz (2014a). This book is the first part to the current one and has all the definitions for the underlying quantities of the derivatives considered in the first part. Furthermore, some basic derivatives have already been considered there.

Part II

Since the concept of volatility is of course not only relevant for modelling interest rates, there are many papers either devoted to volatility or covering volatility modelling for other asset classes. For volatility modelling a standard reference is Gatheral (2006). That book gives a great overview of many techniques and gives hints to further reading. The ground breaking articles for local volatility are Dupire (1994) and Derman and Kani (1994). These references are cited in many papers and books covering volatility modelling. Another good source of information and worth for building your intuition is Rebonato (2004). Here, different approaches with many illustrations and outlining their practical relevance are covered.

A very recent book that is written by a market practitioner is Bergomi (2016). This book covers the instruments that have volatility as well as the dynamics of the volatility as risk factors. For instance, forward starting options are covered, volatility index futures and options, the dynamics of local volatility, uncertain volatility and its usage and many more facts are considered in great detail.

Now, for the special case of the Heston Stochastic Volatility model which was introduced in Heston (1993) many papers and even a book dedicated to the model do exist. The book is Rouah (2015) and covers the standard but also many variants of the Heston model and numerical methods. Since then many researchers and practitioners used this model and contributed in terms of

applications or numerical methods. Relevant literature for implementing the Heston model and applications to calibration are Lord and Kahl (2005), Albrecher et al. (2006), Forde et al. (2012), Antonov et al. (2008), for simulation Andersen (2008), Staunton (2007) and Chan and Joshi (2010), for long stepping schemes (Bin 2007). The Heston model is also applied for enhancing existing models with a stochastic volatility component such as market models or for considering hybrid models. For enhancing market models, see Piterbarg (2003), Kiesel and Lutz (2010) and for an example of a hybrid model we recommend Kammeyer and Kienitz (2012a, b, c).

The other popular model is the SABR model. There is also a large body of literature available. The main reference for the SABR model is Hagan et al. (2002) but there have been research papers and books thereafter. For instance Hagan et al. (2005) propose an expression for the density which is often necessary when dealing with CMS derivatives.

After the events in 2007 and 2008 we saw that the standard method of applying SABR namely using the approximation technique was not valid anymore and methods had to be considered to remove arbitrage and cover with low rates and high volatility. We refer to Doust (2012), Hagan et al. (2015), Hagan et al. (2016), Antonov and Spector (2012), Antonov and Spector (2013), Kienitz (2015), Kienitz et al. (2017). Other methods to account for the negative rates include Antonov et al. (2015). The authors introduce a new local volatility function to the standard SABR model that changes the model behaviour and leading to a new way of modelling rates.

For considering the SABR model together with term structure models, we refer to Mercurio and Morini (2009) or Rebonato et al. (2009). The latter covers all the aspects necessary to use a market model with SABR-type stochastic volatility.

If you are interested in implementing the models we suggest to consult Kienitz and Wetterau (2012). This reference covers most of the techniques described in the above references. It also provides working Matlab source code and the reader can see how the models work and can play around with parameters, run simulations and calibration.

Part III

Term structure models are covered in a three volume compendium Andersen and Piterbarg (2010a, b, c). Another standard reference has already been mentioned for the products covered in Part I of this book. It is Brigo and Mercurio (2006). Both books have a wealth of information, tips and tricks from practitioners and well-known researchers.

If you are interested in short rate modelling you can work through several research papers but the above-cited references have all the stuff you need to

successfully apply short rate models. From pricing basic instruments as well as numerical methods to tackle exotic products are covered in the cited books. Furthermore, the references there point to the original papers if you wish to consider reading the original articles.

For the instantaneous forward rate models, we are not aware of a book that has a broad coverage of the models and the numerical techniques which are applied here. We suggest to take Andreasen (2005), Cheyette (1994) or Trolle and Schwartz (2009) as a starting point. A nice summary was written by a student of J. Kienitz from UCT, see Schumann (2016).

The case of the LGM model is considered in many papers by P. Hagan. For a detailed description, you can also consult Lichters et al. (2015). They treat the case of multi-currency LGM and combining it with different markets by using for instance foreign exchange extensions.

If you consider to work with a Libor market model we suggest to take Rebonato (2002) as a reference. Modern extensions with stochastic volatility are covered in Piterbarg (2003), Kiesel and Lutz (2010), Antonov et al. (2008) and Rebonato et al. (2009).

Another very useful reference is the homepage of John Schoenmakers at WIAS Berlin (http://www.wias-berlin.de/people/schoenma/). There you find many papers on different aspects of Libor Modelling. Furthermore, his book Schoenmakers (2005) covers the basics as well as advanced and very technical aspects of modelling Libor rates.

For the modern aspects of multi curve models and stochastic basis approaches, we suggest to consider Grbac et al. (2015), Mercurio and Xie (2012) and Mercurio (2010).

Acknowledgements **Jörg**: This book would not have been written without the support and help of many people. Foremost of course I would like to thank my family for their support and patience. For fruitful discussions and further insights, I wish to thank my colleagues Dr. Ventsislav Petkov and Weijun Yu. It was and is a pleasure to work with you and without your coding and mathematical skills some goals would not have been achieved.

The following people from the University of Cape Town for interesting discussions, good conversations and pushing forward research have to be mentioned: Prof. Thomas McWalter, Ralph Rudd and Gareth Schumann and all of the hard working Masters students. Without Prof. David Taylor from UCT the latter would not have happened. Thanks for making it possible to joining the faculty of Acturial Science at UCT as an Adjunct Associate Professor. Finally, my colleagues from the University of Wuppertal, namely, Prof. Michael Günther and Prof. Matthias Erhardt for their collaboration and their patience during my habilitation and for their encouragement to keep on going.

Peter: First and foremost I would like to thank my wife and my children for their backing and patience, it would not have been possible to write this book without them. For constant support and inspiration during many discussions, I want to thank Roland Lichters, Roland Stamm and Donal Gallagher from Quaternion Risk Management. It is very enjoyable to work on current topics in quantitative finance in this firm's lively and dynamic setting. Finally, I owe Luigi Ballabio and Ferdinando Ametrano from the QuantLib project a lot, the work on the library and having this fantastic toolbox available for so many years is invaluable.

References

Albrecher, H., Mayer P., Schoutens, W., & Tistaert, J. (2006). The little heston trap. *Wilmott Magazine*, 3.

Andersen, L. (2008). Simple and efficient simulation of the Heston stochastic volatility model. *Journal Compuational Finance, 7,* 1–32, 2008.

Andersen, L., & Piterbarg, V. (2010a). *Interest rate modeling - Volume I: Foundations and Vanilla Models*. New York: Atlantic Financial Press.

Andersen, L., & Piterbarg, V. (2010b). *Interest rate modeling - Volume II: Term Structure Models*. New York: Atlantic Financial Press.

Andersen, L., & Piterbarg, V. (2010c). *Interest rate modeling - Volume III: Products and Risk Management*. New York: Atlantic Financial Press.

Andreasen J. (2005). Back to the future. *RISK, 18*(9),104–109.

Antonov, A., Konikov, M., & Spector, M. (2015). Free boundary SABR. *RISK*.

Antonov, A., & Spector, M. (2012). Advanced analytics for the SABR Model. *SSRN*.

Antonov, A., & Spector, M. (2013). SABR spreads its wings. *RISK*.

Bergomi, L. (2016). Chapman and Hall. CRC Financial Mathematics Series, Boca Raton. *Stochastic volatility modeling*.

Bin, C. (2007). *Calibration of the heston model with application in derivative pricing and hedging.* Thesis. Retrieved from www.quantcode.com.

Brigo, D., & Mercurio, F. (2006). *Interest rate models —Theory and practice.* (2nd ed.). Berlin: Springer.

Chan, J. H., & Joshi, M. (2010). *Fast and accurate long stepping simulation of the heston stochastic volatility model.* Preprint. Retrieved from www.ssrn.com.

Cheyette, O. (1994). Markov representation of the Heath-Jarrow-Morton model. *Barra - Working paper and SSRN*.

Derman, E., & Kani, I. (1994). Riding on a smile. *RISK, 7,* 32–39.

Doust, P. (2012). No-arbitrage SABR. *Journal of Computational Finance, 15,* 3–31.

Dupire, B. (1994). Pricing with a smile. *RISK, 7,*18–20.

Forde, M., Jacquier, A., & Lee, R. (2012). The small-time smile and term structure of implied volatility under the Heston model. *SIAM Journal on Financial Mathematics, 3*(1), 690–708.

Gatheral, J. (2006).*The volatility surface*. Chichester: Wiley.

Grbac, Z., Papapantoleon, A., Schoenmakers, J., & Skovmand, D. (2015). Affine LIBOR models with multiple curves: Theory, examples and calibration. *SIAM Journal on Financial Mathematics, 6,*, 984–1025.

Hagan, P., Kumar, D., Lesniewski, A. S., & Woodward, D. E. (2015). Arbitrage free SABR. *Wilmott Magazine, 69,* 60–75.

Hagan, P., Kumar, D., Lesniewski, A. S., & Woodward, D. E. (2016). Universal smiles. *Wilmott Magazine, 84,* 40–55.

Hagan, P., Lesniewski, A., & Woodward, D. (2005). Probability distribution in the SABR model of stochastic volatility. *Working Paper*. Retrieved from http://lesniewski.us/papers/ProbDistForSABR.pdf.

Hagan, P. S., Kumar, D., Lesniewski, A. S., & Woodward, D. E. (2002). Managing smile risk. *Wilmott Magazine, 1,* 84–108.

Henrad, M. (2014).*Interest rate modelling in the multi-curve framework: Foundations, evolution and implementation.* Basingstoke: Palgrave McMillan.

Heston, S. (1993). A closed form solution for options with stochastic volatility with applications to bond and currency options. *The Review of Financial Studies, 6,* 327–343.

Kammeyer, H., & Kienitz, J. (2012a, January). The Heston Hull White Model I - Finance and Analytics. *Wilmott Magazine, 57,* 46–53.

Kammeyer, H., & Kienitz, J. (2012b, March). The Heston Hull White Model II - Fourier Transform and Monte Carlo Simulation. *Wilmott Magazine, 58,* 34–45.

Kammeyer, H., & Kienitz, J. (2012c, May). The Heston Hull White Model III - The Implementation. *Wilmott Magazine, 59,* 44–49.

Kenyon, C., & Stamm, R. (2012).*Discounting, libor, CVA and funding*. Basingstoke: Palgrave McMillan.

Kienitz J., McWalter T., & Sheppard R. (2017). Approximate and PDE solution to the boundary free SABR Model - Applications to pricing and calibration. In M. Ehrhardt., M. Günther., & J. Ter Maten (Eds.),*STRIKE –Novel methods in computational finance* (pp. 231–252). Berlin: Springer.

Kienitz, J. (2014a) .Transforming Volatility - Multi curve cap and swaption volatilities. *International Review of Applied Financial Issues and Economocs, 5*(1).

Kienitz, J. (2014b). *Interest rate derivatives explained: Volume 1 products and markets*. Palgrave McMillan: Palgrave McMillan.

Kienitz, J. (2015). Approximate and PDE solution to the boundary free SABR Model - Applications to pricing and calibration. *SSRN*. Retrieved from http://papers.ssrn.com/sol3/papers.cfm?abstractid=2647344.

Kienitz, J. & Wetterau, D. (2012). *Financial modeling - Theory, implementation and practice - (with Matlab source)*. Chichester: Wiley.

Kiesel, R. & Lutz, M. (2010). Efficient pricing of CMS spread options in a stochastic volatility LMM. *Working paper, SSRN*.

Lichters, R., Stamm, R., & Gallagher, D. (2015). *Modern derivatives pricing and credit exposure analysis - Theory and practice of CSA and XVA pricing, exposure simulation and backtesting*. Basingstoke: Palgrave McMillan.

Lord, R. & Kahl, C. (2005). Complex logarithms in Heston-like models. *Preprint*. Retrieved from www.christiankahl.com/publications/complexlogarithmsheston.pdf.

Mercurio, F. (2010). Libor market models with stochastic basis. *RISK,* 23.

Mercurio, F. & Xie, Z. (2012). The basis goes stochastic. *RISK, 12*: 78–83.

Mercurio, F. & Morini, M. (2009). Joining the SABR and libor models together. *Risk, 3*: 80–85.

Piterbarg, V. (2003). A stochastic volatility forward LIBOR model with a term structure of volatility smiles. Retrieved from http://papers.ssrn.com/sol3/papers.cfm?abstractid=472061.

Rebonato, R. (2002).*Modern pricing of interest-rate derivatives*. Chichester: Wiley.

Rebonato, R. (2004).*Volatility and correlation.* (2nd ed.). Chichester: Wiley.

Rebonato, R., McKay, K., & White, R. (2009). *The SABR/LIBOR market model.* Chichester: Wiley.

Rouah, F. (2015).*The heston model and its extensions in VBA*. Chichester: Wiley.

Schoenmakers, J. (2005).*Robust libor modelling and pricing of derivative products*. Chapman hall/CRC financial mathematicss series.

Schumann, G. W.(2016). *Trolle-Schwartz HJM interest rate model*. MSc thesis, University of Cape Town.

Staunton, M. (2007). Monte Carlo for Heston. *Wilmott Magazine*, 29.

Trolle, A. B., & Schwartz, E. S. (2009). A general stochastic volatility model for the pricing of interest rate derivatives. *Review of Financial Studies, 22*(5), 2007–2057.

Part I

Products

1

Vanilla Bonds and Asset Swaps

1.1 Introduction and Objectives

In this chapter, we introduce some common vanilla interest rate products with a focus on securities and the corresponding hedge swaps. Here "vanilla" means that we exclude exotic features like callability that are discussed in later chapters.

In our valuation examples for the hedge swaps for risk from other financial trades in this chapter, we do not go into further detail about value adjustments, the so-called XVAs. That is we do not consider CVA, DVA, FVA—type adjustments coming from residual credit risk which might arise despite having full collateralization due to thresholds, margin periods of risk, or other features of the collateral process. There are also other adjustments like MVA and KVA coming from initial margin and capital requirements. For a comprehensive introduction to these topics, see Chap. 5 or Lichters et al. (2015).

We start with the introduction of a basic measure of credit risk commonly used for bond pricing.

1.2 The Z-Spread

When pricing a security we need to incorporate some credit risk measure, because both the coupon and the final capital payments are subject to credit risk, these are paid conditional on the survival of the issuer up to the respective

© The Author(s) 2017

J. Kienitz and P. Caspers, *Interest Rate Derivatives Explained: Volume 2*,
Financial Engineering Explained, DOI 10.1057/978-1-137-36019-9_1

payment date. One common way of accounting for this default risk is by weighing each coupon and the final notional payment by a factor

$$e^{-\lambda T_i} \tag{1.1}$$

where λ in Eq. (1.1) is the so-called Z-spread. The capital Z refers to zero volatility. This is a name that becomes more clear when we consider callability in Sect. 2.2. There the option adjusted spread is introduced. The time T_i is the payment time of the respective cashflow. The Z-spread is continuously compounded with respect to Actual/365 (Fixed) day counting in our formulation here, but other conventions like yearly compounding are common in practice as well.

Note that neither the default event nor a recovery payment is modelled explicitly, but rather a constant (in the sense that λ is constant) decay factor is applied to all cashflows simultaneously.

Although unrealistic in a sense, this way of accounting for the credit risk is very common and practical. Note that λ is dependent on the maturity of the bond, thus, it has to be interpreted as an average default rate over the lifetime of the bond.

Usually $\lambda \geq 0$, but negative values are not strictly excluded, and depending on the benchmark discounting curve chosen, negative Z-spreads can be perfectly reasonable. In this light, the Z-spread is different from a hazard rate, and (1.1) cannot always be interpreted as a survival probability up to time T_i.

On the other hand, (1.1) obviously looks the same as a discounting factor, with λ playing the role of the (continuously compounded) zero rate.

The Z-spread to apply in a bond's valuation depends directly on the benchmark discounting curve chosen, that is it does not make any sense to speak of a Z-spread as such, but instead only as a Z-spread relative to a certain benchmark discounting curve.

1.3 Fixed Rate Bonds

Fixed rate bonds and the corresponding vanilla fix versus float hedge swaps are among the most basic products in fixed income.

A fixed rate bond with bullet notional structure pays periodic coupons as a percentage of its notional, and at maturity the notional itself. Table 1.1 gives an example with a 5% coupon paid over a lifetime of 10 years.

The valuation of a fixed rate bond is straightforward once a benchmark discounting curve is specified, given by its discounting factors $DF(0, t)$ for each $t > 0$, and a Z-spread λ accounting for the credit risk.

Table 1.1 Fix rate bond schedule, with annual coupon payments @5%, Actual/Actual bond basis, unadjusted accrual dates (which leads to identical coupon amounts for each period) and payment dates adjusted with respect to the TARGET calendar and ''Following'' rolling convention

Accrual start	Accrual end	Payment	Amount
2016-05-25	2017-05-25	2017-05-25	50,000.00
2017-05-25	2018-05-25	2018-05-25	50,000.00
2018-05-25	2019-05-25	2019-05-27	50,000.00
2019-05-25	2020-05-25	2020-05-25	50,000.00
2020-05-25	2021-05-25	2021-05-25	50,000.00
2021-05-25	2022-05-25	2022-05-25	50,000.00
2022-05-25	2023-05-25	2023-05-25	50,000.00
2023-05-25	2024-05-25	2024-05-27	50,000.00
2024-05-25	2025-05-25	2025-05-26	50,000.00
2025-05-25	2026-05-25	2026-05-25	50,000.00
		2026-05-25	1,000,000.00

Let N denote the notional, R the fixed coupon rate being paid, τ_i the day count fraction applicable to the ith accrual period and T_i the payment time of the ith payment, then the present value of the bond (1.2) as of today is given by

$$V^{\text{Fix Bond}} = N\left(\sum_{i=1}^{n} R\tau_i DF(0, T_i)e^{-\lambda T_i} + DF(0, T_n)e^{-\lambda T_n}\right) \tag{1.2}$$

In our example $N = 1{,}000{,}000.00$, $n = 10$, $R = 0.05$, $\tau_i = 1$ for all i and $T_i \approx 1, 2, \ldots, 10$. The exact values for T_i are calculated by the day count fraction between the evaluation date and the payment dates in the third column of Table 1.1 using the day count convention of the benchmark discounting curve: Table 1.2 gives a valuation of the bond as of 2016-05-23. We assume a benchmark discounting curve flat @2%. Again, the yield is continuously compounded in our example here, with respect to Actual/365(Fixed) day counting and a Z-spread of 300 basis points.

The column "Discount" contains the discount factor coming from the benchmark curve applicable to the respective payment date. The product of the payed amount and the discount factor gives the risk free present value NPV_{rf} of that payment, discounted to the valuation date 2016-05-23. The sum of all discounted payments gives the risk free present value of the bond, that is its value without taking credit risk into account. In our example, it is 1,267,122.99 EUR or 126.7123% relative to the nominal.

Table 1.2 Fix rate bond valuation as of 2016-05-23 (flat yield term structure @2% and Z-spread $\lambda = 3\%$) the risk free net present value NPV_{rf} is the product of the amount and the discount factor, the final NPV is the product of this and the credit risk damping factor $e^{-\lambda T_i}$

Payment	Amount	Discount	NPV_{rf}	$e^{-\lambda T_i}$	NPV
2017-05-25	50,000.00	0.980091	49,004.56	0.970286	47,548.44
2018-05-25	50,000.00	0.960684	48,034.21	0.941610	45,229.48
2019-05-27	50,000.00	0.941558	47,077.91	0.913631	43,011.82
2020-05-25	50,000.00	0.922965	46,148.23	0.886702	40,919.72
2021-05-25	50,000.00	0.904689	45,234.43	0.860496	38,924.04
2022-05-25	50,000.00	0.886775	44,338.73	0.835064	37,025.69
2023-05-25	50,000.00	0.869215	43,460.77	0.810384	35,219.93
2024-05-27	50,000.00	0.851864	42,593.18	0.786240	33,488.47
2025-05-26	50,000.00	0.835041	41,752.07	0.763066	31,859.58
2026-05-25	50,000.00	0.818551	40,927.57	0.740575	30,309.92
2026-05-25	1,000,000.00	0.818551	818,551.32	0.740575	606,198.41
	1,500,000.00		1,267,122.99		989,735.49

Note that the accruals are zero as of the valuation date (which lies 2 days before the first accrual start date of the bond), so the percentage figures above are clean prices. Also, note that the valuation does not assume any settlement days, in contrast to the usual market quotation which does incorporate a settlement delay, usually a few (often two) days. The reason is that if a bond is traded, the cash amount is paid on this date and not immediately on the trade date. In this sense, our valuation is more a theoretical one, as some banks use it for their internal profit and loss reporting, and less a valuation for trading purposes. However, note that the conversion between the two is very simple, since they only differ by a factor given as the discount factor, (1.3) for the settlement period

$$DF(0, t_s) \text{ with } t_s = \text{Actual365(Fixed)}\ (2016\text{-}05\text{-}23,\ 2016\text{-}05\text{-}25) \tag{1.3}$$

Under credit risk the value becomes 989,735.49 EUR or 98.9735%. The intuition that the bond should be worth 100% when it pays a 5% coupon and is valued under a yield term structure at 2% and a credit spread of 3% is correct. However, note that the bond coupon is simply compounded while the yield and credit spread are continuously compounded (and the day counters of the coupon and the term structure are different as well), which explains that the discounting effect overcompensates the coupon in this case, despite the numeric match of $2\% + 3\%$ valuation rate against the 5% coupon.

It is usual to take a swap curve with respect to certain tenor as the benchmark discounting curve, for example, a Euribor 6M curve for EUR bonds or a USD Libor 3M curve for USD bonds. A justification for this can be given as follows: Without taking credit risk into account, the valuation should reflect

the value of the investment taking into account the funding costs for it. If these funding costs are assumed to be those of an average bank contributing quotes to the Euribor or Libor fixing, it is appropriate to use a swap curve as the discounting curve (in addition we assume that the refinancing frequency is equal to the tenor of the swap curve). This way, average funding costs of a number of representative big banks are incorporated into the risk free NPV of the bond.

While each investor has its own funding curve, possibly largely deviating from others and therefore leading to significantly different bond prices. Assuming a swap curve gives a unique, objective market price for the bond. If a bank's funding curve significantly deviates from the swap curve, it is still a good basis for the construction of an individual funding curve by adding (or subtracting) an appropriate spread reflecting the relative funding disadvantage (or advantage) compared to the average swap funding curve.

Other popular choices for the benchmarking curve are yield curves stripped from government bonds. Here the interpretation is different from the funding perspective above, reflecting more directly the relative credit spread to the credit risk level of the government. Historically, that is before the 2007 financial crisis, both curve constructions of swap and government curve could basically be interpreted as giving a risk free curve.

Finally, when a bond can be used as a repo transaction underlying, the corresponding repo curve reflects the funding costs for that bond and is therefore a sensible choice as a benchmark curve as well.

1.4 Fixed Versus Float Vanilla Swaps

A natural hedge for a long position in the fix rate bond would be an interest swap paying the bond coupons and receiving floating coupons based on Ibor (like for example Euribor 6M, USD Libor 3M, etc.), possibly plus a margin. The package consisting of the long position in the bond and the hedge swap would then produce the same (net) cash flows as an Euribor 6M floating bond, which is much less exposed to interest rate risk than the fix bond. Note though that there are different curves involved in the valuation of the bond and swap cashflows

1. A benchmark discount curve for bond valuation, for example Ibor (Euribor 6M, USD Libor 3M, …) based, which together with the Z-spread is used to discount the bond cashflows

2. The discount curve for the swap, which is an OIS (Eonia, Fedfund …) curve, in case the swap is collateralized (which is the usual case and matches our general assumption, see above)
3. The forward curve for the Ibor (Euribor 6M, USD Libor 3M, …) coupons

If $DF_{\text{OIS}}(0,\cdot)$ denotes the discounting curve for the swap's cash flows (that is we assume discounting on an OIS curve) and $F_T(\tilde{T}_i, \tilde{T}_{i+1})$ the forward rate estimated for the index estimation start time $\tilde{T}_i$ and end time $\tilde{T}_{i+1}$ for the floating leg's Libor tenor T, typically $T = 1, 3, 6$ and 12 m. We have chosen to denote the dates appearing in a schedule corresponding to some floating rate index by a tilde on top, thus using $\tilde{T}$ instead of T. On an appropriate forward curve $DF_T(0,\cdot)$, that is

$$F_T(\tilde{T}_i, \tilde{T}_{i+1}) = \frac{DF_T(0, \tilde{T}_i) - DF_T(0, \tilde{T}_{i+1})}{\tau_{F,i} DF_T(0, \tilde{T}_{i+1})} \tag{1.4}$$

with $\tau_{F,i}$ denoting the day count fraction between the index estimation start and end date using the applicable forward's rate convention. Using (1.4), then, a payer swap's value with margin s_i on the float leg is given by

$$V^{\text{Payer Swap}} = \sum_{i=1}^{m} \tilde{\tau}_i (F_T(\tilde{T}_i, \tilde{T}_{i+1}) + s_i) DF_{\text{OIS}}(0, \tilde{T}_i) - \sum_{i=1}^{n} R\tau_i DF_{\text{OIS}}(0, T_i) \tag{1.5}$$

where again T_i, $\tilde{T}_i$ denote the payment times and τ_i, $\tilde{\tau}_i$ the day count fractions of the fixed and float leg coupons, respectively. In (1.5) the first summand corresponds to the floating leg and the second to the fixed leg. Note that m, the number of floating coupons, is typically a multiple of n, the number of fixed rate coupons, for example for a Euribor 6M swap we have $m/n = 2$, since the fixed leg pays yearly coupons, while the float leg pays semiannual coupons.

Since in particular on the float leg of a swap there are many different dates involved, we list all of them in Table 1.3 for an Euribor 6M hedge swap for the bond above, each row corresponding to one coupon period.

Note that the future fixing dates do not enter the valuation (1.5) directly, because only the index estimation start and end dates enter the formula for the forward rate estimation.

Also note that the index estimation start and end dates are not necessarily identical to the accrual start and end dates: While the index and accrual start dates agree for a plain vanilla, in particular in advanced fixed, swap, the index

Table 1.3 Hedge swap versus Euribor 6M Actual/360, floating leg fixing, index estimation, accrual and payment dates, the index start and accrual start are identical here, as well as the accrual end and payment dates; in general all these dates are independent of each other though

Fixing	Index start	Index end	Accrual start	Accrual end	Payment
2016-05-23	2016-05-25	2016-11-25	2016-05-25	2016-11-25	2016-11-25
2016-11-23	2016-11-25	2017-05-25	2016-11-25	2017-05-25	2017-05-25
2017-05-23	2017-05-25	2017-11-27	2017-05-25	2017-11-27	2017-11-27
2017-11-23	2017-11-27	2018-05-28	2017-11-27	2018-05-25	2018-05-25
2018-05-23	2018-05-25	2018-11-26	2018-05-25	2018-11-26	2018-11-26
2018-11-22	2018-11-26	2019-05-27	2018-11-26	2019-05-27	2019-05-27
2019-05-23	2019-05-27	2019-11-27	2019-05-27	2019-11-25	2019-11-25
2019-11-21	2019-11-25	2020-05-25	2019-11-25	2020-05-25	2020-05-25
2020-05-21	2020-05-25	2020-11-25	2020-05-25	2020-11-25	2020-11-25
2020-11-23	2020-11-25	2021-05-25	2020-11-25	2021-05-25	2021-05-25
2021-05-21	2021-05-25	2021-11-25	2021-05-25	2021-11-25	2021-11-25
2021-11-23	2021-11-25	2022-05-25	2021-11-25	2022-05-25	2022-05-25
2022-05-23	2022-05-25	2022-11-25	2022-05-25	2022-11-25	2022-11-25
2022-11-23	2022-11-25	2023-05-25	2022-11-25	2023-05-25	2023-05-25
2023-05-23	2023-05-25	2023-11-27	2023-05-25	2023-11-27	2023-11-27
2023-11-23	2023-11-27	2024-05-27	2023-11-27	2024-05-27	2024-05-27
2024-05-23	2024-05-27	2024-11-27	2024-05-27	2024-11-25	2024-11-25
2024-11-21	2024-11-25	2025-05-26	2024-11-25	2025-05-26	2025-05-26
2025-05-22	2025-05-26	2025-11-26	2025-05-26	2025-11-25	2025-11-25
2025-11-21	2025-11-25	2026-05-25	2025-11-25	2026-05-25	2026-05-25

estimation end date may differ by a few days from the accrual end date for some periods (for example 2018-05-28 vs. 2018-05-25 in our example). The payment date is also identical to the accrual end date here, because both are adjusted using the same conventions, but note that this is not the case on the fixed leg (which has an identical schedule as the bond), where the accrual dates are not adjusted (see Table 1.1).

At this point, we recall the basic fact that a convexity adjustment applies to the forward rate estimation as soon as the index estimation end date is different from the payment date of the corresponding coupon. However, it is usually negligible and therefore ignored in situations, where the mismatch is only a few days (as in our example here), and only taken into account for in arrears fixed coupons, or coupons with significantly delayed payment date, see Andersen and Piterbarg (2010), 16.4, 16.5.

Because of the different discounting curves involved, even the risk free valuation of the bond cashflows do not match the valuation of the same cashflows coming from the fix leg of the hedge swap, see Table 1.4. Table 1.5 shows the estimated cashflows of the swap's float leg as well as their NPV. Finally, Table 1.6

Table 1.4 Hedge swap, fix leg valuation as of 2016-05-23 (discount curve for a collateralized swap is assumed to be flat @1.9%)

Payment	Amount	Discount	NPV
2017-05-25	−50,000.00	0.981077	−49,053.86
2018-05-25	−50,000.00	0.962613	−48,130.64
2019-05-27	−50,000.00	0.944397	−47,219.87
2020-05-25	−50,000.00	0.926671	−46,333.57
2021-05-25	−50,000.00	0.909231	−45,461.55
2022-05-25	−50,000.00	0.892119	−44,605.93
2023-05-25	−50,000.00	0.875328	−43,766.42
2024-05-27	−50,000.00	0.858720	−42,936.00
2025-05-26	−50,000.00	0.842602	−42,130.11
2026-05-25	−50,000.00	0.826787	−41,339.35
	−500,000.00		−450,977.30

Table 1.5 Hedge swap versus Euribor 6M Actual/360, with zero margin, float leg valuation as of 2016-05-23 (discount curve is flat @1.9%, Euribor 6M forward curve is flat @2%)

Accrual start	Accrual end	Payment	Est. amount	Discount	NPV
2016-05-25	2016-11-25	2016-11-25	10,133.19	0.990365	10,035.55
2016-11-25	2017-05-25	2017-05-25	9,967.15	0.981077	9,778.55
2017-05-25	2017-11-27	2017-11-27	10,243.89	0.971624	9,953.21
2017-11-27	2018-05-25	2018-05-25	9,856.48	0.962613	9,487.97
2018-05-25	2018-11-26	2018-11-26	10,188.54	0.953387	9,713.62
2018-11-26	2019-05-27	2019-05-27	10,022.49	0.944397	9,465.22
2019-05-27	2019-11-25	2019-11-25	10,022.49	0.935492	9,375.97
2019-11-25	2020-05-25	2020-05-25	10,022.49	0.926671	9,287.56
2020-05-25	2020-11-25	2020-11-25	10,133.19	0.917838	9,300.63
2020-11-25	2021-05-25	2021-05-25	9,967.15	0.909231	9,062.44
2021-05-25	2021-11-25	2021-11-25	10,133.19	0.900564	9,125.58
2021-11-25	2022-05-25	2022-05-25	9,967.15	0.892119	8,891.88
2022-05-25	2022-11-25	2022-11-25	10,133.19	0.883615	8,953.83
2022-11-25	2023-05-25	2023-05-25	9,967.15	0.875328	8,724.53
2023-05-25	2023-11-27	2023-11-27	10,243.89	0.866894	8,880.37
2023-11-27	2024-05-27	2024-05-27	10,022.49	0.858720	8,606.52
2024-05-27	2024-11-25	2024-11-25	10,022.49	0.850623	8,525.36
2024-11-25	2025-05-26	2025-05-26	10,022.49	0.842602	8,444.98
2025-05-26	2025-11-25	2025-11-25	10,077.84	0.834614	8,411.10
2025-11-25	2026-05-25	2026-05-25	9,967.15	0.826787	8,240.71
			201,114.13		182,265.60

Table 1.6 Asset Swap calculation, all values in EUR except fair margin, which is in basis points. The BPS is the NPV of 1bp payments on the float leg payment dates, the fair margin is then the difference between the nominal (discounted from the settlement date to today) and the NPV of Bond + Swap, divided by the BPS

	Risk free	Risky
Bond NPV	1,267,122.99	989,735.49
Swap fix leg NPV	−450,977.30	n.a.
Swap float leg NPV	182,265.60	n.a.
Bond + Swap NPV	998,411.28	721,023.79
Swap float leg BPS	919.37	n.a.
Swap fair margin	1.61	303.33

summarizes the calculations and computes fair asset swap margins for the risk free and the credit-risky cases.

The fair asset swap margin is defined to be the margin to be put on the swap's floating leg in such a way that the package of the bond and the swap is worth the notional of the bond (as of the settlement date). It is mainly the different discounting curves we use for the bond and swap valuation that constitute a non-zero margin of 1.63 basis points for the risk free case.

The par asset swap hedge construction is particularly popular, since it allows to pay the notional amount for the package, the same way one would do for a floater priced @100% on its issue date. The asset swap construction can also be done during the lifetime of the bond, even within a coupon period, so that on each possible trade date an investor can enter into the position of the bond and the asset swap paying 100% as a (dirty, that is effective settlement) price.

1.5 Hedging with Asset Swaps, the Credit Trap

Looking closer at the hedge construction in Sect. 1.4 one notices that the bond cashflows are indeed converted to floating Euribor coupons. However, in case of a default this construction breaks down and leaves the investor with a collateralized swap and whatever he receives as a recovery from the defaulted bond. The swap may both have an unfavourable NPV and may carry an unwanted market risk. This imperfection of the hedge originates in the possibility for a non-zero Z-spread. A full hedge could be obtained, though, by replacing the vanilla swap by a credit linked swap that terminates whenever the bond terminates due to a default event. These credit linked swaps are actually traded as hedge swaps for more exotic credit products like first to

default notes but they are less common for a vanilla bond hedge. We call this the credit trap.

There is another important consequence of this observation which is worth pointing out. The margin on the asset swap's floating leg making the package of the bond and the asset swap worth the notional is called the asset swap spread of the bond. It can be calculated at any time during the lifetime of the bond and is therefore another "spread" apart from the Z-spread we already introduced.

Since the package of the bond and the swap superficially looks like a defaultable floater, it is tempting to interpret the asset swap spread directly as the fair spread over Libor that the issuer had to pay when issuing a new plain vanilla floating rate note. This way, the asset swap spread would be a direct measure of credit risk, just like the Z-Spread.

However, this is not true, because as we saw the package actually is not a defaultable floater, since in case of a default event the swap survives. Actually, the knowledge of the asset swap spread directly enables us to compute the current bond price and thus it is an "all in" spread. That is a spread that contains information about all price drivers, not just the credit risk, which might include interest rate levels, volatility levels, inflation rate levels and whatever other market observables influence the bond's price.

Thus, a change in the asset swap spread level might not only arise from a change in the credit risk, but it is also induced from a change in other risk drivers.

As a conclusion, it is tempting but not entirely correct to use the asset swap spread as an indicator for credit risk. However for moderate spread levels there is a strong relationship between the asset swap spread level and the Z-spread level, see Caspers (2013) for some example calculations and more details on this.

1.6 Conclusion and Summary

In this section, we introduced fixed rate bonds and the corresponding asset swaps commonly used to hedge the interest rate risk of positions in such bonds. We explain how both products are valued and discuss the different interest rate curves involved in this and how they can be constructed. The zero volatility spread and the asset swap spread are measures of credit risk coming naturally into play when valuing non-collateralised cash products such as bonds. However, we explain why the asset swap construction is not a perfect hedge and how this is also reflected in these two kinds of spreads.

References

Andersen, L., & Piterbarg, V. (2010). *Interest rate modeling—Volume III: Products and risk management*. London: Atlantic Financial Press.

Caspers, P. (2013). Zero yield and asset swap spreads. *SSRN*. Retrieved from http://www.papers.ssrn.com/sol3/papers.cfm?abstract_id=2465847.

Lichters, R., Stamm, R., & Gallagher, D. (2015). *Modern derivatives pricing and credit exposure analysis—Theory and practice of CSA and XVA pricing exposure simulation and backtesting*. Palgrave MacMillan.

2

Callability Features

2.1 Introduction and Objectives

In this chapter, we introduce callability which gives one party in a transaction the right (but not the obligation) to terminate the transaction early. The valuation of such optional rights requires more than a static curve as in Chap. 1. A starting point is the dynamic term structure model as presented in Chap. 10. We give valuation examples in terms of this model in the following sections.

2.2 Callability

In order to pay a higher coupon, thus making the bond look more attractive to the investor, one can add features that have a positive value from the issuer perspective. This excess value can then be distributed via the coupon payments such that in effect a higher coupon can be paid without any economical disadvantage taken by the issuer. One of the most common of such features is callability. This gives the issuer the right to pay back the notional of the bond before its scheduled maturity, usually at par and without any compensation for the outstanding coupon payments. There are variations to this repayment style, which we look at in Chap. 3. The call right is a one-sided right owned by the issuer that he may, but is not obliged, exercise, thus a long option held by the issuer.

There are also bonds that are puttable, meaning that the investor instead of the issuer has the right to early terminate the bond and receive the notional before reaching its maturity. Clearly, this constitutes a long option for the investor. Finally, there are bonds which are both callable and puttable.

© The Author(s) 2017

J. Kienitz and P. Caspers, *Interest Rate Derivatives Explained: Volume 2*,
Financial Engineering Explained, DOI 10.1057/978-1-137-36019-9_2

We focus on callable bonds, that is bonds with a call right owned by the issuer. On the one hand, they are more common than puttable bonds and on the other hand, a put right is similar to a call in terms of valuation methodology.

A general remark about the exercise of an early redemption option is in order. While for the derivative side, that is the hedge swaps the exercise is usually purely driven by what is captured in (an appropriate) valuation model, the early redemption decision of a bond goes usually beyond the exercise criterion given by a pure valuation model: Firstly, the valuation model itself is harder to calibrate to the current market, since variables like the dynamic of the credit spread and its correlation to the interest rate dynamics are required as an input which are much harder to derive from market observables than the pure interest rate swap curves and vanilla options that are required for a callable swap valuation. This is, however, not entirely true, since the inter-temporal correlation of rate movements is essential for multi-callable swap valuation as well, which is, for example, represented by a parameter mean reversion in, for example, a LGM called model, see the exposition in later chapters, in particular Chap. 9 or Sect. 10.3. Furthermore, liquidity considerations may influence an early redemption decision to a great extent, which are rarely part of the valuation model at all or if so, very hard to calibrate to any objective reference. We take this model as a placeholder for any other term structure model in the sequel.

In the fixed rate bond example from Chap. 1 suppose that the issuer has a call right after 5 year of the bond's lifetime (say exactly on the start of the 6th coupon accrual period). Whenever the NPV of the remaining 5 year bond is above par (that is the notional amount), the issuer should buy back the bond and issue a new 5 year bond at the same time at par. Since the NPV of the original bond was above par, the coupon of the new bond is necessarily below the original coupon, such that the issuer then has a gain from this switch. If on the other hand the NPV is below par on the option date, the issuer does not exercise the option. It is this one-sided option right which constitutes a positive value of the call option to the issuer.

Note that both interest rate and credit spread movements influence the NPV of the bond, such that the option value is driven by the common dynamics in particular their volatilities and mutual correlation of the two quantities in general.

The early exercise right can be the right to pay back the notional early at only one predefined date in the future. In this case, it is known as an European exercise right. If the right can be exercised at one of the several predefined future dates, it is known as a Bermudan exercise right. It is understood that a Bermudan right is at least as valuable as the most valuable European right corresponding to its exercise dates. Actually, in general the value is not equal

to the maximum of the corresponding European rights, but greater than this maximum. This is because the decision which exercise date will potentially be chosen to pay back the notional early has not to be taken until a certain exercise date is reached. Only then the single decision if this particular exercise opportunity is taken has to be made or if one rather hopes that a later exercise may be more favourable. There is also the notion of an American Exercise right, which means that the notional can be paid back on each day during the life time of the bond. Technically, this is nothing else than a Bermudan exercise right with each day being an exercise date.

While for a plain bond without any early redemption rights a swap exchanging the bond coupons against a floating rate like Euribor or Libor plus a spread is the natural hedging instrument, for a callable bond it is a swap that can be terminated early at the same dates as the bonds. Such swaps are known as callable swaps, again European, Bermudan or American callable swaps depending on how many exercise opportunities exist.

A certain period at the beginning of the lifetime of a bond where it can not be called is common, for example 2 years in a 10-year bond, and only after this period a Bermudan call right may start with yearly call rights. In this case, the bond would be callable after 3, 4, 5, 6, 7, 8 and 9 years. If it is not called then the notional is paid back at maturity.

As explained in Sect. 1.5, callable swaps are imperfect hedges unless they are made credit-linked. The situation is, in a sense, worse than for the non-callable case though, since even without a default event the swap may be called on an exercise date while the bond does not. This happens, for example, if a low interest rate level suggests a call of the swap, but an overcompensating high credit spread level lets the issuer keep the bond as is (because in economical terms he would have to pay a higher coupon for a new issue despite the low interest rates because their credit spread is high enough).

We note that a call right may not be exercised purely by interest rate level and credit spread level considerations, but that in practice the liquidity situation of the issuer and the actual ability to place a new issuance may play a role whether an exercise right is executed or not. It is important to add that the credit spread is in general a quantity that is not directly observable in the market, but has to be implied from other instruments like other bonds (with similar characteristics) of the same issuer or even CDS. Since between the bond and CDS market there is a basis, the latter approach is even more difficult to apply.

2.3 Callable Fixed Bonds, Callable Swaps and Swaptions

We continue to give a valuation example. As above, we assume a flat yield term structure @2% as the benchmark discounting curve and an OAS spread of 300 basis points. The bond is a 10-y bond with fixed, yearly coupons @5%, as above, but now the bond is callable by the issuer @100% at the start of each coupon accrual period. In practice, the issuer has to decide whether or not to exercise a few days before the start of such a period. In our example we assume 5 business days. Table 2.1 lists the exercise dates and corresponding accrual start dates on which the redemption amount (in our case the notional) has to be paid.

We assume the model's interest rate volatility to be 0.0050 and the reversion speed to be 0.0020. Likewise, we assume the credit spread volatility to be 0.0080 and its reversion speed to be 0.0040. The joint dynamics of interest rates and credit spreads is specified by the correlation between their driving Brownian motions. We assume this to be 50% for the moment. When we consider short rate models, you notice that the above numbers are quite small, especially for the mean reversion.

In terms of numerical procedures, PDEs, numerical integration or Monte Carlo Simulation are all possible, whereas PDEs are probably most common for the product in question here. For the example calculation, however we use a general Monte Carlo Engine for structured bonds valuation which was designed to handle the possibility of a larger number of price factors (like

Table 2.1 Exercise and settlement dates for a callable fix rate bond, the exercise decision has to be taken on the exercise date, while in case of an exercise the redemption amount is to be paid on the settlement date. Here, the exercise date is chosen to have a 5 business days notice period before the settlement date, which is the accrual start date of the first coupon period that is part of the exercise

Exercise date	Settlement date
2017-05-18	2017-05-25
2018-05-18	2018-05-25
2019-05-20	2019-05-25
2020-05-18	2020-05-25
2021-05-18	2021-05-25
2022-05-18	2022-05-25
2023-05-18	2023-05-25
2024-05-20	2024-05-25
2025-05-19	2025-05-25

Table 2.2 NPV of a callable fix rate bond and its Asset Swap (Euribor 6M + 315.6bp) for OAS = 3%, IR volatility 0.0050, CR volatility 0.0080, IR-CR correlation 50%

	NPV (EUR)	NPV (relative) (%)
Bond underlying	989,763.11	98.9763
Bond call option	−49,783.90	−4.9783
Callable bond total	939,979.21	93.9979
Swap underlying NPV	21,441.42	2.1441
Swap call option	38,218.36	3.8218
Callable swap total	59,659.78	5.9660

Inflation, FX) as well as path dependency. Numerical methods are outlined in Appendix A.

Table 2.2 lists the NPV of the bond and its asset swap under these assumptions. The margin on the asset swap's float leg evaluates to 315.6 basis points to make the package of the callable bond and callable asset swap worth the notional on the settlement date 25-May-2016. Note that, this is not exactly the same as the asset swap spread for the non-callable bond (which was 303.33 basis points, cf. Table 1.6), which once again illustrates that the asset swap spread is not a pure measure of credit risk but reflects other price drivers as well.

The small difference of the bond's underlying price compared to the calculation in Table 1.2, which is 27.62 EUR or 0.2 basis points relative to the nominal, comes from the fact that we use a Monte Carlo valuation model here which introduces a simulation error.

We already noted that the asset swap belonging to the callable fixed rate bond is a callable fix versus float vanilla swap, that is a swap with schedule as in Table 1.4 plus an early termination right given by an exercise schedule identical to Table 2.1, meaning that all payments with respect to accrual periods with accrual start date greater or equal to the exercise date are cancelled in case of an exercise. This is the prototype of a Bermudan callable fix versus float swap. Note that the call right is held by the investor to offset the bond's call right held by the bond's issuer.

The option to enter into the tail of the underlying swap on one of the exercise dates is called a Bermudan swaption. If from the option holder perspective the underlying is a payer swap, the option is a payer swaption and otherwise a receiver swaption. The call option of a Bermudan callable swap is actually a Bermudan swaption: For a vanilla payer swap, a Bermudan receiver swaption represents the right to enter into a swap whose cashflows exactly offset the original swap's flows. In other words, the portfolio consisting of a vanilla payer swap and a Bermudan receiver swaption is equivalent to a Bermudan callable payer swap.

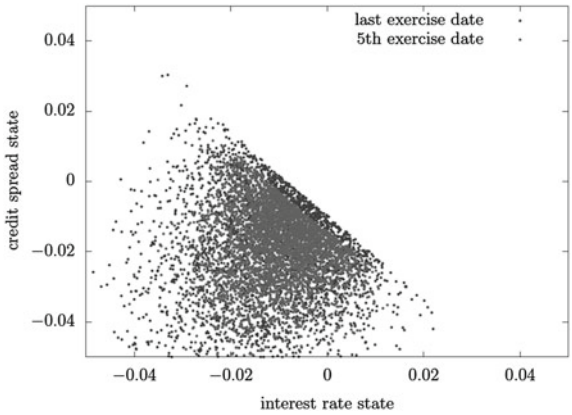

Fig. 2.1 Exercise region for 9th (the last, 2025-05-19) and the 5th (2021-05-18) exercise dates of a fixed rate bond, states in which the bond is exercised are taken from the Monte Carlo simulation used for pricing

Figure 2.1 shows points in the (x, y) plane for which the fix bond is called at the 9th and the 5th exercise dates.

Firstly, the shape of the exercise region (for both exercise dates) indicates that the bond is exercised when either the interest rate level or the credit spread level is low enough. More specifically, the picture confirms the intuition that the exercise boundary is given by the condition $ax + by < 1$ for some constants a, b. x is the level of interest rate and y that of credit spread.

In addition to this, one sees that the exercise region moves to the lower left for earlier exercise dates. This is because the exercise decision depends on two criteria:

1. the exercise as such must make sense economically, that is the bond's fair value at exercise must be greater or equal to the redemption price (usually the nominal);
2. the pay-off from the exercise (that is the difference of the bond's fair value and the redemption value) must exceed the present value of future early redemption rights.

The second point is exactly the reason why the pay-off at earlier exercise dates must increase.

Next, we look at how the callable bond price reacts to changes in

1. credit and interest rate volatility levels,
2. correlation of credit and interest rates,
3. credit and interest rates reversion.

Table 2.3 NPV of a callable fix rate bond under different model parameter scenarios

	NPV (relative) (%)	NPV change (%)
Original parameters	93.9979	0.0000
IR volatility $+0.0010$	93.6350	-0.3628
CR volatility $+0.0010$	93.5664	-0.4315
IR reversion $+0.0010$	94.0095	$+0.0116$
CR reversion $+0.0010$	94.0229	$+0.0250$
IR-CR correlation $+10\%$	93.8504	-0.1475
IR-CR correlation -10%	94.1653	$+0.16740$

Table 2.3 summarizes the results. The qualitative behaviour of the NPV under the different scenarios for the model parameters can be explained as follows: an increase both in IR or CS volatility increases the bond's price volatility at each exercise date; therefore, the value of the call option increases as well and, thus, the callable bond prices decrease then, since there is a higher chance of a price increase then.

For a term structure model that we consider later, a parameter governing the behaviour that control the tendency towards a long-term average, the mean reversion, for instance in a LGM model controls two things:

1. the inter-temporal correlations between rates (see above) and a higher reversion produces a lower inter-temporal correlation, which in turn increases the call option value;
2. the effective volatility for rates which is lower for higher reversion rates (given the same model volatility parameter) and, therefore, decrease the call option value.

Here, the second effect outweighs the first which effectively decreases the call option value then (and increases the callable bond's price). It should be noted that if the model volatility is calibrated to a market instrument that is discussed below, the second effect is washed away, since after increasing the model's reversion the recalibration of the model volatility will lead to an increased model volatility compensating for the change in the reversion. Then, the role of the reversion parameter is solely to control the inter-temporal correlations and an increase in reversion would lead to an increase in option value opposite to the result here. We give an example for this in Sect. 2.4.

Finally, a higher correlation between interest rates and credit spreads increases the effective price volatility of the bond at the exercise dates again and, therefore, increases the call option value and decreases the callable bond's value.

2.4 Hedging and Model Calibration

Up to now, we have looked at valuations in a model with arbitrary volatility, reversion and correlation parameters. To get market consistent prices, one has to calibrate the model's parameters in such a way that relevant market prices of reference instruments are matched. Here, "reference instruments" refer to instruments that are liquidly traded and for which a tradable market premium is known. "Relevant" means that the reference instruments whose value is reproduced by the model are related to the features of the exotic structure to be priced.

In case of a Bermudan call right, the usual choice is the underlying single European call rights, which in turn are given by European swaptions, at least in the case of a vanilla Bermudan callable swap. In some sense, the Bermudan option can be seen as a (dynamically) weighted sum of the single European rights, since as seen from today the exercise of the Bermudan option coincides with the exercise of each of the European rights with a certain probability (which changes over time). Indeed, one approximation for the Bermudan option value is simply the maximum of the values of the European options. See also below for the influence of inter-temporal correlations on the Bermudan option value.

As soon as the underlying instrument of the exotic call deviates from the market swaption's standard underlying, one has to perform some matching procedures to find a basket of market swaptions that appropriately describes the European call rights on the non-standard underlying of interest.

In our case, the callable bond's underlying deviates from the standard market swaption's underlying (with equal fixed rate as the bond, notional, underlying start date and underlying maturity date) in a number of points:

1. most importantly, the market swaption is not driven by the bond's credit spread, while for the bond it is one of the main price drivers;
2. the valuation of the underlying on the bond's benchmark discounting curve plus OAS spread versus the valuation of the swaption's underlying on the O/S curve;
3. the exchange of the redemption amount against the remaining bond cash-flows in case of the bond being called versus the exchange of the fixed and the Euribor 6M floating leg on exercise of the swaption;
4. the expiry date of the call, which is 5 business days in case of the bond and 2 in case of the market swaption;
5. the accrual schedule, which is unadjusted in the case of the bond and adjusted modified following in case of the market swaption's underlying swap.

Considering the first point, the only way out would be to use a swaption with a credit-linked swap underlying for hedging. However, such a product is not a liquidly quoted instrument in the market, so it does not help to follow this route in terms of model calibration. Also, one usually relies on standard market swaptions for hedging, since those are the instruments liquidly available and therefore cheap to trade.

There are several possible ways of accounting for the remaining differences, such as,

1. roughly adjusting parameters, like setting the swaption's strike to the bond fixed rate minus the Z-spread (appropriately converted to take the different rate conventions into account), or (more usual) adding an appropriate margin to the floating leg of the swaption's underlying swap;
2. ignoring other parameters such as the different notification periods of the call, the different exchanged financial instruments in case of the bond's and swaption's exercise (see above), or the different accrual schedules;
3. applying some numerical optimization to find the best-matching market instrument, for example by matching the NPV, Delta and Gamma of the respective underlying instruments in the model on the relevant expiry date, see Andersen and Piterbarg (2010b), 19.4 (representative basket approach), and Caspers (2013) for a specific application of the method to callable fixed bonds and other situations;
4. applying other matching methods, see Andersen and Piterbarg (2010b), 19.4.4, 19.4.5.

In the following, we illustrate the representative basket method on our examples.

So far we have identified market instruments to calibrate the model's interest rate volatility. To calibrate the model's volatility parameter to more than one instrument, it is usual to use a piecewise constant or piecewise linear volatility function with step times equal to the expiry times of the instrument one calibrates to. This gives the model's volatility exactly the same number of degrees of freedom as there are number of calibration instruments.

Likewise, one has to calibrate the credit volatility to market instruments like CDS options, if available. If no such appropriate instruments are liquidly quoted in the market (which is likely to happen), a historical estimation of the volatility can be used as a second best solution. Lichters et al. (2015), 12.3.3 provides a matching procedure to translate a historical estimate to a model parameter.

The reversion parameters of the model fine-tune the difference of the value of the Bermudan exercise right compared to the underlying European rights. See Andersen and Piterbarg (2010a), 19.2 for several possibilities to determine this parameter (in the case of interest rates at least):

1. calibrated to inter-temporal correlation from a global model such as a Libor Market Model;
2. used as an external, free parameter to match market prices for Bermudan swaptions directly;
3. calibrated to additional vanilla options such as caps and floors.

Finally, the correlation between interest rates and credit has to be specified. Since there are most probably no liquid market instruments quoted which are sensitive to this correlation, one again has to rely on a historical estimate. Again, see Lichters et al. (2015), 12.3.3 for a procedure to match the historical estimate with the model correlation.

We continue the valuation example from above by calibrating the interest rate component of our model to a basket of market-quoted swaptions. As indicated above, we ignore the credit spread dynamics, but adjust for the remaining differences listed in Sect. 2.4 by looking for a best-matching basket of market swaptions in the sense of Andersen and Piterbarg (2010b), 19.4.

Table 2.4 lists the resulting calibration basket. The expiry dates are exactly the exercise dates of the bond. The start dates of the underlying swaps however correspond to a standard market swaption's start delay of 2 business days opposed to the notice period of the bond's exercise of 5 business days. This causes the accrual periods and coupon payment dates of the swap are shifted by a few days compared to the bond. The nominal is a bit lower than the bond's nominal, which accounts for the default possibility of the bond leading

Table 2.4 Calibration basket for a callable fixed rate bond, following the representative basket approach

Expiry	Maturity	Nominal	Strike
2017-05-18	2025-12-22	929,972.53	0.019965
2018-05-18	2026-01-22	936,966.66	0.019968
2019-05-20	2026-02-23	942,693.56	0.020010
2020-05-18	2026-03-20	950,322.17	0.019965
2021-05-18	2026-04-20	957,875.24	0.019967
2022-05-18	2026-04-20	965,760.47	0.019960
2023-05-18	2026-05-22	976,226.73	0.019949
2024-05-20	2026-05-22	976,006.14	0.020122
2025-05-19	2026-05-21	958,570.07	0.020133

to a reduced hedge nominal for the swaptions. Note that, the nominal for the calibrating swaptions is not really relevant for the model calibration. For the same reason, the maturity dates lie before the bond's maturity, by 6 months for the first swaption up to only the few days we already observed for the last swaption. Finally, the strike of the calibrating swaptions is close to 2%, which is expected since the bond's coupon is 5% and the valuation spread (OAS) is 3%.

In summary, this basket is the result of a numerical optimization which accounts for the before-mentioned differences between the actual bond's call right and the standard market swaptions available for hedging.

We now calibrate the interest rate component of our LGM model to this basket assuming a (normal) market volatility of 0.0050. Table 2.5 shows the calibrated interest rate volatility. Note that, we keep the reversion fixed at the level we assumed before. Note also that the model volatility is close to the market volatility. This is, however, due to the facts that we use a normal market volatility (which corresponds to the nature of the model volatility) and that the reversion of the model is close to zero. Otherwise, the model volatility—in numeric terms—might significantly deviate from the market volatility.

Table 2.7 shows the effect of a reversion shift like in Table 2.3 before, but now when re-calibrating the model volatility to the market swaption basket. Now, the effect on the NPV is indeed negative because of the lower inter-temporal correlations increasing the call option's value. Table 2.6 shows the calibrated model volatility under the shifted reversion 0.0030. Although the calibration instruments have exactly the same value, the model volatility is slightly different because of the different reversion, which shows that reversion and volatility are interconnected.

Table 2.5 Calibrated model interest rate volatility, reversion is fixed at 0.0020

Swaption expiry	Market premium	Model premium	Model volatility
2017-05-18	13,321.19	13,321.19	0.00495
2018-05-18	17,143.09	17,143.09	0.00496
2019-05-20	18,694.90	18,694.90	0.00497
2020-05-18	18,638.26	18,638.26	0.00501
2021-05-18	17,561.88	17,561.88	0.00499
2022-05-18	15,326.62	15,326.62	0.00500
2023-05-18	12,691.53	12,691.53	0.00501
2024-05-20	9,131.95	9,131.95	0.00506
2025-05-19	4,716.95	4,716.95	0.00504

Table 2.6 Calibrated model interest rate volatility, with different reversion, now fixed at 0.0030

Swaption expiry	Market premium	Model premium	Model volatility
2017-05-18	13,321.19	13,321.19	0.00498
2018-05-18	17,143.09	17,143.09	0.00499
2019-05-20	18,694.90	18,694.90	0.00500
2020-05-18	18,638.26	18,638.26	0.00505
2021-05-18	17,561.88	17,561.88	0.00504
2022-05-18	15,326.62	15,326.62	0.00505
2023-05-18	12,691.53	12,691.53	0.00507
2024-05-20	9,131.95	9,131.95	0.00512
2025-05-19	4,716.95	4,716.95	0.00511

Table 2.7 NPV of a callable fix rate bond with calibrated interest rate volatility, both with and without recalibration under the reversion shift

	NPV (relative) (%)	NPV change (%)
Calibrated IR volatility	94.0075	0.0000
IR reversion $+0.0010$	94.0095	+0.0020
Recalibrated IR volatility	94.0043	−0.0032

2.5 Amortizing Structures

While in a bullet structure the full notional is paid back at maturity, there are also bonds that pay back part of the notional during the lifetime, most commonly together with the coupon payments. For example, the 10-year bond example from above may be modified such that on each coupon payment date 10% of the notional is paid back to the investor, leaving a final payment of only 100,000 USD on an initial investment of 1,000,000 USD. The coupon amounts are then computed with respect to the current notional of the period, that is these amounts shrink in the same proportion as the notional itself. Table 2.8 gives an example of such a bond's payment schedule.

Callability works in the same fashion for amortizing structures as it does for bullet structures: at an exercise date, the outstanding notional may be paid back to the investor.

Other than the amortizing notional payments which are scheduled to be paid back, the early redemption amounts are paid back if and only if the issuer chooses to do so. This distinction is important to remember. In this sense, amortization does not constitute an additional positive value to the issuer, while the one-sided early redemption rights do. It is important to distinguish these two kinds of repayments.

Table 2.8 Fix rate amortizing bond schedule

Accrual start	Accrual end	Payment date	Notional	Payment
2016-05-25	2017-05-25	2017-05-25	1,000,000.00	50,000.00
2017-05-25	2018-05-25	2018-05-25	900,000.00	45,000.00
2018-05-25	2019-05-25	2019-05-27	800,000.00	40,000.00
2019-05-25	2020-05-25	2020-05-25	700,000.00	35,000.00
2020-05-25	2021-05-25	2021-05-25	600,000.00	30,000.00
2021-05-25	2022-05-25	2022-05-25	500,000.00	25,000.00
2022-05-25	2023-05-25	2023-05-25	400,000.00	20,000.00
2023-05-25	2024-05-25	2024-05-27	300,000.00	15,000.00
2024-05-25	2025-05-25	2025-05-26	200,000.00	10,000.00
2025-05-25	2026-05-25	2026-05-25	100,000.00	5,000.00
		2026-05-25		100,000.0

Table 2.9 Asset swap of an amortizing fix rate bond, fixed leg schedule

Accrual start	Accrual end	Payment date	Notional	Payment
2016-05-25	2017-05-25	2017-05-25	1,000,000.00	−50,000.00
2017-05-25	2018-05-25	2018-05-25	900,000.00	−45,000.00
2018-05-25	2019-05-25	2019-05-27	800,000.00	−40,000.00
2019-05-25	2020-05-25	2020-05-25	700,000.00	−35,000.00
2020-05-25	2021-05-25	2021-05-25	600,000.00	−30,000.00
2021-05-25	2022-05-25	2022-05-25	500,000.00	−25,000.00
2022-05-25	2023-05-25	2023-05-25	400,000.00	−20,000.00
2023-05-25	2024-05-25	2024-05-27	300,000.00	−15,000.00
2024-05-25	2025-05-25	2025-05-26	200,000.00	−10,000.00
2025-05-25	2026-05-25	2026-05-25	100,000.00	−5,000.00

The natural hedge swap for an amortizing bond is again a fix versus float swap, but with the same amortizing notional structure as the bond (on both legs). Again, if the bond is callable, the hedge swap is made callable in the same way and the same remarks about the imperfectness of the hedge (and making it perfect by credit-linking it) apply. Table 2.9 displays the schedule of the fixed leg of the asset swap, and Table 2.10 the schedule of the floating leg, assuming an Euribor 6M index and a zero margin.

Concerning model calibration, similar remarks as in Sect. 1.3 apply; a suitable set of market instruments to calibrate the valuation model can be found by a Delta-Gamma best-matching approach (Andersen and Piterbarg 2010b, 19.4, Caspers 2013), or other matching methods as outlined in Andersen and Piterbarg (2010b), 19.4.4, 19.4.5.

We compute a best-matching calibration basket for the amortizing bond again following Andersen and Piterbarg (2010b), 19.4. Table 2.11 shows the

Table 2.10 Asset swap of an amortizing fix rate bond (zero margin), floating leg schedule, Euribor 6M rates are estimated on a flat forward curve @2%

Accrual start	Accrual end	Payment date	Notional	Payment
2016-05-25	2016-11-25	2016-11-25	1,000,000.00	10,133.19
2016-11-25	2017-05-25	2017-05-25	1,000,000.00	9,967.15
2017-05-25	2017-11-27	2017-11-27	900,000.00	9,219.50
2017-11-27	2018-05-25	2018-05-25	900,000.00	8,870.83
2018-05-25	2018-11-26	2018-11-26	800,000.00	8,150.83
2018-11-26	2019-05-27	2019-05-27	800,000.00	8,018.00
2019-05-27	2019-11-25	2019-11-25	700,000.00	7,015.75
2019-11-25	2020-05-25	2020-05-25	700,000.00	7,015.75
2020-05-25	2020-11-25	2020-11-25	600,000.00	6,079.91
2020-11-25	2021-05-25	2021-05-25	600,000.00	5,980.29
2021-05-25	2021-11-25	2021-11-25	500,000.00	5,066.59
2021-11-25	2022-05-25	2022-05-25	500,000.00	4,983.58
2022-05-25	2022-11-25	2022-11-25	400,000.00	4,053.28
2022-11-25	2023-05-25	2023-05-25	400,000.00	3,986.86
2023-05-25	2023-11-27	2023-11-27	300,000.00	3,073.17
2023-11-27	2024-05-27	2024-05-27	300,000.00	3,006.75
2024-05-27	2024-11-25	2024-11-25	200,000.00	2,004.50
2024-11-25	2025-05-26	2025-05-26	200,000.00	2,004.50
2025-05-26	2025-11-25	2025-11-25	100,000.00	1,007.78
2025-11-25	2026-05-25	2026-05-25	100,000.00	996.72

Table 2.11 Calibration basket for an amortizing bond, following the representative basket approach

Expiry	Maturity	Nominal	Strike
2017-05-18	2023-05-22	693,427.09	0.019946
2018-05-18	2023-10-23	620,913.74	0.019936
2019-05-20	2024-03-22	545,833.24	0.020013
2020-05-18	2024-08-20	472,931.84	0.019962
2021-05-18	2024-12-20	400,376.58	0.019953
2022-05-18	2025-05-20	327,004.67	0.019921
2023-05-18	2025-09-22	251,921.83	0.019884
2024-05-20	2026-01-22	173,156.94	0.020173
2025-05-19	2026-05-21	95,848.96	0.020133

result. The strike of the calibrating swaption is again close to 2% for all expiries. The maturity, however, for the first calibrating swaption is 3 years shorter than the bond's maturity, which is due to the decreasing notional over the lifetime of the bond. Likewise, the nominal is reduced. The same applies to the following calibrating swaptions, but to a lesser degree until the last swaption, which has its maturity date close to the bond maturity.

2.6 Callable Floater and Inverse Floater

A plain vanilla floating rate bond pays a Libor rate, plus possibly a spread, as the coupon. The accrual periods have the same tenor as the Libor rate itself, which in turn is fixed at the beginning of the period, usually a few business days before the accrual start date. We also call such a bond a floating rate note or floater for short.

The valuation of the floater is given by

$$V^{\text{Float Bond}} = N\left(\sum_{i=1}^{m} \tau_i (F_T(\tilde{T}_i, \tilde{T}_{i+1}) + s_i) DF_B(0, T_i) e^{-\lambda T_i} + DF_B(0, T_m) e^{-\lambda T_m}\right) \tag{2.1}$$

The natural hedge swap of a (callable) floater with price given by (2.1) would be a (callable) Libor against Libor swap, but with possibly different tenors and spreads on each of its legs. For example, an Euribor 1Y + 100bp floater may be hedged by a Euribor 1Y + 100bp against Euribor 6M + 212bp swap. Here, the margin on the Euribor 6M leg is determined by the tenor basis spread between Euribor 6M and Euribor 1Y and the credit spread of the bond, such that the package trades at par (assuming that a par asset swap is used for hedging).

The valuation of the hedge swap is given by

$$\begin{aligned} V^{\text{Float-Float Swap}} = & \sum_{i=1}^{n} \tilde{\tau}_i' (F_T(\tilde{T}_i', \tilde{T}_{i+1}') + s_i') DF_{\text{OIS}}(0, \tilde{T}_i') \\ & - \sum_{i=1}^{m} \tilde{\tau}_i (F_T(\tilde{T}_i, \tilde{T}_{i+1}) + s_i) DF_{\text{OIS}}(0, \tilde{T}_i) \end{aligned} \tag{2.2}$$

with m, n the number of coupon periods of the payer, resp. the receiver side of the swap, $\tilde{\tau}_i'$, $\tilde{\tau}_i$ the day count fractions of the coupons, T, T' the tenors of the two legs, $\tilde{T}_i'$, $\tilde{T}_i$ the index estimation start dates, $\tilde{T}_{i+1}'$, $\tilde{T}_{i+1}$ the index estimation end dates, s_i', s_i the spreads and T_i', T_i the payment times of the coupons.

At this point, it becomes particularly apparent that the plain hedge swap construction (without credit-linking) gives an imperfect hedge construction.

We illustrate the situation by looking at a 10-y floater paying half-yearly coupons at Euribor 6M + 300bp, which is callable yearly. Table 2.12 shows the estimated flows, and Table 2.13 the call schedule.

Table 2.14 shows the valuation of this floater. Looking at the effect of rate and volatility shifts in the model's interest rate and credit parameters, see Table 2.16,

Table 2.12 Euribor 6M floater schedule without the notional repayment at the end

Accrual start	Accrual end	Payment	Est. fixing (%)	Spread (%)	Est. amount
2016-05-25	2016-11-25	2016-11-25	1.9826	3.0000	25,466.52
2016-11-25	2017-05-25	2017-05-25	1.9824	3.0000	25,050.49
2017-05-25	2017-11-27	2017-11-27	1.9827	3.0000	25,743.89
2017-11-27	2018-05-25	2018-05-25	1.9825	3.0000	24,773.96
2018-05-25	2018-11-26	2018-11-26	1.9826	3.0000	25,605.21
2018-11-26	2019-05-27	2019-05-27	1.9825	3.0000	25,189.16
2019-05-27	2019-11-25	2019-11-25	1.9826	3.0000	25,189.71
2019-11-25	2020-05-25	2020-05-25	1.9825	3.0000	25,189.16
2020-05-25	2020-11-25	2020-11-25	1.9826	3.0000	25,466.52
2020-11-25	2021-05-25	2021-05-25	1.9824	3.0000	25,050.49
2021-05-25	2021-11-25	2021-11-25	1.9826	3.0000	25,466.52
2021-11-25	2022-05-25	2022-05-25	1.9824	3.0000	25,050.49
2022-05-25	2022-11-25	2022-11-25	1.9826	3.0000	25,466.52
2022-11-25	2023-05-25	2023-05-25	1.9824	3.0000	25,050.49
2023-05-25	2023-11-27	2023-11-27	1.9827	3.0000	25,743.89
2023-11-27	2024-05-27	2024-05-27	1.9825	3.0000	25,189.16
2024-05-27	2024-11-25	2024-11-25	1.9826	3.0000	25,189.71
2024-11-25	2025-05-26	2025-05-26	1.9825	3.0000	25,189.16
2025-05-26	2025-11-25	2025-11-25	1.9826	3.0000	25,328.12
2025-11-25	2026-05-25	2026-05-25	1.9824	3.0000	25,050.49

we see that both the interest rate level and the interest rate volatility have comparatively little impact on the valuation than the credit spread level and volatility. Table 2.15 shows the impact of the IR-CR correlation underlying's NPV: an increased correlation decreases the value of the float coupons.

It is interesting to look at the exercise region for a callable floater, see Fig. 2.2, and compare it to the corresponding picture for a callable fix bond, see Fig. 2.1. The interest rate level now has practically no impact on the exercise decision; it is solely driven by the credit spread level.

Finally, what would be a suitable calibration basket built from market swaptions? The answer is that there is not really a particularly appropriate one, since the call right in the floater does not have a significant sensitivity to the interest rate levels (it has sensitivity to the credit spread level, but regarding this the market instruments have no sensitivity on the other hand). This corresponds to the fact that there is no effective natural hedge for the callable floater.

It is market practice to just calibrate to a strip of ATM co-terminal swaptions to pick up the general market volatility in the model.

We should mention that the pay-off of a Libor floater is usually floored at an effective coupon rate of zero percent, so that negative coupon payments are avoided. This is not much of a difference if interest rates or the margin paid on top of the Libor fixing is sufficiently high, but for low interest rate markets and a low margin the embedded floor becomes a significant price driver. While

Table 2.13 Euribro 6M Floater call schedule, the settlement dates are chosen to be equal to the accrual start date of the first period that is part of the exercise right, the exercise date has a 5 business days (TARGET) notice period

Exercise date	Settlement date
2016-11-18	2016-11-25
2017-05-18	2017-05-25
2017-11-20	2017-11-27
2018-05-18	2018-05-25
2018-11-19	2018-11-26
2019-05-20	2019-05-27
2019-11-18	2019-11-25
2020-05-18	2020-05-25
2020-11-18	2020-11-25
2021-05-18	2021-05-25
2021-11-18	2021-11-25
2022-05-18	2022-05-25
2022-11-18	2022-11-25
2023-05-18	2023-05-25
2023-11-20	2023-11-27
2024-05-20	2024-05-27
2024-11-18	2024-11-25
2025-05-19	2025-05-26
2025-11-18	2025-11-25

Table 2.14 NPV of a callable floater

	NPV (EUR)	NPV (relative) (%)
Bond underlying	996,509.47	99.6509
Bond call option	−36,135.67	−3.6136
Callable bond total	960,373.81	96.0374

Table 2.15 NPV of a floating rate bond under different IR-CR correlations

	NPV (relative) (%)	NPV change (%)
IR-CR correlation 0	99.8909	0.0000
IR-CR correlation 0.5	99.6509	−0.2400
IR-CR correlation −0.5	100.1294	+0.2385

we ignored such a floor up to now, we go into more detail about this in the following, discussing inverse floaters.

An inverse floater has a similar pay-off as a vanilla floater, but it reverses the sign of the Libor part of the pay-off and typically introduces a multiplier. An example would be a pay-off of the form $9\% - 2 \cdot$ Euribor 6M, where the coupon is floored at 0% to avoid negative coupons in the floater.

Roughly assuming a fixing of 2% for the Euribor 6M one arrives at a coupon of 5%, just as in the case of the floater above.

Table 2.16 NPV of a callable floating rate bond under different model parameter scenarios and IR and CR rate shifts

	NPV (relative) (%)	NPV change (%)
Original parameters	96.0374	0.0000
IR rate level $+0.0010$	96.0529	$+0.0155$
CR spread level $+0.0010$	95.5608	-0.4766
IR volatility $+0.0010$	96.0100	-0.0274
CR volatility $+0.0010$	95.5631	-0.4743

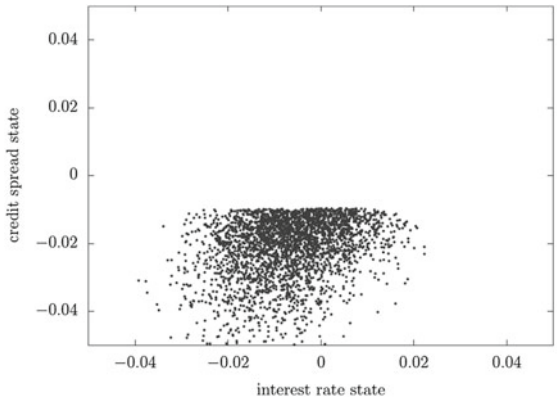

Fig. 2.2 Exercise region for 10th exercise date (2020-11-28) of a floating rate bond; exercise states are taken from the Monte Carlo simulation used for pricing

One interesting point in the pay-off is the embedded floor. Obviously, it is activated if Euribor 6M fixings exceeding 4.5%, that is the floored coupon rate can actually be understood as a long position in a 2% standard market cap from the bond's investors perspective. Table 2.17 shows an example of realized cashflows under simulated Euriobr 6M fixings. The embedded floors produce a pay-off for the accrual periods starting on 2022-05-25, 2022-11-25, 2023-11-27 and 2024-05-27.

From the valuation perspective, for a non-callable inverse floater, the embedded cap can be valued separately using the market Black76 formula. However, note that the discounting has to be done on the bond's benchmark curve with the credit spread added. The latter is also called the Asset Swap spread since it is tied to the bond.

If the inverse floater is callable, the situation gets more complicated. The model we used so far for interest rates, the LGM model, has not enough flexibility to be calibrated to both caplet smiles and a strip of co-terminal swaptions. Possible alternatives are models with local volatility like the Markov functional model, or a full Libor market model.

Table 2.17 Inverse floater schedule with a simulated series of fixings

Accrual start	Accrual end	Payment	Sim. fixing (%)	Spread (%)	Sim. amount
2016-05-25	2016-11-25	2016-11-25	1.9000	9.0000	26,577.78
2016-11-25	2017-05-25	2017-05-25	2.1000	9.0000	24,133.33
2017-05-25	2017-11-27	2017-11-27	2.5000	9.0000	20,666.67
2017-11-27	2018-05-25	2018-05-25	3.0000	9.0000	14,916.67
2018-05-25	2018-11-26	2018-11-26	3.1000	9.0000	14,388.89
2018-11-26	2019-05-27	2019-05-27	2.8000	9.0000	17,188.89
2019-05-27	2019-11-25	2019-11-25	3.5000	9.0000	10,111.11
2019-11-25	2020-05-25	2020-05-25	3.7000	9.0000	8,088.89
2020-05-25	2020-11-25	2020-11-25	3.9000	9.0000	6,133.33
2020-11-25	2021-05-25	2021-05-25	4.0000	9.0000	5,027.78
2021-05-25	2021-11-25	2021-11-25	3.8000	9.0000	7,155.56
2021-11-25	2022-05-25	2022-05-25	4.1000	9.0000	4,022.22
2022-05-25	2022-11-25	2022-11-25	4.6000	9.0000	0.00
2022-11-25	2023-05-25	2023-05-25	5.0000	9.0000	0.00
2023-05-25	2023-11-27	2023-11-27	4.3000	9.0000	2,066.67
2023-11-27	2024-05-27	2024-05-27	4.8000	9.0000	0.00
2024-05-27	2024-11-25	2024-11-25	4.5000	9.0000	0.00
2024-11-25	2025-05-26	2025-05-26	4.0000	9.0000	5,055.56
2025-05-26	2025-11-25	2025-11-25	3.9000	9.0000	6,100.00
2025-11-25	2026-05-25	2026-05-25	4.0000	9.0000	5,027.78

2.7 Zero Bonds, Callable Zeros and Accreting Swaps

A Zero Coupon Bond does not pay coupons during his lifetime but only the final capital. There are two types: the first paying a deterministic amount at maturity and the second a stochastic amount.

Although there are no coupon payments, it is useful to think of these bonds as coupon paying bonds with the coupons immediately reinvested in the bond again.

For example, consider a fixed rate bond with a notional of 1,000,000 USD paying a yearly coupon of 5% which is immediately reinvested in the notional of the bond. Table 2.18 shows the reinvested coupons in the nominal column as well as the actual, physical flow of the instrument at maturity. This is an example of a compounding zero bond.

Table 2.19 shows an equivalent bond, but with rescaled nominal, such that the final nominal corresponds to the notional of the bond. This is in contrast to the compounding zero bond where the initial notional equals the notional of the bond. This type of zero bond is called discounted zero bond.

In case the reinvested coupon is not deterministic that is not known in advance, as is the case for "Libor plus spread" coupons as the most basic

Table 2.18 Fixed rate compounded zero bond schedule, the only physical payment occurs at maturity

Accrual start	Accrual end	Payment	Nominal	Amount
2016-05-25	2017-05-25	2017-05-25	1,000,000.00	0.00
2017-05-25	2018-05-25	2018-05-25	1,050,000.00	0.00
2018-05-25	2019-05-25	2019-05-27	1,102,500.00	0.00
2019-05-25	2020-05-25	2020-05-25	1,157,625.00	0.00
2020-05-25	2021-05-25	2021-05-25	1,215,506.25	0.00
2021-05-25	2022-05-25	2022-05-25	1,276,281.56	0.00
2022-05-25	2023-05-25	2023-05-25	1,340,095.64	0.00
2023-05-25	2024-05-25	2024-05-27	1,407,100.42	0.00
2024-05-25	2025-05-25	2025-05-26	1,477,455.44	0.00
2025-05-25	2026-05-25	2026-05-25	1,551,328.22	1,628,894.63

Table 2.19 Fixed rate discounted zero bond schedule; the repayment at maturity is equal to the nominal of the bond

Accrual start	Accrual end	Payment	Nominal	Amount
2016-05-25	2017-05-25	2017-05-25	613,913.25	0.00
2017-05-25	2018-05-25	2018-05-25	644,608.91	0.00
2018-05-25	2019-05-25	2019-05-27	676,839.36	0.00
2019-05-25	2020-05-25	2020-05-25	710,681.33	0.00
2020-05-25	2021-05-25	2021-05-25	746,215.40	0.00
2021-05-25	2022-05-25	2022-05-25	783,526.16	0.00
2022-05-25	2023-05-25	2023-05-25	822,702.47	0.00
2023-05-25	2024-05-25	2024-05-27	863,837.60	0.00
2024-05-25	2025-05-25	2025-05-26	907,029.48	0.00
2025-05-25	2026-05-25	2026-05-25	952,380.95	1,000,000.00

example or for other structured coupons (for example CMS coupons, CMS spread coupons or PIK note coupons), only a compounding zero bond can be constructed. That is a zero bond with unknown final notional to be paid back. Table 2.20 shows an example with simulated fixings, based on a coupon of Euribor 6M plus 300 basis points spread.

Callability of zero bonds has the same mechanics as for fixed rate bonds, but the notional be paid back if the early redemption right is exercised follows a non-constant schedule. Usually, this is equal to the current accreted nominal. Table 2.23 shows an example corresponding to the zero bond shown in Table 2.18.

The natural hedge instrument of a (callable) zero bond is a (callable) accreting swap, which exchanges the virtual coupon of the zero bond, but this time as a physical payment in the swap, against an Libor plus spread coupon. In

Table 2.20 Floating zero bond schedule with simulated fixings

Accrual start	Accrual end	Payment	Sim. fixing (%)	Spread (%)	Sim. nominal	Sim. amount
2016-05-25	2016-11-25	2016-11-25	1.9000	3.0000	1,000,000.00	0.0
2016-11-25	2017-05-25	2017-05-25	2.1000	3.0000	1,025,044.44	0.0
2017-05-25	2017-11-27	2017-11-27	2.5000	3.0000	1,051,328.29	0.0
2017-11-27	2018-05-25	2018-05-25	3.0000	3.0000	1,081,203.54	0.0
2018-05-25	2018-11-26	2018-11-26	3.1000	3.0000	1,113,459.44	0.0
2018-11-26	2019-05-27	2019-05-27	2.8000	3.0000	1,148,363.30	0.0
2019-05-27	2019-11-25	2019-11-25	3.5000	3.0000	1,182,035.87	0.0
2019-11-25	2020-05-25	2020-05-25	3.7000	3.0000	1,220,878.88	0.0
2020-05-25	2020-11-25	2020-11-25	3.9000	3.0000	1,262,232.76	0.0
2020-11-25	2021-05-25	2021-05-25	4.0000	3.0000	1,306,747.50	0.0
2021-05-25	2021-11-25	2021-11-25	3.8000	3.0000	1,352,737.76	0.0
2021-11-25	2022-05-25	2022-05-25	4.1000	3.0000	1,399,752.91	0.0
2022-05-25	2022-11-25	2022-11-25	4.6000	3.0000	1,449,720.20	0.0
2022-11-25	2023-05-25	2023-05-25	5.0000	3.0000	1,506,033.77	0.0
2023-05-25	2023-11-27	2023-11-27	4.3000	3.0000	1,566,609.80	0.0
2023-11-27	2024-05-27	2024-05-27	4.8000	3.0000	1,625,697.10	0.0
2024-05-27	2024-11-25	2024-11-25	4.5000	3.0000	1,689,803.75	0.0
2024-11-25	2025-05-26	2025-05-26	4.0000	3.0000	1,753,875.48	0.0
2025-05-26	2025-11-25	2025-11-25	3.9000	3.0000	1,815,943.18	0.0
2025-11-25	2026-05-25	2026-05-25	4.0000	3.0000	1,879,637.39	0.0
		2026-05-25				1,945,790.19

Table 2.21 Asset swap for fixed rate compounded zero bond schedule, fixed leg

Accrual start	Accrual end	Payment	Nominal	Amount
2016-05-25	2017-05-25	2017-05-25	1,000,000.00	50,000.00
2017-05-25	2018-05-25	2018-05-25	1,050,000.00	52,500.00
2018-05-25	2019-05-25	2019-05-27	1,102,500.00	55,125.00
2019-05-25	2020-05-25	2020-05-25	1,157,625.00	57,881.25
2020-05-25	2021-05-25	2021-05-25	1,215,506.25	60,775.31
2021-05-25	2022-05-25	2022-05-25	1,276,281.56	63,814.08
2022-05-25	2023-05-25	2023-05-25	1,340,095.64	67,004.78
2023-05-25	2024-05-25	2024-05-27	1,407,100.42	70,355.02
2024-05-25	2025-05-25	2025-05-26	1,477,455.44	73,872.77
2025-05-25	2026-05-25	2026-05-25	1,551,328.22	77,566.41

addition, the notional of the swap is not constant, but increases by each virtual coupon. Tables 2.21 and 2.22 show the schedules of the legs of such an asset swap.

Finally, the representative basket method can be applied here as well to determine a calibration basket. Table 2.24 lists the calibration instruments for the callable zero bond given by Tables 2.18 and 2.23. We observe that the strike

Table 2.22 Asset swap for fixed rate compounded zero bond schedule, floating leg (amount is estimated on a flat 2%) forward curve

Accrual start	Accrual end	Payment	Nominal	Est. amount
2016-05-25	2016-11-25	2016-11-25	1,000,000.00	9,711.11
2016-11-25	2017-05-25	2017-05-25	1,000,000.00	10,558.33
2017-05-25	2017-11-27	2017-11-27	1,050,000.00	13,562.50
2017-11-27	2018-05-25	2018-05-25	1,050,000.00	15,662.50
2018-05-25	2018-11-26	2018-11-26	1,102,500.00	17,563.44
2018-11-26	2019-05-27	2019-05-27	1,102,500.00	15,606.50
2019-05-27	2019-11-25	2019-11-25	1,157,625.00	20,483.53
2019-11-25	2020-05-25	2020-05-25	1,157,625.00	21,654.02
2020-05-25	2020-11-25	2020-11-25	1,215,506.25	24,229.09
2020-11-25	2021-05-25	2021-05-25	1,215,506.25	24,445.18
2021-05-25	2021-11-25	2021-11-25	1,276,281.56	24,788.22
2021-11-25	2022-05-25	2022-05-25	1,276,281.56	26,309.13
2022-05-25	2022-11-25	2022-11-25	1,340,095.64	31,507.14
2022-11-25	2023-05-25	2023-05-25	1,340,095.64	33,688.52
2023-05-25	2023-11-27	2023-11-27	1,407,100.42	31,261.08
2023-11-27	2024-05-27	2024-05-27	1,407,100.42	34,145.64
2024-05-27	2024-11-25	2024-11-25	1,477,455.44	33,612.11
2024-11-25	2025-05-26	2025-05-26	1,477,455.44	29,877.43
2025-05-26	2025-11-25	2025-11-25	1,551,328.22	30,755.08
2025-11-25	2026-05-25	2026-05-25	1,551,328.22	31,198.93

Table 2.23 Zero fix compounded call schedule, the exercise amount is equal to the compounded nominal schedule, the exercise date is chosen to have a notice period of 5 business days (TARGET) before the settlement date

Exercise date	Settlement date	Exercise amount
2017-05-18	2017-05-25	1,050,000.00
2018-05-18	2018-05-25	1,102,500.00
2019-05-20	2019-05-27	1,157,625.00
2020-05-18	2020-05-25	1,215,506.25
2021-05-18	2021-05-25	1,276,281.56
2022-05-18	2022-05-25	1,340,095.64
2023-05-18	2023-05-25	1,407,100.42
2024-05-20	2024-05-27	1,477,455.44
2025-05-19	2025-05-26	1,551,328.22

is again, and expected close to 2% for all calibrating instruments, while the notional increases over the lifetime and the maturity decreases starting from a date beyond the maturity of the zero bond for the first calibration instruments, matching the maturity for the last (two) calibration instruments.

Table 2.24 Zero fix compounded calibration basket, following the representative basket approach

Expiry	Maturity	Nominal	Strike
2017-05-18	2026-08-24	1,096,497.57	0.019967
2018-05-18	2026-08-24	1,143,772.29	0.019964
2019-05-20	2026-07-22	1,191,195.80	0.019999
2020-05-18	2026-07-20	1,242,027.65	0.019969
2021-05-18	2026-06-22	1,294,664.97	0.019970
2022-05-18	2026-06-22	1,348,914.20	0.019969
2023-05-18	2026-06-22	1,409,093.35	0.019962
2024-05-20	2026-05-22	1,455,776.38	0.020127
2025-05-19	2026-05-21	1,487,009.51	0.020133

2.8 Conclusion and Summary

In this section, we introduced callability as an important exotic feature that is often added to bonds and swaps, typically in the form of multiple ("Bermudan") call rights. We gave valuation examples and explain how different model parameters influence the pricing of the call option of a bond. We explained the asset swap construction for callable bonds via callable swaps and go into some detail about how a model can be calibrated to liquid vanilla market options representing the bond's call right as suitable as possible. We covered callable fixed rate bonds as well as amortizing structures, floater and zero bonds as the corresponding asset swaps.

References

Andersen, L., & Piterbarg, V. (2010a). *Interest rate modeling—Volume I: Foundations and vanilla models*. London: Atlantic Financial Press.

Andersen, L., & Piterbarg, V. (2010b). *Interest rate modeling—Volume III: Products and risk management*. London: Atlantic Financial Press.

Caspers P. (2013). Representative basket method applied. *SSRN*. Retrieved from http://www.papers.ssrn.com/sol3/papers.cfm?abstract_id=2320759.

Lichters, R., Stamm, R., & Gallagher, D. (2015). *Modern derivatives pricing and credit exposure analysis—Theory and practice of CSA and XVA pricing. Exposure simulation and backtesting*. Basingstoke: Palgrave McMillan.

3

Structured Finance

3.1 Introduction and Objectives

Loans and loan-like instruments in structured finance are often structured in a similar way as bonds. They often contain call rights for example. However, these call rights are less standardized typically in structured finance, and other optionalities may be present that do not usually appear in structured bonds at all. In this chapter, we describe these specialities and give some valuation examples.

3.2 Redemption Amount Variations

In the case of bonds, we assumed that on an early redemption date the whole notional is paid back. In structured finance it is common to have the right of paying back only a part of the notional, and possibly other portions on later exercise dates or only at maturity. It is also possible that an upper bound for this ratio is applied for a certain period. For example, only 10% of a structured investment may be callable within the first two years, and the full amount only after that period.

In terms of valuation, this variation can be handled by slicing the loan into several layers representing the different redemption terms. As an example, consider a 1,000,000 EUR loan paying annual fixed coupons at 5% for 10 years. Assume that 10% of the notional may be redeemed after 1 and 2 years

© The Author(s) 2017

J. Kienitz and P. Caspers, *Interest Rate Derivatives Explained: Volume 2*,
Financial Engineering Explained, DOI 10.1057/978-1-137-36019-9_3

and after that the whole remaining notional is eligible for redemption on a yearly basis until maturity. This gives rise to two layers:

- The first layer has size 100,000 EUR, which is 10% of the total notional. This layer is equipped with a yearly call right after 1, 2, . . . , 9 years.
- The second layer has size 900,000 EUR and is callable only in the third year for the first time and after that on a yearly basis.

For both layers we compute the value of the call option, and their sum is the value of the call option for the whole bond. At first sight this approach may look problematic since the exercise decision after 3 years onwards seemed to be decoupled for both layers, while the actual callability terms require the redemption of either 1, 000, 000 EUR (if the 10% portion was not called within the first 2 years) or 900, 000 EUR (if the 10% portion was called in the first or second year). However, one can verify that either the full notional is redeemed on one of the exercise dates in years 3, . . . , 9 or the 10% portion is called within the first 2 years by looking at an actual valuation scheme. The decision to exercise the call right on a path is made first for year 9 and coincides for both layers. Then, the decision for year 8 is made using the expected value of the exercise option of year 9, again, this leads to an identical decision in year 8. This scheme is continued until year 3. As seen from the third year's exercise date, both layers are still called exactly on the same paths. Only if the exercise in the second (and after that in the first) year of the first layer is more favourable than exercising from the third year on, the 10% portion is called within the first 2 years, differently from the second layer, but this is of course in line with the callability terms stated above.

Apart from this slicing, there may be certain penalties associated with the execution of the call right: It may, for example, be specified that on a call date, if exercised, 102% of the notional has to be paid back instead of 100%. This increased amount reduces the value of the early exercise option. These penalties might themselves have a schedule, that is within the first 2 years a redemption price of 102% applies, for years three and four 101% and after that the par value of 100% has to be paid back.

Since the redemption value stays deterministic at this stage this does not cause any complication in the valuation procedure—instead of the notional the notional times a multiplier has to be taken into account in the exercise decision.

This becomes different if instead of a predefined factor times the notional a stochastic amount is paid back on exercise. In case of whole redemption rights the present value of certain future payments on the exercise date is part of the

redemption value. There are many variants to this; two typical cases for the determination of the redemption amount are:

1. The notional (times a factor) plus the present value of outstanding coupons; sometimes only coupons in a certain "phase" of the loan are considered in this present value in addition.
2. The present value of outstanding coupons plus the present value of outstanding notional payments, possibly this value is floored by the outstanding notional on exercise times a factor.

To complicate things further, the present value of coupon and notional payments is usually not computed on the model's valuation curve, but on a curve explicitly specified in the terms of the loan.

3.3 Draw Down Options

It may happen that the notional amount is not paid to the issuer in full, but that parts of the notionals are paid only at later dates during the lifetime of the investments. These payments may follow a predefined schedule, but they can also constitute an option that the issuer holds. They may or may not draw portions of the notional at certain future exercise dates.

This kind of option is similar to early exercise options, but is always exercised by the issuer in exactly opposite conditions compared to the former. For instance, in a fixed rate structure it is attractive to draw amounts when rates are high or the issuer's credit level is high. In this situation, a new issue would be more expensive than under the original conditions, so it may be favourable to exercise the draw option at such a date. Like an early redemption right the draw option can be European, or more commonly Bermudan/American. If at the same time early redemption rights are present in the structure, the exercise of the draw option generates the early exercise option: Only if an amount is drawn it can be paid back early, that is an early redemption right comes into existence only when the draw options are exercised. Therefore, it might be favourable to exercise a draw option although the exercise alone has a negative value to the issuer, because the generated early redemption option has a positive value and the sum of both is still positive. This reasoning only works in a pure valuation context. We have already remarked that other considerations are likely to drive the decision whether to draw a certain portion of the notional or not (Table 3.1).

Table 3.1 NPV of a draw option, 1,000,000.00 EUR can be drawn yearly, after being drawn the notional is then yearly callable

	NPV (EUR)	NPV (relative) (%)
Draw option	−63, 474.76	−6.3475

Table 3.1 shows the valuation of a draw option on 1,000,000.00 EUR open notional with a coupon schedule as in Table 1.1 and an early redemption schedule as in Table 2.1 which we assume to be the schedule for the draw option at the same time. The benchmark discounting curve is 2% flat, and the OAS is 3% as before. The call option alone was worth −4.9783%, see Table 2.2, so the draw option adds another 1.3% of value to it.

3.4 PIK Options and Capital Deferral Options

Payment in kind coupons and deferred amortization payments refer to the option to defer a coupon or a nominal amortization payment until the maturity of a trade. Clearly, these options constitute a positive value to the issuer: If, for example, the credit spread is so high that the funding of the current coupon payment is more expensive than the coupon rate of the investment itself, they choose to include this payment into the notional. From a valuation point of view, this means that the discounted later coupon payment is less (for example, due to high credit spreads) than the coupon amount to be paid now.

Note that the deferral of a payment does not mean that this works without paying interest on this deferred amount, as it is paid on the usual notional of the loan. This can also be understood as reinvesting the deferred payment amount into the loan's notional. In addition it may also be the case that the exercise of a deferral option is coupled with the payment of an additional penalty fee on top of that.

As in the case of draw options, also payment in kind coupons and deferred amortization payments interact with the early exercise option in the following ways:

1. The exercise value of a payment in kind coupon option depends on the value of future early exercise rights and future payment in kind coupon options since both affect the continuation value of one unit of notional of the bond into which the deferred payment is invested.

Table 3.2 NPV of a PIK option, all coupons of the bond are eligible for deferral

	NPV (EUR)	NPV (relative) (%)
Bond underlying	989, 684.46	98.9684
PIK option	−16, 211.93	−1.6212
Bond total	973, 472.53	97.3473

2. The early redemption decision must take into account both the continuation value of future early exercise rights and payment in kind coupon options, plus a payoff from a payment in kind coupon option on the same date as the exercise, if any.

Table 3.2 gives the value of a payment in kind option for the fix bond example given before in Table 1.1, again valued on a benchmarking curve at 2% flat and an OAS of 3%.

3.5 Tenor Options

In a Libor-based floating rate loan, the issuer often has the option to choose the underlying index tenor and—connected to this—the payment frequency of the coupons. For example, they might choose between paying monthly Libor 1M fixing (plus a spread s) or quarterly Libor 3M fixing (plus the same (!) spread s) or semiannual Libor 6M fixings (plus s).

If one assumes that under all usual circumstances the tenor basis between 1M, 3M and 3M, 6M is positive respectively, from a pure valuation viewpoint, the issuer should almost always choose the Libor 1M index as the basis for their coupon payments and the tenor option does actually have only a small value. There are situations where the basis might get negative for a short period of time, but we exclude this possibility for the discussion here. With a small basis near zero, it might be favourable also from the valuation perspective to choose a larger tenor because of the later payment time of the coupon.

If on the other hand one considers liquidity constraints or costs associated with the different tenors in the valuation model, this leads to a completely different type of valuation model which is beyond the scope of this book, see also Sect. 3.6.

3.6 Behavioural Models

In Sect. 2.2, we already mentioned that liquidity considerations may influence option exercise decisions regardless of the pure economical viewpoint of our valuation model. Thus, we need to take into account this behaviour. This demands for a behavioural model. In the field of structured finance this remark applies in a particular strong way since the repayment of a loan is tightly coupled to the project progress and cash flows produced in each project phase. Therefore, it may be desirable to use a model that accounts for such variables and not purely relies on the economic value of exercise decisions; recall, for example, Sect. 3.5. The downside of this approach is that it is unlikely that such a model can be calibrated on observable market variables. Instead a lot of case-specific expert judgement enters into the model which therefore provides a rather subjective view on the valuation of the transaction.

3.7 Conclusion and Summary

In this section we explained the typical features occurring in structured finance deals. This included deferred payment options that are applicable both to coupons and amortizing notional payments, draw options which represent the issuer's right to draw down additional notional and variations of redemption right terms like the whole valuation of outstanding coupons and capital payments. We explained how these optional components interact with each other, which poses an extra challenge to the valuation procedure and give valuation examples for all such features.

4

More Exotic Features and Basis Risk Hedging

4.1 Introduction and Objectives

In this chapter we discuss a number of additional exotic features beyond callability. Most of the features can be combined among each other and also with callability. We then conclude the product part with a brief overview on basis products.

4.2 TaRNs and TaRN Swaps

In the previous sections we have seen that callable structures allow for higher coupon payments due to the embedded call option sold implicitly by the investor to the issuer. Target redemption notes (TaRNs) exhibit a similar feature, but the rule for the termination of the structure is simply determined by the already realized coupon payments: As soon as the sum of the coupon payments reaches a predefined target level, the notional together with the last coupon triggering the termination is paid back to the investor. This feature bears a positive value for the issuer, this is like callability.

To explain this further, consider a note that pays 2% – Euribor 6M, floored at zero, with start date on 25 May 2016 and a maturity of 10y. The note is terminated early when a target coupon of 10% of the notional is accumulated. Assume also that the issuer's credit quality would allow him or her to issue a floater paying Euribor 6M flat coupons. If the Euribor 6M fixings are near zero at the issue date and remain at this level for a while, the note terminates shortly after 5y and, then have paid coupons all near 2%, which would be a highly attractive scenario for the investor compared to the income generated

© The Author(s) 2017

J. Kienitz and P. Caspers, *Interest Rate Derivatives Explained: Volume 2*,
Financial Engineering Explained, DOI 10.1057/978-1-137-36019-9_4

Table 4.1 Example TaRN payments in Scenario 1, the investor receives high coupons, but the note is terminated after 5.5 years

Accrual start	Accrual end	Payment	Sim. fixing (%)	Sim. amount	Acc. amount (%)
2016-05-25	2016-11-25	2016-11-25	0.0005	9,966.67	0.0100
2016-11-25	2017-05-25	2017-05-25	0.0010	9,552.78	0.0195
2017-05-25	2017-11-27	2017-11-27	0.0012	9,713.33	0.0292
2017-11-27	2018-05-25	2018-05-25	0.0020	8,950.00	0.0382
2018-05-25	2018-11-26	2018-11-26	0.0018	9,352.78	0.0475
2018-11-26	2019-05-27	2019-05-27	0.0030	8,594.44	0.0561
2019-05-27	2019-11-25	2019-11-25	0.0025	8,847.22	0.0650
2019-11-25	2020-05-25	2020-05-25	0.0020	9,100.00	0.0741
2020-05-25	2020-11-25	2020-11-25	0.0010	9,711.11	0.0838
2020-11-25	2021-05-25	2021-05-25	0.0015	9,301.39	0.0931
2021-05-25	2021-11-25	2021-11-25	0.0018	9,302.22	0.1024
		2021-11-25		1,000,000.00	

by the vanilla floater. Yet the total coupon that might be received is bounded by definition of the payoff and the note is already terminated after about the half of its original maturity in this scenario. See Table 4.1 for a sample payment schedule in this scenario.

On the other hand, there is the chance that Euribor rates rise over the lifetime of the note, such that the investor might even end up receiving zero coupon payments from a certain point on, but this time for the whole original lifetime of the underlying inversed floater; see Table 4.2 for a sample payment schedule in this scenario. Thus, the lifetime of the underlying is cut in scenarios that are fortunate from the investors point of view, but not in adverse scenarios. This constitutes a positive net present value for the issuer.

In general, the value at $t = 0$ of a TaRN can be written as

$$V^{\mathrm{TaRn}} = \mathrm{Nom} \cdot N(0) \cdot \mathrm{E}^N \left(\sum_{i=1}^{n} \frac{1_{\{A_i < \Lambda\}} \cdot \tilde{\tau}_i \cdot C_i(\omega) + 1_{\{A_{i-1} < \Lambda\}} 1_{\{A_i \geq \Lambda\}}}{N(\tilde{T}_i, \omega)} S(\tilde{T}_i, \omega) \right) \quad (4.1)$$

In Eq. (4.1), $N(T_i, \omega)$ is the numeraire at time $\tilde{T}_i$ and $S(\tilde{T}_i, \omega)$ is the survival probability up to time $\tilde{T}_i$ and we take the expectation E^N in the measure associated to the numeraire N. Specifically, if we choose the LGM Rates–Credit model described in Chap. 10, these quantities are given by formulas (10.8) and (10.11), respectively.

We write $A_i = \sum_{j=1}^{i-1} \tilde{\tau}_i C_i$ for the accumulated coupon before the ith coupon payment; Nom for the notional of the note; $\tilde{T}_i$ for the payment time

Table 4.2 Example TaRN payments in Scenario 2, the investor receives low coupons, and the note runs until its original maturity

Accrual start	Accrual end	Payment	Sim. fixing (%)	Sim. amt.	Acc amt. (%)
2016-05-25	2016-11-25	2016-11-25	0.0050	7,666.67	0.0077
2016-11-25	2017-05-25	2017-05-25	0.0120	4,022.22	0.0117
2017-05-25	2017-11-27	2017-11-27	0.0130	3,616.67	0.0153
2017-11-27	2018-05-25	2018-05-25	0.0150	2,486.11	0.0178
2018-05-25	2018-11-26	2018-11-26	0.0160	2,055.56	0.0198
2018-11-26	2019-05-27	2019-05-27	0.0130	3,538.89	0.0234
2019-05-27	2019-11-25	2019-11-25	0.0140	3,033.33	0.0264
2019-11-25	2020-05-25	2020-05-25	0.0160	2,022.22	0.0284
2020-05-25	2020-11-25	2020-11-25	0.0180	1,022.22	0.0295
2020-11-25	2021-05-25	2021-05-25	0.0210	0.00	0.0295
2021-05-25	2021-11-25	2021-11-25	0.0220	0.00	0.0295
2021-11-25	2022-05-25	2022-05-25	0.0200	0.00	0.0295
2022-05-25	2022-11-25	2022-11-25	0.0190	511.11	0.0300
2022-11-25	2023-05-25	2023-05-25	0.0220	0.00	0.0300
2023-05-25	2023-11-27	2023-11-27	0.0240	0.00	0.0300
2023-11-27	2024-05-27	2024-05-27	0.0260	0.00	0.0300
2024-05-27	2024-11-25	2024-11-25	0.0240	0.00	0.0300
2024-11-25	2025-05-26	2025-05-26	0.0230	0.00	0.0300
2025-05-26	2025-11-25	2025-11-25	0.0250	0.00	0.0300
2025-11-25	2026-05-25	2026-05-25	0.0230	0.00	0.0300
		2026-05-25		1,000,000.00	

of the ith coupon; τ_i for the applicable day count fraction for that coupon period, C_i for the structured coupon amount and Λ for the target level.

The structured coupon C_i can be any floating rate coupon, as simple as a plain Ibor rate, possibly plus spread, but also inverse Ibor coupons with capped/floored rate and straight or inverse CMS or CMS spread coupons, for instance the ones we have listed in Sect. 4.6. The coupon is usually fixed a few days before its payment date.

As in other structures, the first or the first few coupons in a TaRN note might be deterministic and relatively high, generating an attractive short-term income to the investor, which is compensated by a lower net present value of the remaining structure.

TaRNs, as other structured bonds, are hedged with swaps exchanging the structured coupon payments against an Ibor plus spread payment and terminating by the same rule as the note. A TaRN asset swap package is therefore equivalent to a floater with stochastic termination date. The last feature may be relevant from the viewpoint of liquidity management.

There are variations to the terminating condition which cap the last coupon payment such that the total target T is hit exactly, or also exclude the coupon payment triggering the termination.

Finally, target redemption triggers can be put on top of other structures, for example, there might be callable snowball bonds (see Sect. 4.3) with TaRN feature, that work just like the underlying structure, but adding a termination event based on the accumulated coupon of the underlying structure.

The valuation of a TaRN requires a model that captures the joint distribution of the coupon payments appropriately. For example, the valuation of a TaRN on an inversed Ibor coupon floored at zero would at best require a model that is able to reproduce the current market's perception of both

1. the caplet/floorlet smile for expiries equal to one of the fixing dates of the structured coupon and
2. the copula, see Kienitz (2014) for instance where it is shown how to connect the marginal distributions of the Ibor rates corresponding to these smiles.

The sensitivity on the smile involves the whole strike range, since the termination indicator corresponds to a digital option with different possible strikes depending on the distance $T - A_i$ of the already accumulated coupon to the target. In addition the smile sensitivity is significant in general because of this digital feature. While smiles are available for the major currencies, there are no quoted vanilla options from which the copula could be derived, which induces a high degree of model risk in the valuation of TaRN structures.

In terms of numerical procedures, a TaRN valuation can be done straightforward with a forward scheme (like Monte Carlo) combined with a Longstaff–Schwartz regression if call rights are also present. Backward schemes (like backward PDEs) are also possible though. To apply them, the accumulated coupon has to be modelled as an additional state variable.

4.3 Snowballs

A snowball note pays coupons defined by a recursive formula, for example, $C_1 = 7\%$, and for the other coupons

$$C_n = \max(\min(C_{n-1} + 3\% - 2 \cdot L_n, 10\%), 0\%), \tag{4.2}$$

where L_n is a Libor rate, fixed in the usual way at the beginning of the nth coupon period. Other structured coupon types like CMS or CMS spread are possible as well and can replace the Libor rate in (4.2). Table 4.3 shows an

Table 4.3 Snowball note schedule with simulated fixings, the average coupon paid is 5.03%

Accrual start	Accrual end	Payment	Sim. fixing (%)	Sim. coupon (%)	Sim. amount
2016-05-25	2016-11-25	2016-11-25	1.9000	7.0000	35,777.78
2016-11-25	2017-05-25	2017-05-25	2.1000	9.1500	46,004.17
2017-05-25	2017-11-27	2017-11-27	2.5000	10.0000	51,666.67
2017-11-27	2018-05-25	2018-05-25	3.0000	10.0000	49,722.22
2018-05-25	2018-11-26	2018-11-26	3.1000	10.0000	51,388.89
2018-11-26	2019-05-27	2019-05-27	2.8000	10.0000	50,555.56
2019-05-27	2019-11-25	2019-11-25	3.5000	10.0000	50,555.56
2019-11-25	2020-05-25	2020-05-25	3.7000	9.7500	49,291.67
2020-05-25	2020-11-25	2020-11-25	3.9000	9.2000	47,022.22
2020-11-25	2021-05-25	2021-05-25	4.0000	8.3500	41,981.94
2021-05-25	2021-11-25	2021-11-25	3.8000	7.3500	37,566.67
2021-11-25	2022-05-25	2022-05-25	4.1000	6.6500	33,434.72
2022-05-25	2022-11-25	2022-11-25	4.6000	5.5000	28,111.11
2022-11-25	2023-05-25	2023-05-25	5.0000	3.6000	18,100.00
2023-05-25	2023-11-27	2023-11-27	4.3000	1.1000	5,683.33
2023-11-27	2024-05-27	2024-05-27	4.8000	0.0000	0.00
2024-05-27	2024-11-25	2024-11-25	4.5000	0.0000	0.00
2024-11-25	2025-05-26	2025-05-26	4.0000	0.0000	0.00
2025-05-26	2025-11-25	2025-11-25	3.9000	0.0000	0.00
2025-11-25	2026-05-25	2026-05-25	4.0000	0.0000	0.00
		2026-05-25			1,000,000.00

example schedule. Note the relatively high coupons paid at the beginning of the structure and how they decrease, so that in the last 2.5 years even zero coupons are paid. The average coupon being paid in this coupon is 5.03%.

The valuation formula for a snowball using our usual notation is given by using the notation $\tilde{T}$ for specifying the dates for a floating-based time schedule:

$$V^{\text{Snowball}} = \text{Nom} \cdot N(0) \cdot \mathbb{E}^N \left(\sum_{i=1}^{m} \tilde{\tau}_i \frac{C_i(\omega) S(\tilde{T}_i, \omega)}{N(\tilde{T}_i, \omega)} + \frac{S(\tilde{T}_m, \omega)}{N(\tilde{T}_m, \omega)} \right). \tag{4.3}$$

The expectation has to be calculated with regard to the numeraire which is denoted by N here. As explained in Sect. 4.2, the snowball feature can be combined with callability. The hedge swap is constructed in the obvious way, exchanging the structured snowball coupons against a Libor plus spread leg.

Relevant calibration instruments are given by the coupon's underlying rate(s) smiles at each fixing date of the structure, that is in the example above caplet

smiles on the underlying Libor rate on each of the note's fixing dates. Furthermore, similar to Sect. 4.2, the common distribution of these rates that is the copula between the marginal rate distribution determines the structure value.

4.4 Range Accruals

A range accrual note pays coupons C_i like the notes described in the previous sections, that is a fixed rate coupon or a coupon based on a floating rate like Libor or CMS, etc. However, the coupon rate is multiplied by a factor. This factor is computed as the number of business days on which a certain condition, *cond*, is met. This could be with respect to another floating rate F. The number of days are divided by all business days in the period. The latter condition could for example be that "the CMS 1Y fixing is between 2.25 % and 2.75 %".

$$V^{\text{Range Note}} = \text{Nom} \cdot N(0) \cdot \mathbb{E}^N \Big(\sum_{i=1}^{m} \frac{\tilde{\tau}_i C_i(\omega) S(\tilde{T}_i, \omega)}{N(\tilde{T}_i, \omega)} \cdot \frac{|\{d \in [\tilde{T}_i, \tilde{T}_{i+1}] | \text{cond}(d) \text{ true}\}|}{|\{d \in [\tilde{T}_i, \tilde{T}_{i+1}]\}|} \tag{4.4}$$

$$+ \frac{S(\tilde{T}_m, \omega)}{N(\tilde{T}_m, \omega)} \Big). \tag{4.5}$$

Suppose for example the payoff of a plain floater Euribor 3M + 300 basis points, and consider the single quarterly coupon period in Table 4.4. The plain coupon determined by the fixing (3% in this example) is multiplied by 22/67 because the whole coupon period contains 67 business days (with respect to the TARGET calendar in this case) and for 22 of them the reference fixing CMS 1Y meets the range condition given above, see Table 4.5 for how these 22 hits might occur within this period.

The hedge swaps for range accruals are again constructed in the usual way, and it is perfectly possible to combine the range feature with callability.

Table 4.4 Single coupon period taken from a range accrual structure

Accrual start	Accrual end	Payment	Sim. fixing (%)	Spread (%)	Hits	Days	Amount
2017-05-25	2017-08-25	2017-08-25	3	3	22	67	1,678.28

Table 4.5 Range condition hit counting for each business day in the coupon period, with simulated fixings

Date	Fixing (%)	Cnt	Date	Fixing (%)	Cnt	Date	Fixing (%)	Cnt
2017-05-25	2.47	1	2017-06-27	2.27	18	2017-07-28	1.52	22
2017-05-26	2.55	2	2017-06-28	2.36	19	2017-07-31	1.44	22
2017-05-29	2.72	3	2017-06-29	2.52	20	2017-08-01	1.43	22
2017-05-30	2.63	4	2017-06-30	2.44	21	2017-08-02	1.30	22
2017-05-31	2.69	5	2017-07-03	2.12	21	2017-08-03	1.38	22
2017-06-01	2.76	5	2017-07-04	2.03	21	2017-08-04	1.41	22
2017-06-02	2.79	5	2017-07-05	2.27	22	2017-08-07	1.32	22
2017-06-05	2.81	5	2017-07-06	2.18	22	2017-08-08	1.29	22
2017-06-06	2.71	6	2017-07-07	2.21	22	2017-08-09	1.30	22
2017-06-07	2.70	7	2017-07-10	2.16	22	2017-08-10	1.51	22
2017-06-08	2.60	8	2017-07-11	2.19	22	2017-08-11	1.53	22
2017-06-09	2.47	9	2017-07-12	2.20	22	2017-08-14	1.53	22
2017-06-12	2.31	10	2017-07-13	1.95	22	2017-08-15	1.36	22
2017-06-13	2.30	11	2017-07-14	1.93	22	2017-08-16	1.47	22
2017-06-14	2.41	12	2017-07-17	1.73	22	2017-08-17	1.49	22
2017-06-15	2.37	13	2017-07-18	1.68	22	2017-08-18	1.54	22
2017-06-16	2.40	14	2017-07-19	1.69	22	2017-08-21	1.44	22
2017-06-19	2.29	15	2017-07-20	1.71	22	2017-08-22	1.43	22
2017-06-20	2.34	16	2017-07-21	1.69	22	2017-08-23	1.28	22
2017-06-21	2.38	17	2017-07-24	1.58	22	2017-08-24	1.06	22
2017-06-22	2.18	17	2017-07-25	1.41	22	2017-08-25	1.22	22
2017-06-23	2.02	17	2017-07-26	1.36	22			
2017-06-26	2.21	17	2017-07-27	1.55	22			

If the underlying coupon is fixed, a range accrual coupon is the sum of plain digital options on the reference rate. In this case (and in absence of callability), it is possible to price the note with the usual methods for digital options, like computing a call spread on the reference rate's smile. Otherwise, that is if the underlying coupon is itself floating, the reference rate's smile is obviously a candidate to calibrate a full-term structure model. In addition, the distribution of the underlying rate and the correlation between this rate and the reference rate are relevant for calibration.

4.5 Volatility Notes

A volatility note pays coupons that depend on the realized volatility of a reference rate R. The reference rate is, for example, a swap rate, that is fixed on a common date for all coupon periods of the note (although it is possible to have different fixing dates as well). Let us assume R to be the 10y swap rate fixed on 2026-05-25, that is on the maturity date of the bond. The general valuation formula for the note is given by

$$V^{\text{Vol Note}} = \text{Nom} \cdot N(0) \cdot \mathbb{E}^N\Big(\sum_{i=1}^{m} \frac{\tilde{\tau}_i |R(\tilde{T}_i) - R(\tilde{T}_{i-1})| S(T_i, \omega)}{N(\tilde{T}_i, \omega)} \tag{4.6}$$

$$+ \frac{S(\tilde{T}_m, \omega)}{N(\tilde{T}_m, \omega)}\Big). \tag{4.7}$$

Table 4.6 shows an example schedule.

The hedge swaps for volatility notes are constructed in the standard way, and it is possible to combine them with a callability feature.

Important calibration instruments for the valuation of a volatility note are the swaptions expiring on the reference rate's fixing date, across the whole strike range, so that the market implied distribution of that rate is reproduced in the valuation model.

For volatility notes and swaps, a stochastic volatility component in the valuation model is of special importance since it hugely influences the price of the volatility exotic, even if there is not a big visible difference in terms of volatility smile fitting to vanilla market options during calibration.

Table 4.6 Volatility note schedule with simulated fixings for the reference 10y swap rate S

Accrual start	Accrual end	Payment	Sim. fixing 1 (%)	Sim. fixing 2 (%)	Sim. amount
2016-05-25	2017-05-25	2017-05-25	1.9000	2.1000	2,000.00
2017-05-25	2018-05-25	2018-05-25	2.1000	2.5000	4,000.00
2018-05-25	2019-05-25	2019-05-27	2.5000	3.0000	5,000.00
2019-05-25	2020-05-25	2020-05-25	3.0000	3.1000	1,000.00
2020-05-25	2021-05-25	2021-05-25	3.1000	2.8000	3,000.00
2021-05-25	2022-05-25	2022-05-25	2.8000	3.5000	7,000.00
2022-05-25	2023-05-25	2023-05-25	3.5000	3.7000	2,000.00
2023-05-25	2024-05-25	2024-05-27	3.7000	3.9000	2,000.00
2024-05-25	2025-05-25	2025-05-26	3.9000	4.0000	1,000.00
2025-05-25	2026-05-25	2026-05-25	4.0000	4.2000	2,000.00
		2026-05-25			1,000,000.00

4.6 Structured Floating Rate Coupons

There are variants of plain vanilla floaters where the plain vanilla Libor coupon is replaced by a structured coupon. We merely list a few common examples here.

1. Non-natural payment times for Libor coupons, in particular
   (a) in arrears fixed Libor coupons (where the fixing date lies a few days before the accrual end instead of the accrual start date)
   (b) delayed Libor coupons with a payment time (significantly) later than the index estimation end date.
2. CMS coupons, inverse CMS coupons, both possibly capped and / or floored
3. CMS spread coupons, inverse CMS spread coupons, again possibly capped and / or floored
4. Digital payoffs based on Libor, CMS, CMS spread rates
5. Quanto payoffs linking the payment to an index in a different currency than it is paid.

All of the given variants, if occurring without a call feature (or TaRN or Snowball, see below) are usually valued using "vanilla" models applied to the single coupons instead of a full-term structure model, see for example Andersen and Piterbarg (2010), Chap. 16.

If callability, a TaRN or Snowball feature are present at the same time, though, these coupons are evaluated applying the same full-term structure

model. Yet the coupon type influences the choice of calibration instruments, of course. For example a strip of CMS coupons would require calibration to the whole market swaption smile on each CMS fixing date with respect to the CMS tenor. CMS spread coupons would require calibration to both components swaption smiles plus the correlation between the swap rates, etc.

If a quanto element is present, the model we present in Sect. 10.3 has to be extended by another currency and a FX process between this and the domestic currency, again see Lichters et al. (2015) on how this can be done.

4.7 In-Currency Tenor Basis Swaps

An in-currency tenor basis swap exchanges one floating rate (Ibor or OIS) against another, with both sides possibly having a spread. An example is a swap exchanging Euribor 3M + X bp coupons against Euribor 6M + Y bp coupons. In-currency basis swaps are suitable to hedge the basis risk between different index tenors of the same currency, that is the risk of changing spreads between the respective forward curves of the two indices. Such trades are also called money market basis swaps.

4.8 Cross-Currency Basis Swaps

A cross-currency basis swap exchanges a fixed or floating rate in one currency against another fixed or floating rate in another currency (possibly the floating tenors are different in both currencies, and there are all combinations fixed–fixed, fixed–float and float–float common in the market). Again, legs with floating rates can have spreads. As an example, a swap might exchange USD Libor 3M coupons against EUR Euribor 3M + X bp coupons. There are two important differences to in-currency tenor basis swaps:

1. Usually at the start and end of the swap, the notionals in the two currencies are exchanged in addition to the coupon payments.
2. In an important variant of the cross-currency swap called “mark to market”, the notional of one side of the swap is adjusted at the start of each coupon period using the current FX rate (technically, a FX index fixing is used to determine the new notional amount) and the difference to the previous notional is exchanged.
3. If the swap is amortizing, the notional differences on each leg are exchanged as well.

This way, (ordinary) cross-currency swaps can directly be used to transform the income from a foreign exchange bond to another currency (that is hedge the FX risk), including amortization payments.

The mark-to-market variant on the other hand has the feature that the exposure of the outstanding notionals is reset on each coupon period, thus creating much smaller absolute NPVs over the lifetime of the swap in case the FX rate has bigger moves, which in turn reduces the NPV exposure of such a swap.

4.9 Conclusion and Summary

In this section, we introduced TaRNs, Snowballs, Range Accruals and Volatility Notes and their corresponding asset swaps as the most common examples of exotic structures beyond callability. We gave a list of structured coupon types and explain how these can be combined with both the exotic structures introduced in this chapter and callability introduced earlier. Finally, we briefly explained the mechanics of in-currency tenor basis swaps and cross-currency basis swaps and for which purposes they are used.

References

Andersen, L., & Piterbarg, V. (2010). *Interest rate modeling—Volume II: Term structure models*. Atlantic Financial Press.

Kienitz, J. (2014). Transforming volatility—Multi curve cap and swaption volatilities. *International Review of Applied Financial Issues and Economocs*, *5*(1).

Lichters, R., Stamm, R., & Gallagher, D. (2015). *Modern derivatives pricing and credit exposure analysis—Theory and practice of CSA and XVA pricing*. Palgrave McMillan: Exposure Simulation and Backtesting.

5

Exposures

5.1 Introduction and Objectives

After August 2007 and with all the new regulatory requirements, term structure models are applied to simulate interest rate scenarios. This is done either under the real world or the risk neutral measure to estimate exposure for interest rate bearing instruments. To this end, it is important to have efficient numerical methods available to simulate and price using your favourite term structure model.

In this short chapter, we review some exposure measures and illustrate the calculation of exposure. Then, we aim to present some exposure profiles of financial instruments which can be tackled with the term structure models and the methods described in this book.

Let us consider the simplified approach for calculating CVA by assuming a constant recovery. Then, we need to calculate

$$CVA \approx (1-R)\int_0^\infty DF(0,t)EE(t)\mathbb{P}^d(t,t+dt)dt]. \tag{5.1}$$

The quantities appearing in Eq. (5.1) are the recovery rate R, the discount factor DF, the probability of default $\mathbb{P}^d$ and the Expected Exposure EE. Thus, to be able to calculate CVA, it is necessary to specify these quantities. In this chapter, we only consider the EE and assume the other components given. The quantity EE is ultimately linked to future scenarios of the risk factors. For interest bearing instruments such as Interest Rate Swaps or Swaptions, we need to apply a term structure model to generate such future scenarios.

© The Author(s) 2017

J. Kienitz and P. Caspers, *Interest Rate Derivatives Explained: Volume 2*,
Financial Engineering Explained, DOI 10.1057/978-1-137-36019-9_5

On these scenarios, we calculate the value of the financial instruments under consideration. This can be done using forward methods where we have to evaluate at every simulated point in time or backward methods where we only evaluate at maturity and, then, use regression to evolve the price backwards. The calculated numbers are aggregated due to netting and collateral assumptions to calculate the exposure. From the calculated exposure, we derive the Expected Exposure.

Many other adjustments such as DVA (Debit Value Adjustment), FVA (Funding Value Adjustment), KVA (Capital Value Adjustment), ColVA (Collateral Value Adjustment), MVA (Marginal Value Adjustment) or DIM (Dynamic Initial Margin) exist and also need the scenarios, respectively, exposures as input to the calculations. We refer to all the adjustments as xVA. Let us now begin to consider exposures.

5.2 Exposures—Summary and Illustrations

The regulatory literature that is mandatory for many financial institutions specifies numerous measures that have to be calculated for quantifying exposure. We give a short overview of the measures and present the formulae that are used for calculation. Let $V(t, T)$ denote the value of a trade, portfolio or Netting Set at time t with longest maturity T.

- Expected Future Value (EFV): The mean value at time t

$$EFV(t) = \mathbb{E}[V(t, T)]$$

- Expected Exposure (EE): The mean value at time t only taking positive values

$$EE(t) = \mathbb{E}[V(t, T)^+]$$

- Expected Positive Exposure (EPE): The mean of EE with respect to time

$$EPE = 1/T \int_0^T EE(s)ds$$

- Expected Negative Exposure (NEE/ENE): The mean at time t taking only negative values

$$NEE(t) = \mathbb{E}[V(t, T)^-]$$

- Effective Exposure

$$EffEE(t) := EEE(t) := max_{0 \leq s \leq t} EE(t)$$

- Potential Future Exposure (PFE): Quantile at time t of the distribution, for instance $q = 95\%$

$$PFE^q(t) = \alpha_q(V(t, T))$$

It is helpful to visualize the measures for some financial instruments. Here we have chosen to use a portfolio of Interest Rate Swaps with different maturities. Figure 5.1 shows the changes of the value of the portfolio on different scenarios generated using a term structure model, the positive values along a given scenario and the portfolio exposure.

Now, using the results shown in Fig. 5.1, we calculate the exposure measures defined at the beginning of this section. The results are displayed in Fig. 5.2.

It is often necessary to study the effect a new trade has on the exposure of a portfolio for a given Netting Set. We use a simplistic example to illustrate this. We take a Payer Interest Rate Swap with maturity 5 years. This is our initial portfolio. Then, we add different trades to this portfolio, namely

(a) Payer Interest Rate Swap with maturity 6 years
(b) Receiver Interest Rate Swap with maturity 5 years
(c) Cross-Currency Basis Swap with maturity 5 years and without periodic notional reset.

Figure 5.3 illustrates the resulting exposure profiles. We show the Expected Exposure profiles for the initial trade, the resulting portfolio, for the portfolio if netting is allowed and for the increment of the exposures. Such analysis can help traders and risk managers to control and manage the exposure profile of a given Netting Set.

Another key driver of the exposure is the collateral and the mechanism of posting it. In Kienitz (2014), we considered the effect of collateral on the exposure and outlined that the underlying CSA determines how the collateral influences the exposure. Now, we use term structure models to not only simulate the exposure of a Netting Set but also include the collateral process here. Figure 5.4 visualizes how the collateral reduces the exposure of a given Netting Set. We not only display the effect for different paths but finally show the averaged reduction of the exposure. This is the graph displayed on the bottom right in Fig. 5.4.

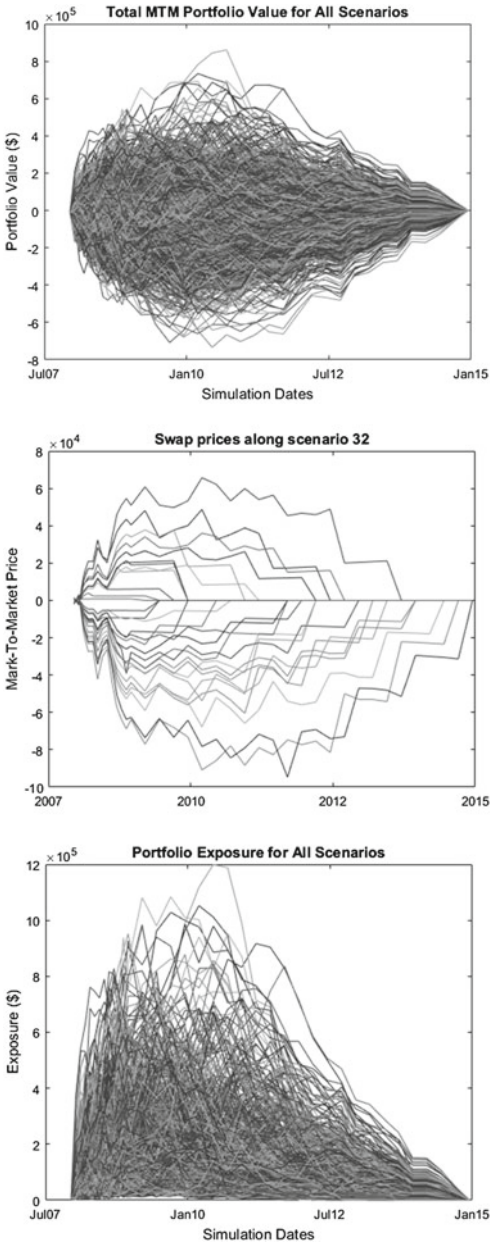

Fig. 5.1 Exposure measures illustrated on a portfolio of interest rate swaps. We show several paths (*top*), a particular one (*mid*) and the values contributing to the exposure (*bottom*)

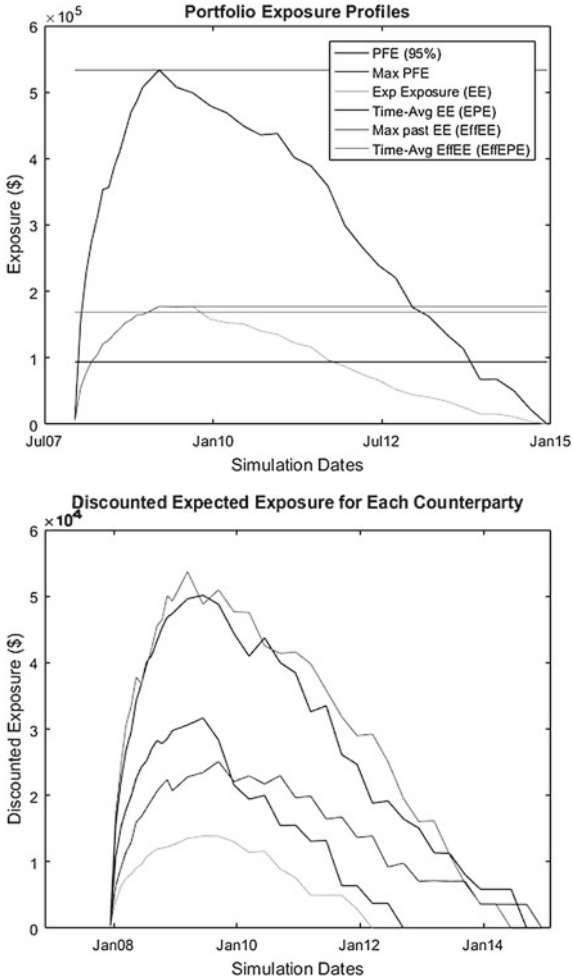

Fig. 5.2 Exposure measures (*top*) and the expected exposure (*bottom*)

Let us shortly summarize the necessary steps of xVA and exposure calculation:

- **Scenario-generation**
  - Identification of risk factors affecting the portfolio
  - Definition and calibration of a stochastic model
  - Determination of simulation times
  - Sampling of several thousand paths for the risk factors

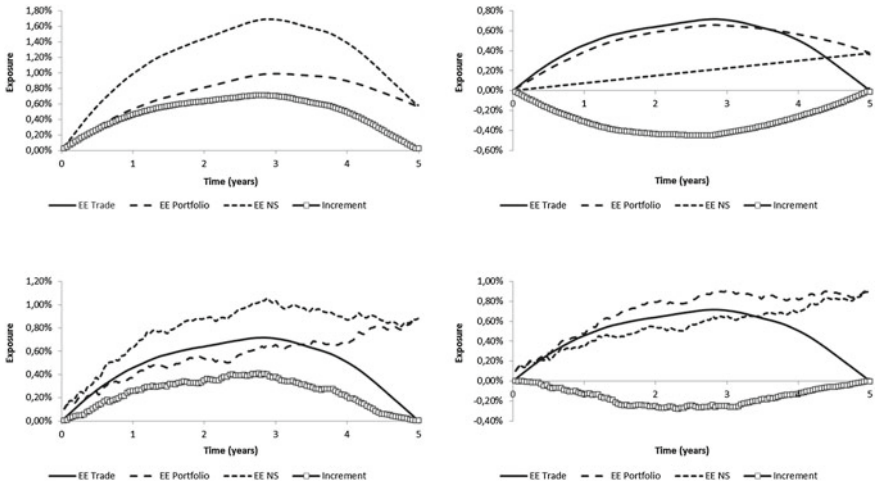

Fig. 5.3 The effect on the exposure of adding trades to a given portfolio. We consider the case **a** (*top left*), **b** (*top right*), **c** (*bottom left*) and adding the trades from (**b**) and (**c**) (*bottom right*)

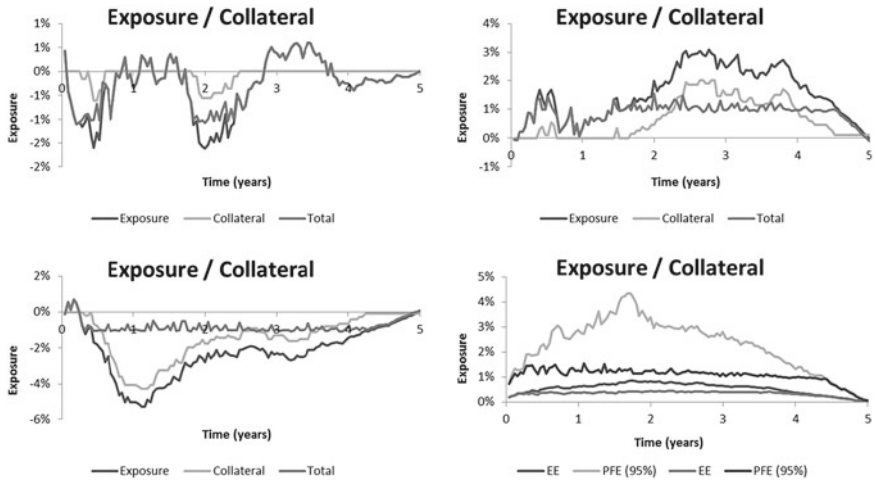

Fig. 5.4 Effect of the collateral on the exposure of a given Netting Set. While the graphs (*top left*), (*top right*) and (*bottom left*) illustrate this on a sampled path, the graph (*bottom right*) shows the averaged effect

- **Assessment of single items**
  - Each instrument has to be assessed in each scenario for each simulation time or using backward methods
  - A three-dimensional matrix, also known as a cube consisting of the value of each instrument, in scenario, at the time k needs to be calculated
  - Use of efficient valuation methods or backward pricing
- **Netting and Collateral**
  - Aggregation of all transactions within a Netting Set
  - Calculating of the exposure for each counterparty under any scenario for any date
  - Consideration of possible specifics of security arrangements
- **Determination of exposure measures**
  - From the calculated exposures in the previous step, PFE, EPE and other measures can be determined and used for further calculating valuation adjustments
  - The calculated figures are then used for pricing, reporting limits, risk management and economic/regulatory capital
- **Reporting and Analysis**
  - Reporting (daily risk reports, reports for CVA desks)
  - Backtesting (P&L Explain, distribution to other units).

5.3 Examples

This section gives some standard examples for illustrating the exposure produced by financial instruments. The figures are produced by simulating the future term structure using a stochastic description of the model and a numerical procedure that is capable of performing the path simulation. Then, we applied the backward pricing approach for efficient calculation of the model prices. This has the advantage that we do not mix models but stay in the same model for generating the scenarios and the pricing of the instruments.

For the risk factor evolution, we used a term structure model which is considered in Chap. 11. It is called the Trolle and Schwartz model.

5.3.1 Interest Rate Swaps

We start with the case of an Interest Rate Swap. Usually a Money Market rate such as LIBOR is exchanged for a fixed rate at pre-specified points in time. Usually the swap is fair at inception. But this is not necessarily the case when a swap is considered during its life time. With regard to the interest rate curves the swap can take either negative or positive values. We have considered all three cases in Fig. 5.5. There, a fair or ATM swap as well as swaps having positive and negative current values is displayed.

The results leading to exposure profiles as shown in Fig. 5.5 are calculated using scenarios for future yield curves. From the scenarios, the exposures for ATM and $ATM \pm 1\%$ are calculated in case of paying, respectively receiving, the fixed coupon. How the underlying exposure simulation could look like is shown in Fig. 5.6.

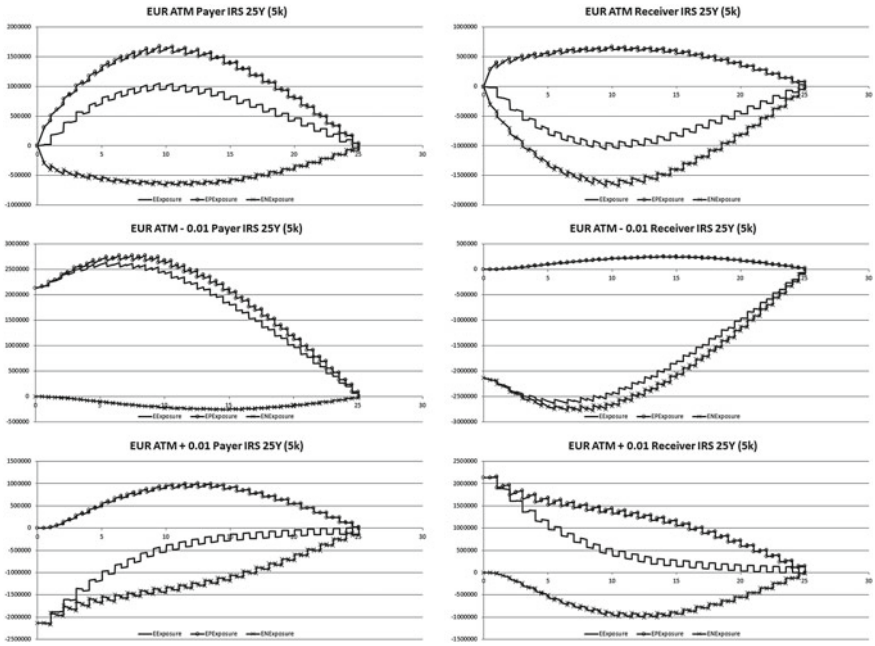

Fig. 5.5 Exposure profiles of different interest rate swaps with maturity 25 years. The ATM pay/receive cases (*top-left* and *right*), ATM −1% pay/receive (*mid-left* and *right*) and ATM + 1% pay/receive (*bottom-left* and *right*)

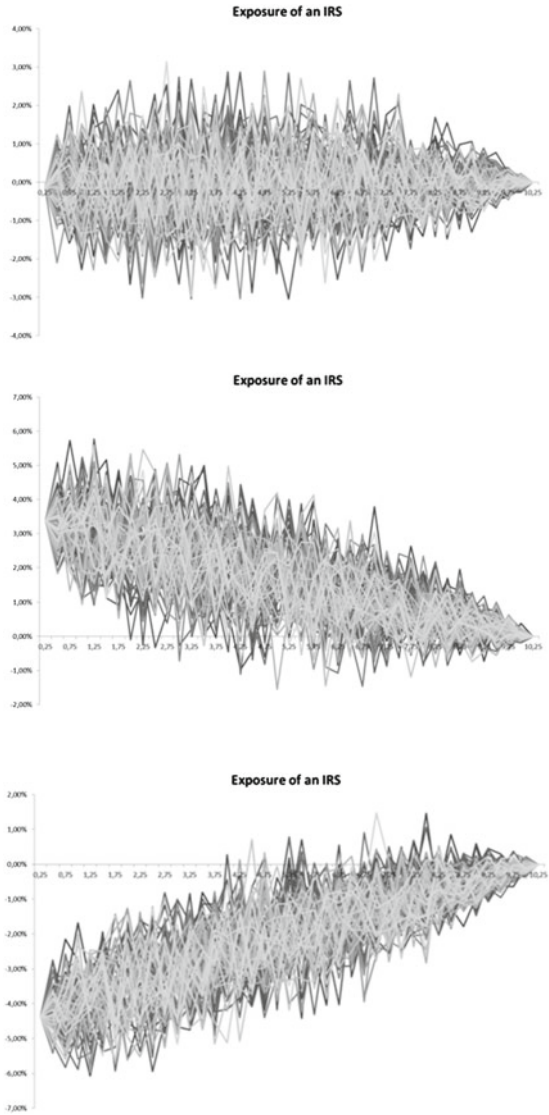

Fig. 5.6 Exposure profiles of different interest rate swaps with maturity 10 years. The ATM case (*top*) and the cases of positive market value (*mid*) and a negative one (*bottom*)

5.3.2 Cross-Currency Swaps

Another standard product is the Cross-Currency Swap and we would like to show exposure profiles for this kind of trade. To this end, we need to simulate

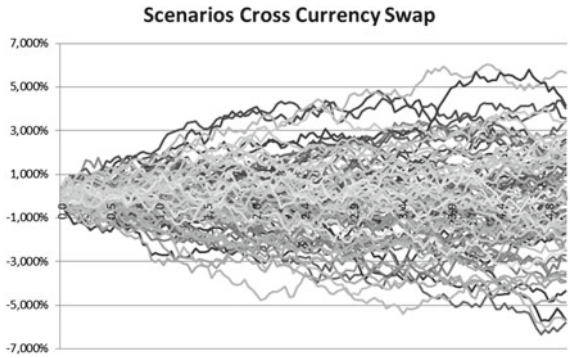

Fig. 5.7 Sample paths of the value of a cross-currency swap without periodic reset

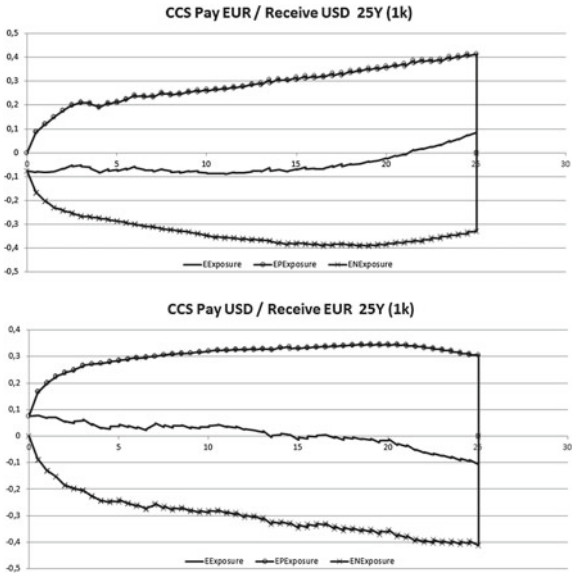

Fig. 5.8 Exposures of cross-currency swaps that are not periodically reset. Perspective EUR/USD (*top*) and USD/EUR (*bottom*)

scenarios with regard to a term structure model. Such scenarios are shown in Fig. 5.7.

Such scenarios are then used to calculate the exposure profiles. We give two profiles for a trade that currently has positive market value and one that has negative market value, namely the opposite trade. See Fig. 5.8 for illustration.

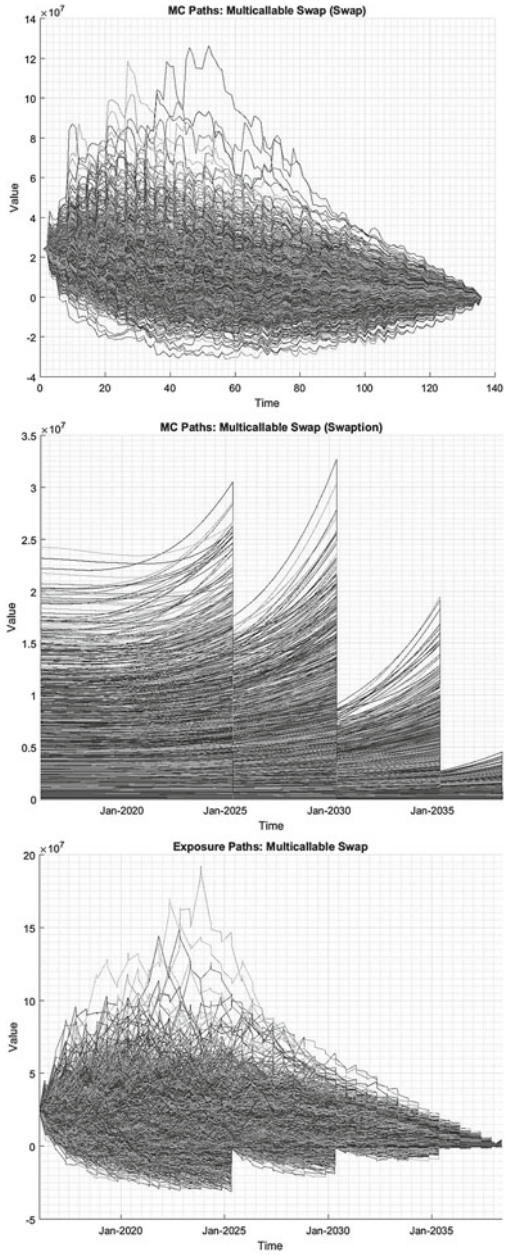

Fig. 5.9 Scenarios generated to calculate the profile of a multi-callable swap. The swap (*top*), the Bermudan Swaption (*mid*) and the combination of both (*bottom*)

5.3.3 Callable Swaps

As a final example, we consider the case of a multi-callable swap. This is essentially the combination of a Swap combined with a Bermudan Swaption. The standard way to calculate the exposures is again, simulating scenarios and use backwards Monte Carlo methods for the pricing. In this case, the backward approach is essential since we consider multiple exercise possibilities. We have shown the scenarios in Fig. 5.9.

If the call feature is such that we enter into a swap, that is we have physical settlement, the exposure of the resulting swap has to be considered. This is shown in Fig. 5.10.

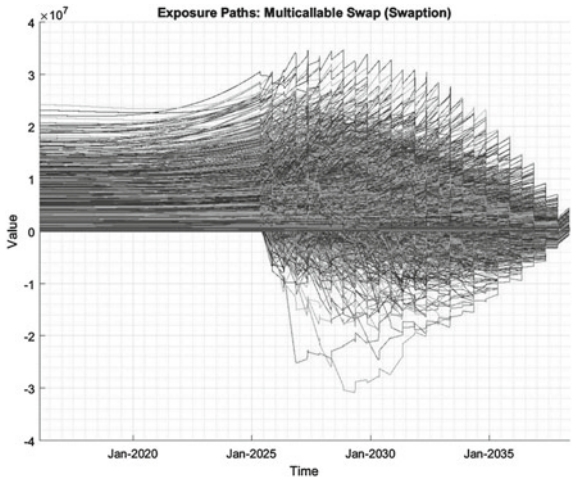

Fig. 5.10 Exposure profile of the swap resulting from physical settlement of the exercised swaption

Using the scenarios, the exposure profiles can be computed and we display these profiles in Fig. 5.11.

The considerations then lead to the final exposure profile displayed in Fig. 5.12.

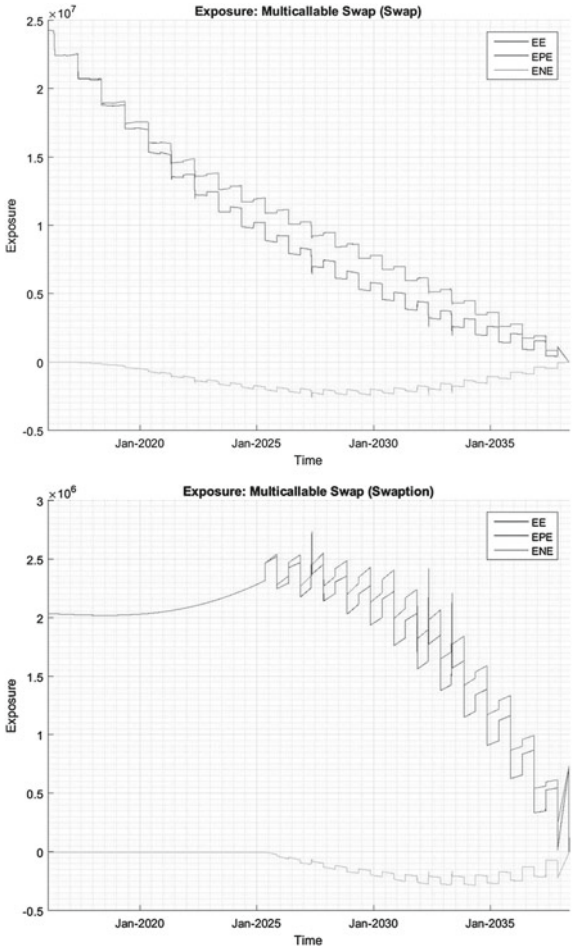

Fig. 5.11 Exposure profiles of the constituting elements. The swap (*top*) and the option (*bottom*)

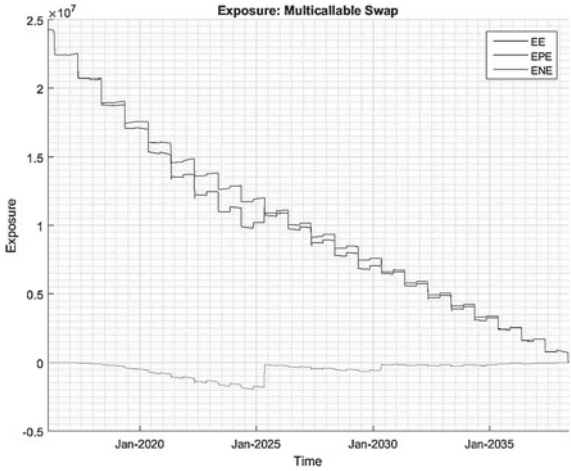

Fig. 5.12 Exposure profile of a multi-callable swap

5.4 Summary and Conclusions

In this section, we considered the calculation of xVA and the necessary steps of exposure calculation. The latter is usually done using term structure models and simulation methods. We outlined how the models considered in this book can help to cope with the task of generating exposure and how they can be applied to manage and analyse the effects of adding trades to a given Netting Set, the effect of collateral or simply the exposure profile of some widely used financial instruments.

Reference

Kienitz, J. (2014). *Interest rate derivatives explained: Volume 1 products and markets.* Palgrave McMillan.

Part II

Volatility

6

The Heston Model

6.1 Introduction and Objectives

In this chapter we introduce the subject of volatility modelling. Some issues have already been tackled in Kienitz (2014). We start with a short general introduction. This is followed by considering one of the most popular Stochastic Volatility models, namely the Heston model. Since its introduction in Heston (1993) it gained a lot of attraction and is used by practitioners for many asset classes including interest rates. Due to its popularity many researchers worked on this model and by today efficient numerical techniques for pricing, simulation and calibration do exist. We introduce the Heston model and give an interpretation of the model parameters. Then, in Sect. 6.5 we show how to calibrate the model. The necessary numerical methods are postponed to Appendix A. The approaches for incorporating non-constant volatility into models basically lead to considering the following model classes:

- Local Volatility models
- Stochastic Volatility models
- Hybrid Volatility models (combination of a Local and a Stochastic Volatility model)

Local Volatility models incorporate a deterministic function $\sigma(S, T)$ depending on the current value of the underlying S and time T. This model class includes the Black76 and the Bachelier as well as Displaced Diffusion and CEV models. But non-parametric methods also exists. The function σ is then determined by purely numerical methods involving inter- and extrapolation. The second class of models allows for another stochastic driver for the volatility

© The Author(s) 2017

J. Kienitz and P. Caspers, *Interest Rate Derivatives Explained: Volume 2*,
Financial Engineering Explained, DOI 10.1057/978-1-137-36019-9_6

component. Such models assign a dynamic (6.1) to the volatility.

$$dV(t) = \mu(t)dt + \nu(t)dW(t) \tag{6.1}$$

where $W(t)$ is a Brownian motion possibly correlated to the Brownian motion driving the asset dynamics. The drift μ and the volatility ν can be chosen appropriately. Finally, it is possible to combine the class of Local Volatility and Stochastic Volatility models which lead to hybrid volatility, respectively Local Stochastic Volatility models.

6.2 Local Volatility Models

The concept of a local volatility can be traced back to the work of Dupire (1994) and Derman and Kani (1994). They realized that under the assumption of risk neutrality a unique state-dependent diffusion process can be constructed that is consistent with all market prices for European Call options. The diffusion coefficient, σ_L of the process is a function of state and time. This is the fact why the model is called Local Volatility model. For a detailed discussion see for instance Gatheral (2006). For our purpose we only need to consider Local Volatility models of a special form. The function C we consider in Eq. (6.2) determines what is called the functional form of the volatility. We already considered some of the models in Kienitz (2014) but reproduce some formulae here for the reader's convenience. We take the dynamics given by (6.2).

$$dS(t) = \sigma(t)C(S)dW(t), \quad S(0) = s_0. \tag{6.2}$$

We can now choose different functional forms by determining the function C in (6.2). The choice $C(S) = 1$ is the Bachelier model, $C(S) = S$ is the Black76 model and $C(S) = (S + a)$ or $C(S) = S^\beta$ lead to the Displaced Diffusion and the CEV model.

Let us shortly come back to the backbone and which role the function C plays here. To this end we remind that the Delta hedging approach to risk management is intimately linked to the dynamic of the model's implied volatility dynamics. If C denotes the model price for a European Call option the Delta is given by

$$\Delta(t) = \frac{\partial C(t)}{\partial S_0}$$

If we consider the Black76 model for instance together with an implied volatility parameterization that may depend on many quantities such as the strike or

the maturity but also on parameters that determine the shape of the skew/smile. Then, the Delta becomes

$$\begin{aligned}\Delta(t) &= \frac{\partial C_B(t)}{\partial S_0} + \frac{\partial C_B(t)}{\partial \sigma_B}\frac{\partial \sigma_B(t)}{\partial S_0} \\ &= \Delta_B(t) + V_B(t)\frac{\partial \sigma_B(t)}{\partial S_0}\end{aligned}$$

This means that the Delta is given in terms of the standard Black76 Delta but another quantity enters the scene which is multiplied by the Black76 Vega and added to the Delta. While $\Delta_B(t) = \mathcal{N}(d_1)$ and $V_B(t) = S(t)\sqrt{T-tn}(d_1)$ with $d_1 = \frac{\ln(S/K)+\frac{1}{2}\sigma^2 T}{\sigma_B\sqrt{T}}$ the calculation of $\frac{\partial \sigma_B}{\partial S_0}$ depends on model parameters. If σ does not depend on the spot value S_0 we have

$$\Delta(t) = \Delta_B(t)$$

This is not the case for other models such as the Heston model. The Delta has an additional contribution which is related to the Vega and the implied Black volatility calculated. Thus, the term $\frac{\partial \sigma_B}{\partial S_0}$ called the backbone determines if the Delta is higher or lower than the corresponding Black one. Thus, the use of a risk management model is not determined by fitting the market in the first place but by the hedging and, thus, how well the skew/strike dynamics is described. Traders use the model implied or exogenously supplied backbone for hedging. This is called *Shadow Delta Hedging*.

Let us consider an approach of controlling the backbone using Displaced Diffusion models. In Kienitz (2014) we considered

$$dS(t) = \sigma_B(S(t) + b)dW(t)$$

Now, we consider a different notation which is

$$dS(t) = \sigma(aS(t) + (1-a)L)dW(t)$$

This leads to

$$\sigma_B(0, S(0), T, K) \approx \sigma\frac{\ln(S(0)/K)}{\int_K^{S(0)}\frac{du}{au+(1-a)L}} = \sigma a\frac{\ln(S(0)/K)}{\ln(\frac{aS(0)+(1-a)L}{aK+(1-b)L})}$$

and the backbone is controlled by the displacement parameters a and L:

$$\left.\frac{\partial \sigma_B(0, S(0), T, K)}{\partial S(0)}\right|_{K=S(0)} \approx -\frac{1-a}{2}\frac{L}{S(0)^2}\sigma \overset{L=S(0)}{=} -\frac{1-a}{2}\frac{\sigma}{S(0)} \tag{6.3}$$

If we had chosen the dynamic

$$dS(t) = \sigma(aS(t) + (1-a)S(0))dW(t)$$

we would have calculated the backbone as

$$\left.\frac{\partial \sigma_B(0, S(0), T, K)}{\partial S(0)}\right|_{K=S(0)} \approx \frac{1-a}{2}\frac{\sigma}{S(0)} \tag{6.4}$$

Equations (6.3) and (6.4) lead to different backbones despite the fact that they look so similar. To be fully flexible we could take

$$dS(t) = \sigma(aS(t) + (m-a)S(0) + (1-m)L)dW(t)$$

with backbone

$$\left.\frac{\partial \sigma_B(0, S(0), T, K)}{\partial S(0)}\right|_{K=S(0)} \approx -\frac{1-a}{2}\frac{(m-a)S(0) - (1-m)L}{S(0)}\frac{\sigma}{S(0)}$$

See for instance Hagan et al. (2002) or Andersen and Piterbarg (2010) for more details and further facts on the backbone. If we have an expression for the implied Bachelier or Black76 volatility we can then simply use the corresponding pricing formulae. We have for the Bachelier model, (6.5)

$$\begin{aligned} C_N(S(0), K, T, \sigma) &= (S(0) - K)\mathcal{N}(d(\sigma_{\mathrm{N}})) + \sigma\sqrt{T}n(d(\sigma_{\mathrm{N}})) \\ P_N(S(0), K, T, \sigma) &= (K - S(0))\mathcal{N}(-d(\sigma_{\mathrm{N}})) + \sigma\sqrt{T}n(d(\sigma_{\mathrm{N}})) \end{aligned} \tag{6.5}$$

and for the Displaced Diffusion model (6.6) where the Black76 formula is a special case, $b = 0$.

$$\begin{aligned} C_{DD}(S(0), K, T, \sigma) &= (S(0) + b)\mathcal{N}(d_1) - (K + b)\mathcal{N}(d_2) \\ P_{DD}(S(0), K, T, \sigma) &= (K + b)\mathcal{N}(-d_2) - (S(0) + b)\mathcal{N}(-d_1) \end{aligned} \tag{6.6}$$

6.3 The Heston Model

The Heston model is given by the following set of SDE's:

$$dS(t) = (r - d)S(t)dt + \sqrt{V(t)}S(t)dW_1(t) \tag{6.7}$$

$$dV(t) = \kappa(\Theta - V(t))dt + \nu\sqrt{V(t)}dW_2(t) \tag{6.8}$$

$$\langle dW_1, dW_2\rangle = \rho dt \tag{6.9}$$

$$(S(0), V(0)) = (S_0, V_0)$$

The parameter κ models the speed of the mean reversion of the variance, Θ is the long term variance. The parameter ν is the volatility of variance, ρ is the correlation of the driving Brownian motions W_1 and W_2, S_0 is the spot asset price and V_0 is the spot variance. Dealing with the Heston model has shown that two variants of parametrizations exist. The variants considered depend on the parameter values. To this end we consider

$$(I)\ \ 2\kappa\Theta \geq \nu^2, \quad (II)\ \ 2\kappa\Theta < \nu^2. \tag{6.10}$$

The model fulfills the *Feller property* if Equation (I) from 6.10 holds. The Feller condition implies that the process never reaches 0. If the condition is not fulfilled the process V may reach 0. In this case, to obtain a unique solution to the system of SDEs we have to specify a boundary condition at 0. In quantitative finance the chosen boundary condition is that the process remains in 0. We call it the absorbing boundary condition. If the process reaches 0 and is allowed to leave 0 it is called a reflecting boundary.

Next, we wish to gain intuition on the model parameters. Let us fix a base scenario by fixing all model parameters. We modify the parameters one by one and study the effect this modification has on the implied volatility generated by the model. The base scenario is given by: $V(0) = 0.03$, $\Theta = 0.025$, $\kappa = 0.3$, $\nu = 0.5$ and $\rho = 0$.

The results are shown in Figs. 6.1 and 6.2. In addition to a base scenario we considered for the Spot Variance 0.02 and 0.04, for the long term variance 0.01 and 0.04, for the Mean Reversion 0.1 and 0.5, for the volatility of Variance 0.3 and 0.7 as well as for the correlation −0.5 and 0.5. The first value is the one determining the lower value and the second value is the one used for increasing the value of the model parameters.

Next, we wish to consider the fullly implied volatility surface. Using the numerical techniques presented in Appendix, especially the Fourier transform methods we study the parameter effects and visualise these using the implied

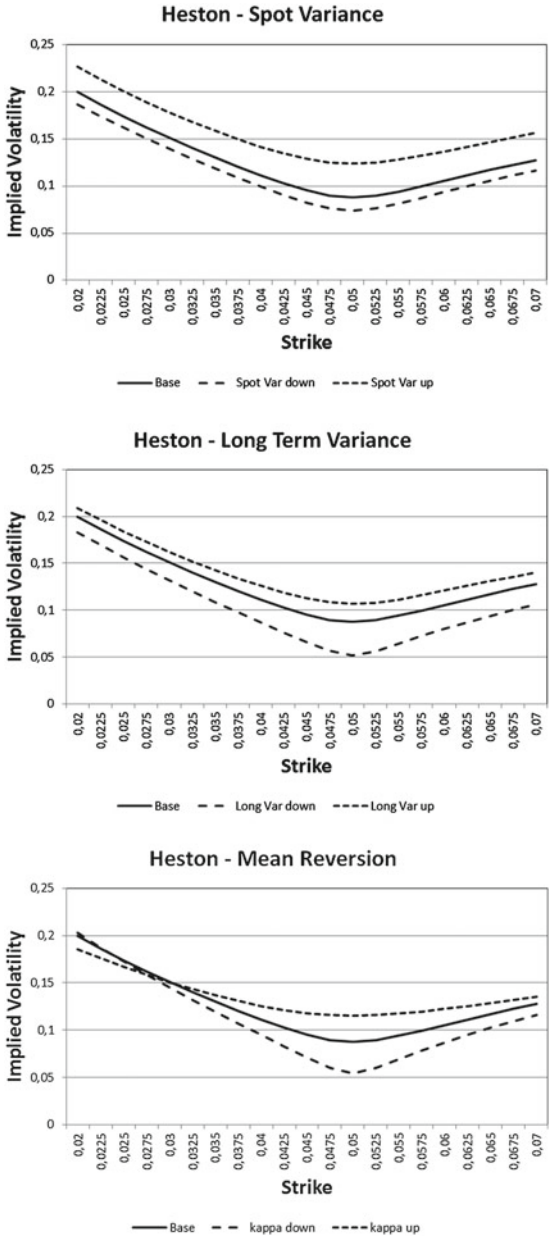

Fig. 6.1 Effect of the model parameters on the Implied Volatility Curve for a fixed maturity. Spot Variance (*top*), long term variance (*mid*) and Mean Rerversion (*bottom*)

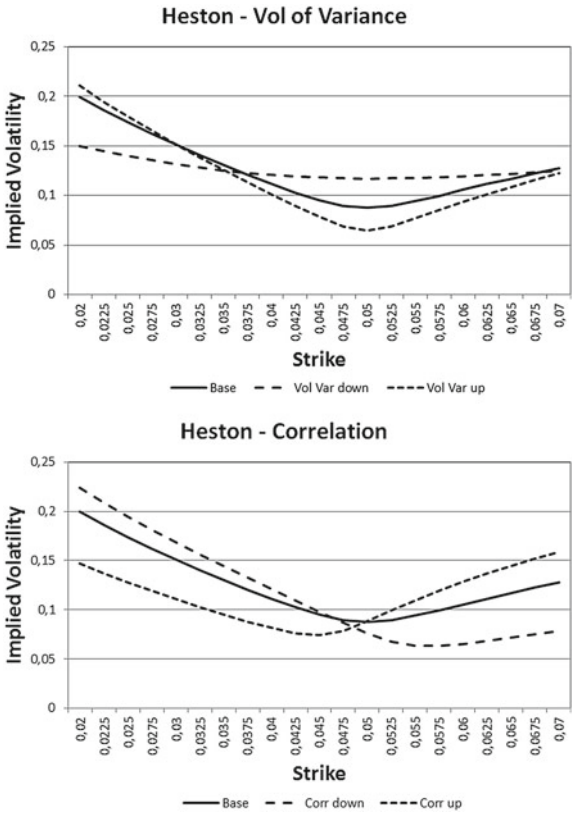

Fig. 6.2 Effect of the model parameters on the Implied Volatility Curve for a fixed maturity. Volatility of Variance (*top*) and Correlation (*bottom*)

volatility surface. Figures 6.3 and 6.4 show the corresponding graphs. This generalizes the findings for an implied volatility curve.

6.4 Pricing

For the Heston model we apply the techniques reviewed in Apendix A. The prices of European Call and Put options are calculated using the results from Sects. A.A.1 or A.A.2. We work with a quantity called the characteristic function. This function is denoted by φ_{H}. Equation (6.11) gives the closed form expression.

$$\varphi_{\mathrm{H}}(u,t,T) = \exp(A_H(u,t,T) + B_\sigma(u,t,T)V(t) + iuX(t)), \qquad (6.11)$$

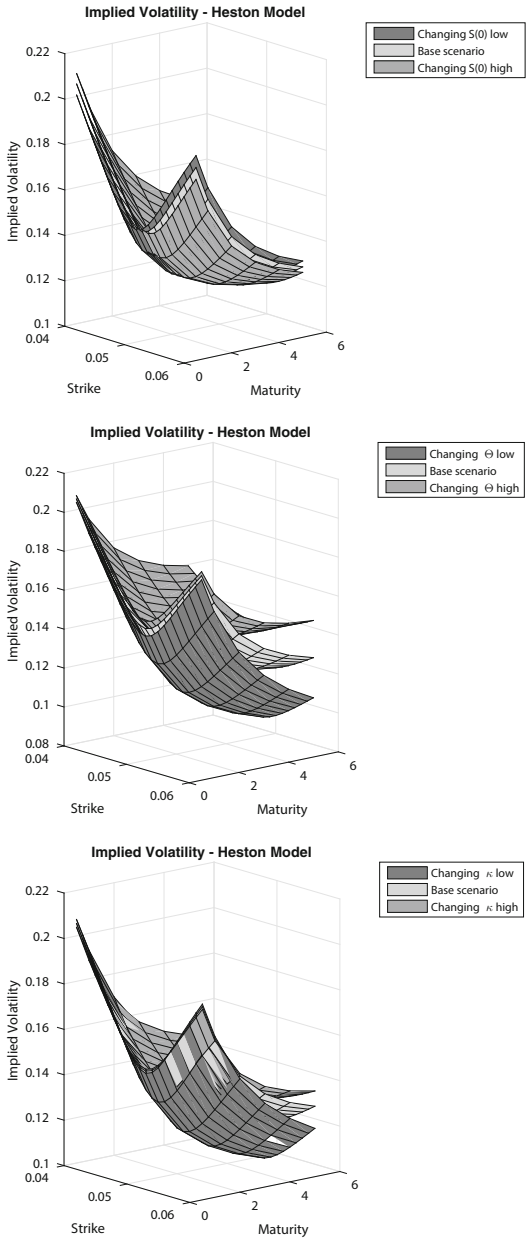

Fig. 6.3 Effect of the model parameters on the Implied Volatility Surface. We consider the Spot Variance (*top*), long term variance (*mid*) and the Mean Reversion (*bottom*)

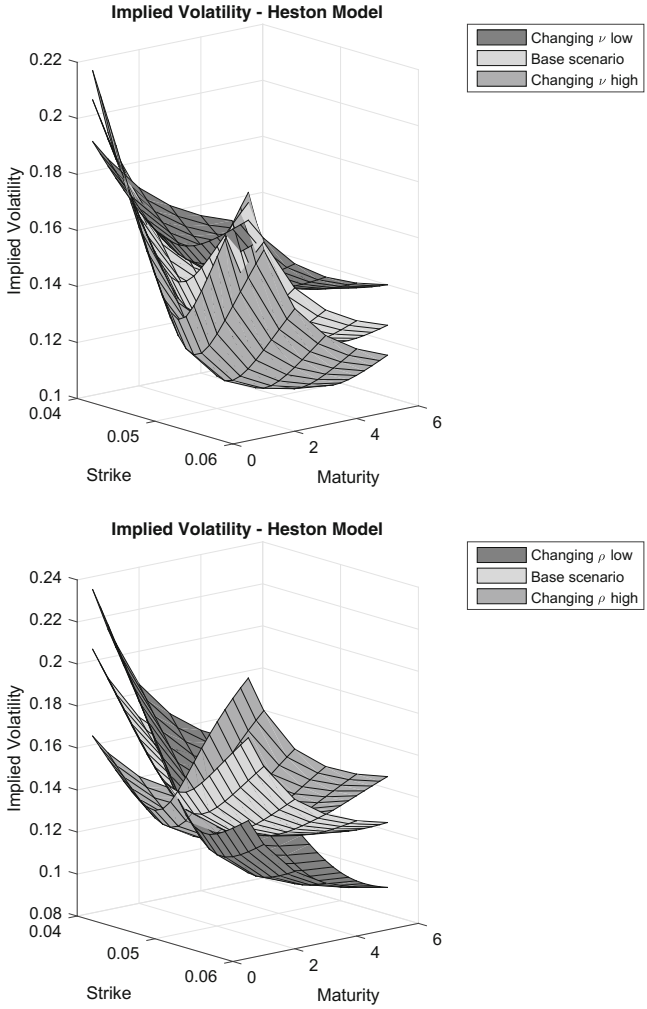

Fig. 6.4 Effect of the model parameters on the Implied Volatility Surface. Volatility of Variance (*top*) and Correlation (*bottom*)

with

$$A_H(u,t,T) = \frac{\kappa\Theta}{\nu^2}\left((\kappa - \rho\nu ui - D)(T-t) - 2\log\left(\frac{Ge^{-D(T-t)}}{G-1} - 1\right)\right)$$

$$B_\sigma(u,t,T) = \frac{\kappa - \rho\nu ui - D}{\omega^2}\left(\frac{1-e^{-D(T-t)}}{1-Ge^{-D(T-t)}}\right)$$

$$G = \frac{\kappa - \rho\nu u i - D}{\kappa - \rho\nu u i + D}$$
$$D = \sqrt{(\kappa - \rho\nu u i)^2 + u(i+u)\nu^2}.$$

Despite the fact that the expression of the characteristic function looks pretty complicated it is very convenient to be applied when it comes to numerical evaluations. It allows us to use established and efficient techniques from numerical mathematics. If we need to simulate paths we use one of the standard numerical schemes from Appendix A, Sect. A.4 or the QE scheme which we have also included in the final chapter, Sect. A.4.4.

6.5 Applications and Calibration

The model parameters have to be determined if we wish to use the model for pricing or simulation. To this end we select market instruments and try to adjust the model parameters such that the model prices are close to the selected market instruments. For instance we consider swaption prices. Let $V(K_i, T)$, $i = 1, \ldots, N$ be N market prices of swaptions of maturity T on a fixed swap rate. We also consider the model prices $\tilde{V}_{\alpha,\beta,\nu,\rho}(K_i, T)$. Then, we take as distance function

$$\frac{1}{N}\sum_{i=1}^{N}\left(V(K_i, T) - \tilde{V}_{\alpha,\beta,\nu,\rho}(K_i, T)\right)^2 \tag{6.12}$$

Now, we need to consider a strategy for efficiently determining the model parameters. To this we apply the smart parameter approach from Forde et al. (2012). This is an efficient method for the calibration task. The starting parameters are most important since if we were able to choose parameters which are close to the parameter set minimizing the function (6.12) we can hope that finding the optimal parameters does not take too long. Thus, a smart guess can be very efficient. The approach is based on the moneyness formulation and it takes the variance for options with moneyness $x_0 = \log(K/S)$ and two maturities T_1, T_2. The variances are $V(\pm x_0, T_j)$ $j = 1, 2$ and $V(0, 0)$. Let $V_0 = V(0, 0)$, $V_\pm = \frac{T_2}{T_2 - T_1}V(\pm x_0, T_1) - \frac{T_1}{T_2 - T_1}V(\pm x_0, T_2)$, $S = \frac{V_+ - V_-}{x_0}$ and $C = \frac{V_+ - 2V_0 + V_-}{2x_0^2}$. The Heston Parameters from the smart parameter approach are given by:

$$\begin{pmatrix} \tilde{V}_0 \\ \tilde{\nu} \\ \tilde{\rho} \end{pmatrix} := \begin{pmatrix} V_0 \\ \sqrt{7S^2 + 12V_0C} \\ 2S/\sqrt{7S^2 + 12V_0C} \end{pmatrix}.$$

and the parameters $\tilde{\epsilon}$ and $\tilde{\kappa}$ by matrix multiplication:

$$\begin{pmatrix} \tilde{\alpha} \\ \tilde{\kappa} \end{pmatrix} = \begin{pmatrix} -\frac{\tilde{\rho}\tilde{\nu}}{12\tilde{V}_0}x_0 & -\frac{\tilde{\rho}\tilde{\nu}}{12}x_0 \\ \frac{1}{2} + \frac{(13\tilde{\rho}^2-6)\tilde{\nu}^2}{96\tilde{V}_0^2}x_0^2 & -\frac{\tilde{V}_0}{2} - \frac{\tilde{\rho}^2\tilde{\nu}^2}{96\tilde{V}_0}x_0^2 \end{pmatrix}^{-1} (q - r)$$

with $\tilde{\alpha} = \tilde{\Theta}\tilde{\kappa}$. We used the vectors q and r:

$$q = \frac{1}{2T_1}\begin{pmatrix} V(x_0, T_1) - V(-x_0, T_1) - V_+ + V_- \\ V(x_0T_1) + V(-x_0, T_1) - V_+ - V_- \end{pmatrix}$$

$$r = \begin{pmatrix} \frac{\tilde{\rho}\tilde{\nu}^3(1-\tilde{\rho}^2)+\tilde{V}_0\tilde{\rho}^2\tilde{\nu}^2}{24\tilde{V}_0}x_0 \\ \frac{12\tilde{V}_0\tilde{\rho}\tilde{\nu}+(\tilde{\rho}^2-4)\tilde{\nu}^2}{48} + \frac{(176-712\tilde{\rho}^2+521\tilde{\rho}^4)\tilde{\nu}^4+40\tilde{V}_0\tilde{\rho}^3\tilde{\nu}^3}{7680\tilde{V}_0^2}x_0^2 \end{pmatrix}$$

Forde et al. (2012) show a small time expansion for the implied volatility σ_{BS} in terms of the Heston parameters. It is given by:

$$\sigma_{\mathrm{BS}}(x, t) \approx \sqrt{\sigma_0^2(x) + a(x)t}$$

with strike $K = S_0 \exp(x)$ and x being close to 0 and

$$\sigma_0 \approx \sqrt{V_0}\left(1 + \frac{\rho\nu x}{4V_0} + \frac{1}{24}\left(1 - \frac{5\rho^2}{2}\right)\frac{\nu^2x^2}{V_0^2}\right)$$

$$\begin{aligned} a(x) \approx & -\frac{\nu^2}{12}\left(1 - \frac{\rho^4}{4}\right) + \frac{V_0\rho\nu}{4} + \frac{\kappa(\Theta - V_0)}{2} + \frac{\rho\nu}{24V_0}(\nu^2(1-\rho^2) \\ & -2\kappa(\Theta + V_0) + V_0\rho\nu)x \\ & + \frac{\nu^2x^2}{7680V_0^2}\Big(176\nu^2 - 480\kappa\Theta - 712\rho^2\nu^2 + 521\rho^4\nu^2 \\ & +40V_0\rho^3\nu + 1040\kappa\Theta\rho^2 - 80V_0\kappa\rho^2\Big) \end{aligned}$$

6.5.1 Extensions of Heston

The standard extension of the Heston model to incorporate negative rates for instance is to consider the displaced dynamic (6.13). It is obtained from the original Heston model (6.7) and (6.8) by replacing the asset dynamic with

$$dS(t) = (r - d)S(t)dt + \sqrt{V(t)}(S(t) + a)dW_1(t) \tag{6.13}$$

This enables the model to accommodate negative values of the asset. Values up to but not including $-a$ are admissible. All the numerical models in Appendix A apply to the displaced version of the model as well. Thus, it is very convenient to replace the standard Heston model with its displaced version.

Another extension is to consider time-dependent model parameters, that is,

$$\begin{aligned} dS(t) &= (r - d)S(t)dt + \sqrt{V(t)}(S(t) + a(t))dW_1(t) \\ dV(t) &= \kappa(t)(\Theta(t) - V(t))dt + \nu(t)\sqrt{V(t)}dW_2(t) \\ \langle dW_1(t), dW_2(t)\rangle &= \rho(t)dt \end{aligned}$$

This makes the model a lot more complicated but even in this case it is still applicable in practice. Kiesel and Lutz (2010) or Andersen and Piterbarg (2010) outline methods of how to tackle the time-dependence in this model. They use the techniques of Markovian Projection and Parameter Averaging together with parsimonious functions for the time-dependent parameters. See Andersen and Piterbarg (2010) for details modelling on the methods.

6.6 Conclusion and Summary

In this chapter we considered the Heston model, Heston (1993). This is a very popular method of modelling volatility skews/smiles. The model is used as a stand alone model for instance to describe a market quoted implied volatility surface using only a handful of parameters. But it can also be one of the best choices to enhance a term structure model with a stochastic volatility feature. We introduced the model and reviewed the parametrization by considering the effect of changing each parameter with respect to an initial parameter set.

References

Andersen, L., & Piterbarg, V. (2010). *Interest rate modeling—Volume I: Foundations and vanilla models*. Atlantic Financial Press.

Derman, E., & Kani, I. (1994). Riding on a smile. *Risk*, *7*, 32–39.

Dupire, B. (1994). Pricing with a smile. *Risk*, *7*, 18–20.

Forde, M., Jacquier, A., & Lee, R. (2012). The small-time smile and term structure of implied volatility under the Heston model. *SIAM Journal on Financial Mathematics*, *3*(1).

Gatheral, J. (2006). *The volatility surface*. Wiley.

Hagan, P. S., Kumar, D., Lesniewski, A. S., & Woodward, D. E. (2002). Managing smile risk. *Wilmott Magazine*, *1*, 84–108.

Heston, S. (1993). A closed form solution for options with stochastic volatility with applications to bond and currency options. *The Review of Financial Studies*, *6* (2), 327–343.

Kienitz, J. (2014). *Interest rate derivatives explained: Volume 1 products and markets*. Palgrave McMillan.

Kiesel, R., & Lutz, M. (2010). Efficient pricing of CMS spread options in a stochastic volatility LMM. *Working Paper, SSRN*.

7

The SABR Model

7.1 Introduction and Objectives

This chapter is devoted to one of the most famous models used for smile and skew modelling in the interest rate markets. The **S**tochastic **A**lpha **B**eta **R**ho model or SABR in short was introduced in Hagan et al. (2002) and due to its ease of use and its flexibility was always among the first choice by practitioners. However, the events starting in August 2007 have also impacted the use of the SABR model. The popular approximation formula for assigning an implied Black–Scholes volatility given a strike and a maturity could not safely be used. This made it necessary to consider more sophisticated numerical techniques and at latest when negative interest rate occured for currencies as CHF or EUR even the model had to be developed further.

The current chapter is not only a description of the SABR model but also gives the different numerical treatments and the model extensions it reflects the changes taken place in the interest rate market. We structured this chapter into seven sections. We introduce the SABR model in Sect. 7.2 and illustrate its applications in Sect. 7.4. To really apply the SABR model in practice it has to be properly implemented and not just using the approximation formula which made it so popular. To understand the necessary numerical techniques we included Sect. 7.5 where an overview of the methods is given. For extensions and special versions of the model we have Sect. 7.6. Here the obvious extensions to cover negative rates can be found and we give guidance on how to adapt

© The Author(s) 2017

J. Kienitz and P. Caspers, *Interest Rate Derivatives Explained: Volume 2*,
Financial Engineering Explained, DOI 10.1057/978-1-137-36019-9_7

the numerics to cope with negative rates. The Sect. 7.7 summarizes recent developments around the SABR model and illustrates its application. Finally, we summarize and conclude this chapter by Sect. 7.8.

7.2 Introduction

The SABR (stochastic α, β, ρ) model was introduced in Hagan et al. (2002) to manage the smile risk.

$$dS(t) = \sigma(t)C(S(t))dW(t) \tag{7.1}$$

$$d\sigma(t) = \sigma(t)\nu dZ(t) \tag{7.2}$$

$$\langle dW(t), dZ(t)\rangle = \rho dt. \tag{7.3}$$

$$(S(0), \sigma(0)) = (S_0, \sigma_0)$$

S_0 is the spot asset price, σ_0 is the spot value of volatility. In Hagan et al. (2002) this parameter was termed α. β is the CEV exponent, the volatility of volatility ν and the correlation ρ between the Brownian motions W and Z. The function $C(\cdot)$ is $C(S) = S^\beta$ for the classic SABR model and can be chosen by the modeller. The choice of C means to determine the local volatility (backbone) of the SABR model. Popular choices include $C(S) = (S + a)^\beta$ or, recently, $C(S) = |S|^\beta$.
Using an approximation formula for implied Black volatility derived in Hagan et al. (2002) it is possible to apply the Black formula to price European Call and Put options. To this end the implied Black volatility σ_{BS} is replaced by a function, σ_{SABR}, depending on the strike K, the maturity T and the SABR model parameters

$$\sigma_{\mathrm{B76}}(K,T) \approx \frac{\sigma_0}{(SK)^{\frac{1-\beta}{2}}\left(1 + \frac{(1-\beta)^2}{24}\log^2(S/K) + \frac{(1-\beta)^4}{1920}\log^4(F/K) + \dots\right)} \frac{z}{x(z)}$$
$$\left(1 + \left(\frac{(1-\beta)^2\sigma_0^2}{24(SK)^{1-\beta}} + \frac{\rho\beta\nu\sigma_0}{4(SK)^{\frac{1-\beta}{2}}} + \nu^2\frac{2-3\rho^2}{24}\right)T + \dots\right),$$

with

$$z = \frac{\nu}{\sigma_0}(SK)^{\frac{1-\beta}{2}}\log(S/K), \quad x(z) = \log\left(\frac{\sqrt{1-2z\rho+z^2}+z-\rho}{1-\rho}\right).$$

We reproduced the original formula given in Hagan et al. (2002) here. Many extensions and improvements upon this formula exist, for instance the version derived in Obloj (2007). For a summary of approximation formulae not only to the implied volatility we refer to Kienitz and Wetterau (2012).

Since the current interest rate markets with very low or even negative rates and high volatility implies that it is often not possible to quote options using the concept of implied Black volatility it is convenient to have a formulae for implied Bachelier volatility (or Normal volatility).

This is due to the fact that for the standard Black 76 approach or even in the displaced diffusion setting it is not always possible to quote option prices in terms of the implied volatility. Formula 6.6 implies an upper bound on the option price if we consider the right hand side of the formula as a function of the volatility parameter. This is not the case for the Bachelier model. Within this model there are no bounds on the European Call option prices.

We have (7.4) for the implied Bachelier volatility:

$$\begin{aligned}\sigma_N(K) = &\frac{\sigma_0}{(F-K)}\frac{\xi}{x(\xi)}\int_K^F \frac{df}{C(f)} \\ &\times\left(1+\left(g\sigma_0^2+\frac{\rho\nu\sigma_0}{4}\frac{C(F)-C(K)}{F_K}+\frac{2-3\rho}{24}\nu^2\right)T+\cdots\right)\end{aligned} \tag{7.4}$$

with

$$\xi = \frac{\nu}{\sigma_0}\int_K^F \frac{df}{C(f)} \quad x(\xi) = \log\left(\frac{\sqrt{1-2\rho\xi+\xi^2}-\rho+\xi}{1-\rho}\right)$$

$$g = \log\left(\frac{1}{F-K}\int_K^F \frac{\sqrt{C(F)C(K)}}{C(f)}df\right) / \left(\int_K^F \frac{df}{C(f)}\right)$$

To account for the different local volatilities we set $C(f) = f^\beta$ for the classic SABR, $C(f) = f + b$ for the displaced stochastic volatility model and $C(f) = (f+b)^\beta$ for displaced SABR. While the approximation formulas are very easy to implement and fast to execute on a computer they also have severe shortcomings. For instance for large values of ν and long maturities the formulas deviate significantly from the results implied by the SABR model. Furthermore, very short rates and large volatilities imply arbitrage. This is due to the fact that the probability density p_{SABR} calculated using $p_{\text{SABR}} \sim \frac{\partial^2 C(K,T)}{\partial K^2}$ where the option prices are calculated by plugging in the implied volatility from (7.4) leads to negative values. Figure 7.1 illustrates this fact.

Before we proceed let us study the effect of the model parameters on the implied Bachelier volatility. Using the methodology described above also affects

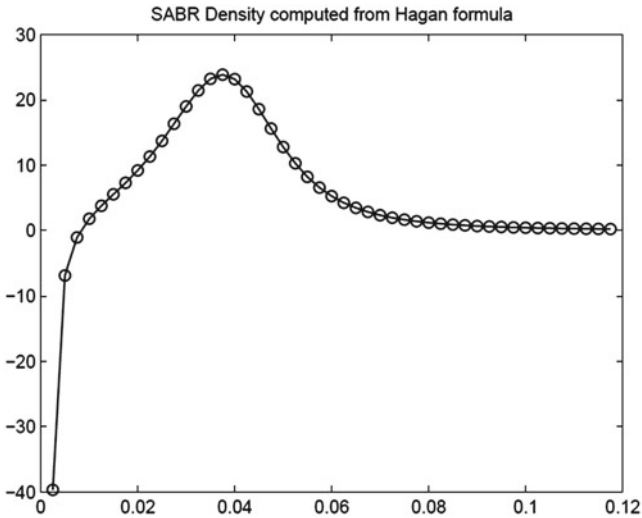

Fig. 7.1 Negative values if the risk neutral density is calculated with the volatility from (7.4) as an input

the risk neutral density. For the SABR model the density is not available in closed form but approximation formulae exist, see Hagan et al. (2005), Henry-Labordere (2005), Paulot (2009) or Wu (2010). From 7.2 we see the effects of changing parameters and expect that the SABR model can be used to fit the observed market smiles due to its flexibility. We wish to gain an intuition for the parameters in this model. To this end we proceed as for the classic SABR model. We take as a base scenario $\sigma_0 = 0.005095939$, $\beta = 0.1$, $\nu = 0.3$, $\rho = -0.3$, $f_0 = 0.005$ and $T = 5$.

From Fig. 7.2 we can see the effects on the implied volatility for a given maturity. The spot value of the volatility determines the overall level of the volatility. It is closely linked to current at the money volatility. Changing this value leads mainly to a parallel shift of the volatility. To a much smaller extent this parameter effects the steepening around the money strike. The exponent β leads to the steepening of the skew/smile when decreased and it lowers the level of the smile as it increases and, finally, it is possible to control the curvature which increases if we decrease β. The correlation parameter ρ is used to control the slope of the skew/smile moving the values into negative territory it gets more negatively sloped. The effect for moving the parameter to positive values is the opposite. It also has a small effect on the curvature and, thus, have a similar effect as β but to a much more smaller extent. The volatility of volatility ν increases the curvature. An increase in β and ρ leads to a decrease in volatility for the out of the money region and an increase in

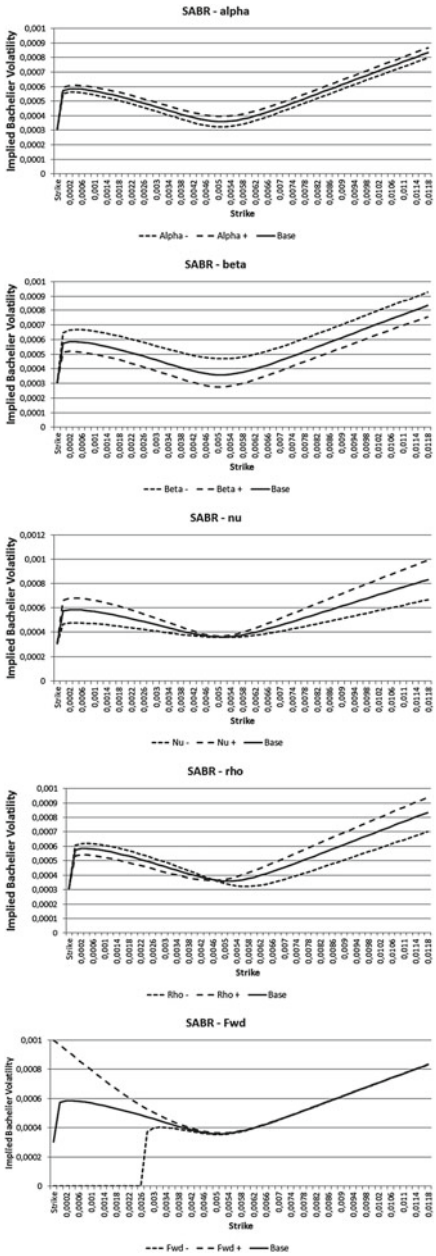

Fig. 7.2 Implied Bachelier volatility—intuition for the parameters determining the SABR model for *top* to *bottom* we have σ_0, resp. α, β, ν, ρ and f_0

the money region. This is the slope. In contrast ν moves both regions which corresponds to a move in curvature. Before we proceed to recent applications of the SABR model we shortly summarize why the model has been attractive to market participants.

- Application of the SABR model is fast and easy to code due to (7.4)
- The model is flexible and can reproduce many shapes of the market implied volatility
- The effect of changing model parameters has an interpretation in terms of changes in the shape of the smile.

The attractive features made the SABR model very popular and still it is widely applied in practice. However, the financial crisis and the new market reality with negative rates and high volatilities makes it necessary to consider the shortcomings which are

- Far in the money prices can lead to negative values of the risk neutral density when calculated using (7.4)
- Implied volatility deviates from the model implied one for large values of ν or T
- The wings of the standard SABR model imply to high prices for CMS products and CMS derivatives.

On one hand we need to incorporate the market reality such as negative rates into our modelling framework. On the other hand we observe that the standard easy to code approximation formulae cannot be applied any longer.

The risk neutral density corresponding to a model is in general not known in closed form. To this end it is only possible to compute the density numerically or deriving approximate solutions. We consider the following methods:

(1) Risk neutral density from Call prices using the second derivative $\frac{\partial^2 C}{\partial K^2}$
(2) Risk neutral density from the characteristic function and application of inversion of Fourier transform
(3) Approximate solutions using Riemannian geometry, Perturbation analysis and Forward and Backward Kolmogorov equations.

Why do we need the full implied volatility skew/smile. In Kienitz (2014) we used the skew/smile to calculate a convexity adjustment for CMS or applied copula methods including the marginal probability distribution of CMS rates to price CMS spread options. Thus, extrapolation for very low and very high

strikes is necessary and numerical experiments show that the standard approximation formula of the SABR model cannot be used since it may produce negative values for the density, see Fig. 7.1. Possible solutions include ad hoc methods such as constant extrapolation, using regimes of volatility, price extrapolation, Benaim et al. (2010), density extrapolation, Kienitz (2011), density approximation, Doust (2012) or more recent methods such as numerical integration, see Antonov and Spector (2012). While such methods can be used in practice the desired method is some efficient robust numerical method that is based on the dynamics of the SABR model and, thus, allows for the interpretation of the parameters. In the sequel we consider some more sophisticated approximation techniques as well as a numerical techniques based on Finite Difference methods.

7.3 Approximation

It is possible to enhance the current approximation methods by including higher order terms to account for the weaknesses of the original approximation formulas or including a parameter which allows to control the slope of the wings implied by SABR. In the sequel we provide some ideas in this direction but our view is that more sophisticated numerical methods such as finite difference methods need to be applied in the current market environment.
Let us start with the more sophisticated approximation formulas. To this end we consider

$$\sigma(K,T) = \underbrace{\sigma_0}_{(1)} \underbrace{\frac{K-f}{\int_f^K C(g)^{-1}dg}}_{(2)} \underbrace{\frac{z}{Y(z)}}_{(3)} \cdot \underbrace{A}_{(4)} \tag{7.5}$$

with A being $\sqrt{1-\Theta T}$ if $\Theta < 0$, Y defined below and $\frac{1}{\sqrt{1+\Theta T}}$ if $\Theta \geq 0$ and

$$\begin{aligned}
\Theta &= -\frac{1}{2}\rho\nu\sigma_0 C'(f_0) - \frac{2}{3}\sigma_0 s_K \\
\Delta &= 2C(f_0)C''(f_0) - (C'(f_0))^2 \\
s_K &= \frac{\nu^2}{8\sigma_0 Y(z)}\left(-Y(z) + 3\frac{z+\rho-\rho\sqrt{1+2\rho z+z^2}}{\sqrt{1+2\rho z+z^2}}\right) \\
&\quad + \frac{\Delta}{16Y(z)}\left((1-\rho)^2 Y(z) + (z+\rho)\sqrt{1+2\rho z+z^2} - \rho\right)
\end{aligned}$$

The formula (7.5) accounts for higher order terms not being represented in the original approximation formulas. We have that (1) is the overall level of volatility, (2) describes the main effect from local volatility, (3) is the main effect from stochastic volatility and (4) accounts for higher order terms.

Now, we consider controlling the slope of the wing. Since we use Geometric Brownian Motion for the stochastic volatility the values can get very large. Especially for large values of ν and T. For instance, we wish to use the whole volatility smile for pricing CMS related products the volatilities for the right wing of the smile might take to large values. To this end we cap this effect using a constant M.

For our purpose we take

$$D_M(F) := \min\left(D(F), M\right) = \min\left(\sqrt{1 + 2\rho\nu z + \nu^2 z^2}, M\right) \tag{7.6}$$

Of course we have to account for (7.6) everywhere in our numerical implementation. To this end we replace the original variables in the approximation formulas using

$$Y(z) = \begin{cases} Y_+ + (z - z_+)/M & , z > z_+ \\ -\log\left(\frac{\sqrt{1-2\rho z+z^2}}{1-\rho}\right) & , z_- < z < z_+ \\ 1Y_+ + (z - z_-)/M & , z < z_- \end{cases}$$

with

$$z_\pm = -\rho \pm \sqrt{M^2 - 1 + \rho^2}, \quad Y_\pm = \log\left(\frac{M \pm \sqrt{M^2 - 1 + \rho^2}}{1 + \rho}\right)$$

Furthermore, we take for $z > z_+$:

$$\begin{aligned} s_K = \frac{\nu^2}{8\sigma_0 Y(z)}&\left(-Y_+ + 3\frac{-M\rho + \sqrt{M^2 - 1 + \rho}}{M}\right) \\ &+ \frac{\Delta}{16Y(z)}\Big(2M^2(Y(z) - Y_+) + (1 - \rho^2)Y_+ \\ &+ M\sqrt{M^2 - 1 + \rho^2} - \rho\Big), \end{aligned}$$

for $z < z_-$

$$s_K = \frac{\nu^2}{8\sigma_0 Y(z)}\left(-Y_- + 3\frac{M\rho + \sqrt{M^2 - 1 + \rho}}{M}\right) + \frac{\Delta}{16Y(z)}\left(2M^2(Y(z) - Y_-) + (1-\rho^2)Y_- + M\sqrt{M^2 - 1 + \rho^2} - \rho\right)$$

and for the standard case $z_- < z < z_+$:

$$s_K = \frac{\nu^2}{8\sigma_0 Y(z)}\left(-Y(z) + 3\frac{z + \rho - \rho\sqrt{1 + 2\rho z + z^2}}{\sqrt{1 + 2\rho z + z^2}}\right) + \frac{\Delta}{16Y(z)}\left((1-\rho^2)Y(z) + (z+\rho)\sqrt{1 + 2\rho z + z^2} - \rho\right)$$

We show the effect of the dampening by considering Fig. 7.3. The right wing of the implied volatility can be controlled by choosing the dampening parameter. This directly impacts the prices for convexity adjustments for instance. Since using the replication method described in Kienitz (2014) the replicating instruments are priced using different values of the implied volatility if different dampening parameters are chosen.

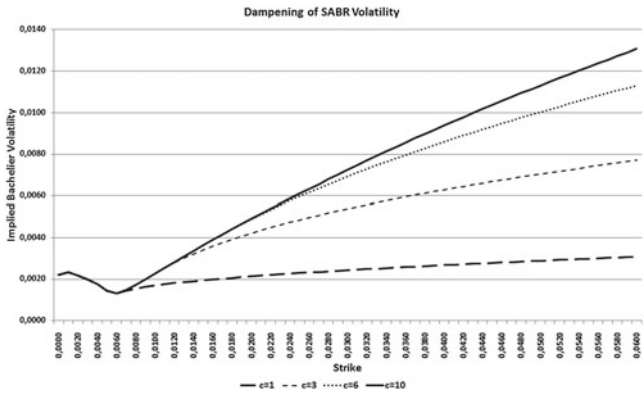

Fig. 7.3 Applying the dampening method to the SABR model for different values of the dampening parameter M

7.4 Applications and Calibration

The main applications of the SABR model is to parameterize the implied volatility surface. In practice, one considers a slice of the surface. A slice consist of the implied volatility values for a fixed maturity. Thus, a slice is a function of the strike values.

The parametrization of one slice consists of finding the SABR parameters σ, β, ν and ρ such that the implied volatility is reasonably fitted. In practice, this is called the calibration of the model. To calibrate the model it is standard to consider a distance measure. This distance measure is a function For instance, consider swaption prices. Let $V(K_i, T)$, $i = 1, \ldots, N$ be N market prices of swaptions of maturity T on a fixed swap rate. We also consider the model prices $\tilde{V}_{\sigma,\beta,\nu,\rho}(K_i, T)$. Then, we take as distance function

$$\frac{1}{N}\sum_{i=1}^{N}\left(V(K_i, T) - \tilde{V}_{\sigma,\beta,\nu,\rho}(K_i, T)\right)^2$$

Strategies for minimizing this function:

- The parameter β
  - **CMS**
    In Kienitz (2014) we saw how to price CMS Caps and Floors by replication. To this end the whole skew/smile has to be taken into account. Since the value of β is one parameter that affects the shape of the skew/smile we can choose the value such that the observed CMS Caps and Floors are priced with the least error.
  - **Regression**
    For the regression method it is a standard practice to take the forward rates on the x-axis and the ATM volatilities on the y-axis and consider the least squares regression. Figure 7.4 illustrates the method. The β value which best matches the market data is taken to determine the backbone of the SABR model.
  - **Fixing**
    Sometimes the parameter is fixed by the modeller and only the other parameters are calibrated.
- Fitting σ
  Once the parameter β is determined by one of the methods described above the calibration strategy is to let only the parameters ρ and ν vary and determine σ to exactly match the ATM volatility. The fitting of σ can be

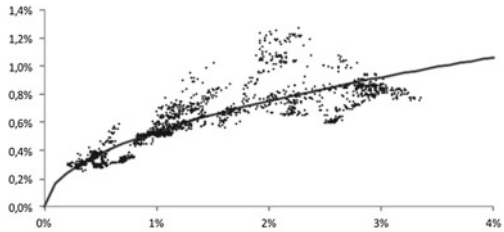

Fig. 7.4 Regression to determine CEV coefficient β

done using either the approximation formula and solve for the parameter value or if one does not wish to rely on approximation formulae the full numerical evaluation using a PDE method, described in Sect. 7.5, can be used.

Now, that we are able to determine the SABR parameters for a given slice we need to glue the slices together. To this end we consider the maturities $T_1, \ldots, T_N$ to which we fitted a SABR model. Call the parameters $\sigma_{0,i}$, β_i, ρ_i and ν_i. Of course there are now many different possibilities to glue the parameters and in practice many of such approaches are found. For instance, the modeller can use a parametric function f_j, $j = 1, 2, 3, 4$ with parameters $\gamma_{j,1}, \ldots, \gamma_{j,m_j}$ and choose the parameters such that the calibrated SABR parameters fits best in a least square sense. For instance we can take of σ:

$$\min_{\gamma_{1,1},\ldots,\gamma_{1,m_1}} \left\{ \left(\sum_{i=1}^{N} \left(\sigma_{0,i} - f(\gamma_{1,1}, \ldots, \gamma_{1,m_1})\right)^2 \right)^{0.5} \right\}$$

Another application of the SABR model is to enhance a term structure model with a stochastic volatility component. This approach is considered in Rebonato et al. (2009) or Mercurio and Morini (2009). In Chap. 12 we show how to do this enhancement but choosing another stochastic volatility model since the SABR setting poses some difficulties. These difficulties are related to the fact that the SABR model is a model for the forward rate and is not that easy combined with a term structure.

7.5 Numerical Technics for SABR

Several numerical techniques are applied to implement financial models. For the SABR model we suggest to apply Finite Difference Techniques, see Hagan (2013), LeFloch and Kennedy (2013).

In Hagan et al. (2015) a single partial differential equation was derived, called the *effective PDE* which approximate the evolution of the probability density of the forward governed by a SABR model, (7.7).

$$\begin{aligned} dF(t) &= D(F)\sqrt{E(T,F)}dW \\ F(0) &= f \end{aligned} \tag{7.7}$$

The effective Eq. (7.8) is given by

$$\begin{aligned} Q_T &= \frac{1}{2}[D^2(F)E(T,F)Q]_{FF} \\ Q(0) &= \delta(F-f) \end{aligned} \tag{7.8}$$

This equation is for the evolution of the density evolving from the point mass which is placed at the current forward level to the density at maturity. The probability Q corresponds to

$$Q(T,F;f)dF = \mathbb{P}\left(\bar{F} < F < \bar{F} + dF | F(0) = f\right)$$

We do not show how to derive this effective equation here but we outline how to solve it numerically to be useful for practical applications. The function D is given by (7.9),

$$D^2(F) = \left[\left(\sigma_0^2 + 2\rho\nu y\sigma_0 + \nu^2 y^2\right)\exp\left(\rho\nu v\Gamma(F)(T-t)\right)C^2(F)\right] \tag{7.9}$$

First, this type of SDE/PDE appears for general local volatility models as well as for stochastic volatility models by considering its effective equation, see Hagan et al. (2016). To this end we numerically compute the density by applying conservation of probability, that is the probability mass is equal to 1 at each step of the procedure. This is often a problem to achieve. But also we wish to apply conservation of forward, that is we wish to obey the martingale property at each step which is often a problem too. The application of conservation needs appropriate boundary conditions and efficient schemes.

Finally, when we have computed the density at maturity we need to think about the actual pricing. Simple numerical summation would be too crude for pricing purposes since the strike is not necessary part of the grid which we construct during the numerical procedure.

While the method can be applied using different numerical schemes and grid construction techniques we outline the procedure from Hagan (2013). First, we consider a standard/equi-distant grid

$$x_i = -a + h \cdot i, \quad i = 0, \ldots, N_x =: N$$
$$t_j = s \cdot j, \quad j = 0, \ldots, N_t =: M$$

with $h = \frac{2a}{N}$ and $s = \frac{T}{M}$. Since, for accurately solving the equation by Finite Difference methods often 4–6 standard deviations above the forward are required. This means that on such a grid nearly all grid points ly above the forward. For instance if the spot is 1% to cover the full range of 4-6 standard deviations we might need rates up to 200%. Keeping equi-distance then only a few rids points ly below 1%. This should be handled more efficiently. We consider the transform

$$z(F) = \int_f^F D(g)^{-1} dg$$

This transformation transforms the original domain to a more suitable one in the new coordinates. For instance taking the values $f = 1$, $\sigma = 0.35$, $\beta = 0.25$, $\rho = -0.1$, $\nu = 1$ and $T = 1$ we get from the standard grid the new coordinates shown in Fig. 7.5.

Thus, we now consider a finite difference scheme for new, the z-coordinates. The obtained solution in terms of z has then be transformed back to the original coordinates, (7.10). The details of the transformation are

$$C(z) = D(F(z)) \tag{7.10}$$

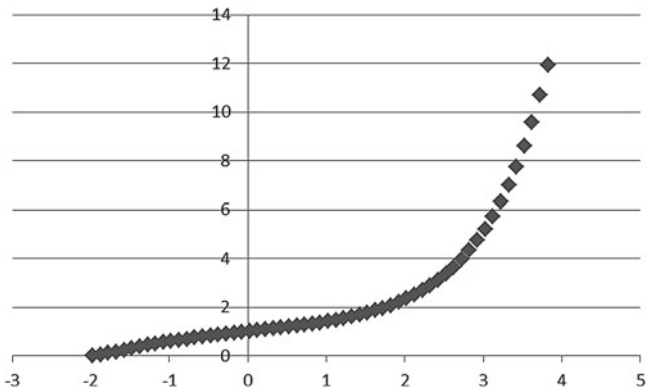

Fig. 7.5 Coordinate transformation for the equidistant grid to a more suited one

This changes the differentiation. But we are able to compute this, (7.11),

$$\frac{dz}{dF} = \frac{1}{D(F)} = \frac{1}{C(z)}, \quad \frac{dF}{dz} = D(F) = C(z) \tag{7.11}$$

and the function F is given by (7.12)

$$F(z) = \int_0^z C(x)dx \tag{7.12}$$

as well as, (7.13)

$$\frac{\partial}{\partial F} = \frac{1}{D(F)}\frac{\partial}{\partial z}. \tag{7.13}$$

To keep track of conserving the probability mass and the martingale property during the solution process, we have to calculate integrals of the form

$$\int_A^B Q(T, F)dF, \quad \int_A^B FQ(T, F)dF$$

which are given in the new coordinates as

$$\int_{z(A)}^{z(B)} Q(T, F)C(z)dz, \quad \int_{z(A)}^{z(B)} F(z)Q(T, z)C(z)dz$$

Writing the original density (for f) in terms of z we have to consider

$$q(T, z) = Q(T, F(z))D(F(z)) = Q(T, z)\frac{dF}{dz}$$

This leads to consider (7.14)

$$q_T = \frac{1}{2}D(F)[D(F)E(T, F)q]_{FF} = \frac{1}{2}\frac{\partial}{\partial z}\left(\frac{1}{C(z)}[C(z)E(T, z)q]_z\right) \tag{7.14}$$

with accounting for the flow on the boundaries

$$q(T, z) = 0 \;\; F \to z^- \left(= z(F^-)\right) \quad q(T, z) = 0 \;\; F \to z^+ \left(= z(F^+)\right)$$

and the initial condition $q(0, z) = \delta(z)$.

$$D(F) = \sqrt{1 + 2\rho\nu\left(\int_f^F |g|^{-\beta} dg\right) + \nu^2\left(\int_f^F |g|^{-\beta} dg\right)^2}$$
$$E(T, F) = \exp(v\rho\nu\Gamma T)C(F)$$
$$\Gamma = \Gamma(F) = \frac{C(F) - C(f)}{F - f}$$

First, conservation of the mass leads to consider

$$Q^L + \int_{F_{\text{Min}}}^{F_{\text{Max}}} Q dF + Q^R = 1 \to 0 = \frac{d}{dT}\left(Q^L + \int_{F_{\text{Min}}}^{F_{\text{Max}}} Q dF + Q^R\right)$$

which requires to take

$$\frac{dQ^L}{dT} = \lim_{F \downarrow F_{\text{Min}}} \frac{1}{2}\left[D^2(F)E(T, F)Q\right]_F, \quad Q^L(0) = 0$$

and

$$\frac{dQ^R}{dT} = -\lim_{F \uparrow F_{\text{Max}}} \frac{1}{2}\left[D^2(F)E(T, F)Q\right]_F, \quad Q^R(0) = 0$$

for the left, respectively right boundary.

Second, to preserve the martingale property we take the conservation given by

$$F_{\text{Min}} Q^L(T) + \int_{F_{\text{Min}}}^{\infty} F Q D F + F_{\text{Max}} Q^R(T) = f$$

which means to consider

$$0 = \frac{d}{dT}\left(Q^L + \int_{F_{\text{Min}}}^{F_{\text{Max}}} Q dF + Q^R\right)$$

and, thus,

$$D^2(F)E(T, F)Q \to 0, \quad F \downarrow F_{\text{Min}} \quad D^2(F)E(T, F)Q \to 0, \quad F \uparrow F_{\text{Max}}$$

For the discretization we let the z-grid start approximately N standard deviations from the forward. This means we consider

$$z^- := \max\left(z_0, -N\sqrt{T}\right), \quad z^+ = N\sqrt{T}$$

In terms of the original variables we have

$$F^- = F(z^-), \quad F^+ = F(z^+)$$

and for the new coordinates the grid is

$$z_j = z^- + jh, \quad j = 1, \ldots, J$$

For the transformed density we set q_j to be equal to the probability for the interval between z_{j-1} and z_j in the spirit that

$$hq_j(T) = \int_{zj-1}^{z_j} q(T, z)dz = \int_{F(z_{j-1})}^{F(z_j)} Q(T, F)dF$$
$$F_{j-\frac{1}{2}}q_j(T) = \int_{zj-1}^{z_j} F(z)q(T, z)dz = \int_{F(z_{j-1})}^{F(z_j)} FQ(T, F)dF$$

where

$$F_{j-\frac{1}{2}} := F(z_{j-\frac{1}{2}}) := F(z_{\text{Min}} + [j - \frac{1}{2}]h)$$

This means that it is the constant, in fact integrated, density between the grid points z_{j-1} and z_j. For the second equality to hold we need to extend our arguments. We choose to discretize the PDE

$$\frac{\partial q_j}{\partial T} = \frac{1}{2h}\left(\frac{S_{j+1} - S_j}{h\bar{C}_j} - \frac{S_j - S_{j-1}}{h\bar{C}_{j-1}}\right)$$

setting

$$S_j := C_{j-\frac{1}{2}}E_{j-\frac{1}{2}}q(T, z_j) = D(F_{j-\frac{1}{2}})E(T, (F_{j-\frac{1}{2}})q(T, z_j)$$

Then, this choice preserves the expected value since (with the bar notation)

$$h\bar{C}_j := F_{j+\frac{1}{2}} - F_{j-\frac{1}{2}} = \int_{z_{j-1}}^{z_j} (C(z)dz)$$

We also have to consider the boundaries and ensure that the conservation is preserved in our numerical procedure. We use the space discretization $z_j = z^- + jh$ leading to $y_j = y(z_j - \frac{h}{2})$. Furthermore for the function values at the discretization nodes we set $F_j = F(y_j), C_j = D(F_j)\,\Gamma_j = \frac{C(F_j)-C(f)}{F_j - f}$ and $E_j(T) = \exp(\rho\nu\sigma\Gamma_j T)$. For the time discretization we take $t_n = nT/N$. This means the value of the quantity q we are interested in can be written in short notation as $q_j^n = q(z_j, t_n)$. This is for $j = 1, \ldots, J, \quad n = 0, \ldots, N-1$. Where we take the differentiation on the inner part of the grid by considering

$$\frac{C_{j-1}}{F_j - F_{j-1}} E_{j-1}(t_n) q_{j-1}^n = -\frac{1}{\Delta}\left(\frac{C_j}{F_{j+1} - F_j} + \frac{C_j}{F_j - F_{j-1}}\right) E_j(t_n) q_j^n + \frac{1}{\Delta}\frac{C_{j+1}}{F_{j+1} - F_j} E_{j+1} q_{j+1}^n$$

and on the boundaries

$$\frac{C_0}{F_1 - F_0} E_0(T) q(t_0, T) = -\frac{C_1}{F_1 - F_0} E_1(T) q(z_1, T)$$
$$\frac{C_{J+1}}{F_{J+1} - F_J} E_{J+1} q(t_{J+1}, T) = -\frac{C_J}{F_{J+1} - F_J} E_J(T) q(z_J, T)$$

Implementation of this procedure leads the SABR density (preserving the probability mass and the martingale property). Figure 7.6 illustrates the outcome of the procedure for the SABR and the Free SABR model.
The well known Crank–Nicolson scheme, see Crank and Nicolson (1996) and Duffy (2006) for an overview and a report on the performance Duffy (2004),

$$q_j^{n+1} - q_j^n = \frac{\Delta}{2}\left(L_j^{n+1} q_j^{n+1} + L_j^n q_j^n\right)$$
$$Q^L(t_{n+1}) - Q^L(t_n) = \frac{\Delta}{2}\frac{C_1}{F_1 - F_0}\left(E_1(t_{n+1}) q_1^{n+1} + E_1(t_n) q_1^n\right)$$
$$Q^R(t_{n+1}) - Q^R(t_n) = \frac{\Delta}{2}\frac{C_J}{F_{J+1} - F_J}\left(E_J(t_{n+1}) q_J^{n+1} + E_J(t_n) q_J^n\right)$$

applied to solve this equation leads to unreasonable and erroneous results. For too few time steps we observe that there are large oscillations from which we conclude that this scheme should be applied with great care or even be

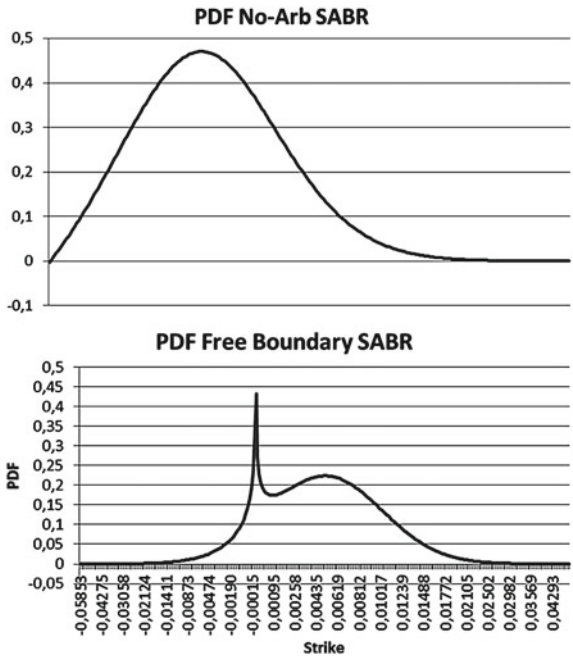

Fig. 7.6 Densities for the SABR (*top*) and the free boundary SABR (*bottom*) models

fully abandoned. We suggest to consider a scheme due to Lawson and Swayne (1976) and suggested to apply to Forward Kolmogorov equation in LeFloch and Kennedy (2013). Setting $b = 1 - \frac{1}{2}\sqrt{2}$ this scheme is given by a three step procedure. The first step determines the densities by solving

$$
\begin{aligned}
q_j^{n+b} - q_j^n &= b\Delta L_j^{n+b} q_j^{n+b} \\
Q^L(t_{n+b}) - Q^L(t_n) &= b\Delta \frac{C_1}{F_1 - F_0} E_1(t_{n+b}) q_1^{n+b} \\
Q^R(t_{n+b}) - Q^R(t_n) &= b\Delta \frac{C_J}{F_{J+1} - F_J} E_J(t_{n+b}) q_J^{n+b}
\end{aligned}
$$

The second one uses the results from the first step and the following system has to be solved

$$
\begin{aligned}
q_j^{n+2b} - q_j^{n+b} &= b\Delta L_j^{n+2b} q_j^{n+2b} \\
Q^L(t_{n+2b}) - Q^L(t_{n+b}) &= b\Delta \frac{C_1}{F_1 - F_0} E_1(t_{n+2b}) q_1^{n+2b} \\
Q^R(t_{n+2b}) - Q^R(t_{n+b}) &= b\Delta \frac{C_J}{F_{J+1} - F_J} E_J(t_{n+2b}) q_J^{n+2b}
\end{aligned}
$$

Finally, to obtain the result at the next grid point we have to solve

$$
\begin{aligned}
q_j^{n+1} &= (\sqrt{2}+1) q_j^{n+2b} - \sqrt{2} q_j^{n+b} \\
Q^L(t_{n+1}) &= (\sqrt{2}+1) Q^L(t_{n+2b}) - \sqrt{2} Q^L(t_{n+b}) \\
Q^R(t_{n+1}) &= (\sqrt{2}+1) Q^R(t_{n+2b}) - \sqrt{2} Q^R(t_{n+b})
\end{aligned}
$$

Stepping through the whole grid leads to a density at maturity T. Knowing this density it is possible to price European options. We outline the procedure for pricing options given the density. First, only pricing of European options depending on the density at maturity is possible. Thus, we take payoffs V, (7.15), which we integrate with respect to this density

$$
V(T, K) = \int_K^\infty h(F) Q(T, F) dF \tag{7.15}
$$

We illustrate our approach by taking the payoff of a European Call option, that is $h(F) = (F - K)^+$. First, we need to remind the reader of the coordinate transformation given by (7.16)

$$
z(F) = \int_f^F D(g)^{-1} dg \tag{7.16}
$$

We assume that for the strike level $z_{k-1} < z(K) \leq z_k$. The call option price is approximated by (7.17)

$$
C(T, K) \approx \int_{z(K)}^{z_J} (F(z) - K) q(T, z) dz + (F_{\text{Max}} - K) Q^L(T) \tag{7.17}
$$

This approximation is illustrated by Fig. 7.7. Each Mathematically, the approximation illustrated in Fig. 7.7 is the sum of the areas of all rectangles. This is Eq. (7.18).

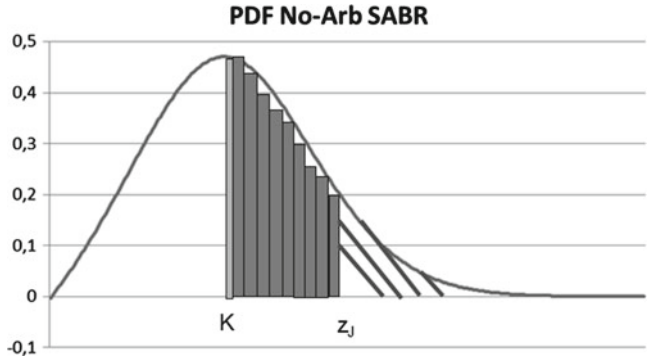

Fig. 7.7 Illustration of the pricing using the effective equation

$$C(T,K) = \int_{z(K)}^{z_k} (F(z) - K) q(T,z) dz + \sum_{j=k+1}^{J} (F_{j-\frac{1}{2}} - K) h q_j(T) + (F_{\text{Max}} - K) Q^R(T) \quad (7.18)$$

Thus, the calculation of the option price is a summation. But we need to approximate the integral which makes it necessary to consider the sub-grid behaviour for the density.

7.6 Extensions of SABR

Let us shortly review some generalisations of the SABR model. First, to be able to consider negative rates we consider a Displaced, respectively a Normal SABR model. This generalisation can be done by simply choosing another function C. Another generalisation is described in Andreasen and Huge (2012). Here the volatility process is taken to be of CEV type. The model is known as the ZABR model.

7.6.1 Displaced/Normal SABR

The Displaced Diffusion and the Normal SABR are simple variants of the original SABR model. The variants correspond to choosing the local volatility function $C(S) = (S + a)^{\beta}$ for the Displaced model and $C(S) = 1$ for the Normal model. The numerical techniques presented so far can directly be applied.

For the Normal SABR model a closed form solution in terms of an integration is available. Different to the Free SABR model this solution is valid for all values of ρ. The price of a European Call option is (7.19)

$$C(T,K) = (f-K)^+ + \frac{V_0}{\pi}\int_{s_0}^{\infty} \frac{G(\gamma^2 T, s)}{\sinh(s)} \sqrt{\sinh^2(s) - (k - \rho\cosh(s))^2} ds \tag{7.19}$$

with

$$\cosh(s_0) = \frac{-\rho k + \sqrt{k^2 + (1-\rho^2)^2}}{(1-\rho^2)^2}, \quad k = \frac{\gamma(K - F_0)}{v_0} + \rho$$

The Displaced and the Normal SABR models can be applied to negative rates. For the Displaced SABR model the displacement parameter a has to be chosen appropriately, see Dimitroff et al. (2016).

7.6.2 ZABR

In practice it is often important to control the behaviour of implied volatility on the wings. One approach is to truncate the stochastic volatility effect by applying dampening. This was discussed earlier in this chapter. There are other methods available and practitioners sometimes apply the ZABR model which assumes a CEV dynamic for the volatility process by introducing another CEV exponent β_v. This model was introduced in Andreasen and Huge (2012). The full description of the model is

$$\begin{aligned} dF(t) &= F(t)^{\beta} dW_1(t) \\ dv(t) &= \gamma v(t)^{\beta_v} dW_2(t) \\ \langle dW_1(t), dW_2(t)\rangle &= \rho dt \\ (F(0), v(0)) &= (f, v_0) \end{aligned}$$

Together with the model numerical methods for implying the volatility and price options is discussed. First, Andreasen and Huge (2013) derive a *short maturity expansion* and, then, apply a one step finite difference scheme. This is very efficient since only one system of equations has to be solved instead of discretizing the whole time interval.

Setting $x := (F-k)/\nu$, the call price with strike k and time to maturity T is given by

$$\begin{aligned} c(t,k,T) &= \mathbb{E}_t[(F_T-k)^+] = g(t,F_t,\nu(t)) \\ &:= (F-k)\mathcal{N}(x/\sqrt{T}) + \nu(t)\sqrt{T}n(x/\sqrt{T}), \end{aligned}$$

with $\nu(t)$ being the implied normal volatility and $\mathcal{N}$, respectively n the cumulative distribution, respectively density of the standard normal distribution. Then, using Ito formula we find for c:

$$dc = -g_t dt + g_F dF + \frac{1}{2} g_{FF} dF^2 + g_\nu d\nu + \frac{1}{2} g_{\nu\nu} d\nu^2 + g_{F\nu} dF d\nu.$$

An application of Ito's formula using the definition of x yields the corresponding processes

$$\begin{aligned} dx &= \frac{1}{\nu} dF - \frac{F-k}{\nu^2} d\nu - \frac{1}{\nu} ds d\nu + \frac{F-k}{\nu^3} d\nu^2 = \frac{1}{\nu}(dF - x d\nu) + O(dt) \\ dx^2 &= \frac{1}{\nu^2}(dF^2 + x^2 d\nu^2 - 2x dF d\nu) \end{aligned}$$

Since the derivatives with respect to ν can be calculated using the Bachelier pricing formula we find $g_\nu = \nu t g_{FF}$, $g_{\nu\nu} = \left(\frac{F-k}{\nu}\right)^2 g_{FF}$, $g_{F\nu} = -\frac{F-k}{\nu} g_{FF}$ and $0 = -g_t + \frac{1}{2}\nu^2 g_{FF}$. Taking expectations, using the martingale property on c leads to

$$0 = -\nu^2 dt + dF^2 + 2\nu t \mathbb{E}[d\nu] + x^2 d\nu^2 - 2x dF d\nu = \nu^2(dx^2 - dt) + 2\nu t \mathbb{E}[d\nu]$$

Now, the interesting thing here is that for small t a condition on the diffusion part is given. This condition is the following Eq. (7.20).

$$\sigma_x^2 \equiv \frac{dx^2}{dt} = 1 \tag{7.20}$$

The standard SABR model is a special case, namely $C_v(v) = \gamma v$. To illustrate the methodology for this choice we transform variables by using

$$y = \frac{1}{z} \int_k^F \frac{du}{C(u)}.$$

Using this (transformed) volatility and applying Ito once more we find

$$\begin{aligned} dy &= dW_1 - \gamma y dW_2 + O(dt) \\ &= \sqrt{a + \gamma^2 y^2 - 2\rho\gamma y} dB + O(dt) \\ &= J(y) dB + O(dt) \end{aligned} \tag{7.21}$$

In Eq. (7.21) B is a (new) Brownian motion which as the same variance as the process composed of W_1 and W_2. Since $y(F = k) = 0$ we get x by normalizing the volatility of y

$$\begin{aligned} x &= \int_0^y \frac{du}{J(u)} = \frac{1}{\gamma} \log\left(\frac{J(y) - \rho + \gamma y}{1 - \rho}\right) \\ \nu &= \frac{F - k}{x}, \bar{\nu} = \frac{\log(F/k)}{x} \\ J(y) &= \sqrt{1 + \gamma^2 y^2 - 2\rho\gamma y} \end{aligned}$$

The latter expression can be interpreted as a local volatility model. The Log-Normal Volatilities can be calculated and we also could determine the corresponding Bachelier ones using numerical methods. We have shown the volatilities all as Lognormal ones in Fig. 7.8. In fact the methodology applied above has led to a representation of the associated local volatility for the SABR model. By the chain rule we find:

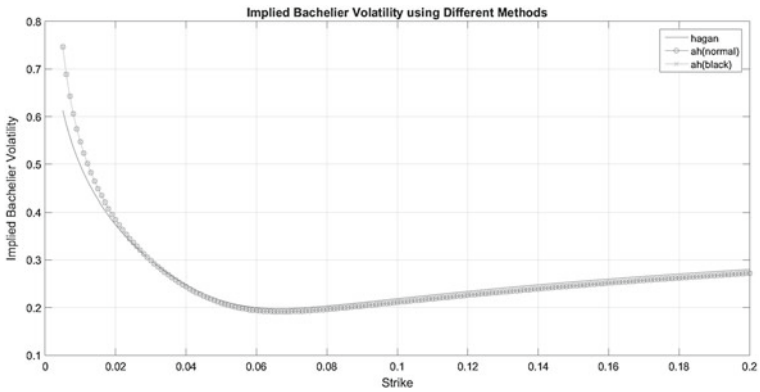

Fig. 7.8 Log-Normal volatilities from Hagan formula, Andreasen–Huge method using log-normal and normal volatilities. The parameters are $v_0 = 0.0873$, $\beta = 0.7$, $\gamma = 0.47$, $\rho = -0.48$, $T = 10$ and $f = 0.0325$

$$\frac{\partial x}{\partial k} = \frac{\partial x}{\partial y}\frac{\partial y}{\partial k} = \frac{1}{J(y)}\left(-\frac{1}{z}\frac{1}{C(k)}\right)$$

Thus, the local volatility $\theta(k)$ is given by:

$$\theta(k) = J(y)zC(k), \quad J(y) := \sqrt{1+\gamma^2 y^2 - 2\rho\gamma y}$$

This gives the guiding idea for the general ZABR model. We have to derive an expression for the local volatility associated to the model. Then, knowing this function specific pricing algorithms can be applied efficiently.

Now, we turn to the general ZABR model. We transform the volatility by considering

$$y = z^{\beta_v - 1}\int_k^F \frac{du}{C(u)}$$

Using Ito's formula it can be shown that

$$dy = z^{\beta_v - 1}(dW_1 + (\beta_v - 2)\gamma y dW_2) + O(dt)$$

Define the process $x = z^{1-\beta_v} f(y)$ and apply Ito to obtain the corresponding SDE. This is

$$dx = f_y(y)dW_1 + ((\beta_v - 2)yf_y(y) + (1-\beta_v)\beta_v f(y))dW_2 + O(dt).$$

To satisfy the diffusion condition (7.20) we need

$$\begin{aligned}
1 &= A(y)f_Y(y)^2 + B(y)f_y(y)f(y) + C \\
A(y) &= 1 + (\beta_v - 2)^2\gamma^2 y^2 + 2\rho(\beta_v - 2)\gamma y \\
B(y) &= 2\rho(1-\beta_v)\gamma + 2(1-\beta_v)(\beta_v - 2)\gamma^2 y \\
C &= (1-\beta_v)^2\gamma^2 \\
f(0) &= 0
\end{aligned}$$

This leads to

$$f_y(y) = \frac{-B(y)f(y)\sqrt{B(y)^2 f(y)^2 - 4A(y)(Cf^2 - 1)}}{2A(y)} (=: F(y, f))$$

This is an ordinary differential equation (ODE). This equation can be solved by discretization. We take

$$\begin{aligned}
\frac{\partial y}{\partial k} &= -\frac{z^{\beta_v - 2}}{C(k)} \\
\frac{\partial x}{\partial k} &= z^{1-\beta_v}\frac{\partial f}{\partial k} = z^{1-\beta_v} f_y(y)\frac{\partial y}{\partial k} = -\frac{F(y, z^{\beta_v - 1}x)}{zC(k)} \\
y(k = s) &= 0, \quad x(k = s) = 0.
\end{aligned}$$

Now, we have a representation for the associated local volatility, Equation (7.22). This is

$$\theta(k) = -\left(\frac{\partial x}{\partial k}\right)^{-1} = zC(k) f_y(y) = \frac{zC(k)}{F(y, z^{\beta_v - 1}, x)}. \tag{7.22}$$

Taking the implied (normal) volatility from the short maturity expansion directly might lead to arbitrage. Thus, we need a refinement. To this end we take the Dupire equation

$$c_t(t, k) = \frac{1}{2}\theta(k)^2 c_{kk}(t, k) \; c(0, k) = (F - k)^+ \tag{7.23}$$

Following the methods from Andreasen and Huge (2012) we also solve

$$c(t, k) - \frac{1}{2}t\theta(k)^2 c_{kk}(t, k) = (F - k)^+ \tag{7.24}$$

The discretization of (7.24) we take

$$(1 - \frac{1}{2}t\theta(k)^2\delta_{kk})c(t, k) = (F - k)^+$$

with δ_{kk} acting on a function f as

$$\delta_{kk} f = \frac{f(x + k) - 2f(x) + f(x - k)}{h^2}.$$

The central difference operator of second order. Now, we consider the one step scheme introduced in Andreasen and Huge (2012):

$$\begin{pmatrix} 1 & 0 & \cdots & \cdots & \cdots & 0 \\ -z_1 & 1+2z_1 & -z_1 & 0 & \cdots & 0 \\ 0 & -z_2 & 1+2z_2 & -z_2 & 0 & 0 \\ 0 & 0 & \ddots & \ddots & \ddots & 0 \\ \vdots & \vdots & \cdots & -z_{n+1} & 1+2z_{n+1} & -z_{n+1} \\ 0 & \cdots & \cdots & \cdots & 0 & 1 \end{pmatrix}$$

$$z_j = \frac{1}{2}\frac{\Delta_t}{\Delta_k^2}\theta_j(k_k)^2, \text{ with } \Delta_t \text{ time step, } \Delta_k \text{ space step.}$$

As for any finite difference solution the boundaries are crucial. The problem can be solved by applying a tridiagonal solver together with the boundary conditions

$$c(t, k_0) = g(t, F, \nu(k_0)) \tag{7.25}$$
$$c(t, k_n) = g(t, F, \nu(k_n)) \tag{7.26}$$

The boundary conditions (7.25) and (7.26) can be specified by adding a vector d

$$d = (c(t, k_n), 0, \ldots, 0, c(t, k_0))^\top.$$

Now, the refined solution is derived by comparing the result to the Dupire equation. Since the prices computed using (7.23) and eq::AndreasenHuge should be the same we substitute c_{kk} from (7.23) in (7.24). Denoting $\xi := |x|/\sqrt{t}$ this leads to

$$\begin{aligned}\Theta(k)^2 &= \theta(k)^2\frac{c(t,k)-(F-k)^+}{tc_t(t,k)} \approx \theta(k)^2\frac{(g(t,F,\nu)-(F-k)^+)}{t\partial g(t,F,\nu)/\partial t} \\ &= \theta(k)^2 2\left(1-\xi\frac{\mathcal{N}(-\xi)}{n(\xi)}\right) = \theta(k)^2 P(x)^2\end{aligned}$$

The function P is given by

$$P(x) = 1 - n(x)\sum_{i=1}^{5} a_i t^i$$

with n denoting the density of the standard normal distribution and the coefficients a_i, $i = 1, \ldots, 5$ and t given by

$$a_1 = 0.319381530\,, \qquad a_2 = -0.356563782$$
$$a_3 = 1.781477937\,, \qquad a_4 = -1.821255978$$
$$a_5 = 1.330274429\,, \qquad p = 0.23164190000$$
$$t = \frac{1}{1 + px}$$

This refined solution does not suffer from the shortcomings of the raw solution. Especially, the observed peak at $k = f$ has been removed.

For a numerical example we consider different Call prices, densities and log-normal volatilities for different values of β_v. We consider the parameters: $v_0 = 0.0873$, $\rho = -0.48$, $\gamma = 0.47$, $f = 0.0325$ and $T = 10$ and different values for β given by $\beta_v = 0, 0.5, 1, 1.5$. In Fig. 7.9 we plot the call prices on the left, densities in the middle and volatilities on the right.

Finally, we consider the implied log-normal and the implied Bachelier volatilities for ZABR. Figure 7.10 shows the values for different values of β_v. This parameter can be used to control the shape of the wings. It decreases and simultaneously increases the slope.

7.7 Recent Developments

7.7.1 Free SABR

To overcome the problem and difficulties with the negative rates environment but at the same time keeping the nice features of the SABR model the *Free Boundary* SABR model was developed, see Antonov et al. (Antonov et al. 2015), Antonov and Spector (2013) or Antonov (2015). Numerical methods in terms of an integral solution have been proposed. However, this is only possible for the case of $\rho = 0$. The general model has to be handled using a projection method. We review the integration as well as the projection method and propose a robust and reliable solution for all model parameter values. This approach is considered in Kienitz (2015).

The free SABR model, that is $C(F) = |F|^\beta$ only has a semi-analytic solution for the case $\rho = 0$. The solution is given by

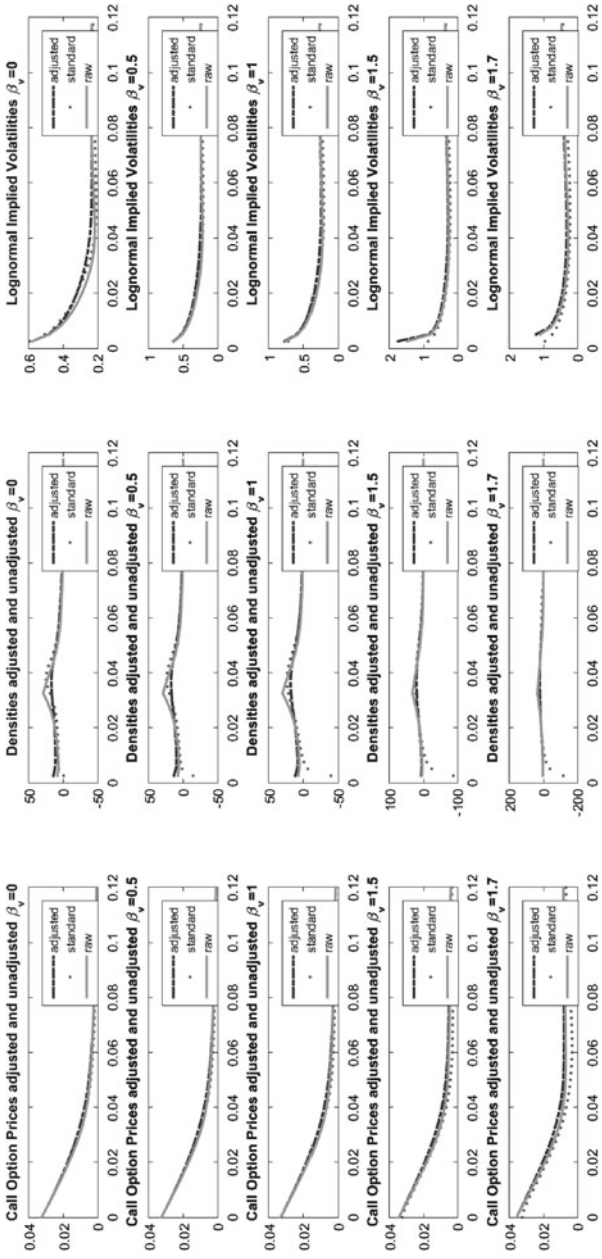

Fig. 7.9 Hagan approximate solution, raw solution and the refined solution for the SABR model are plotted for different values of β_v

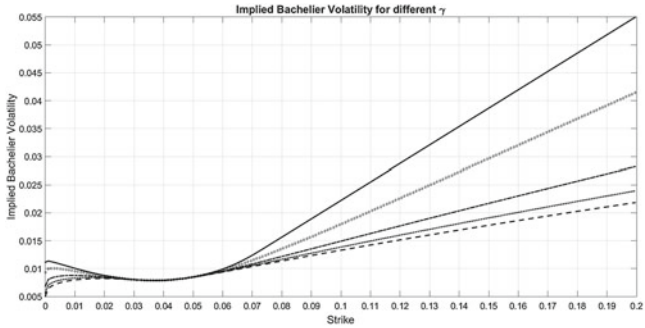

Fig. 7.10 ZABR implied Bachelier volatilities (*right*) for $\beta_v = 0, 0.5, 1, 1.5, 1.7$ and the parameters from $\sigma_0 = 0.0873$, $\beta = 0.7$, $\rho = -0.48$, $\gamma = 0.47$, $f = 0.0325$ and $T = 10$

$$C(K,T) = (S-K)^+ + \mathcal{O}(K,T) = (S-K)^+ + \frac{1}{\pi}\sqrt{|Kf_0|}\{1_{K\geq 0}A_1 + \sin(\nu\pi)A_2\}$$

The case $\rho \neq 0$ has to be handled with care and it is suggested to use a Projection technique. The projection is to adjust the parameters of a zero correlation model to resemble the shape of the distribution of the non-zero case. There are several possibilities to choose a distribution for the projection but the best results are obtained by choosing a zero correlation Free SABR model where we approximate the volatility by

$$\tilde{\nu} = \tilde{\nu}^{(0)} + T\tilde{\nu}^{(1)} + \cdots$$

However, the projection is not available for all values for the correlation and No-arbitrage problems might arise. Among these problems are negative values for the density. Figure 7.11 shows the quantity under the square root for different values of the parameters. If the corresponding graph is negative the formulas given above cannot be applied since one has to take the square root of a negative value.

The integration limits need to be adjusted with respect to the parameters and we observe that small values of the CEV parameter lead to erroneous results as well as small values for the forward rates leverage this phenomenon. In Antonov et al. (2015) the general recipe for the projection is to choose a mimicking zero correlation model such that

$$\tilde{\beta} = \beta \quad \tilde{\nu} = \sqrt{\nu^2 - \frac{3}{2}\left(\rho^2\nu^2 + \sigma_0\nu\rho(1-\beta)F^{\beta-1}\right)}$$

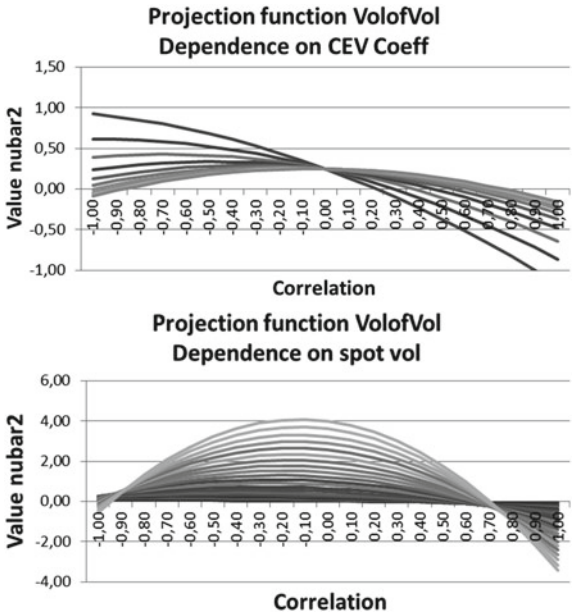

Fig. 7.11 Values of the function under the square root in the above equation. We have chosen different CEV coefficients (*top*) and different values for the correlation (*bottom*)

$$\tilde{\nu}^{(0)} = \frac{2\theta\Delta\tilde{\nu}}{\theta^2 - 1}, \qquad \left.\frac{\tilde{\nu}^{(1)}}{\tilde{\nu}^{(0)}}\right|_{K=F} = \frac{1}{12}\left(1 - \frac{\tilde{\nu}^2}{\nu^2} - \frac{3}{2}\rho^2\right)\nu^2 + \frac{1}{4}\beta\rho\sigma_0\nu F^{\beta-1}$$

with

$$\Delta = \frac{K^{1-\beta} - F^{1-\beta}}{1-\beta}, \qquad \theta = \left(\frac{\sqrt{\nu^2\Delta^2 + 2\rho\nu\Delta\sigma_0 + v_0^2} + \rho\sigma_0 + \nu\Delta}{(1+\rho)\sigma_0}\right)^{\frac{\tilde{\nu}}{\nu}}$$

We have for instance illustrated the difficulties arising from choosing inappropriate upper bounds in Fig. 7.12. There the prices for European Call options and the corresponding implied Bachelier volatilities are displayed. It is obvious that the choice of the upper bound is crucial to produce reliable results. This problem may be resolved by applying a transform which leads to only considering evaluations of the integral within a bounded domain. Then, advanced integration methods like adaptive integration.

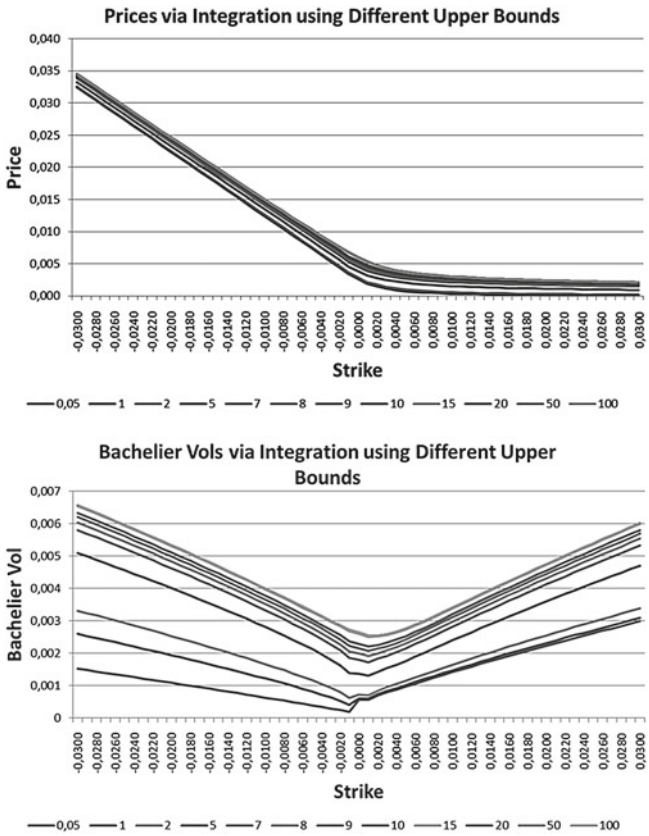

Fig. 7.12 Prices for European call options (*top*) and implied Bachelier volatilities for choosing different upper bounds in the integration formula (*bottom*)

We wish to gain an intuition for the parameters in this model. To this end we proceed as for the classic SABR model. We take as a base scenario $\sigma_0 = 0.005095939$, $\beta = 0.1$, $\nu = 0.3$, $\rho = -0.3$, $f_0 = 0.005$ and $T = 5$. The results are shown in Fig. 7.13.

7.7.2 Mixing SABR

If the modeller feels that the different parameters of the SABR model are not enough for building the volatility skew/smile there is yet more flexibility to adjust it. To this end a convex combination of models can be considered. This is known as the *mixture of models* approach. The idea is to take models of the same model class, for instance a zero correlation free SABR and a normal SABR model. For both models semi-analytic methods exist.

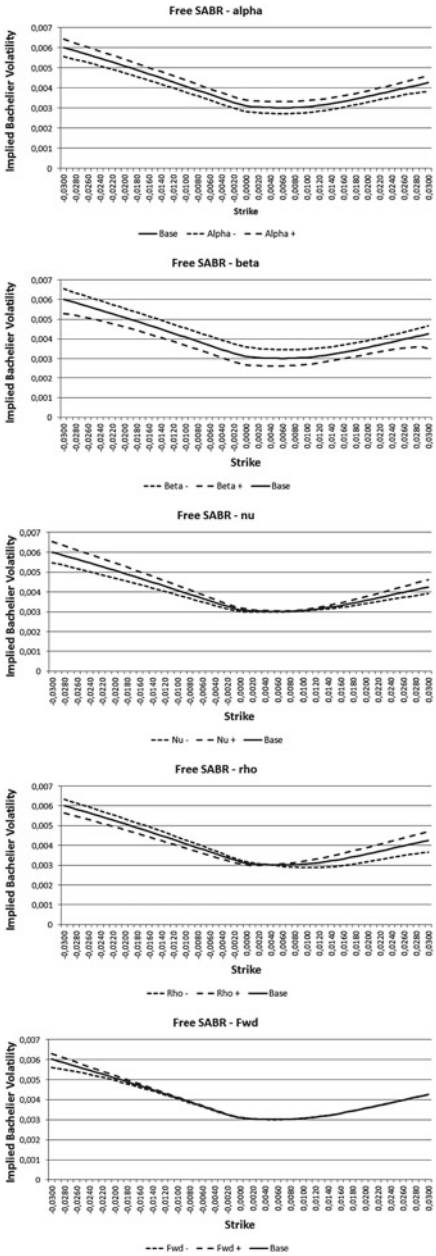

Fig. 7.13 Intuition for the effect of the parameters on the implied Bachelier volatility for the Free SABR model from *top* to *bottom* σ_0, resp. α, β, ν, ρ and f_0

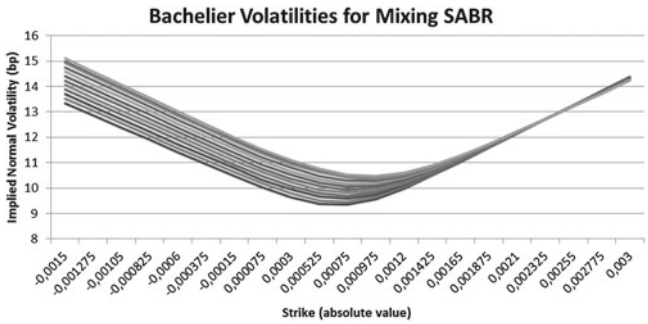

Fig. 7.14 Mixing of a normal and a Free boundary SABR model with zero correlation. We have varied the mixing parameter to toggle between the impact of a model

By applying a mixed approach we introduce a parameter $\omega \in [0, 1]$ that is used to determine how much of the models is mixed, that means we consider $\omega M_1 + (1 - \omega) M_2$. Figure 7.14 shows this for different values of the mixing parameter ω.

The method of mixing is not restricted to the above mentioned models. For instance we can combine different ZABR models. Furthermore, there can be more than two models involved. However, we have to remark that this model is only suitable for modelling one single maturity. It has to be handled with care. For further pitfalls see Piterbarg (2005).

7.8 Summary and Conclusions

In this chapter we considered the well known SABR model which is used by many market participants. The closed form solution in terms of implied Black volatility was given and the possible shortcomings of this approach were highlighted. Especially, that the formula is not applicable for negative rates and for low values of the forwards. Then, we proceed by considering several improvements to the formula. First, switching from Black implied volatility to Bachelier volatility which is very often used by market practitioners. Furthermore, we considered a displaced version of the SABR model that allows to consider negative rates to some extent. Finally, we reviewed and contributed to the most recent results by considering the ZABR and the Free SABR model. To this end we showed the applicability and proposed some numerical techniques which are robust, reliable and can be used in many market environments.

References

Andreasen, J., & Huge, B. N. (2012). Volatility interpolation. *RISK*, *3*, 76–79.
Andreasen, J., & Huge, B. N. (2013). Expanded forward volatility. *RISK*, *1*.
Antonov, A. (2015). Mixing SABR models. In *ICBI global derivatives conference*.
Antonov, A., & Spector, M. (2012). Advanced analytics for the SABR model. *SSRN*.
Antonov, A., & Spector, M. (2013). SABR spreads its wings. *RISK*, *26* (8), 58.
Antonov, A., Konikov, M., & Spector, M. (2015). Free boundary SABR. *RISK*.
Benaim, S., Dodgson, M., & Kainth, D. (2010). An arbitrage free method for smile extrapolation. *Preprint*. http://www.quarchhome.org/RiskTailsPaper_v5.pdf.
Crank, J., & Nicolson, P. (1996). A practical method for numerical evaluation of solutions of partial differential equations of the heat-conduction type. *Advances in Computational Mathematics*, *6* (1), 207–226.
Dimitroff, G., Fries, C., Lichtner, M., & Rodi, N. (2016). Lognormal vs normal volatilities and sensitivities in practice. *SSRN*.
Doust, P. (2012). No-arbitrage SABR. *Journal of Computational Finance*, *15*, 3–31.
Duffy, D. (2004). A critique of the crank nicolson scheme strengths and weaknesses for financial instrument pricing. *Wilmott Magazine*, *2017* (88), 1–60.
Duffy, D. (2006). *Finite difference methods in financial engineering*. Wiley, 2006.
Hagan, P. S. (2013). Change of variables and conservative numerical schemes. *Not published*.
Hagan P. S., Kumar D., Lesniewski A. S., & Woodward, D. E. (2015). Arbitrage free SABR. *Wilmott Magazine*, *69*, 60–75.
Hagan, P. S., Kumar, D., Lesniewski, A. S., & Woodward, D. E. (2016). Universal smiles. *Wilmott*, 40–55.
Hagan, P. S., Lesniewski, A., & Woodward, D. (2005). Probability distribution in the SABR model of stochastic volatility. *Working Paper*. http://www.lesniewski.us/papers/ProbDistForSABR.pdf.
Hagan, P. S., Kumar, D., Lesniewski, A. S., & Woodward, D. E. (2002). Managing smile risk. *Wilmott Magazine*, *1*, 84–108.
Henry-Labordere, P. (2005). A general asymptotic implied volatility for stochastic volatility models. *SSRN*. http://www.ssrn.com/abstract=698601.
Kienitz, J. (2011). *Pricing CMS spread options*. Paris: Talk at ICBI Global Derivatives.
Kienitz, J. (2014). *Interest rate derivatives explained: Volume 1 products and markets*. Palgrave McMillan.
Kienitz, J. (2015). Approximate and PDE solution to the boundary free SABR model—Applications to pricing and calibration. *SSRN*. http://www.papers.ssrn.com/sol3/papers.cfm?abstract_id=2647344.
Kienitz, J., & Wetterau, D. (2012). *Financial modeling—Theory, Implementation and practice—(with Matlab source)*. Wiley.
Lawson, J. D., & Swayne, D. A. (1976). A simple efficient algorithm for the solution of heat conduction problems. In *Proceedings of the 6th Manitoba Conference on Numerical Mathematics* (pp. 239–250).

LeFloch, F., & Kennedy, G. (2013). Finite difference techniques for arbitrage free SABR. *unpublished*.

Mercurio, F., & Morini, M. (2009). Joining the SABR and libor models together. *Risk*, *3*, 80–85.

Obloj, J. (2007). Fine tune your smile. *Wilmott Magazine*, *3*, 84–108.

Paulot, L. (2009). Asymptotic implied volatility at the second order with applications to the SABR model. *Preprint*. http://www.ssrn.com/sol3/papers.cfm?abtract_id=1413649.

Piterbarg, V. (2005). Mixture of models: A simple recipe for a ... hangover? *Wilmott Magazine*, *1*, 72–77.

Rebonato, R., McKay, K., & White, R. (2009). *The SABR/LIBOR market model*. Chichester: Wiley.

Wu, Q. (2010). Series expansion of the SABR joint Density. *Mathematical Finance*, *11*, 269–286. http://www.ssrn.com/sol3/papers.cfm?abtract_id=1367966.

Part III

Term Structure Models

8

Term Structure Models

8.1 Introduction and Objectives

This chapter gives an introduction to term structure modelling without focusing on a single model but on different classes of models. First, we consider why it is necessary to assign a future evolution of the current yield curve. Then, we summarize different approaches to term structure models and outline how they can be enhanced by considering stochastic volatility or stochastic basis spreads. The latter becomes necessary to better fit market observed structures and account for observations on the financial markets. Typical representatives of each model class are considered in this chapter but are described in detail in subsequent chapters.

8.2 Different Models for the Term Structure

For term structure modelling, we wish to consider Zero Coupon Bond prices given by

$$P(\cdot, T) : [0, T] \to \mathbb{R}^+. \tag{8.1}$$

This function takes values in the positive real numbers and $T < \infty$. The value of the Zero Bond at time $t \leq T$ is the function

$$T \mapsto P(t, T). \tag{8.2}$$

© The Author(s) 2017

J. Kienitz and P. Caspers, *Interest Rate Derivatives Explained: Volume 2*,
Financial Engineering Explained, DOI 10.1057/978-1-137-36019-9_8

Remark From Kienitz (2014), we know that there are different curves for discounting and for calculating forward rates. But it is of course possible to transform all these curves into their corresponding zero curves. Then, we have an OIS zero curve and one for 1, 3, 6 and 12M. Whenever necessary, we indicate the corresponding curve by writing P_{OIS} or P_{nM}.

We may choose one of the rates that we wish to use as a base for modelling the future term structure. The Zero Bond price P are also sometimes called discount factors and denoted by DF.

- **Short Rate Models**
  The short rate denoted by r is defined as the limit of the continuously compounded interest rate term structure (8.3).

$$r(t) = \lim_{T \downarrow t} -\frac{\log(P(t,T))}{T-t} \tag{8.3}$$

  The short rate is not observable and a rather theoretic concept. However, most of the models assigning an evolution of the short rate allow to construct all Zero Bond prices using model parameters. Thus, we model only one quantity but implicitly the whole future term structure.
- **Instantaneous Forward Rate Models (HJM)**
  Such term structure models assign a stochastic dynamic to the instantaneous forward rate $f(t,T)$. To define the instantaneous forward rate, we consider

$$F(t,T_1,T_2) := \frac{1}{\tau(T_1,T_2)} \frac{P(t,T_1) - P(t,T_2)}{P(t,T_2)}$$

  with τ being the year fraction measuring the fraction of a year between the dates T_1 and T_2; see Kienitz (2014). Now, letting T_2 tend to T_1 we get the instantaneous forward rate. To this end, let $\delta > 0$

$$f(t,T) := \lim_{\delta \to 0} F(t;T,T+\delta) = -\frac{\log(P(t,T))}{\partial T}. \tag{8.4}$$

  Equation (8.4) is the mathematical definition. The short rate and the instantaneous forward rate are related by (8.5)

$$r(t) = f(t,T)|_{T=t}\,. \tag{8.5}$$

- **Market Models**
  Such models consider market observable rates such as Libor or Swap rates and model these quantities directly by assigning some stochastic evolution

to them. The main advantage is that the model parameters often have an interpretation in terms of market observable structures.

8.2.1 Short Rate Models

Short rate models appeared in the early stages of interest rate modelling but since then they are invaluable tools for risk management and pricing. Figure 8.1 illustrates the evolution. A single stochastic variable governs the whole term structure. As a consequence, all rates have a single common stochastic risk factor.

To make the modelling approach more flexible, the stochastic dynamic can be assumed to be driven by several factors. The latter choice allows for a more realistic dynamic since using multiple factors it is possible to achieve de-correlation for certain parts of the yield curve. For instance, de-correlation means that the short end of the curve and the long end may show different dynamics since they are linked to different market drivers, see Kienitz (2014). In practice, it is of importance that the models are numerically tractable and allow for fast pricing and stable simulation. To this end, a class called affine models is used in practice.

Let us consider the arbitrage free price of a payoff h on the underlying S. To this end we take the risk-neutral measure. If $D(t, T)$ denotes the stochastic discount factor, then the price at t is given by

$$h_t = \mathbb{E}\left[D(t, T)h_T \,|\mathcal{F}_t\right],$$

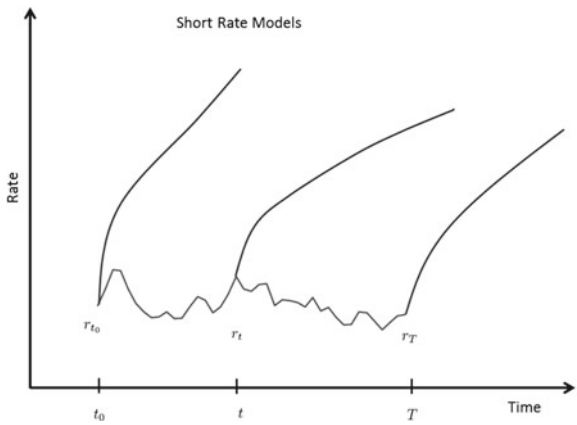

Fig. 8.1 Illustration of the modelling of short rates

where the expression means that we only use information available at time t. This is expressed by the concept of a filtration $\mathcal{F}_t$. This mathematical concept is not studied in detail but we can think of information which is revealed in a special way. If $s < t$, we wish to have that $\mathcal{F}_s \subset \mathcal{F}_t$ meaning that all the information available at time s is also available at time t. Thus, the information increases if time goes by. The expected value is given by

$$\mathbb{E}\left[e^{\left(-\int_t^T r(s)ds\right)} h_T \,|\mathcal{F}_t\right],$$

where r is the spot rate process. In particular, if $h_T = 1$ we have

$$P(t,T) = \mathbb{E}\left[e^{\left(-\int_t^T r(u)du\right)} |\mathcal{F}_t\right].$$

The latter means that the Zero Bond dynamics are specified whenever the dynamics of r is. This was indeed the pioneering work undertaken in Vasicek (1977). There a dynamic for the spot process r was considered and the successful application gave rise to a lot of research and practical applications extending and generalizing the models. In this exposition, we consider the following:

- Gaussian Short Rate models including the Ho-Lee, Ho and Lee (1986), Vasicek model, Vasicek (1977) or Hull–White model, Hull and White (1990);
- affine models and especially Square Root models also known as CIR models, see Cox et al. (1985); and
- model extensions to multiple dimensions (G2++, 2F Hull–White).

The reader should consult Brigo and Mercurio (2006) or Andersen and Piterbarg (2010b) and the references therein for an extensive survey.

In general, we consider the *Short Rate Model* given by

$$dr(t) = \mu(r(t),t)dt + \sigma(r(t),t)dW(t), \quad r(0) = r_0. \tag{8.6}$$

There are many issues a modeler has to consider. First, the question is does the dynamics imply reasonable dynamics for the zero bond prices? For instance, in the early years the short rate was required to generate only positive values leading to zero bond prices below 1. Of course, since the advent of negative rates this feature is not desirable anymore.

But there are other features we have to cope with. The probability distributions implied by the model dynamic should be reasonable, Zero Bond prices

and basic options should have analytic representations or should at least be easily computed. Can the model be easily adapted to include market observed features as modelling a skew or a smile? Are there any known restrictions?

Of course, we can extend the list but we proceed by choosing another way here. We only consider two types of short rate models. On the one hand, it is the general Gaussian Short Rate model and on the other hand it is the Cox–Ingersoll–Ross model.

We consider the general Gaussian Short Rate model together with the Linear Gauss Markov representation in the next chapter. The Gaussian nature of the model implies that negative rates can occur. In the second section, we consider a model which only generates positive rates. The third section considers multi-factor extensions of general short rate models.

8.2.2 Instantaneous Forward Rate Models

The modelled quantity is the instantaneous forward rate f, see Kienitz (2014). The model set-up is based on the well-known Heath–Jarrow–Morton framework. To be able to use such models, we need to restrict the broad class to a bunch of tractable models. This approach was taken by Cheyette (1994), Babbs (1990), Ritchken and Sankarasubramanian (1995) or Jamshidian (1991). They independently researched a method for choosing the volatility structure to end up with a Markovian model driven by some state variables. The number of state variables and the dynamic they follow can be chosen by the modeler. In this way, factor models can be considered that are flexible enough for practical purposes while at the same time allowing for extensions using local or stochastic volatilities. The general idea is to use the factors and from the dynamic retrieve the full future yield curve; see Fig. 8.2.

For a detailed description and any further information, see Chap. 11, Andersen and Piterbarg (2010b) or Andreasen (2005). Both references show how to extend the basic set-up and give examples for possible choices of local and stochastic volatility processes.

8.2.3 Market Models

Market Models aim to specify a dynamic for market observable rates. Popular models are the Libor or the Swap Market Models. Historically, Brace et al. (1997), Miltersen et al. (1997) and Jamshidian (1997) outlined approaches where market observable quantities are directly modelled. In a Libor Market

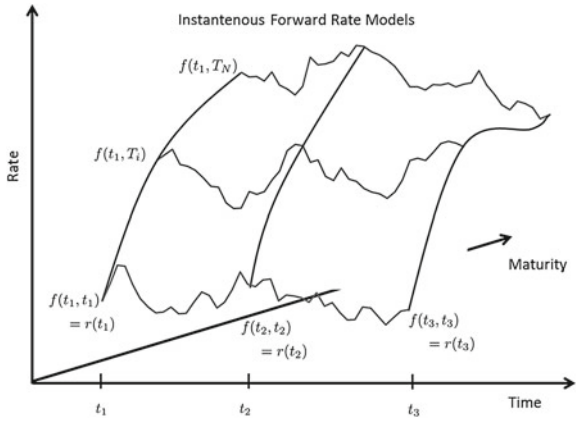

Fig. 8.2 Illustration of the modelling of instantaneous forward rates

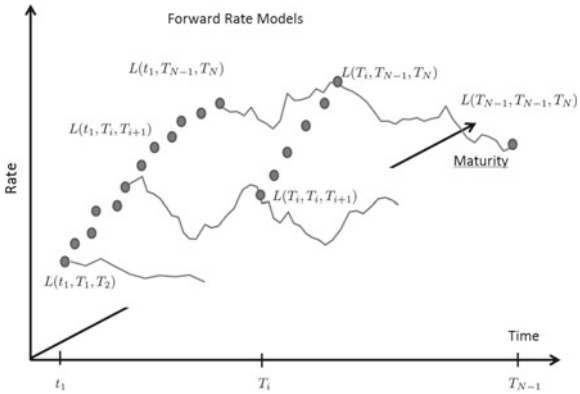

Fig. 8.3 Illustration of the modelling of market rates

Model, it is common to choose a Libor period, for instance, of 3 months and assign a dynamic for each of the forward Libor rates up to a given maturity. To this end, a term structure $T_0 < T_1 < T_2 < \ldots < T_N$ is fixed and the rates $L(T_1, T_2)$, $L(T_2, T_3)$, …, $L(T_{N-1}, T_N)$ are modelled as stochastic variables. Here not only the volatilities leveraging the dynamics of each rate but also the co-movement has to be accounted for. Taking for example a 3-month Libor period and considering derivatives with a maturity of 20 years, we need to jointly model the evolution of $4 \cdot 20 - 1 = 79$ rates. Furthermore, since only a discrete set of rates is modelled, it becomes necessary to research inter- and extrapolation methods to be able to calculate any value of a Zero Coupon Bond in between Libor periods. This includes the Zero Coupon Bonds which do not pay at one of the time points constituting the term structure. Figure 8.3 illustrates this modelling approach. We review the methodology in Chap. 12.

8.3 Stochastic Volatility Enhancements

For adding more modelling realism to financial models, it is a common approach to account for skew and smile in implied volatility to enhance the model by a stochastic volatility component. For interest rates, many widely applied models do only model unobservable rates and use these rates as well as the model parameters to express observable quantities such as Zero Coupon Rates, Libor Rates or Swap Rates implicitly. To this end, it is not easy to separate the uncertainty arising from the interest rate dynamic and the stochastic volatility component.

Therefore, we distinguish models which have a true stochastic volatility component from those which have not. They are called unspanned stochastic volatility models since it is not possible to hedge the risk arising from this component by standard instruments such as Zero Bonds. For such models, to hedge this risk the trader needs to take positions in options. In Andersen and Piterbarg (2010b), two conditions are specified for a model to be a true stochastic volatility model. To this end, let z be the component modelling the stochastic volatility. Then, such a model should fulfil

$$\frac{\partial \sigma}{\partial r} \neq 0, \quad \frac{\partial P}{\partial z} = 0. \tag{8.7}$$

Essentially, (8.7) means that the effects from the stochastic volatility cannot be eliminated by hedging trades in the underlying rates. For the models we consider in the sequel, we give examples if the enhancement using a stochastic volatility component is feasible or not.

8.4 Stochastic Basis Spreads

In Kienitz (2014), we have shown that after August 2007 the money market basis spread as well as the cross currency basis spread have become significant and it is often necessary to assume that these spreads are stochastic. The basic interest rate models considered, for instance, in Brigo and Mercurio (2006) do assume a constant basis spread. More recent textbooks such as the Andersen and Piterbarg (2010a) allow the spreads to be stochastic. Common to all approaches modelling stochastic basis spread is that they are based on standard interest rate models. Common approaches assume

- **Additive Spread**
  This means that the spread is the difference between the nM-Forward rate calculated on the OIS curve and the same rate calculated from the nM-Libor curve. Mathematically, this means

$$S_k^{nM}(t) := L_k^{nM}(t) - F_k^{OIS}(t).$$

- **Multiplicative Spread**
  Here it is assumed that the spread is linear compounded and this compounding is a factor calculated as the quotient from the linear compounded nM-Forward rate calculated on the OIS curve divided by the same amount calculated from the nM-Libor curve. In terms of a formula, this means

$$S_k^{nM}(t) := \frac{1}{\tau_k^{nM}} \frac{1 + \tau_k^{nM} L_k^{nM}}{1 + \tau_k^{nM} L_k^{OIS}} - 1.$$

- **Instantaneous Spread**
  This concept directly relates the discount factors on the OIS curve and the nM-Libor curve. The discount factor on the Libor curve is the product of the discount factor from the OIS curve times the exponential of the integral of the spread over the considered time interval. This concept is illustrated in terms of an equation by

$$P_{nM}(t, T) = P_{OIS}(t, T) e^{\int_t^T s(u)du}.$$

There is no common best practice approach to determine which of the spread concepts to apply. The set-up is often chosen with respect to the model that is used for interest rate modelling. We use the approach of modelling the spreads as additive for illustration. Let us consider a set of time points $T_1^{nM}, T_2^{nM}, \ldots, T_N^{nM}$ corresponding to an nM-tenor structure. The forward rate F_k^{nM} defined in (8.8) is calculated on the OIS curve.

$$F_k^{nM}(t) := \frac{1}{\tau_k^{nM}} \left(\frac{P(t, T_{k-1}^{nM})}{P(t, T_k^{nM})} - 1 \right) \tag{8.8}$$

The Forward Libor Rate L_k^{nM} is given by (8.9) for the same period:

$$L_k^{nM}(t) := \mathbb{E}_{OIS}^{T_k^{nM}} \left[L^{nM}(T_{k-1}^{nM}, T_k^{nM}) | \mathcal{F}_t \right]. \tag{8.9}$$

The Forward Libor Rate (8.9) is the conditional expectation of the Libor Rate realized between T_{k-1}^{nM} and T_k^{nM} with respect to the risk-neutral measure (the T_k^{nM} Forward Measure) induced by the T_k^{nM} Zero Bond on the OIS curve. This definition in Eq. (8.9) insures that the Forward Libor Rates are martingales with respect to the OIS T_k^{nM} Forward Measure. For the spread, we set

$$S_k^{nM}(t) = S_k^{nM}(0) + \alpha_k^{nM}(F_k^{nM}(t) - F_k^{nM}(0)) + \beta_k^{nM}(\mathcal{X}_k^{nM}(t) - \mathcal{X}_k^{nM}(0). \tag{8.10}$$

The parameters α_k^{nM} and β_k^{nM} in Eq. (8.10) are used to model volatility (β_k^{nM}) and correlation (α_k^{nM}) for the stochastic basis. Mercurio and Xie (2012) remark that to avoid unrealistic modelling the parameters should not be modelled to be completely independent and suggest to take $\alpha_k^{nM} = \gamma_k^{nM}\beta_k^{nM}$. If there is no stochastic component, $\beta_k^{nM} = 0$, we have a purely deterministic spread model since if α_k^{nM} is a multiple of β_k^{nM} then this implies $\alpha_k^{nM} = 0$.

To introduce Forward Libor and Swap Rates in this setting, let us consider two sets of time points:

$$\mathcal{T}_{\text{float}} := \{T_{a+1}^{nM}, \ldots, T_b^{nM}\}$$
$$\mathcal{T}_{\text{fix}} := \{T_{c+1}, \ldots, T_d\}.$$

The Forward Libor Rates are given by (8.11)

$$L_k^{nM}(t) = L_k^{nM}(0) + (1 + \alpha_k^{nM})(F_k^{nM}(t) - F_k^{nM}(0)) + \beta_k^{nM}(\mathcal{X}_k^{nM}(t) - \mathcal{X}_k^{nM}(0). \tag{8.11}$$

For the definition of the Swap Rates, we assume $T_d = T_b^{nM}$ and $\mathcal{T}_{\text{fix}} \subset \mathcal{T}_{\text{float}}$.

$$\begin{aligned} S_{a,b,c,d}(T_a^{nM}) = & \frac{\sum_{k=a+1}^{b} \tau_k^{nM} P(t, T_k^{nM}) L_k^{nM}(0)}{A(t)} \\ & + \frac{\sum_{k=a+1}^{b} \tau_k^{nM}(1 + \alpha_k^{nM})(F_k^{nM}(t) - F_k^{nM}(0))}{A(t)} \\ & + \frac{\sum_{k=a+1}^{b} \tau_k^{nM} P(t, T_k^{nM}) \beta_k^{nM}(\mathcal{X}_k^{nM}(t) - \mathcal{X}_k^{nM}(0))}{A(t)} \end{aligned} \tag{8.12}$$

with A denoting the annuity

$$A(t) := \sum_{j=c+1}^{d} \tau_j P(t, T_j).$$

To further shed light on the role of the parameters, Mercurio and Xie (2012) give an alternative representation

$$\alpha_k^{nM} = \mathrm{Corr}(\mathrm{S_k^{nM}}(\mathrm{T_{k-1}^{nM}}), \mathrm{F_k}(\mathrm{T_{k-1}^{nM}}))\sqrt{\frac{\mathbb{V}[\mathrm{S_k^{nM}}(\mathrm{T_{k-1}^{nM}})]}{\mathbb{V}[\mathrm{F_k}(\mathrm{T_{k-1}^{nM}})]}}$$

$$\beta_k^{nM} = \sqrt{(1 - \mathrm{Corr}(\mathrm{S_k^{nM}}(\mathrm{T_{k-1}^{nM}}), \mathrm{F_k}(\mathrm{T_{k-1}^{nM}}))^2)\frac{\mathbb{V}[\mathrm{S_k^{nM}}(\mathrm{T_{k-1}^{nM}})]}{\mathbb{V}[\mathrm{F_k^{nM}}(\mathrm{T_{k-1}^{nM}})]}}.$$

They proceed by computing FRA, Futures, Caps, Floors and Swaptions prices. Let us start with the FRA. It is possible to write down the exact formula for the FRA. To use this formula, in practice a conditional expectation has to be calculated. The value is not available in closed form but Mercurio and Xie (2012) give approximate expressions which we show in Eq. (8.13):

$$\begin{aligned} V^{FRA}(t, T_{k-1}^{nM}, T_k^{nM}) = L_k^{nM}(t) - \tau_k^{nM}\alpha_k^{nM}(1 + \alpha_k^{nM})\mathbb{V}[F_k^{nM}(T_{k-1}^{nM})] \\ -\tau_k^{nM}(\beta_k^{nM})^2\mathbb{V}[\mathcal{X}_{k-1}^{nM}]. \end{aligned} \tag{8.13}$$

A corresponding formula holds true for the case of a Future. The interested reader should consult Mercurio and Xie (2012) on the details. We summarize that using this general set-up it is possible to enhance any of the standard term structure models. In order to apply the models in practice, we have to choose the model dynamics in a way that the resulting model including the stochastic basis can be implemented. Thus, we have to take care that the relevant formulas are reasonably simple. We consider examples in Chap. 9, Sect. 9.4 and 12, Sect. 12.9 to illustrate this abstract concept. We finally remark that the outlined approach may lead to negative realisations of the basis and before applying a careful analysis should be conducted.

8.4.1 Deterministic Basis

Many practitioners still use a deterministic basis approach. To partly justify this, we assume that the basis spreads and the zero curve used for discounting are independent. Let us denote by $DF_{nM}(t, T)$ the discount factor on the Libor curve and by $DF(t, T)$ the discount factor on the discount curve. The basis adjustment factor is given by $S_{nM}(t, s) = \frac{DF(t,T)}{DF_{nM}(t,T)}$. For a constant continuously compounded basis spread s_c, we have $S_{nM}(t, s) = e^{s_c(t,T_m,T_n)(s-t)}$. This is for a swap starting at T_m and ending at T_n. The present value of the

swap at time t is given by

$$V^{\text{Swap}}(t) = c\sum_{i=m}^{n-1}\tau_i DF(t,T_i) - \sum_{i=m}^{n-1}F_{nM}(t,T_i,T_{i+1})DF(t,T_{i+1}).$$

For the floating leg, we find

$$V^{\text{Float}}(t) = 1 - DF(t,T_n) - \sum_{i=m}^{n-1}DF(t,T_i)\left(\frac{DF(t,T_i)}{DF(t,T_{i+1})} - \frac{DF_{nM}(t,T_i)}{DF_{nM}(t,T_{i+1})}\right).$$

Keeping the basis constant corresponds to a freezing argument very common in interest rate modelling; see, for instance, Brigo and Mercurio (2006). After freezing, we write

$$V^{\text{Float}}(t) = 1 - DF(t,T_n) - \sum_{i=m}^{n-1}DF(t,T_i)\left(\frac{DF(0,T_i)}{DF(0,T_{i+1})} - \frac{DF_{nM}(0,T_i)}{DF_{nM}(0,T_{i+1})}\right).$$

The time t expression of the difference

$$\frac{DF(t,T_i)}{DF(t,T_{i+1})} - \frac{DF_{nM}(t,T_i)}{DF_{nM}(t,T_{i+1})}$$

would be approximated by its current value and the basis spread is the weighted average of the period forward components with weights

$$w_j := \frac{DF(t,T_{j+1})}{\sum_{j=m}^{n-1}DF(t,T_{j+1})}.$$

8.5 Pricing and Path Simulation

To apply a term structure model in practice for pricing or exposure generation, we need to take into account two things. On the one hand, the model needs to be robust and flexible. This means that it should be possible to determine market observed rates from the modelled quantities. For instance, from the short rate it should be possible to calculate Zero Coupon Bond prices or Swap rates. Furthermore, the parameters should have a sound and clear meaning such that we could build an intuition of what the different model parameters are and what they are used for. On the other hand, we need efficient numerical

techniques for turning the model risk factors into market variables as well as efficiently computing derivatives prices.

This all boils down to be able to implement the model in a computer. There are many cutting-edge numerical techniques that can be applied. Among them are

- Monte Carlo Simulation and
- PDE/FDM Methods.

From the basic instruments, all the products considered in Part I of this book can be constructed. For instance consider a short rate model. The modelled quantity r is neither observable nor is there a financial instrument based on the short rate. But if we have a representation of Zero Coupon Bonds, then it is possible to construct other rates.

In the Appendix A, we consider the basics of the two numerical methods. When we consider representatives of models, we often give recipes and extensions to the basic methods that can be used for valuing derivatives or exposure generation.

8.6 Summary and Conclusions

In this short chapter, we gave a very short introduction to term structure modelling and identified the main modelling approaches. For the purpose of this book, we considered Short Rate Models, models of the instantaneous Forward Rate and Market Models. Then, we proceed by explaining the possible extension using stochastic volatilities and stochastic basis spreads. We outlined what a true or unspanned stochastic volatility is. Finally, we summarized the numerical methods necessary to implement the described models. Many more details on the numerical implementation can be found in Appendix A.

References

Andersen, L., & Piterbarg, V. (2010a). *Interest rate modeling—Volume I: Foundations and Vanilla models*. Atlantic Financial Press.

Andersen, L., & Piterbarg, V. (2010b). *Interest rate modeling—Volume II: Term structure models*. Atlantic Financial Press.

Andreasen, J. (2005). Back to the Future. *RISK, 18*(9), 104–109.

Babbs S. (1990). *The term structure of interest rates: Stochastic processes and contingent claims*. Ph.D. Thesis—University of London.

Brace, A., Gatarek, D., & Musiela, M. (1997). The market model of interest rate dynamics. *Mathematical Finance*, *7*, 127–155.

Brigo, D., & Mercurio, F. (2006). *Interest rate models—Theory and practice* (2nd ed.). Berlin, Heidelberg, New York: Springer.

Cheyette O. (1994). Markov representation of the Heath-Jarrow-Morton model. *Barra—Working paper and SSRN*.

Cox, J. C., Ingersoll, J. E, Jr., & Ross, S. A. (1985). A theory of the term structure of interest rates. *Econometica*, *53*, 363–384.

Ho., & Lee S. B. (1986). Term structure movements and pricing interest rate contingent claims. *Journal of Finance 41*, 1011–1029.

Hull, J. C., & White, A. (1990). Pricing interest rate derivative securities. *The Review of Financial Studies*, *3*, 573–592.

Jamshidian, F. (1991). Bond and option evaluation in the gaussian interest rate model. *Research in Finance*, *9*, 131–170.

Jamshidian, F. (1997). LIBOR and swap market models and measures. *Finance and Stochastics*, *1*, 293–330.

Kienitz, J. (2014). *Interest rate derivatives explained: Volume 1 products and markets*. Palgrave McMillan.

Mercurio, F., & Xie, Z. (2012). The basis goes stochastic. *RISK*, *12*, 78–83.

Miltersen, K. R., Sandmann, K., & Sondermann, D. (1997). Closed form solution for term structure derivatives with log-normal interest rates. *The Journal of Finance*, *52*(1), 409–430.

Ritchken, P., & Sankarasubramanian, L. (1995). Volatility structures of forward rates and the dynamics of the term structure. *Mathematical Finance*, *5*(1), 55–72.

Vasicek, O. (1977). An equilibrium characterization of the term structure. *Journal of Financial Economics*, *5*, 177–188.

9

Short Rate Models

9.1 Introduction and Objectives

In this chapter, we consider two of the favourite short rate models, the Gaussian Short Rate, respectively Linear Gauss Markov (LGM), model and the Cox–Ingersoll–Ross (CIR) model. We give a short introduction to the models and show how to price quoted financial instruments such as caplets or European swaptions. This is necessary to calibrate the model. Then, we outline how to generate paths corresponding to the model dynamic. The paths can be used for pricing path-dependent and exotic options and can as well be used for exposure simulation. Many software packages use variants of Gaussian Short Rate and CIR models for creating exposures for interest rates.

Finally, we outline of how to extend the modelling approach to take into account N-factor models.

Since in this book we do not derive all the equations but give a practical introduction, the interested reader can consult the standard references on the mathematical details of interest rate modelling including Brigo and Mercurio (2006), Andersen and Piterbarg (2010) and Lichters et al. (2015). The latter has detailed references and derivations for the models considered in the Appendix A.

© The Author(s) 2017

J. Kienitz and P. Caspers, *Interest Rate Derivatives Explained: Volume 2*,
Financial Engineering Explained, DOI 10.1057/978-1-137-36019-9_9

9.1.1 Gaussian Short Rate Model and the Hull–White Model

We first consider a Gaussian model, called the (general) *Gaussian Short Rate*. We take deterministic functions θ, κ and σ and specify the model dynamic of the short rate by (9.1); see, for instance, Brigo and Mercurio (2006).

$$\begin{aligned} dr(t) &= (\theta(t) - \kappa(t)r(t))dt + \sigma(t)dW(t) \\ r(0) &= r_0 \end{aligned} \tag{9.1}$$

In the literature, for instance Andersen and Piterbarg (2010), another specification of the model is found, namely

$$\begin{aligned} dr(t) &= \kappa(t)(\theta(t) - r(t))dt + \sigma(t)dW(t) \\ r(0) &= r_0. \end{aligned}$$

This specifies the same model but the final formulas for prices and the specifications of the solutions differ due to the parameterization.
If $\theta(t) = \theta$, $\kappa(t) = \kappa$ and $\sigma(t) = \sigma$, the solution is given by Eq. (9.2):

$$r(t) = f(s)e^{-\kappa(t-s)} + \theta\left(1 - e^{-\kappa(t-s)}\right) + \sigma\int_s^t e^{-\kappa(t-u)}dW(u). \tag{9.2}$$

In this case, the first and the second moments can be computed and are given by

$$\mathbb{E}[r(t)|\mathcal{F}_s] = r(s)e^{-\kappa(t-s)} + \theta\left(1 - e^{-\kappa(t-s)}\right) \tag{9.3}$$

$$\mathbb{V}[r(t)|\mathcal{F}_s] = \frac{\sigma^2}{2\kappa}\left[1 - e^{-2\kappa(t-s)}\right]. \tag{9.4}$$

Obviously, in general this model with constant coefficients (θ, κ and σ) cannot fit the observed term structure of interest rates. This is unsatisfactory for practical purposes since at least the instruments that can be evaluated using the current yield curve should be priced correctly. A solution is to consider θ to be a deterministic function. We take

$$\theta(t) := \frac{\partial^2 \ln(P(0,t))}{\partial t^2} - \kappa\frac{\partial \ln(P(0,t))}{\partial t} + \frac{\sigma^2}{2\kappa}\left(1 - e^{-2\kappa t}\right). \tag{9.5}$$

In Eq. (9.5), we denote the market observed zero coupon bond prices derived from the current yield curve by $P(0,t)$. In practice, the derivative $\frac{\partial}{\partial t}$ used

to determine the rates has to be calculated numerically and, thus, the values depend on the used interpolation method; see Kienitz (2014). Again, the solution $r(t)$ is available and is given by Eq. (9.6):

$$r(t) = r(s)e^{-\kappa(t-s)} + \int_s^t e^{-\kappa(t-u)}\theta(u)du + \sigma \int_s^t e^{-\kappa(t-u)}dW(u). \quad (9.6)$$

The first integral in (9.6) is given by

$$-\frac{\partial \ln(P(0,t))}{\partial t} + \frac{\sigma^2}{2\kappa^2}\left(1-e^{-\kappa t}\right)^2 + \frac{\partial \ln(P(0,s))}{\partial s} - \frac{\sigma^2}{2\kappa^2}\left(1-e^{-\kappa s}\right)^2 e^{-\kappa(t-s)}.$$

For practical reasons, it is often easier to work with another variable x instead of r and using the relation (9.7)

$$r(t) = x(t) - f(0,t). \quad (9.7)$$

We provide the rationale for this at the end of this chapter where we consider the most general Gaussian Short Rate model. It is possible to determine the zero coupon bond prices $P(t,T)$ explicitly. They are given by

$$\begin{aligned}
P(t,T) &= A(t,T)e^{-B(t,T)r(t)} \\
A(t,T) &= \frac{P(0,T)}{P(0,t)} \exp\left(-B(t,T)\frac{\partial \ln(P(0,t))}{\partial t} - \frac{\sigma^2}{4\kappa}\left(1-e^{-2\kappa T}\right)B(t,T)^2\right) \\
B(t,T) &= \frac{1-e^{-\kappa(T-t)}}{\kappa}.
\end{aligned} \quad (9.8)$$

Figure 9.1 shows how the term structure varies for choosing different values of $r(0)$. We have chosen to start with -1% and increase the value by 0.5%. In a simulation, we evolve r with respect to the given dynamic, use (9.8) to determine the term structure and use this for pricing more complex financial instruments.

Figure 9.2 shows some term structure evolution for the Gaussian Short Rate model paths with constant coefficients. We used the representation of the mean and the variance. Then we sampled standard normal variates with the mean and standard deviation calculated using the formulas (9.3) and (9.4). This is furthermore an illustration of the effects of the parameters κ and θ. The short rate tends to the long-term value θ and the parameter κ determines how fast the process is pulled back if it deviated from θ. However, using a Gaussian Short Rate model the skew/smile is fixed by the normal assumption. This means that there is no possibility for the modeler to adjust it. We address this problem when we consider Affine Short Rate models in Sect. 9.1.2.

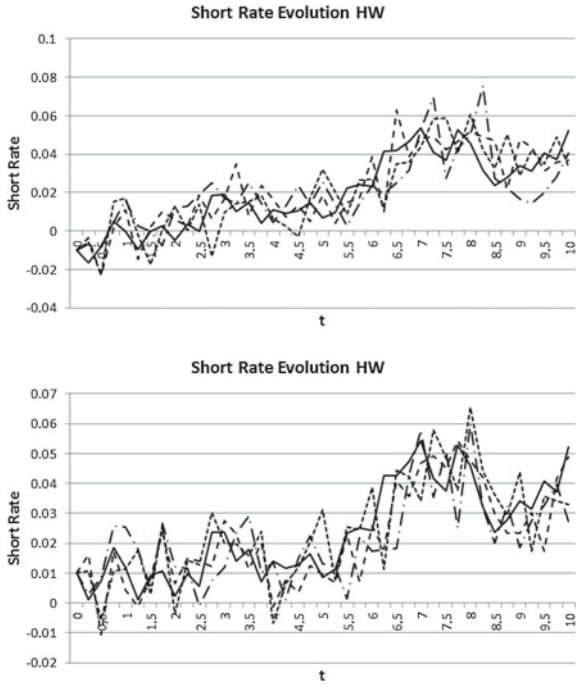

Fig. 9.1 Simulated short rate paths for different spot rates. We let $r(0) = -0.01$ (*top*) and $r(0) = 0.01$. The other parameters are $\kappa = 0.2$, $\theta = 0.03$ and $\sigma = 0.02$ (*bottom*)

We already mentioned that instruments that depend only on the current yield curve should be priced correctly in the model. Since we wish to use the model to price interest rate derivatives which are not quoted in the market, we would need that the model prices quoted instruments correctly. To this end, we select some interest rate options and try to determine the model parameters that lead to the smallest pricing error. This method is known as the *calibration*. For a calibration, it is beneficial if the model allows to calculate the prices for common options in closed form or using efficient approximation formulas. For the model under consideration, it is possible to derive prices for Call and Put options on Zero Coupon Bonds, (9.9) and (9.10).

$$V^{\text{ZCCall}}(t, T, S, K) = KP(t, S)\mathcal{N}(-h) - P(t, T)\mathcal{N}(h - \Sigma) \tag{9.9}$$

$$V^{\text{ZCPut}}(t, T, S, K) = KP(t, T)\mathcal{N}(-h + \Sigma) - P(t, S)\mathcal{N}(-h) \tag{9.10}$$

We used

$$\Sigma := \sigma\sqrt{\frac{1 - e^{-2\kappa(T-t)}}{2\kappa}}B(T, S), \quad h = \frac{1}{\Sigma}\ln\left(\frac{P(t, S)}{P(t, T)K}\right) + \frac{\Sigma}{2}.$$

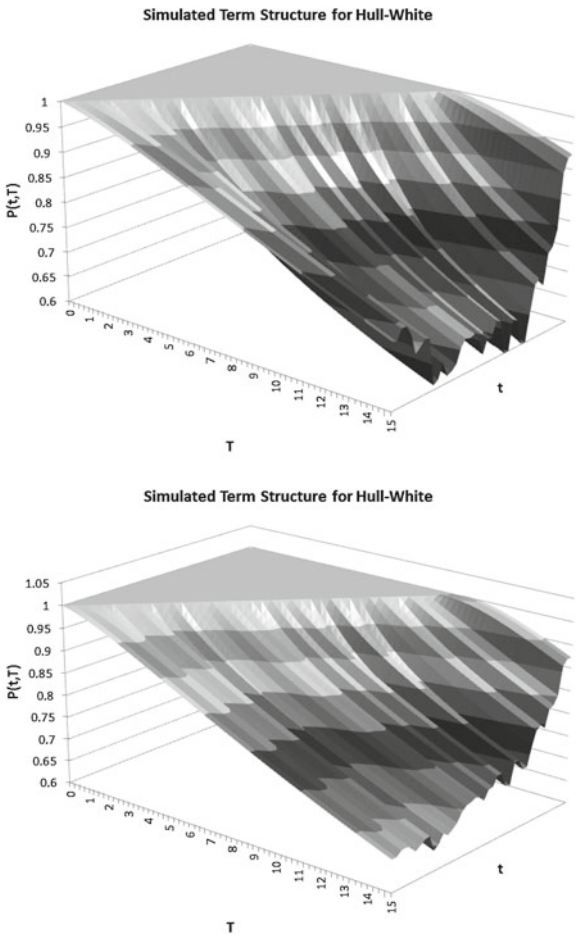

Fig. 9.2 Two simulated term structures for the Gaussian short rate model with $\kappa = 0.2$ (*top*) and $\kappa = 0.5$ (*bottom*), $\theta = 0.03$, $\sigma = 0.02$ and $r = 0.01$

With this result, the prices for Caplets and Floorlets as well as swaptions can be derived; see (9.11), (9.12), (9.14) and (9.15).
However, it is not possible to find the corresponding prices if the functions $\kappa(t)$ and $\sigma(t)$ are non-constant. The next subsection shows a different formulation of the Gaussian Short Rate model which allows for handling the more general cases. But for now, let us consider the pricing of basic options. Let $\mathcal{T} := \{t_0, \ldots, t_N = T\}$ be a discretization of $[0, T]$.

$$V^{\text{Cap}}(K, T) = \sum_{i=1}^{N} \left[P(t, t_{i-1})\mathcal{N}(-h_i + \sigma_i) - (1 + K\tau_i)P(t, t_i)\mathcal{N}(-h_i) \right]$$

with the volatility

$$\sigma_i = \sigma\sqrt{\frac{1-e^{-2\kappa(t_{i-1}-t)}}{2\kappa}B(t_{i-1},t_i)}, \quad h_i = \frac{1}{\sigma_i}\log\left(\frac{P(t,t_i)(1+K\tau_i)}{P(t,t_{i-1})}\right)+\frac{\sigma_i}{2}.$$

The corresponding value for the Floor is

$$V^{\text{Floor}}(K,T) = \sum_{i=1}^{N}\left[P(t,t_i)\mathcal{N}(h_i) - (1+K\tau_i)P(t,t_{i-1})\mathcal{N}(h_i-\sigma_i)\right].$$

Each Caplet is a Put option, respectively each Floorlet is a Call option, on a Zero Coupon Bond. This means that we can reuse the corresponding formulas. To calculate the expectation

$$\mathbb{E}[e^{-\int_t^T r(s)ds}(P(T,S)-K)^+|\mathcal{F}(t)]$$

for pricing a Zero Coupon Bond call, we have a complex expression which we wish to simplify. This can be done by changing the numeraire, and we can resort to the pricing equation

$$P(t,T)\mathbb{E}^T[(P(T,S)-K)^+|\mathcal{F}(t)].$$

This gives new insight which is helpful for future pricing problems. Namely, we applied the change of numeraire technique often applied in interest rate derivative pricing. We find for the dynamic of $\tilde{r}$ in the T-Fwd measure:

$$d\tilde{r}(t) = [-B(t,T)\sigma^2 - a\tilde{r}(t)]dt + \sigma dW^T(t).$$

Thus, the solution is given by

$$\tilde{r}(t) = \tilde{r}(s)e^{-a(t-s)} - M^T(s,t) + \sigma\int_s^t e^{-a(t-u)}dW^T(u)$$

with

$$M^T(s,t) = \frac{\sigma^2}{a^2}\left[1-e^{-a(T_t)}\right] - \frac{\sigma^2}{2a^2}\left(e^{-a(T-t)} - e^{-a(T+t-2s)}\right).$$

In the T-Forward measure, the short rate is also Gaussian but with a different mean. We have

$$\mathbb{E}^T[r(t)|\mathcal{F}(s)] = \tilde{r}e^{-a(t-s)} - M^T(s,t) + f^M(0,t) + \frac{\sigma^2}{2a}\left(1 - e^{-a(t-s)}\right)^2$$
$$\mathbb{V}^T[r(t)|\mathcal{F}(s)] = \frac{\sigma^2}{2a}\left(1 - e^{-2a(t-s)}\right).$$

Let us consider the pricing of a Cap. We calculate the expectation given by

$$\mathbb{E}\left[e^{-\int_t^{T_i} r(s)ds} N\tau_i(L(T_{i-1},T_i) - K)^+|\mathcal{F}(t)\right].$$

Using the tower property of conditional expectations and the definition of the forward rate (in a single-curve setting!) we find

$$\mathbb{E}\left[e^{-\int_t^{T_i} r(s)ds}(1 - (1+\tau_i K)P(T_{i-1},T_i))^+|\mathcal{F}(t)\right].$$

The latter expression allows to view a Cap with strike K on a forward rate as an option on a Zero Coupon Bond with strike $(1+\tau_i K)^{-1}$ and notional $N(1+\tau_i K)$. The pricing formulae for Caps and Floors become

$$V^{\text{Cap}}(K,T) = \sum_{i=1}^{N}(1+\tau_i K)V^{ZCPut}(t, T_{i-1}, T_i, \frac{1}{1+\tau_i K}) \tag{9.11}$$

$$V^{\text{Floor}}(2,K)T = \sum_{i=1}^{N}(1+\tau_i K)V^{ZCCall}(t, T_{i-1}, T_i, \frac{1}{1+\tau_i K}). \tag{9.12}$$

For the pricing of swaptions, we derive the corresponding pricing equation. However, the Equation is again based on pricing zero coupon bond options but this time an additional quantity called r^* has to be determined. We consider the payoff $N(SR-K)^+A(T,T_N)$. Let r^* be the solution of

$$\sum_{i=1}^{N} c_i A(T,T_i)e^{-B(T,T_i)r^*} = 1. \tag{9.13}$$

With this value r^*, the prices of a maturity T payer/receiver swaptions are given by

$$V_{\text{Pay}}^{\text{Swptn}}(K,t) = N\sum_{i=1}^{N} c_i V^{ZCPut}(t,T,T_i,A(t,T_i)e^{-B(t,T_i)r^*}) \tag{9.14}$$

$$V_{\text{Rec}}^{\text{Swptn}}(K,t) = N\sum_{i=1}^{N} c_i V^{ZCCall}(t,T,T_i,A(t,T_i)e^{-B(t,T_i)r^*}). \tag{9.15}$$

The formulas (9.14) and (9.15) are not closed form solutions since the parameter r^* has to be derived numerically from (9.13). We are in a position to compute the risk-neutral density for the model using the normal distribution.

Path Simulation

For our purposes, we need to evolve not only the short rate but also the discount factor into the future. The short rate is used to determine the future term structure, while the discount factor is then used to produce prices for the current time. We use the notation

$$\begin{aligned}
E_{x,i} &:= \mathbb{E}[x(t_i)|x(t_{i-1})] = e^{-\int_{t_{i-1}}^{t_i}\kappa(s)ds}x(t_{i-1}) + \int_{t_{i-1}}^{t_i} e^{-\int_s^{t_i}\kappa(u)du}y(s)ds \\
E_{I,i} &:= \mathbb{E}[I(t_i)|I(t_{i-1}),x(t_{i-1})] = I(t_{i-1}) - x(t_{i-1})G(t_{i-1},t_i) \\
&\quad - \int_{t_{i-1}}^{t_i}\int_{t_{i-1}}^{u} e^{-\int_s^u \kappa(v)dv}y(s)dsdu \\
V_{x,i} &:= \mathbb{V}[x(t_i)|x(t_{i-1})] = \int_{t_{i-1}}^{t_i}\left(e^{-\int_s^{t_i}\kappa(u)du}\sigma(s)\right)^2 ds \\
V_{I,i} &:= \mathbb{V}[I(t_i)|I(t_{i-1}),x(t_{i-1})] \\
&= 2\int_{t_{i-1}}^{t_i}\int_{t_{i-1}}^{u} e^{-\int_s^u \kappa(v)dv}y(s)dsdu - y(t_{i-1})G(t_{i-1},t_i)^2 \\
C_i &:= \mathrm{COV}[x(t_i),I(t_i)|x(t_{i-1}),I(t_{i-1})] \\
&= \int_{t_{i-1}}^{t_i}\int_{t_{i-1}}^{u} \sigma(u)^2 e^{-2\int_s^u \kappa(v)dv} e^{-\int_s^{t_i}\kappa(v)dv}dsdu \\
\rho_i &:= \frac{C_i}{\sqrt{V_{I,i}}\sqrt{V_{x,i}}}
\end{aligned}$$

with $G(t,T) = \int_t^T e^{-\int_t^u \kappa(s)ds}du$. Let $Z_1, Z_2 \sim \mathcal{N}(0,1)$ be independent standard normal variates. Then we use

$$\begin{aligned}
r(t_i) &= E_x + \sqrt{V_x}Z_1 \\
I(t_i) &= E_I + \sqrt{V_I}(\rho_i Z_1 + \sqrt{1-\rho_i^2}Z_2).
\end{aligned}$$

Finally, let us consider the general Gaussian Short Rate model again. We now show how all the models together with time-dependent parameters embed into this class.

For a most general Gaussian Short Rate model to match the initial term structure, the function ϕ is of the following form:

$$\phi(t) = \frac{1}{\kappa(t)}\frac{\partial f(0,t)}{\partial t} + f(0,t) + \frac{1}{\kappa(t)}\int_0^t e^{-2\int_u^t \kappa(s)ds}\sigma(u)^2 du.$$

We considered the notation $r = x - f(0,t)$. For the general Gaussian Short Rate model, we have

$$dx(t) = (\underbrace{\int_0^t e^{-2\int_u^t \kappa(s)ds}\sigma(u)^2 du}_{y(t)} - \kappa(t)r(t))dt + \sigma(t)dW(t), \quad x(0) = 0$$

with bond pricing formulas

$$P(0,T) = \frac{P(0,T)}{P(0,t)}\exp\left(-x(t)G(t,T) - \frac{1}{2}y(t)G(t,T)^2\right)$$
$$G(t,T) = \int_t^T e^{-\int_u^t \kappa(s)ds}du,$$

and we understand the different notations used at the beginning of this section.

LGM Formulation of Gaussian Short Rate

The *Linear Gauss Markov* (LGM) formulation of the Gaussian Short Rate is due to Hagan and Woodward (1999). In the following, we consider this approach and derive the pricing formulae for standard instruments, that is Caps, Floors and Swaptions. Then we give an overview of possible calibration methodologies with time-dependent functions $\kappa(t)$ and $\sigma(t)$.
First, we consider the stochastic differential Eq. (9.16)

$$dX = a(t)dW(t). \tag{9.16}$$

The solution is a Gaussian variable $X(t)$ and the transition probability density is specified by (9.17):

$$\begin{aligned} p(t,x;T,X) &= \mathbb{P}\left(X < X(T) \leq X + dX \,|\, X(t) = x\right) \\ &= \frac{1}{\sqrt{2\pi\,\Delta\xi}} \exp\left(-\frac{(X-x)^2}{2\Delta\xi}\right) \end{aligned} \tag{9.17}$$

with

$$\Delta\xi := \Delta\xi_t^T := \xi(T) - \xi(t), \quad \xi(t) := \int_0^t a(s)^2 ds.$$

Next, for pricing financial instruments we need to specify the measure we apply when calculating the expected values. Due to the change of numeraire theorem from Kienitz (2014), we can use any positive quantity as the numeraire. In contrast to take a numeraire and specify the dynamic, we propose to use the numeraire

$$N(t,x) = \frac{1}{R(0,t)} \exp\left(H(t)x + \frac{H(t)^2\xi(t)}{2}\right). \tag{9.18}$$

In (9.18) N is a function of t and x. The last ingredient we need to successfully apply the model is a pricing equation. We wish to price the payoff V at time T with state x. To this end, we consider (9.19)

$$\begin{aligned} V(t,x) &= N(t,x)\mathbb{E}\left[\frac{V(T,X)}{N(T,X)}\middle| X(t) = x\right] \\ &= \frac{N(t,x)}{\sqrt{2\pi\,\Delta\xi}} \int \frac{V(T,X)}{N(T,X)} \exp\left(-\frac{(X-x)^2}{2\Delta\xi}\right) dX. \end{aligned} \tag{9.19}$$

Sometime instead of using the pricing Eq. (9.19), it is better to consider already discounted prices and, thus, consider

$$\tilde{V}(t,x) = \frac{V(t,x)}{N(t,x)}.$$

The pricing equation is given by (9.20):

$$V(t,x) = \frac{1}{\sqrt{2\pi\,\Delta\xi}} \int V(T,X) \exp\left(-\frac{(X-x)^2}{2\Delta\xi}\right) dX. \tag{9.20}$$

We use the same notation for standard and deflated prices but we remark which is the specific setting where appropriate! First, it is not necessary that

the process X is one dimensional. Second, the pricing equation is the standard martingale pricing and, thus, strictly speaking not an ingredient of the LGM model. Third, the functions $a(t)$, $H(t)$ and, thus, $\xi(t)$ have to be determined, which is central to the calibration to market data.
Now, we show that the LGM model is essentially a Gaussian Short Rate model. To this end, we start with an LGM model and we set

$$\kappa(t) = -\frac{H''(t)}{H'(t)}, \quad \sigma(t) = H'(t)\sqrt{\xi'(t)}. \tag{9.21}$$

Using these two functions, we can consider the corresponding Gaussian Short Rate model. Thus, any LGM model specifies some Gaussian Short Rate model by (9.21).
Now, the other way round, starting with an Hull–White model we set

$$H(t) = c_1 \int_0^t \exp\left(-\int_0^s \kappa(u)du\right) ds + c_2 \tag{9.22}$$

and

$$\xi(t) = \frac{1}{c_1^2} \int_0^t \sigma^2(s) + \exp\left(2\int_0^s \kappa(u)du\right) ds. \tag{9.23}$$

Thus, (9.22) and (9.23) specify some LGM model with c_1 and c_2 being arbitrary positive constants. To clarify the connection of Gaussian Short Rate and LGM models further, let us consider the transformations:

$$(I)\begin{matrix} H(t) \to c_1 H(t) \\ \xi(t) \to c_2^{-1}\xi(t) \end{matrix}; \quad (II)\begin{matrix} H(t) \to H(t) + c_1 \\ \xi(t) \to \xi(t) \end{matrix}.$$

Since we do obtain the same Gaussian Short Rate model using either the start values or the transformed values, we get the same zero bond prices and option prices! The invariance properties can be applied for calibrating the model.

In a swap, we exchange payments corresponding to the deal's fixed swap rate SR_{mn} according to a payment schedule

$$\mathcal{T}_{\mathrm{Y}} = \{T_m^Y, T_{m+1}^Y, \ldots, T_n^Y\}$$

against the Libor rates $L(T_i, T_{i+1})$ for the corresponding payment schedule

$$\mathcal{T}_{\mathrm{Libor}} = \{T_m^L = T_m^Y, T_{m+1}^L, \ldots, T_N^L = T_n^Y\}.$$

The last payment on the fixed, respectively Libor, leg might include the nominal. For the fix leg, we have

$$V_{\text{Fix}}^{\text{Swap}}(t,x) = SR^{\text{f}} \sum_{j=m+1}^{n} \tau_j^Y P(t,x,T_j^Y).$$

For the floating leg, we have (eventually adjusted for a deterministic basis spread)

$$V_{\text{Float}}^{\text{Swap}}(t,x) = P(t,x,T_m^L) \sum_{j=m+1}^{N} \tau_j^L P(t,x,T_j^L).$$

Remember that in a multiple curve setting we have

$$V_{\text{Float}}^{\text{Swap}}(t,x) = \sum_{j=m+1}^{N} \tau_j^L L(t,x,T_i,T_{i+1}) P(t,x,T_j^L)$$

with L being a Libor index and D being the OIS discount factor.

$$\begin{aligned} V^{\text{Floorlet}} &= (1+\tau_{01}K)\,P(0,T_1)\mathcal{N}(d_1^f) - P(0,T_0)\mathcal{N}(d_2^f) \\ V^{\text{Caplet}} &= P(0,T_0)\mathcal{N}(d_1^c) - (1+\tau_{01}K)P(0,T_1)\mathcal{N}(d_2^c) \end{aligned}$$

with τ_{01} denoting the Floating rate period and

$$\begin{aligned} d_{1,2}^f &= \frac{\log\left(\frac{1+\tau_{01}K}{1+\tau_{01}L}\right) \pm \frac{1}{2}(H_1-H_0)^2\xi_T}{(H_1-H_0)\sqrt{\xi_T}} \\ d_{1,2}^c &= \frac{\log\left(\frac{1+\tau_{01}L}{1+\tau_{01}K}\right) \pm \frac{1}{2}(H_1-H_0)^2\xi_T}{(H_1-H_0)\sqrt{\xi_T}}. \end{aligned}$$

The formulae for a Floorlet/Caplet can be seen as special cases of a Swaption. To this end, we analyse the derivation in more detail.
The payoff of a Receiver Swaption is given by

$$V_{\text{Rec}}^{\text{Swptn}}(T,x) = \left(\sum_{i=m+1}^{n} \tau_i K P(T,x,T_i) + P(T,x,T_n) - P(T,x,T_m) \right)^+.$$

Thus, using the LGM formalism we have

$$V_{\text{Rec}}^{\text{Swptn}}(0) = \frac{1}{2\pi\xi(T)} \int \exp\left(-\frac{X^2}{2\xi(T)}\right) V_{\text{Rec}}^{\text{Swptn}}(T, X)dX.$$

The latter integral can be evaluated and is given by

$$\frac{1}{\sqrt{2\pi\xi(T)}} \int \exp\left(-\frac{y^2}{2\xi(T)}\right) \times \Big[\sum_{i=m+1}^{n} \tau_i KP(0, T_i) e^{-(H_i - H_0)y - \frac{(H_i - H_0)^2 \xi(T)}{2}}$$
$$+ P(0, T_n) e^{-(H_n - H_0)y - \frac{(H_n - H_0)^2 \xi(T)}{2}} - P(0, T_m) \Big]^+ dy.$$

To state a Black–Scholes-type equation, we need to find y^* with

$$\sum_{i=m+1}^{n} \tau_i KP(0, T_i) e^{-(H_i - H_0)y^* - \frac{(H_i - H_0)^2 \xi(T)}{2}}$$
$$+ P(0, T_n) e^{-(H_n - H_0)y^* - \frac{(H_n - H_0)^2 \xi(T)}{2}} = P(0, T_m).$$

Using y^* for the integration limits, we find

$$V_{\text{Rec}}^{\text{Swptn}}(0) = \sum_{i=m+1}^{n} \tau_i KP(0, T_i)\mathcal{N}(d_i) + P(0, T_n)\mathcal{N}(d_n) - P(0, T_m)\mathcal{N}(d)$$

with

$$d_i = \frac{y^* + (H_n - H_0)\xi(T)}{\sqrt{\xi(T)}}, \quad d = \frac{y^*}{\sqrt{\xi(T)}}.$$

For the Payer Swaption, we have

$$\begin{aligned} V_{\text{Pay}}^{\text{Swptn}}(0) &= -\sum_{i=m+1}^{n} \tau_i KP(0, T_i)\mathcal{N}(-d_i) - P(0, T_n)\mathcal{N}(-d_n) \\ &\quad + P(0, T_m)\mathcal{N}(-d) \\ &= V_{\text{Rec}}^{\text{Swptn}}(0) + P(0, T_m) - \sum_{i=m+1}^{n} \tau_i KP(0, T_i) - P(0, T_n). \end{aligned}$$

The value y^* can be computed by a root searching procedure. For the latter, the derivatives need to be calculated but this can be done analytically for this

model parametrization. In general, it would be very useful to be able to quickly price a contract. Thus, having some kind of approximation formula could be beneficial. Here we have an approximation to the Black76 implied volatility and use

$$V_{\text{Rec}}^{\text{Swptn}}(0) = K\mathcal{N}(d_1) - SR_{m,n}(0)\mathcal{N}(d_2)$$
$$V_{\text{Pay}}^{\text{Swptn}}(0) = SR_{m,n}(0)\mathcal{N}(-d_2) - K\mathcal{N}(-d_1)$$

with $d_{1,2} = (P(0, T_m) - P(0, T_n))/\sum_{i=m+1}^{n} \tau_i P(0, T_i)$. Then, the implied Black76 volatility is approximately given by

$$\sigma_{\text{BS}}\sqrt{T} \approx \frac{\sqrt{T}}{\sqrt{KSR_{m,n}(0)}} \frac{\sum_{i=1}^{n} \tau_i SR_{m,n}(0)P(0, T_i)(H_i - H_0) + P(0, T_n)(H_n - H_0)}{\sum_{i=1}^{n} \tau_i P(0, T_i)}.$$

But it is also very convenient to use the implied Bachelier volatility. Using the results in Dimitroff et al. (2016), we can apply the approximation above to calculate the Bachelier volatility.

Let us come back to the calibration. For instance, we consider a Bermudan Swaption. Specify a set of early exercise dates $\mathcal{T}_e = \{T_{m+k}, \ldots, T_n\}$ where we have to decide if we enter into a T_{m+k}, T_n swap or if we enter into a corresponding swap later. The Bermudan value should be larger than the largest one of the constituting European swaptions and the option of exercise at a later point in time could be interpreted as a switch option.

As explained earlier for the hedging of the interest rate risk, we need to specify a hedge strategy. The hedge strategy should involve standard instruments which are liquid. This is of utmost importance to be able to rebalance the hedge as the trader needs. The model should price the hedging instruments correctly. This is now the calibration problem. To solve it, we specify some error measure including model and market prices for the hedge instruments. Seen this way, the hedge resembles the approximate price for the exotic. The calibrated model is now the best approximation to the exotic option.

For the example of a Bermudan swaption, the co-terminal (European) swaptions are the standard hedge instruments. Thus, our model should be calibrated to these instruments. The calibration instruments in this case are determined by the implied volatility quotes of the diagonal of the implied volatility swaption matrix. In the case of the LGM formulation of the Gaussian Short Rate model, we describe several calibration strategies that relate to standard instruments.

The first calibration strategy, (I), is to calibrate the diagonals with fixed κ values and use the relation $H'(T)/H(T) = -\kappa$ and, thus,

$$H(T) = Ae^{-\kappa T} + B \tag{9.24}$$

Applying invariance properties of LGM, we take

$$H(T) = \frac{1 - e^{-\kappa T}}{\kappa}. \tag{9.25}$$

Then, $H(T)$ is specified and we are left with determining ξ. To this end, we use the longest maturity swaption to fit $\xi(T_N)$ and the representation of H to fit the market values for T_i by finding $\xi(T_i)$, $i = N-1, \ldots, 1$. The values of κ are often related to quotes of Bermudan swaptions and practitioners use to set κ to some fixed number or take the numbers from a table that is obtained by a full calibration procedure to Bermudan swaptions.

Another strategy, (II), is to calibrate to a column again with fixed κ values and applying the relation $H'(T)/H(T) = -\kappa$ and, thus, again use Eqs. (9.24) and (9.25). This determines $H(T)$ and it remains to determine ξ. To this end, we use the longest maturity swaption to fit $\xi(T_N)$ for the selected column. Use the representation of H and fit the market values for T_i by finding $\xi(T_i)$, $i = N-1, \ldots, 1$ for the selected column.

Yet another one can be to determine ξ, first. To this end, we choose any increasing or a linear function. Determine the values of $H(T_i)$ by matching the diagonal swaptions.

The next calibration strategy, (III), is to calibrate the diagonal with the given values for ξ. To this end, ξ is specified as any increasing function, for instance a linear one. Then, the values of $H(T_i)$ are used to match the diagonals of the given swaption matrix.

Yet another strategy, (IV), could be to match a column and the diagonal. First, the specified column is fitted and, then, the ξ values are determined from the values for the column instruments and $H(T_i)$ by matching the diagonal swaptions. This is often referred to as the standard LGM calibration procedure.

Finally, instead of a column we might use a row, (V). To this end, set $H(T_0) = 0$ and $\xi(T_0)$ to some fixed value. Then, first match the first price in the specified row. This determines $H(T_N), \ldots, H(T_1)$. Then use ξ to match the diagonal.

In the sequel, we consider the calibration to Bermudan swaptions. To this end, the hedging instruments are the diagonal (co-terminal) swaptions for a given strike. In addition to the diagonal swaptions, people use columns or rows to fit the parameters of the LGM model. Figure 9.3 illustrates the setting.

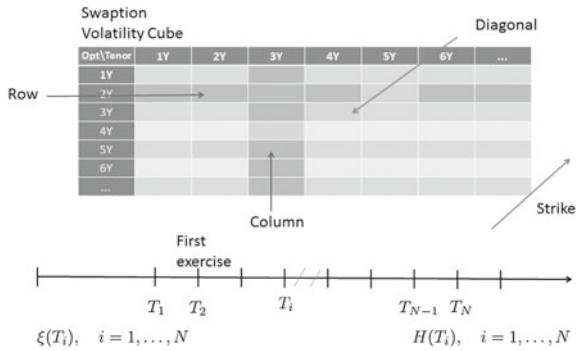

Fig. 9.3 Hedging Instruments for the calibration of the LGM model to Bermudan swaptions

In the sequel, we consider the following calibration strategies:

- **Diagonal with fixed ξ – I**
  We fix the values of ı and use linear interpolation. Then, we consider the $N-1$ into 1, $N-2$ into 2, ... swaptions to determine H assuming without loss of generality the final value $H(T_N) = 0$. Each of the quotes gives us a value of $H(T_i)$. Figure 9.4 shows the values that are fixed in black and the ones to be calibrated in blue.
- **Diagonal with fixed κ – II**
  First, we fix the value of κ that determines the values of H by $H(T) = (1 - e^{-\kappa T})/\kappa$. Thus, only ξ needs to be determined. To this end, we fit the value to the swaption with the longest maturity, namely $\xi(T_N)$. Use the representation of H and fix the market value for all the remaining T_i by fixing $\xi(T_i)$ using the quotes. We illustrated the calibration in Fig. 9.5.
- **Diagonal and column–Standard LGM calibration – III**
  The standard LGM calibration uses market data from a column and a diagonal, namely the N into 1, $N-1$ into 1, $N-2$ into 1, ... quotes from the column and the $N-1$ into 2, $N-2$ into 3, ... quotes from the diagonal. This means we have two quotes to determine two unknown values. We only need to fix the values of $H(T_N)$ and $H(T_{N-1})$ which we do by setting them to 0 and 1, respectively. This is without loss of generality due to the transformation properties of the LGM model. Figure 9.6 illustrates the standard LGM calibration.
- **Diagonal and row – IV**
  The following instruments are taken to determine the model parameters: 2 into 1, 2 into 2, 2 into 3, ... from the row and 3 into $N-3$, 4 into $N-4$, ..., from the diagonal, Fig. 9.7. This means that we can use two

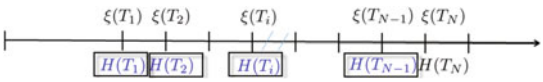

Fig. 9.4 Calibration strategy I

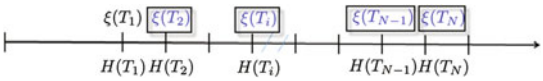

Fig. 9.5 Calibration strategy II

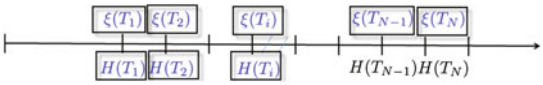

Fig. 9.6 Calibration strategy III

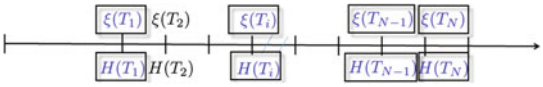

Fig. 9.7 Calibration strategy IV

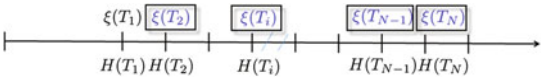

Fig. 9.8 Calibration strategy V

given values to determine the values of ξ and H at a given point in time T_i. We need to fix the values of ξ and H at the first exercise T_2.

- **Column with fixed κ – V**
  This is essentially the calibration to Caplets, Fig. 9.8. We fix the value of κ to determine all the values of H. Then, we use the $N-1$ into 1, $N-2$ into 1, ... swaptions. From the quotes, we determine the values of ξ assuming that the first value, $\xi(T_1)$, is fixed.

Many more calibration strategies can be considered. We have also to remark that it is common that the natural hedging instruments might not be available. This could be the case if no market data are available for the swaption strike. Then, we have to rely on liquid market instruments for hedging. We may wish to account for this mismatch by considering the technique of an adjuster which is described in Hagan (2002).

It is obvious from Fig. 9.9 that each calibration methodology assigns importance to different parts of the swaption implied volatility matrix and, thus, to different hedging instruments. This means that the error is small if the

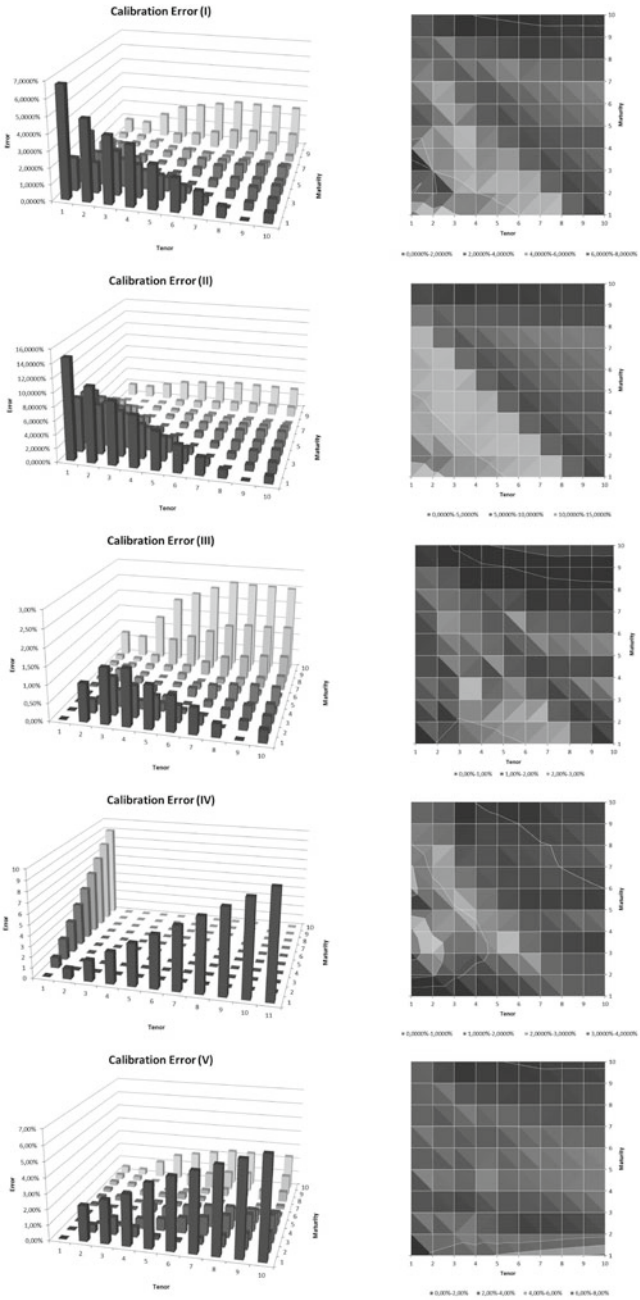

Fig. 9.9 Calibration Error for the strategies (**I**–**V**)

instrument is determined as a hedging instrument or not. Figure 9.9 shows the absolute difference between the quotes and the prices on the left and the same data but in a heat map fashion on the right.

After calibrating the model, it is possible to price exotic instruments since as we remember the calibration resembles an approximation to the instruments that are available for hedging. Essentially, in a calibration we choose hedge instruments and choose the model parameters that the hedging instruments are reasonably priced. Then, any trading strategy in the hedging instruments leads to a price for the exotic. The shortcut is to use the pricing formula from the model, respectively some numerical method, to calculate the exotic price.

9.1.2 Affine Short Rate Models and the Cox–Ingersol–Ross Model (CIR)

Before the financial crisis, many people regarded interest rate models accommodating negative interest rates as flawed and unrealistic. Of course this has changed now. Since the versions of the Gaussian Short Rate model lead to a Gaussian dynamic for the Short Rate, it would be possible to generate negative rates. However, other than Gaussian Short Rate models played and still play a fundamental role in the financial modeling. For instance, we identified that the skew/smile cannot be controlled reasonably using this approach. To this end, the class of Affine Short Rate models is considered. The main representative of a model belonging to this class is the Cox–Ingersoll–Ross or CIR model, Cox et al. (1985), for short. A general model of the Affine Short Rate model class is given by

$$dr(t) = \kappa(t)(\theta(t) - r(t))dt + \sigma(t)C(r(t))dW(t). \tag{9.26}$$

The function C can be chosen by the modeler. Often it is assumed to be of the form $C(r) = (a + br)^{\beta}$. We have to remark that not all choices of functions κ, θ and σ lead to reasonable dynamics; see Andersen and Piterbarg (2010) for details.

The Zero Coupon Bonds are determined by

$$P(t, T) = e^{A(t,T) - B(t,T)r(t)}, \tag{9.27}$$

where A and B satisfy the so-called Riccati differential equation:

$$\frac{dA}{dt} - \kappa(t)\theta(t)B + \frac{1}{2}\sigma(t)^2 aB^2 = 0$$
$$-\frac{dB}{dt} + \kappa(t)B + \frac{1}{2}\sigma(t)^2 bB^2 = 0$$

subject to the terminal conditions $A(T,T) = 0$ and $B(T,T) = 0$. This is a special case of a more general result involving the existence of the joint density of r and $e^{-\int_t^T r(u)du}$, from which the Zero Coupon Bond prices are a special case. Furthermore, this sheds light on the fact why such models are popular among financial modelers; see Andersen and Piterbarg (2010) for details.
We consider a representative of this class, namely the CIR model. This model is given by the following set of SDEs with κ, θ and σ being constants:

$$\begin{aligned} dr(t) &= \kappa(\theta - r(t))dt + \sigma\sqrt{r(t)}dW(t) \\ r(0) &= r_0. \end{aligned} \tag{9.28}$$

This means that it embeds into the general Affine Short Rate model class by choosing the function $C(r) = \sqrt{r}$. The first and second moments can be calculated. They are given by Eqs. (9.29) and (9.30):

$$\mathbb{E}[r(t)|\mathcal{F}_s] = r(s)e^{-\kappa(t-s)} + \theta\left(1 - e^{-\kappa(t-s)}\right) \tag{9.29}$$

$$\begin{aligned} \mathbb{V}[r(t)|\mathcal{F}_s] = r(s)\frac{\sigma^2}{\kappa}&\left(e^{-\kappa(t-s)} - e^{-2\kappa(t-s)}\right) \\ &+ \theta\frac{\sigma^2}{2\kappa}\left(1 - e^{-\kappa(t-s)}\right)^2. \end{aligned} \tag{9.30}$$

Very convenient is that the CIR model allows to explicitly determine the Zero Coupon Bond prices. Using the general formula (9.27), a solution for the Riccati equation can be given in closed form, and thus denoting $\gamma = \sqrt{\kappa^2 + 2\sigma^2}$, the prices are given by

$$P(t,T) = A(t,T)e^{-B(t,T)r(t)} \tag{9.31}$$
$$A(t,T) = \left(\frac{2\gamma e^{(\kappa+\gamma)(T-t)/2}}{2\gamma + (\kappa+\gamma)(e^{(T-t)\gamma} - 1)}\right)^{\frac{2\kappa\theta}{\sigma^2}}$$
$$B(t,T) = \frac{2(e^{(T-t)\gamma} - 1)}{2\gamma + (\kappa+\gamma)(e^{(T-t)\gamma} - 1)}.$$

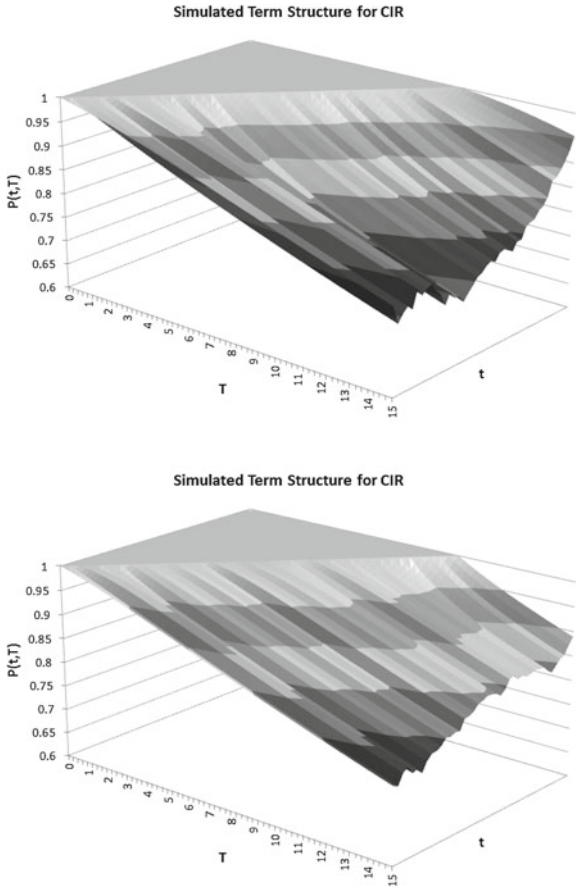

Fig. 9.10 Two simulated term structures for the CIR model with $\kappa = 0.2$ (*top*) and $\kappa = 0.5$ (*bottom*), $\theta = 0.02$, $\sigma = 0.02$ and $r = 0.01$

Fig. 9.10 shows some term structure evolution for the CIR model paths with constant coefficients. We evolved the short rate r and used (9.31) to calculate the term structure. We used the representation of the mean and the variance. Then, we sampled realizations of standard normal variables with the mean and standard deviation calculated using the formulas (9.29) and (9.30). This is furthermore an illustration of the effects of the parameters κ and θ. The short rate tends to the long-term value θ and the parameter κ determines how fast the process is pulled back if it deviated from θ.

As we already found for other short rate models, there are closed form pricing formulas available for European Call and Put options on Zero Coupon Bonds:

$$V^{ZCCall}(K,T) = P(t,S)\chi^2\left(2\bar{r}(\rho+\psi+B(T,S)); \frac{4\kappa\theta}{\sigma^2}, \frac{2\rho^2 r(t)e^{\gamma(T-t)}}{\rho+\psi+B(T,S)}\right)$$
$$-KP(t,T)\chi^2\left(2\bar{r}(\rho+\psi); \frac{4\kappa\theta}{\sigma^2}, \frac{2\rho^2 r(t)e^{\gamma(T-t)}}{\rho+\psi}\right)$$

with

$$\rho = \rho(T-t) = \frac{2\gamma}{\sigma^2(e^{\gamma(T-t)}-1)}, \quad \psi = \frac{\kappa+\gamma}{\sigma^2}, \quad \bar{r} = \frac{\ln(A(T,S)/K)}{B(T,S)}.$$

As for the Gaussian Short Rate models, the dynamic when the Zero Bond maturing at time T is the numeraire is known. Let W be a Brownian Motion with respect to this numeraire. Then

$$dr(t) = (k\theta - (k + B(T,S)\sigma^2)r(t))dt + \sigma\sqrt{r(t)}dW^T(t).$$

This is often useful if we wish to price European options maturing at T.
It is tempting as for the Gaussian Short Rate models to make the parameter θ time dependent to match the initial term structure. However, there are to the best knowledge of the authors no closed form formulas available for determining the necessary quantities.

The CIR model plays an important role either for interest rate models but also for volatility and credit models. The model as described above is in general not able to fit the initial term structure. To this end, we consider an extension which is known as the CIR++ model; see Brigo and Mercurio (2006) or Lichters et al. (2015). This model is obtained from the CIR model by applying a general shift extension; see Brigo and Mercurio (2006). To explain what happens here is that we consider a generalized version of (9.7) and use a CIR dynamic for modelling $x(t)$. In the setting of CIR++, we use the following ansatz:

$$r(t) = x(t) + \phi(t).$$

As opposed to (9.7), we use the difference of the instantaneous forward rated $f(0,t)$ and the instantaneous forward rates implied by a CIR model $f_C(0,t)$. This means we consider

$$\phi(t) = f(0,t) - f_C(0,t)$$

with

$$f_C(0,t) = \frac{2\kappa\theta\left(e^{t\gamma}-1\right)}{2\gamma+(\kappa+\gamma)\left(e^{t\gamma}-1\right)} + x(0)\frac{4\gamma^2 e^{t\gamma}}{\left(2\gamma+(\kappa+\gamma)\left(e^{t\gamma}-1\right)\right)^2}.$$

Using this set-up, prices of Zero Coupon Bonds are explicitly given and the corresponding pricing formulae for European Call and Put options can be derived; see Brigo and Mercurio (2006) or Lichters et al. (2015) for details. Such formulas then lead to pricing formulas for Caps, Floors and Swaptions. Working with the CIR++ model is not straightforward. Here, we have to mention that the generated rates are not always positive. While not that important for interest rates, sometimes the modeler wish to apply term structure models to quantities which should be positive, for instance hazard rates. The rates in CIR++ are always positive if $\phi(t) > 0$ for all $t \geq 0$. This turns out to be a very restrictive assumption leading to a low fitting quality for Cap, Floor or Swaption volatilities. This is due to restrictions in the model parameters implied by the assumption. However, the assumptions can be weakened but, then, the rates are not necessarily positive but only get negative for extreme parameters. For all the issues arising here we point to Brigo and Mercurio (2006).

9.2 Multi-dimensional Models/N-Factor Models

As already mentioned, using just one stochastic risk factor might not be enough. For the models considered so far, the movement of all rates is only determined by the movement of the driving Brownian motion. Thus, the stochastic shocks are the same for all the rates regardless if they are short-, mid- or long-term rates. The different movements of short-, mid- and long-term rates, known as de-correlation of rates cannot be modelled in a one-factor framework. Furthermore, options such as spread options depending on, for instance, the 10y and the 2y swap rate having a payoff $\max(SR_{10} - SR_2, K)$ are known to depend on the co-movement of the rates. Historically, there are periods where the 10Y rate and the 2Y rate show different movements. This means that the correlation is not perfect and is an important risk factor to take into account. Thus, to realistically model the evolution of the yield curve we should use multiple factors $x_i(t)$, $i = 1, \ldots, d$, each being, for instance, a Gaussian model. The driving Brownian motions can then be correlated. The short rate is the sum of the factors $x_i(t)$, and we have

$$dr(t) = \sum_{j=1}^{n} x_j(t).$$

We can also extend the short rate models to cover multiple tenor curves, for instance the 1-, 3- or 6-month curves.
In this modelling framework, the *affine models* gained a lot of attention since pricing and calibration can be done efficiently since the characteristic function, that is a very useful tool for numerically pricing options, of the model is available in closed form.

9.2.1 Example: The Two-Factor Gaussian Short Rate/G2++ Model

In this subsection, we consider a two-dimensional Gaussian short rate model. The G2++ model is popular among practitioners. We closely follow Brigo and Mercurio (2006). The model is given in terms of the set of SDEs:

$$\begin{aligned} r(t) &= x_1(t) + x_2(t) + \phi(t) \\ dx_1(t) &= -\kappa_1 x_1(t)dt + \sigma_1 dW_1(t) \\ dx_2(t) &= -\kappa_2 x_2(t)dt + \sigma_2 dW_2(t) \\ \langle dW_1(t), dW_2(t)\rangle &= \rho dt \\ (x_1(0), x_2(0)) &= (x_0, y_0). \end{aligned}$$

The G2++ model has a lot of good features such as closed form or semi-analytic formulae for basic derivatives which are necessary when we wish to calibrate the model. We start with the Zero Coupon Bond $P(t, T)$:

$$\begin{aligned} P(t,T) = \exp\Big(&-\int_t^T \varphi(u)du + \frac{1}{2}V(t,T) \\ &-\frac{1-e^{-\kappa_1(T-t)}}{\kappa_1}\cdot x_1(t) - \frac{1-e^{-\kappa_2(T-t)}}{\kappa_2}\cdot x_2(t)\Big) \end{aligned} \tag{9.32}$$

with

$$V(t,T) = \sum_{i=1}^{2} \frac{\sigma_i^2}{\kappa_i^2}\left[T - t + \frac{2}{\kappa_i}e^{-\kappa_i(T-t)} - \frac{1}{2\kappa_i}e^{-2\kappa_i(T-t)}\right]$$
$$+2\rho\frac{\sigma_1\sigma_2}{\kappa_1\kappa_2}\left[T - t + \sum_{i=1}^{2}\frac{e^{\kappa_i(T-t)} - 1}{\kappa_i} - \frac{e^{-(\kappa_1+\kappa_2)(T-t)}}{\kappa_1+\kappa_2}\right].$$

Again, the instantaneous forward $f^M(0,T)$ rates are $f^M(0,T) = -\frac{\partial \log(P^M(0,T))}{\partial T}$ and the function ϕ which is used to recover the initial yield curve

$$\varphi(t) = f^M(0,T) + \sum_{i=1}^{2}\frac{\sigma_i^2}{2\kappa_i^2}\left(1 - e^{-\kappa_i T}\right) + \rho\frac{\sigma_1\sigma_2}{\kappa_1\kappa_2}\left(1 - e^{-\kappa_1 T}\right)\left(1 - e^{-\kappa_2 T}\right).$$

This holds if and only if the model fits the initial term structure. The Zero Coupon Bonds have a representation, (9.33), in terms of the model variables:

$$P(t,T) = \frac{P^M(0,T)}{P^M(0,t)}e^{A(t,T)} \tag{9.33}$$

with the function (9.34)

$$A(t,T) = \frac{1}{2}\left[V(t,T) - V(0,T) + V(0,t)\right] - \sum_{i=1}^{2}\frac{1 - e^{-\kappa_i(T-t)}}{\kappa_i}x_i(t). \tag{9.34}$$

To be able to give the pricing formulas for Call and Put options on Zero Coupon Bonds, we need to specify Σ. It is given by

$$\Sigma(t,T,S) = \sum_{i=1}^{2}\frac{\sigma_i^2}{2\kappa_i^3}\left(1 - e^{-\kappa_i(S-T)}\right)\left(1 - e^{-2\kappa_i(T-t)}\right)$$
$$+2\rho\frac{\sigma_1\sigma_2}{\kappa_1\kappa_2(\kappa_1+\kappa_2)}\left(1 - e^{-\kappa_1(S-T)}\right)\left(1 - e^{-\kappa_2(S-T)}\right)\left(1 - e^{-(\kappa_1+\kappa_2)(T-t)}\right).$$

Using the defined quantities, there are closed form pricing formulas available for European Call and Put options on Zero Coupon Bonds:

$$V^{\text{ZCall}}(t,T,S,K) = NP(t,S)\mathcal{N}\left(\frac{\log\left(\frac{NP(t,S)}{KP(t,T)}\right)}{\Sigma(t,T,S)} + \frac{1}{2}\sigma(t,T,S)\right) \tag{9.35}$$

$$- P(t,T)K\mathcal{N}\left(\frac{\log\left(\frac{NP(t,S)}{KP(t,T)}\right)}{\Sigma(t,T,S)} - \frac{1}{2}\Sigma(t,T,S)\right)$$

$$V^{\text{ZPut}}(t,T,S,K) = -NP(t,S)\mathcal{N}\left(\frac{\ln\left(\frac{KP(t,T)}{NP(t,S)}\right)}{\Sigma(t,T,S)} - \frac{1}{2}\sigma(t,T,S)\right) \tag{9.36}$$

$$+ P(t,T)K\mathcal{N}\left(\frac{\ln\left(\frac{KP(t,T)}{NP(t,S)}\right)}{\Sigma(t,T,S)} + \frac{1}{2}\Sigma(t,T,S)\right).$$

Using (9.35), it is again possible to price Caplets and Floorlets. If x^* is the solution of $x^* = \frac{1}{1+x\tau(T_1,T_2)}$, $N^* = N(1+x\tau(T_1,T_2))$, then the Caplet prices are

$$V^{\text{Caplet}}(t,T_1,T_2,N,K) = N^* V^{\text{ZCPut}}(t,T_1,T_2,X^*).$$

For pricing swaptions, we have to work a bit harder to arrive at the pricing Eq. (9.37). This is based on the considerations in Brigo and Mercurio (2006).

$$N\omega P(0,T)\int_{-\infty}^{\infty}\left[\mathcal{N}(-\omega h_1(x)) - \sum_{i=1}^{n}\lambda_i(x)e^{\kappa_i(x)}\mathcal{N}(-\omega h_2(x))\right]\frac{e^{-\frac{(x-\mu_{x_1})^2}{2\sigma_{x_1}}}}{\sigma_{x_1}\sqrt{2\pi}}dx \tag{9.37}$$

The abbreviations are $\omega = \pm 1$ and

$$h_1(x) = \frac{x_2^* - \mu_{x_2}}{\sigma_2\sqrt{1-\rho_{1,2}^2}} - \frac{\rho_{1,2}(x-\mu_{x_1})}{\sigma_{x_1}\sqrt{1-\rho_{1,2}^2}}$$

$$h_2(x) = h_1(x) + B(\kappa_2,T,t_i)\sigma_{x_2}\sqrt{1-\rho_{1,2}}$$

$$\lambda_i(x) = c_i A(T,t_i)e^{-B(\kappa_2,T,t_i)}$$

$$\kappa_i(x) = -B(\kappa_2,T,t_i)\left(\mu_{x_2} - \frac{1}{2}(1-\rho_{1,2}^2)\sigma_{x_2}^2 B(\kappa_2,t,T) + \rho_{1,2}\sigma_{x_2}^2\frac{x-\mu_{x_1}}{\sigma_{x_1}}\right),$$

and the value x_2^* is the solution of Eq. (9.38)

$$\sum_{i=1}^{n} c_i A(t_i, T) e^{-B(\kappa_1, t_i, T)x_1 - B(\kappa_2, t, T)x_2^*} = 1 \tag{9.38}$$

with $B_j(\kappa, t, T) = \frac{1-e^{-\kappa(T-t)}}{u}$ and the parameters μ_{x_i}, σ_{x_i} for $i = 1, 2$ and $\rho_{1,2}$ given by

$$\mu_{x_i} = -M_{X_i}^T(0, T), \quad \sigma_{x_i} = \sigma_i \sqrt{\frac{1 - e^{-2\kappa_i T}}{2\kappa_i}}, \quad \rho_{1,2} = \frac{\rho\sigma_1\sigma_2}{(\kappa_1 + \kappa_2)\kappa_1\kappa_2}\left(1 - e^{-(\kappa_1+\kappa_2)T}\right)$$

$$\begin{aligned} M_{X_i}(s, t) = &\left(\frac{\sigma_i^2}{\kappa_i^2} + \rho\frac{\sigma_1\sigma_2}{\kappa_2\kappa_2}\right)\left(1 - e^{-\kappa_i(t-s)}\right) \\ &- \left[e^{\kappa_i(T-t)} - e^{\kappa_i(T+t-2s)}\right] \\ &-\rho\frac{\sigma_1\sigma_2}{\kappa_i(\kappa_1 + \kappa_2)}\left[e^{-\kappa_{\bar{j}}(T-t)} - e^{\kappa_{\bar{i}}T - \kappa_i t + (\kappa_1+\kappa_2)s}\right] \end{aligned}$$

with the notation $\kappa_{\bar{1}} = \kappa_2$, $\kappa_{\bar{2}}\kappa_1$. It is possible to give the conditional expectation and the conditional variance with respect to the T-Forward measure.

$$\mathbb{E}^T[r(t)|\mathcal{F}_s] = \sum_{i=1}^{2} x_i(s)e^{-\kappa_i(t-s)} - \sum_{i=1}^{2} M_{X_i}^T(s, t) + \varphi(t)$$

$$\mathbb{V}^T[r(t)|\mathcal{F}_s] = \sum_{i=1}^{2} \frac{\sigma_i^2}{2\kappa_i}\left(1 - e^{-2\kappa_i(t-s)}\right) + 2\rho\frac{\sigma_1\sigma_2}{\kappa_1 + \kappa_2}\left(1 - e^{-(\kappa_1+\kappa_2)(t-s)}\right).$$

Assuming the short rate dynamics in the G2++ model, it is possible to determine the probability distribution since it is a Gaussian model. Thus, it suffices to determine the mean and the variance. The quantities are given by Eqs. (9.39) for the mean and (9.40) for the variance:

$$\begin{aligned} \mathbb{E}[r(t)] = &f^M(0, t) + \frac{\sigma_1^2}{2\kappa_1^2}\left(1 - e^{-2\kappa_1 t}\right)^2 + \frac{\sigma_2^2}{2\kappa_2^2}\left(1 - e^{-2\kappa_2 t}\right)^2 \\ &+\rho\frac{\sigma_1\sigma_2}{\kappa_1\kappa_2}\left(1 - e^{-2\kappa_1 t}\right)\left(1 - e^{-2\kappa_2 t}\right) \end{aligned} \tag{9.39}$$

$$\mathbb{V}[r(t)] = \frac{\sigma_1^2}{2\kappa_1}\left(1 - e^{-2\kappa_1 t}\right) + \frac{\sigma_2^2}{2\kappa_2}\left(1 - e^{-2\kappa_2 t}\right) + 2\frac{\rho\sigma_1\sigma_2}{\kappa_1 + \kappa_2}\left(1 - e^{-(\kappa_1+\kappa_2)t}\right). \tag{9.40}$$

This can be used for generating sample paths as well as to determine the probability of negative rates.

9.2.2 Short Rate Models for Hybrids

The current regulatory pressure makes it necessary to calculate several risk figures based on exposures, for instance CVA. See Kienitz (2014) or Lichters et al. (2015). To this end, we need to be able to model several risk factors at once. We consider the case of an interest rate derivative which is in a foreign currency. In this case, we need to model with respect to the domestic currency which we use for the exposure calculation. In the sequel, we specify the dynamic of the domestic interest rate term structure, the foreign term structure and the foreign exchange rate. The dynamic has to be expressed with the money market numeraire for the domestic currency. Both interest rate processes are Gaussian short rate models and the foreign exchange rate is taken to be Geometric Brownian motion.

Consider a hybrid IR–IR–FX model. The domestic and foreign interest rates r_D, r_F are modelled by two Hull–White (HW) models and the FX rate is modelled by a Geometric Brownian motion (GBM). The equations are given by

$$dr_D(t) = \kappa_D(\theta_D(t) - r_D(t))dt + \sigma_D(t)dW_D^{Q_D}(t), \tag{9.41}$$

$$dr_F(t) = \kappa_F(\theta_F(t) - r_F(t))dt + \sigma_F(t)dW_F^{Q_F}(t), \tag{9.42}$$

$$\frac{dX(t)}{X(t)} = \mu_X(t)dt + \sigma_X(t)dW_X^{Q_D}(t). \tag{9.43}$$

Let ρ_{DF}, ρ_{DX} and ρ_{FX} be the correlations between the Brownian motions $W_D^{Q_D}$, $W_F^{Q_F}$ and $W_X^{Q_D}$, respectively.

9.2.3 Dynamics of Zero-Coupon Bonds in a Gaussian Short Rate Model

First, the dynamics of zero-coupon bond under the dynamic are given by

$$dr(t) = \kappa(\theta(t) - r(t))dt + \sigma(t)dW^Q(t). \tag{9.44}$$

The zero-coupon bond $P(t,T)$ of the model is given by $P(t,T) = E^Q\left[e^{-\int_t^T r(s)ds} \mid F_t\right]$. Then, using the Ito formula we find for the zero bond dynamic:

$$\frac{dP(t,T)}{P(t,T)} = r(t)dt + B(t,T)\sigma(t)dW^Q(t). \tag{9.45}$$

with $B(t,T) = \frac{1}{\kappa}e^{-\kappa(T-t)} - 1$.

9.2.4 Dynamics of HW-GBM FX Model Under the Domestic Risk-Neutral Measure Q_D

The zero-coupon bond of the foreign interest rates under the foreign risk-neutral measure Q_F is given by

$$\frac{dP_F(t,T)}{P_F(t,T)} = r_F(t)dt + B_F(t,T)\sigma_F(t)dW_F^{Q_F}(t).$$

Consider the drift adjustment $dW^{Q_F}(t) = dW^{Q_D}(t) - \gamma(t)dt$. Then the equation becomes

$$\frac{dP_F(t,T)}{P_F(t,T)} = \left(r_F(t) - B_F(t,T)\sigma_F(t)\gamma(t)\right)dt + B_F(t,T)\sigma_F(t)dW_F^{Q_D}(t). \tag{9.46}$$

In order to determine $\gamma(t,T)$, one needs to consider the discounted domestic price of $P_F(t,T)$, that is $\tilde{P}_F^D(t,T) = B_D(t)^{-1}X(t)P_F(t,T)$. The equation of the spot FX rate $X(t)$ is given by (9.43). Furthermore, we have $\frac{dB_D(t)^{-1}}{B_D(t)^{-1}} = -r_D(t)dt$. Therefore, the equation of $\tilde{P}_F^D(t,T)$ turns out to be

$$\begin{aligned}\frac{d\tilde{P}_F^D(t,T)}{\tilde{P}_F^D(t,T)} = \Big(&- r_D(t) + r_F(t) - B_F(t,T)\sigma_F(t)\gamma(t) + \mu_X(t) \\ &+ B_F(t,T)\sigma_F(t)\sigma_X(t)\rho_{FX}\Big)dt \\ &+ B_F(t,T)\sigma_F(t)dW_F^{Q_D}(t) + \sigma_X(t)dW_X^{Q_D}(t).\end{aligned}$$

Under the domestic risk-neutral measure Q_D, $\tilde{P}_F^D(t,T)$ must be a martingale and hence the drift term vanishes, that is

$$-r_D(t) + r_F(t) - B_F(t,T)\sigma_F(t)\gamma(t) + \mu_X(t) + B_F(t,T)\sigma_F(t)\sigma_X(t)\rho_{FX} = 0.$$

Since the equation holds for all $T > 0$, we get

$$\mu_X(t) = r_D(t) - r_F(t),$$
$$\gamma(t) = \sigma_X(t)\rho_{FX}.$$

At last, the dynamics of the HW-GBM FX model under Q_D are given by

$$\begin{aligned}
\frac{dP_D(t,T)}{P_D(t,T)} &= r_D(t)dt + B_D(t,T)\sigma_D(t)dW_D^{Q_D}(t) \\
\frac{dP_F(t,T)}{P_F(t,T)} &= (r_F(t) - B_F(t,T)\sigma_F(t)\sigma_X(t)\rho_{FX})\,dt + B_F(t,T)\sigma_F(t)dW_F^{Q_D}(t) \\
\frac{dX(t)}{X(t)} &= (r_D(t) - r_F(t))dt + \sigma_X(t)dW_X^{Q_D}(t).
\end{aligned}$$

9.2.5 Dynamics of HW-GBM FX Model Under the Domestic T-forward Measure Q_D^T

In order to give the dynamics of the FX model under the measure Q_D^T which is often useful for pricing, we need to find the related drift. This can be done using the change of numeraire technique. We just state the final outcome that can be used in practice.

$$\begin{aligned}
\frac{dP_D(t,T)}{P_D(t,T)} &= \left(r_D(t) + B_D(t,T)^2\sigma_D(t)^2\right)dt + B_D(t,T)\sigma_D(t)dW_D^{Q_D^T}(t), \\
\frac{dP_F(t,T)}{P_F(t,T)} &= \Big(r_F(t) - B_F(t,T)\sigma_F(t)\sigma_X(t)\rho_{FX} \\
&\quad + B_D(t,T)\sigma_D(t)B_F(t,T)\sigma_F(t)\rho_{DF}\Big)dt + B_F(t,T)\sigma_F(t)dW_F^{Q_D^T}(t), \\
\frac{dX(t)}{X(t)} &= (r_D(t) - r_F(t) + B_D(t,T)\sigma_D(t)\sigma_X(t)\rho_{DX})\,dt + \sigma_X(t)dW_X^{Q_D^T}(t).
\end{aligned}$$

9.3 Stochastic Volatility

In Chap. 8, we considered the extension of interest rate models by adding a stochastic volatility component. Common short rate models are not able to fully resemble market structures such as the skew/smile observed in market quotes for Caps, Floors or Swaptions. Let us consider the Zero Coupon Bond

dynamics if we assume some Short Rate Model:

$$\frac{dP(t,T)}{P(t,T)} = r(t)dt + \sigma(t)dW(t)$$

Now, for illustration let us focus on the Vasicek model and simply add a stochastic volatility to the short rate; thus, we take

$$\begin{aligned} dr(t) &= \kappa_r(\theta_r - r(t))dt + \sigma_r\sqrt{z(t)}dW_1(t) \\ dz(t) &= \kappa_z(\theta_z - z(t))dt + \sqrt{z(t)}dW_2(t). \end{aligned}$$

Consider the zero bonds $P(t, T_1)$ and $P(t, T_2)$. Within the stochastic volatility Vasicek model, we have

$$\frac{\partial P(t,T_1)}{\partial r} \neq 0, \qquad \frac{\partial P(t,T_2)}{\partial z} \neq 0. \tag{9.47}$$

Thus, the condition specified by Eq. (9.47) is violated. This means that this is not a true, respectively unspanned, stochastic volatility model. Let us briefly expand on this issue here. If V is the price of a derivative security, then we have

$$dV = \frac{\partial V}{\partial r}dr(t) + \frac{\partial V}{\partial z}dz(t) + \ldots dt.$$

Since the prices of the Zero Bond maturing at time T_1 and time T_2 have non-zero partial derivatives with respect to r and z, we construct a portfolio using the bonds such that

$$dV = w_1\frac{\partial P(t,T_1)}{\partial r}dr(t) + w_2\frac{\partial P(t,T_2)}{\partial z}dz(t).$$

But this means that the volatility risk can be eliminated by hedging trades in zero bonds alone. To this end, we verified that this is not a true stochastic volatility model. For true stochastic volatility models, the risk arising from a stochastic volatility component has to be hedged using options.

9.4 Stochastic Basis

We consider the general framework from Chap. 8 Sect. 8.4 in the context of Short Rate Models by giving an example. We take a Vasicek model using the notation $r(t) = x(t) + \phi(t)$ with the dynamics of x given by

$$dx(t) = -\kappa x(t)dt + \sigma(t)dW(t), \quad x(0) = 0.$$

For the dynamics of the spreads, we choose the set-up that each spread $\mathcal{X}_k^x$ is driven by a Geometric Brownian Motion, that is

$$d\mathcal{X}_k^{nM}(t) = \sigma^{nM}\mathcal{X}_k^{nM}dZ^{nM}(t).$$

Further assumptions such that this dynamic applies to all values of k further simplify the model and make it easier to apply in practice. The price to pay is that some of the risk is not well captured. We wish to illustrate the applicability of the model pricing a swaption. Using the notation from Chap. 8 Sect. 8.4, we illustrate the methodology in this case.
Since we know that for the Vasicek dynamics the expectation and the variance are known and being sufficient to describe the distribution of the short rate, we can use this to calculate the price of a European physically settled swaption. When a realization of the short rate is assumed given we price the option using the Black76 formula. This is possible due to the assumption of basis spread following a Geometric Brownian motion. But this means that we may compute the price with respect to the full model by integrating over all realizations of the short rate weighted by the probability density. Each value of the short rate would imply a different price for the Zero Coupon Bond. We denote this dependence by $P(t, T; x)$. Equation (9.48) gives the formula and allows to enhance the short rate model with a stochastic basis component:

$$V_\omega^{\text{Swptn}}(K) = P(0, T_a^{nM})\int_{-\infty}^{\infty} h(x)\frac{1}{\sqrt{2\pi\sigma(T_a^{nM})}}\exp\left(-\frac{(x+\mu(T_a^{nM}))^2}{2\sigma(T_a^{nM})}\right)dx \tag{9.48}$$

with the notation

$$\begin{aligned}
h(x) &:= h(A_\beta(x), B_\alpha(x), \sqrt{\mathbb{V}[\ln(\mathcal{X}^{nM}(T_a^{nM}))]}) \\
A_\beta(x) &:= \sum_{k=a+1}^{b} \tau_k^x P(T_a^x, T_k^x; x)\beta_x^k \\
B_\alpha(x) &:= K\sum_{j=c+1}^{d} \tau_j P(T_a^{nM}, T_b^{nM}; x) - 1 - \alpha_{a+1}^{nM} \\
&\quad +(1+\alpha_B^{nM} - \tau_b^{nM}\xi_b^{nM})P(T_a^{nM}, T_k^{nM}; x)
\end{aligned}$$

$$- \sum_{k=a+1}^{b-1} \left(\alpha_{k+1}^{nM} - \alpha_k^{nM} + \tau_k^{nM} \xi_k^{nM} \right) P(T_a^{nM}, T_k^{nM}; x)$$

$$\xi_k^{nM} := L_k^{nM}(0) - (1 + \alpha_k^{nM}) F_k^{nM} - \beta_k^{nM}.$$

The function h is the option value with regard to the realization x. This means that we have

$$h(S, K, \Sigma) := \begin{cases} B(S, K, \Sigma, 1) & , S, K > 0 \\ B(S, K, \Sigma, -1) & , S, K < 0 \\ S - K & , S \geq 0, K \leq 0 \\ 0 & , S \leq 0, K \geq 0 \end{cases}.$$

The function B is nothing but the Black76 formula with spot S, strike K and volatility Σ for a European Call, respectively Put, option. This means that if we have a numerical integration algorithm and an implementation of the Black76 formula, we are in a position to calculate Swaption prices in a Short Rate model setting with Stochastic Basis. We used the presented formula to consider the same example as in Mercurio and Xie (2012) to produce Fig. 9.11. It is obvious from the figure that the additional modelling freedom allows for a more flexible modelling and to reproduce different shapes of the skew/smile.

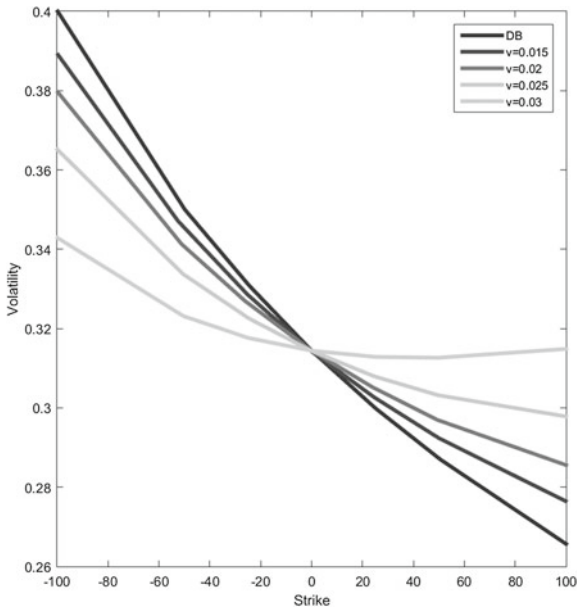

Fig. 9.11 Implied Volatility for a short rate model extended by a stochastic basis component. We displayed different levels of correlation

9.5 Conclusion and Summary

In this chapter, we considered models for the short rate. This rate is not an observable rate but it is used to determine the whole term structure using representations of Zero Coupon Bonds in terms of functions of the model parameters and the current state. We considered the General Gaussian Short Rate model and the Affine Short Rate Model classes as well as well-known and widely applied models such as the Hull–White or the Cox–Ingersoll–Ross model. For the examples we considered, the generation of future realizations of the short rate that can be used to either price derivatives or generate exposure needed to determine any kind of valuation adjustment, for instance CVA. Finally, we considered extensions of the models by increasing the number of risk factors which led to consider multi-dimensional short rate models and by combining different models to consider the pricing of hybrid products. Our example shows two short rate models for the domestic and a foreign term structure and the exchange rate between the involved currencies. This can further be extended to consider term structure and equity dynamics. See Kammeyer and Kienitz (2012a, b, c).

References

Andersen, L., & Piterbarg, V. (2010). *Interest rate modeling—Volume II: term structure models*. Atlantic Financial Press.

Brigo, D., & Mercurio, F. (2006). *Interest rate models—Theory and practice* (2nd ed.). New York: Springer.

Cox, J. C., Ingersoll, J. E, Jr., & Ross, S. A. (1985). A theory of the term structure of interest rates. *Econometica*, *53*, 363–384.

Dimitroff G., Fries C., Lichtner M., & Rodi N. (2016). Lognormal vs normal volatilities and sensitivities in practice. *SSRN*.

Hagan, P., & Woodward, D. (1999). Equivalent black volatilities. *Applied Mathematical Finance*, *6* (3).

Hagan, P. S. (2002). Adjusters—Turning good prices into great prices. *Wilmott Magazine 1*.

Kammeyer, H., & Kienitz, J. (2012a). The Heston Hull White model I—Finance and analytics. *Wilmott Magazine, 57*, 46–53.

Kammeyer, H., & Kienitz, J. (2012b). The Heston Hull White model II—Fourier transform and Monte Carlo simulation. *Wilmott Magazine, 58*, 34–45.

Kammeyer, H. & Kienitz, J. (2012c). The Heston Hull White model III—The implementation. *Wilmott Magazine, 59*, 44–49.

Kienitz, J. (2014). *Interest rate derivatives explained: Volume 1 products and markets*. Palgrave McMillan.

Lichters, R., Stamm, R., & Gallagher, D. (2015). *Modern derivatives pricing and credit exposure analysis—Theory and practice of CSA and XVA pricing*. Palgrave McMillan: Exposure Simulation and Backtesting.
Mercurio, F., & Xie, Z. (2012). The basis goes stochastic. *RISK*, *12*, 78–83.

10

A Gaussian Rates-Credit Pricing Framework

10.1 Introduction and Objectives

In this section, we introduce a pricing model that is used to capture the joint dynamics of interest rates and credit spreads. In general, a full dynamic model for the interest rate curve and jointly the credit spread curve is required to value the call option on a bond, while for a (collateralized) callable swap a model for the interest rate curve alone suffices assuming that no XVAs have to be computed. A straight forward approach for this is probably to use a two-factor LGM model for interest rates and credit spreads, respectively, the detailed description of which can be found in Lichters et al. (2015). In this chapter we briefly summarize this model.

10.2 The Option-Adjusted Spread (OAS)

At this point, we need to introduce some new terminology. For callable bonds, there are two kinds of valuation spreads that must be distinguished. The Z-spread which we introduced in one of the earlier chapters has the particular meaning of a zero volatility spread meaning that this is the spread yielding the fair bond price including the call option right by pure discounting of the bond's cash flows on the benchmark curve plus the Z-spread. This spread is without the valuation of the call right.

© The Author(s) 2017

J. Kienitz and P. Caspers, *Interest Rate Derivatives Explained: Volume 2*,
Financial Engineering Explained, DOI 10.1057/978-1-137-36019-9_10

The option-adjusted spread, denoted by *OAS*, on the other hand is the spread to be used in a full valuation model. This is necessary to account for the call option valuation and we can, for instance, use the LGM model to obtain the fair bond price. Thus, since the call right, if held by the issuer, decreases the bond's fair value, the Z-spread is higher than the OAS. Equation (10.11) can also be described in terms of the OAS λ^* which we consider in this section.

In formulas, we have the value of a callable bond

$$V^{\text{Callable Note}} = \text{Nom} \cdot N(0) \cdot \mathrm{E}^N \Big(\sum_{i=1}^{m(\omega)} \frac{\tau_i C_i S(T_i, \lambda^*, \omega)}{N(T_i, \omega)} + \frac{S(T_{m(\omega)}, \lambda^*, \omega)}{N(T_{m(\omega)}), \omega} \Big) \tag{10.1}$$

with $S(t) = S(t, \lambda^*)$ denoting the survival probability up to time t dependent on the OAS λ^*· $m = m(\omega)$ being the coupon period dependent on the path taken at which the bond terminates by execution of a call right or just because it matures anyway. To calculate the net present value for the payoff given by Eq. 10.1, we take the expectation E^N with respect to the numeraire N (which in the case of the 2F LGM model is given by 10.8).

Once we have the value of the callable bond, the Z-spread λ is, by definition, given by solving

$$V^{\text{Callable Note}} = N \sum_{i=1}^{m} \tau_i C_i D(0, T_i) e^{-\lambda T_i} + D(0, T_m) e^{-\lambda T_m} \tag{10.2}$$

for λ. This way, Eq. (10.2) allows to explicitly calculate the Z-spread.

10.3 The 2F Rates-Credit LGM Model

Before we describe the particular model, we point out that the model is in a sense the most basic approach and as such unique, that is the choice is not arbitrary. There are two main categories of interest rate model construction: the first one using instantaneous forward rates and providing a general framework for arbitrage free interest rate models in this context, known as the HJM (Heath–Jarrow–Morton) framework, and the second approach models discrete Libor rates directly and is known as the Libor market model framework that is considered in Chap. 12.

In the HJM class, the following statement holds: Any Gaussian one-factor HJM model which satisfies the *separability* condition, that is for which

$$\sigma_f(t, T) = g(t)h(T)$$

for the instantaneous forward rate volatility with deterministic $g, h > 0$, necessarily fulfils

$$dr(t) = (\theta(t) - a(t)r(t))dt + \sigma(t)dW(t)$$

for the short rate r, which means that it is a version of the models from the one-factor Gaussian Short rate model class.

The LGM model we use is equivalent to the extended Vasicek model also known as the Hull–White model. The only difference in fact is the choice of another measure—the LGM model measure. Note that by shifting the H parameter, the T-Forward measure, for any T, can be recovered as well, which is a usual measure used in the Hull–White model.

Since in general we wish to model an interest rate and in addition a credit spread factor, we start with stochastic processes for these quantities as follows:

$$dx = \alpha(t)dW(t) \tag{10.3}$$

$$dy = \alpha_c(t)dV(t) \tag{10.4}$$

$$\langle dW, dV \rangle = \rho dt. \tag{10.5}$$

The state variables x are for the interest rate level and y for the credit spread level. α determines the volatility of the interest rate process, while α_c determines the volatility of the credit spread process. Both processes are coupled by a correlation parameter ρ.

The model's interest rate discount bond conditional on the model's state $x(t)$ at time t is given by

$$P(t, T, x) = \frac{P(0, T)}{P(0, t)} e^{-(H(T)-H(t))x - \frac{1}{2}(H(T)^2 - H(t)^2)\zeta(t)} \tag{10.6}$$

with $P(0, \cdot)$ denoting the initial discount curve to be matched by the model, the variance ζ given by

$$\zeta(t) = \int_0^t \alpha(s)^2 ds$$

and a function H that can be parametrized by a mean reversion $\kappa(t)$ as follows:

$$H(t) = \int_0^t e^{-\int_0^s \kappa(u)du} ds. \tag{10.7}$$

The model's numeraire conditional on the model state $x(t)$ at time t is given by

$$N(t, x) = \frac{1}{P(0, t)} e^{H(t)x + \frac{1}{2}H(t)^2\zeta(t)}. \tag{10.8}$$

The credit component is characterized by another function H_c, parametrized by a mean reversion $\kappa_c(t)$,

$$H_c(t) = \int_0^t e^{-\int_0^s \kappa_c(u)du} ds. \tag{10.9}$$

Let us introduce a new variable y' by considering

$$dy' = H(t)\alpha_c(t)dW \tag{10.10}$$

and quantities

$$\begin{aligned} V_0 &= \frac{1}{2}H_c(t)^2\zeta_{c,0} - H_c(t)\zeta_{c,1} + \frac{1}{2}\zeta_{c,2} + H(t)H_c(t)\zeta_{n,c,0} - H(t)\zeta_{n,c,1} \\ V' &= -\frac{1}{2}(H_c(T)^2 - H_c(t)^2)\zeta_{c,0} + (H_c(T) - H_c(t))\zeta_{c,1} \\ &\quad -(H(T)H_c(T) - H(t)H_c(T))\zeta_{n,c,0} + (H(T) - H(t))\zeta_{n,c,1}, \end{aligned}$$

where

$$\begin{aligned} \zeta_{c,i}(t) &= \int_0^t H_c(s)^i \alpha_c(s)^2 ds \\ \zeta_{n,c,i}(t) &= \int_0^t \rho H_c(s)^i \alpha(s)\alpha_c(s) ds. \end{aligned}$$

Conditional on $y(t)$ at time t, the survival probability $S(t)$ up to time t is given by

$$S(t) = e^{-\lambda^* t} e^{-H_c(t)y + y' - V_0}, \tag{10.11}$$

while the survival probability $S'(t, T)$ up to time T conditional on survival up to time t is given by

$$S'(t, T) = e^{-\lambda^*(T-t)} e^{-(H_c(T)-H_c(t))y+V'} \tag{10.12}$$

with the option-adjusted spread λ^*, which we introduce in Sect. 10.2.

To better understand the role of the reversion parameter in the given context, assume the model volatility α (or α_c) and the reversion κ (respectively κ_c) constant for a moment. Then, the correlation can be calculated and is given by

$$\mathrm{corr}(x(T_1), x(T_2)) = \sqrt{\frac{e^{2\kappa T_2} - 1}{e^{2\kappa T_1} - 1}} = e^{-\kappa(T_2-T_1)} \sqrt{\frac{1 - e^{-2\kappa T_1}}{1 - e^{-2\kappa T_2}}} \tag{10.13}$$

which shows that for $\kappa = 0$ the correlation is $\sqrt{T_1/T_2}$ and tends to zero if $a \to \infty$. If instead $a \to -\infty$ it tends to one. This means that via the reversion parameter κ the inter-temporal correlation of rates, respectively credit spreads, at different times can be controlled. De facto, it turns out that this is an important price driver for multi-callable structures; see, for instance, Andersen and Andreasen (2001).

10.4 Monte Carlo Paths in the 2F Rates-Credit LGM Model

One possible way of using a model for pricing purposes is to perform a Monte Carlo Simulation. Applying the Monte Carlo method we simulate a number of random paths for the possible future evolution of a set of relevant price drivers, like interest rates, FX rates and credit spreads. Along each path, the cash flows of the product to be priced are generated and discounted yielding the discounted scenario value of the product. The today's price is then computed as the average over all such scenario values. The basis for the scenario paths is in general an arbitrary model describing the dynamics of the price factors, for instance a term structure model in the case of interest rates. The randomness in the models is sourced from a Brownian motion which has normally distributed increments of variance dt over a time interval of length dt and mean zero. Brownian motion generates continuous paths for the evolution of the price factors. Some models also include jumps on top of that (jump diffusion models) or even simulate the volatility of price drivers as random quantities through time (stochastic volatility models).

It remains to point out that the pricing expectations are usually taken in an artificial measure like the risk-neutral measure, in which probabilities for an event can be drastically different from the actual real-world probabilities for the same events. The risk-neutral measure is constructed such that expectations of future derivative prices discounted on the risk-free interest rate curve corresponding to safe investments are equal to today's price, although in the real world investors would require a higher rate of return for taking the risk of volatile returns. The pricing in the risk-neutral measure is convenient because it does not require knowledge for this market risk premium and at the same time yields prices that are valid in the real world.

Figure 10.1 shows one Monte Carlo path for the interest rate and credit spread state variables x and y, respectively, over 10 years. Both paths start at $x(0) = y(0) = 0$ and thereafter diffuse: $x(t)$ with a volatility of $\alpha = 0.00050$, and $y(t)$ with a volatility of $\alpha_c = 0.0080$. The correlation between the two processes is $\rho = 0.5$. Figure 10.2 shows only the interest rate factor $x(t)$, but for 10 Monte Carlo paths. Note that the LGM model can produce negative states $x(t)$ and interest rates (as well as credit spreads), see 10.6. Note that at each time point t we only have two numbers $x(t)$ and $y(t)$ that determine the whole interest rate and credit spread term structure. We calculate the term structure using Eqs. (10.6), (10.11) and (10.12). In addition, from (10.8) we get the numeraire value at each time point t and for each state $x(t)$ or $y(t)$. Then, we are able to compute the value of each cash flow of a deal in terms of the numeraire. This is done by dividing the expression by $N(t, x)$ during the

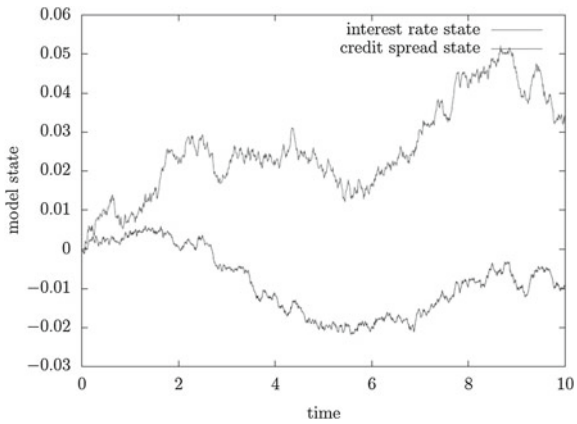

Fig. 10.1 One Monte Carlo path for the interest rate model state x and the credit spread model state y in an LGM 2F model with volatilities $\alpha = 0.0050$, $\alpha_c = 0.0080$ and correlation $\rho = 0.5$

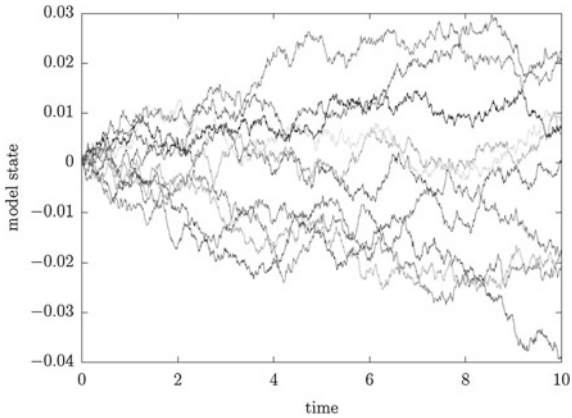

Fig. 10.2 Ten Monte Carlo paths for the interest rate model state x, with a volatility of $\alpha = 0.0050$

simulation. Averaging over all such values and multiplying by the numeraire value at $t = 0$ which in fact happens to be 1 in the LGM model gives the Monte Carlo estimator of the net present value of the deal.

10.5 Conclusion and Summary

In this chapter, we introduced a basic model suitable for the pricing of structures that depend on both rates and credit spreads. One example is a callable bond. The model is a two-factor Gaussian model with one factor representing the interest rate and the other representing the credit spread dynamics. The Brownian motions driving the components are linked by a correlation parameter. We provide a formal description in terms of a two-factor LGM model. This model is equivalent to the two-factor Hull–White model. The only difference is the corresponding numeraire and its associated measure. Finally, we illustrated how a Monte Carlo pricing is done in this model.

References

Andersen, L., & Andreasen, J. (2001). Factor dependence of Bermudan swaptions: Fact or fiction? *Journal of Financial Economics*, *62*(1), 3–37.

Lichters, R., Stamm, R., & Gallagher, D. (2015). *Modern derivatives pricing and credit exposure analysis—Theory and practice of CSA and XVA pricing*. Palgrave McMillan: Exposure Simulation and Backtesting.

11

Instantaneous Forward Rate Models and the Heath–Jarrow–Morton Framework

11.1 Introduction and Objectives

This chapter gives an overview of the general Heath–Jarrow–Morton framework, Heath et al. (1992), and some particular examples. This framework specifies the stochastic evolution of the entire term structure of interest rates. The methodology applied is based on the instantaneous forward rate

$$f(t,T) = -\frac{\partial \ln(P(t,T))}{\partial T}$$

for all maturities. The main achievement of Heath et al. (1992) was to establish the conditions on the volatility structure such that the stochastic evolution is arbitrage-free. In fact it can be shown that any arbitrage-free diffusion-based term structure model is a special case of this framework. This includes not only the well-known short rate models, see Chap. 9 for examples, but also the class of market models, see Chap. 12 for examples.

However, the general setting suffers from some disadvantages. It is not easy to apply the general model in practice. One general issue with this model is that it is in general non-Markovian which means that the future evolution may depend on the whole history and not only on the current realization. A class of tractable Heath–Jarrow–Morton models was developed in Cheyette (1994), Ritchken and Sankarasubramanian (1995). We sketch the models and assumptions necessary to use such models in practice. Finally, we consider a specific model which is a multi-factor Gaussian model with a true Stochastic Volatility component. This Cheyette-type model was first considered in Trolle and Schwartz (2009). Since the number of factors is flexible, we have enough

© The Author(s) 2017

J. Kienitz and P. Caspers, *Interest Rate Derivatives Explained: Volume 2*,
Financial Engineering Explained, DOI 10.1057/978-1-137-36019-9_11

degrees of freedom for pricing applications but also the possibility to scale it down for time-consuming applications such as exposure modelling.

11.2 The Heath–Jarrow–Morton Framework

We take a m-dimensional Brownian motion $W(t), \sigma_f(t,T) = (\sigma_1(t,T), \ldots, \sigma_m(t,T)^\top$ and consider (11.1).

$$df(t,T) = \mu(t,T)dt + \sigma_f(t,T)dW(t) \tag{11.1}$$
$$f(0,T) = f_M(0,T). \tag{11.2}$$

We have denoted the current instantaneous forward rates by $f_M(0,T)$. We can numerically calculate these quantities by taking the current yield curve together with a suitable interpolation algorithm and calculate the rates by applying numerical differentiation.
It can be shown that under the risk-neutral measure, there is a restriction on the drift coefficient $\mu(t,T)$. For all $t \leq T$, it can be shown that

$$\mu(t,T) = \sigma_f(t,T)\left(\int_t^T \sigma_f(t,u)du\right).$$

This means that

$$f(t,T) = f(0,T) + \int_0^t \sigma_f(s,T)\left(\int_s^T \sigma_f(s,u)du\right)ds + \int_0^T \sigma_f(s,T)dW(s)$$
$$f(0,T) = f_M(0,T).$$

From this dynamic the corresponding short rate dynamic can be calculated using the Ito formula. In general the short rate is path-dependent since there is a stochastic integral in the drift. For completeness, we give the formulation of a multi-dimensional Heath–Jarrow–Morton model by (11.3). The driving Brownian motions are $W_1, \ldots, W_m$. The dynamic is

$$df(t) = \sum_{i=1}^m \int_0^t \sigma_i(u,t)\int_u^t \sigma_i(u,s)dsdu + \sum_{i=1}^m \int_0^t \sigma_i(s,t)dW_i(s). \tag{11.3}$$

The Heath–Jarrow–Morton result is fundamental in interest rate modelling. It means that the specification of the volatility structure determines the drift by no-arbitrage arguments. Thus, if we specify the volatility structure as well

as the initial condition the yield curve dynamic is completely determined. The essential ingredient is the volatility function σ_f. In fact several specific choices lead to well-known financial models including short rate models such as the GSR class or the Libor Market model class.
However, using general volatility functions has severe drawbacks. For instance, such functions can lead to non-Markovian models. From a practical point of view, this means that such models are very hard to tackle numerically since, for instance, PDE methods are not applicable. This is due to the fact that the Feynman–Kac theorem does not hold in the non-Markovian setting. Despite this technical difficulty we like to make the reader aware that this model does not have a finite-dimensional state space since the initial condition is the current instantaneous forward curve.

11.3 The Cheyette, Ritchken and Sankarasubramanian Model Class

For the general Heath–Jarrow–Morton formulation of the dynamics of the instantaneous forward rate, we observe that the time variable t determines the upper bound of the stochastic integral and appears in the volatility function. This resulting stochastic process for f being not necessarily Markovian and, thus, it can depend on the whole history of the process. To overcome this problem, Cheyette O. (1994) and Ritchken and Sankarasubramanian (1995) suggest to take a specific representation of the volatility. If the volatility of the forward rate f is taken to be

$$\sigma_f = H(t, \omega)g(T), \tag{11.4}$$

then the forward rate is Markovian and determined by two state variables x and y and we have

$$f(t, T) = f(0, T) + \sigma(t, T)x_t + \left(\sigma(t, T)\int_t^T \sigma(t, s)ds\right) y_t$$

with

$$\sigma(t, T) = \exp\left(-\int_t^T \kappa(s)ds\right). \tag{11.5}$$

It is worth to give some additional remarks with respect to the Cheyette representation (11.4). The function H is a function with respect to time t and a stochastic variable ω and the function g is a deterministic function of time.

The stochastic variable ω for all financial applications comes in via the state variable x. Thus, it is often appropriate to take H to be a function of t and (the Markovian state variables) $x(t)$ and $y(t)$. From the above it can be deduced that

$$\kappa(t) = -\frac{g'(t)}{g(t)}$$

holds, leading to $\eta(t, x(t), y(t)) = H(t, x(t), y(t))g(t)$. Sometimes it is more convenient to use the formulation in terms of (11.5). That is specifying the volatility σ and not σ_f. To this end, set

$$\sigma_f(t, T) = \eta(t, x(t), y(t))\sigma(t, T) = \eta(t, x(t), y(t)) \exp\left(\int_t^T \kappa(s)ds\right). \tag{11.6}$$

The function η in (11.6) can be interpreted as the instantaneous volatility and κ is a deterministic function determining the mean reversion speed. For the short rate, this leads to a dynamic given by (11.7)

$$\begin{aligned} dr(t) &= \left(\kappa(t)[f(0,t) - r(t)] + y(t) + \frac{\partial f(0,t)}{\partial t}\right) dt + \eta(t)dW(t) \\ dy(t) &= \left(\eta^2(t,t) - 2\kappa(t)y(t)\right) dt \end{aligned} \tag{11.7}$$

The variable y is the cumulated variance and we have

$$y(t) = \int_0^t \sigma^2(u, t)du.$$

As seen in the short rate model setting, we consider

$$x(t) = r(t) - f(0, t) \tag{11.8}$$

to avoid the computation of quantities including the instantaneous forward rate. Thus, we have

$$\begin{aligned} dx(t) &= (y(t) - \kappa(t)x(t))dt + \eta(t)dW(t) \\ dy(t) &= (\eta^2(t) - 2\kappa(t)y(t))dt \end{aligned} \tag{11.9}$$

with $x(0) = y(0) = 0$. The modeller has to choose the volatility representation not only with regard to the application but also with regard to the numerical tractability of the model.

- In general the function H can depend on the Markovian state vector $(x(t), y(t))$. This is the general case.
- Adding further Markovian state variables is possible.
- Choosing H to be a constant or time-dependent leads to an ODE for $y(t)$. This means that there is only one source of randomness left. One-factor short rate models can be recovered using this modelling assumption.
- Popular choices for specifying the volatility function η are $\eta(t, x(t)) = \sigma_{\text{CEV}}(t)R(t)^{\beta(t)}$ or $\eta(t, x(t)) = \sigma_{\text{DD}}(t)(a(t)r(t) + (1 - a(t))r_0)$. The deterministic functions $\sigma_{\text{CEV}}(t)$, $\sigma_{\text{DD}}(t)$, $\beta(t)$ or $a(t)$ need to be determined using market quotes. Using this set-up, it is possible to derive pricing formulas for Caps and European Swaptions.

11.3.1 The Hull–White Model

We already remarked that specific choices of the volatility function lead to well-known financial models. Let us consider the Hull–White or Vasicek model that we already considered. Choosing σ_f as given in (11.10) leads to the Hull–White model.

$$\sigma_f(t, T) = \sigma \exp(-a(T - t)) \tag{11.10}$$

This corresponds to choosing $H(t, \omega) = \exp(at)$ and $g(T) = \sigma \exp(-aT)$ and means that the dynamics becomes

$$\begin{aligned} dx(t) &= (y(t) - ax(t))dt + \eta dW(t) \\ dy(t) &= (\eta^2 - 2ay(t))dt. \end{aligned}$$

The function $y(t)$ satisfies an ODE. In fact this is an inhomogeneous linear ODE which has closed-form solutions. The solution is

$$y(t) \exp(-2at) \left(c + \frac{\eta^2}{2a} (\exp(2at) - 1) \right), \quad y(0) = c.$$

We use this result together with the Markovian short rate dynamics and get

$$dr(t) = \left. \frac{\partial_T f(s, T)}{\partial T} \right|_{(s,T)=(0,t)} + \left(\frac{\eta^2}{2a} (1 - \exp(-2at)) - ax(t) \right) dt + \eta dW(t)$$

Since $x(t) = r(t) - f(0, t)$ we find

$$dr(t) = \left(\left. \frac{\partial_T f(s, T)}{\partial T} \right|_{(s,T)=(0,t)} + af(0, t) + \frac{\eta^2}{2a} (1 - \exp(-2at)) - ar(t) \right) dt + \eta dW(t)$$

11.4 Cheyette Model Example

We consider a modelling approach which accommodates negative rates as well as unspanned volatility factors. While negative rates are market reality there are numerous papers on the existence of unspanned volatility factors in interest rate modelling among other Collin-Dufresne and Goldstein (2002), Casassus et al. (2005), Fan et al. (2003), Heidari and Wu (2003) or Andersen and Benzoni (2010). Unspanned volatility factors are sources of uncertainty that effect the prices of interest rate derivatives, for instance, via increasing volatility skews or smiles but leave the term structure as it is. Essentially this means that interest rate derivatives cannot be hedged using the underlying bonds and, thus, it is the postulation of true stochastic volatility. For instance, Li and Zhao (2006) report such observations. To formulate the Trolle and Schwartz model as introduced by Trolle and Schwartz (2009), we take N Brownian motions W_i and Z_i and consider the following model:

$$df(t,T) = \mu_f(t,T)dt + \sum_{i=1}^{N} \sigma_{f,i}(t,T)\sqrt{v_i(t)}dW_i(t) \tag{11.11}$$

$$dv_i(t) = \kappa_i(\theta_i - v_i)dt + \sigma_i\sqrt{v_i(t)}\left(\rho_i dW_i(t) + \sqrt{1-\rho_i^2}dZ_i(t)\right) \tag{11.12}$$

We assigned a dynamic for the instantaneous forward rate (11.11) and for the volatility (11.12). Both dynamics are linked by the correlation parameters $\rho_i \in [-1, 1]$. The deterministic volatility $\sigma_{f,i}(t,T)$ in this model is specified to be separable in the sense of Cheyette O. (1994). This leads to a Markovian model. Furthermore, a parametric form is assumed, see (11.13).

$$\sigma_{f,i}(t,T) = \left(\alpha_{0,i} + \alpha_{1,i}(T-t)\right)e^{-\gamma_i(T-t)} \tag{11.13}$$

This corresponds to a hump-shaped volatility, see Fig. 11.1. With regard to the Heath–Jarrow–Morton framework considered in this chapter, we find for the drift (11.14)

$$\mu_f(t,T) = \sum_{i=1}^{N} v_i(t)\sigma_{f,i}(t,T)\int_t^T \sigma_{f,i}(t,u)du. \tag{11.14}$$

A way of dealing with this model is to write the dynamics of the instantaneous forward rate in a more handy way. The form we have chosen is the form of an affine diffusion process with a finite number of state variables, (11.15).

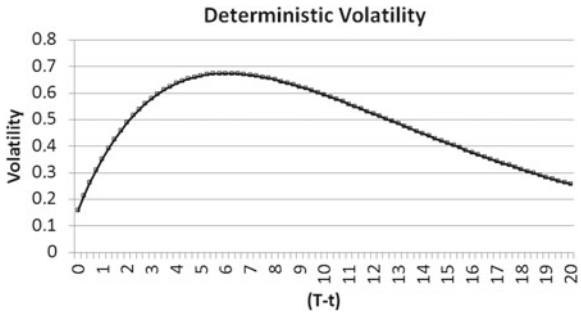

Fig. 11.1 Typical hump shape realized using the deterministic volatility for the Trolle and Schwartz model (parameters $N = 1$, $\alpha_{01} = 0.16$, $\alpha_{11} = 0.25$ and $\gamma_1 = 0.15$)

$$f(t,T) = f(0,T) + \sum_{i=1}^{N} B_{x_i}(T-t)x_i(t) + \sum_{i=1}^{N}\sum_{j=1}^{6} B_{\phi_{j,i}}(T-t)\phi_{j,i}(t). \tag{11.15}$$

$$\begin{aligned}
B_{x_i}(t) &= (\alpha_{0,i} + \alpha_{1,i}t)e^{-\gamma_i t} \\
B_{\phi_{1,i}}(t) &= \alpha_{1,i}e^{-\gamma_i t} \\
B_{\phi_{2,i}}(t) &= \frac{\alpha_{1,i}}{\gamma_i}\left(\frac{1}{\gamma_i} + \frac{\alpha_{0,i}}{\alpha_{1,i}}\right)(\alpha_{0,i} + \alpha_{1,i}t)e^{-\gamma_i t} \\
B_{\phi_{3,i}}(t) &= -\left(\frac{\alpha_{0,i}\alpha_{1,i}}{\gamma_i}\left(\frac{1}{\gamma_i} + \frac{\alpha_{0,i}}{\alpha_{1,i}}\right) + \frac{\alpha_{1,i}}{\gamma_i}\left(\frac{\alpha_{1,i}}{\gamma_i} + 2\alpha_{0,i}\right)t + \frac{\alpha_{1,i}^2}{\gamma_i}t^2\right)e^{-2\gamma_i t} \\
B_{\phi_{4,i}}(t) &= \frac{\alpha_{1,i}^2}{\gamma_i}\left(\frac{1}{\gamma_i} + \frac{\alpha_{0,i}}{\alpha_{1,i}}\right)e^{-\gamma_i t} \\
B_{\phi_{5,i}}(t) &= -\frac{\alpha_{1,i}}{\gamma_i}\left(\frac{\alpha_{1,i}}{\gamma_i} + 2\alpha_{0,i} + 2\alpha_{1,i}t\right)e^{-2\gamma_i t} \\
B_{\phi_{6,i}}(t) &= -\frac{\alpha_{1,i}^2}{\gamma_i}e^{-2\gamma_i t}
\end{aligned}$$

and the state variable

$$dx_i = -\gamma_i x_i(t)dt + \sqrt{v_i(t)}dW_i \tag{11.16}$$

The equations for the state variables $\phi_{j,i}$ are given by the following system of ODEs:

$$d\phi_{1,t} = \big(x_i(t) - \gamma_i\phi_{1,i}(t)\big)\,dt;\;\; d\phi_{2,t} = \big(v_i(t) - \gamma_i\phi_{2,i}(t)\big)\,dt$$
$$d\phi_{3,t} = \big(v_i(t) - 2\gamma_i\phi_{3,i}(t)\big)\,dt;\;\; d\phi_{4,t} = \big(\phi_{2,i}(t) - \gamma_i\phi_{4,i}(t)\big)\,dt$$
$$d\phi_{5,t} = \big(\phi_{3,i}(t) - 2\gamma_i\phi_{5,i}(t)\big)\,dt;\;\; d\phi_{6,t} = \big(2\phi_{5,i}(t) - 2\gamma_i\phi_{6,i}(t)\big)\,dt$$

To be able to use this model for simulation, the state variables and the correlated stochastic variance have to be simulated first. This can be done by applying an Euler scheme for small time steps or a more advanced scheme taking into account the model properties.

The dynamics of the Zero Coupon Bond prices can be found by

$$\frac{dP(t,T)}{P(t,T)} = r(t)dt + \sum_{i=1}^{N} B_{x_i}(T-t)\sqrt{v_i(t)}dW_i(t) \tag{11.17}$$

The modeller chooses the number of factor. For instance for correct pricing and accurately recovering the market quotes, we might wish to choose $N = 3$ or $N = 4$. If we are interested in exposure modelling for risk management $N = 1$ could be a feasible choice since many instruments—a whole netting set—need to be evaluated. This is very time-consuming and, thus, if a reduced number of factors is applied this saves lots of computational time.

From (11.17), it is possible to deduce

$$P(t,T) = \frac{P(0,T)}{P(0,t)} \exp\left(\sum_{i=1}^{N} B_{x_i}(T-t)\sqrt{v_i(t)}dW_i(t)\right) \tag{11.18}$$

Fig. 11.2 shows a simulation of this quantity.

As outlined the key to pricing are expressions for Zero Coupon Bonds and corresponding options since other instruments such as Caps, Floors or Swaptions can then as well be valued. For (11.18) the functions B_{x_i} are called the volatility loading functions and are given by (11.19).

$$B_{x_i}(t) = \frac{\alpha_{1,i}}{\gamma_i}\left(\left(\frac{1}{\gamma_i} + \frac{\alpha_{0,i}}{\alpha_{1,i}}\right)\left(e^{\gamma_i t} - 1\right) + te^{-\gamma_i t}\right) \tag{11.19}$$

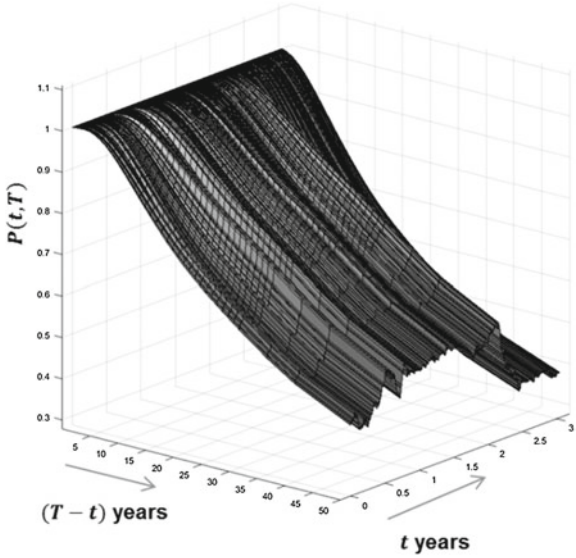

Fig. 11.2 Term structure generated using the Trolle and Schwartz model

Using the affine diffusion process representation we have the alternative representation (11.20)

$$P(t,T) = \frac{P(0,T)}{P(0,t)} \exp\left(\sum_{i=1}^{N} B_{x_i}(T-t)x_i(t) \sum_{i=1}^{N}\sum_{j=1}^{6} B_{\phi_{j,i}}(T-t)\phi_{j,i}(t)\right) \tag{11.20}$$

and the functions $B_{\phi_{j,i}}$ can be determined from the corresponding ones for f.

Using the term structure for the model it is possible to price any financial product based on a single interest rate curve. We used the model to price Zero Coupon Bonds, Caplets and Swaptions. The results are shown in Fig. 11.3. Of course the model parameters need to be specified. To this end we have to calibrate the model and this can only be done efficiently if the basic quoted financial instruments can be valued using fast computational methods. In Trolle and Schwartz (2009) two methods are considered, namely a volatility approximation and a semi-analytical one. These methods are shown to accomplish fast and efficient pricing of zero bonds, Caps and Swaptions. Figure 11.4 shows the performance of the methods for the case of a single Caplet. The obtained results are compared to a Monte Carlo simulation. We clearly see that the number of driving factors N impacts the quality of the volatility approximation, while the semi-analytic method is verified by the results obtained via simulation.

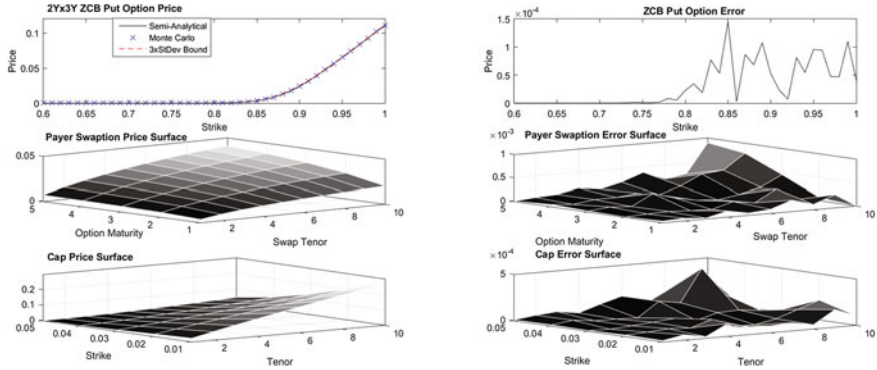

Fig. 11.3 Pricing of interest rate options using the Cheyette model with unspanned stochastic volatility. The prices for zero coupon bonds (*top*), Swaptions (*mid*) and Caps (*bottom*) are shown together with the error with a Monte Carlo simulation as the benchmark. Generated with codes implemented by G. Schumann for a MSc supervised by J. Kienitz, see Schumann (2016)

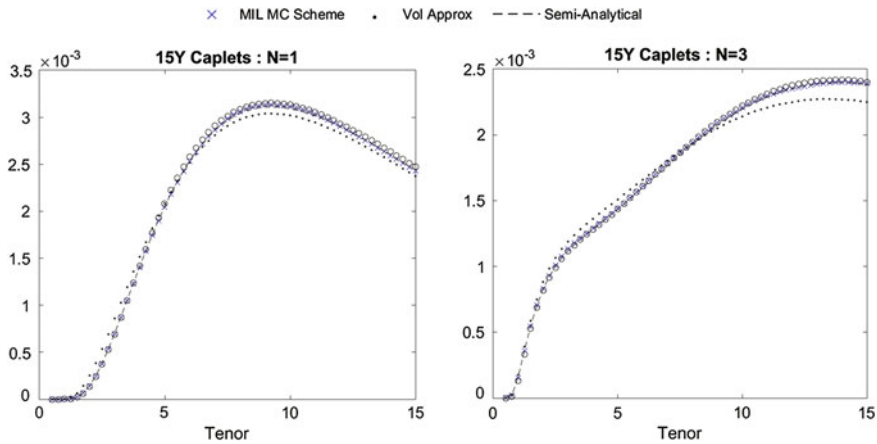

Fig. 11.4 We applied the approximation formulae to the pricing of Caplets and compared them to Monte Carlo simulations. $N = 1$ (*left*) and $N = 3$ (*right*). Generated with codes implemented by G. Schumann for a MSc supervised by J. Kienitz, see Schumann (2016)

Path Simulation

We denote by $f(t_k, t_j)$ the simulated instantaneous forward rate and by $v_i(t_k)$ the volatility state variables. Furthermore let $X_{i,k}, Y_{i,k} \sim \mathcal{N}(0,1)$ independent standard normal random variables and $\Delta_k := t_k - t_{k-1}$ then the scheme with full truncation Milstein updates for the volatility is given by

$$\begin{aligned} f(t_k, t_j) &= f(t_{k-1}, t_j) + \frac{\sum_{i=1}^{N} v_i(t_{k-1})\,(A(j) - A(j-1))}{2} \\ &\quad + \sum_{i=1}^{N} \sigma_{f,i}(t_{k-1}, t_j)\sqrt{v_i(t_{k-1})^+}\sqrt{\Delta_k}X_{i,k} \\ A(j) &:= \left(\sum_{l=k}^{j} \sigma_{f,i}(t_{k-1}, t_l)\Delta_k\right)^2 \\ v_i(t_k) &= v_i(t_{k-1}) + \kappa_i(\theta_i - v_i(t_{k-1})^+)\Delta_k \\ &\quad \sigma_i\sqrt{v_i(t_{k-1})^+}\sqrt{\Delta_k}Y_{i,k} + \frac{1}{4}\sigma_i^2\left(\Delta_k Y_{i,k}^2 - 1\right) \end{aligned}$$

The full truncation is reflected in the fact that we take $(\cdot)^+ := \max(\cdot, 0)$.

We consider further schemes to the Euler scheme. There is the Milstein scheme which improves upon the Euler scheme as well as the QE scheme which is an efficient numerical method when considering Heston-type models, see Andersen (2008) or Kienitz and Wetterau (2012) for an implementation and Appendix A. The results are shown in Fig. 11.5. Furthermore, we applied

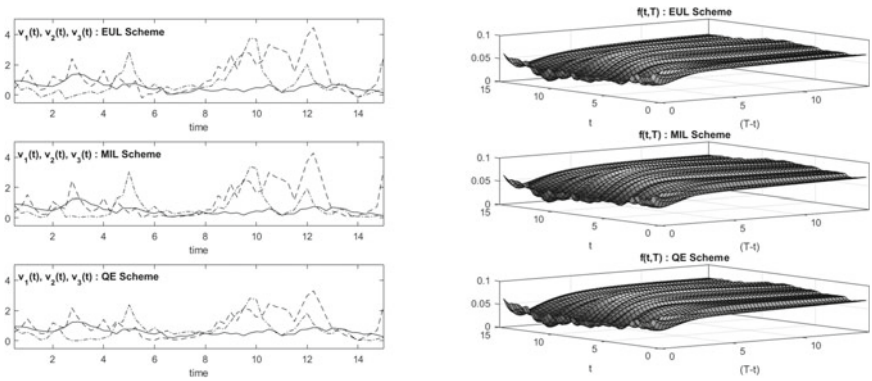

Fig. 11.5 Application of three different numerical schemes for generating the sample path namely the Euler method, the Milstein method and the QE method. We have chosen three driving factors which are plotted (*left*) and the corresponding forward rates (*right*). Generated with codes implemented by G. Schumann for a MSc supervised by J. Kienitz, see Schumann (2016)

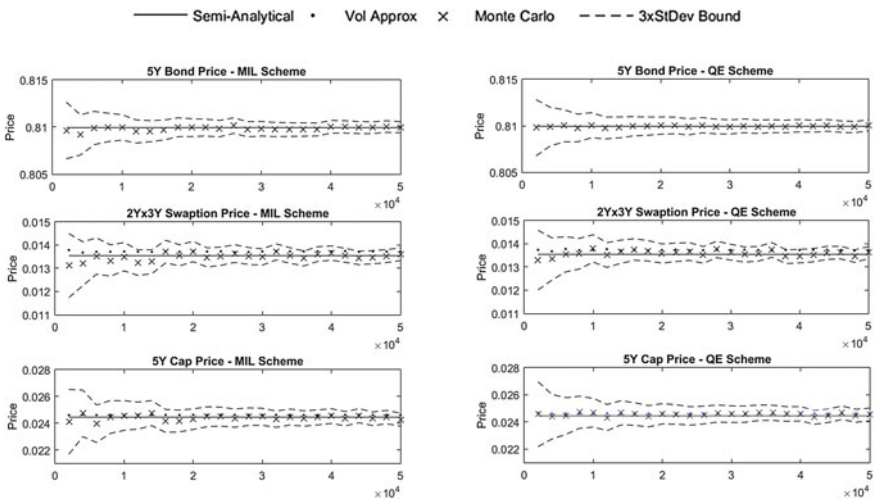

Fig. 11.6 Pricing of Zero Coupon Bond options (*top*), Swaption (*mid*) and a Cap (*bottom*) with a Milstein and a QE scheme. Generated with codes implemented by G. Schumann for a MSc supervised by J. Kienitz, see Schumann (2016)

the path generation method to Monte Carlo pricing of different financial instruments. We have chosen Zero Coupon Bonds, Caps and Swaptions. The results are displayed in Fig. 11.6.

11.5 Summary and Conclusions

In this chapter, we considered the general Heath–Jarrow–Morton result. This is very important for interest rate modelling since it shows that the dynamics of the instantaneous forward rate and, thus, the yield curve are completely determined by the volatility structure if we wish no-arbitrage to hold. However, we pointed to some drawbacks for using this result in practice. Then, we proceed by reviewing an application of the general theory to practical pricing and simulation problems. The results are very appealing since the model allows for simulation to determine exposure profiles and is flexible enough for considering many different market scenarios, for instance, negative interest rates.

References

Andersen, L. (2008). Simple and efficient simulation of the Heston stochastic volatility model. *Journal of Computational Finance*, *11*, 1–42.

Andersen, T. G., & Benzoni, L. (2010). Do Bonds span volatility risk in the US treasury market? A specification test for affine term structure models. *The Journal of Finance*, *65*(2), 603–653.

Casassus, J., Collin-Dufresne, P., Goldstein, P., & Goldstein, G. (2005). Unspanned stochastic volatility and fixed income derivatives pricing. *Journal of Banking and Finance*, *29*(11), 2723–2749.

Cheyette O. (1994). Markov representation of the heath-Jarrow-Morton model. *Barra—Working paper and SSRN*.

Collin-Dufresne, P., & Goldstein, R. S. (2002). Do Bonds span the fixed income markets? Theory and evidence for unspanned stochastic volatility. *The Journal of Finance*, *57*(4), 1685–1730.

Fan, R., Gupta, A. and Ritchken, P. (2003). Hedging in the possible presence of unspanned stochastic volatility: Evidence from swaption markets. *Journal of Finance*, 2219–2248.

Heath, D., Jarrow, R., & Morton, A. (1992). Bond pricing and the term structure of interst rates: A new methodology for contingent claims valuation. *Econometrica*, *60*, 77–105.

Heidari, M., & Wu, L. (2003). Are interest rate derivatives spanned by the term structure of interest rates? *Journal of Fixed Income*, *13*(1), 75–86.

Kienitz, J. and Wetterau, D. (2012). *Financial modeling—Theory, implementation and practice - (with matlab source)*. Wiley.

Li, H., & Zhao, F. (2006). Unspanned stochastic volatility: Evidence from hedging interest rate derivatives. *The Journal of Finance*, *61*(1), 341–378.

Ritchken, P., & Sankarasubramanian, L. (1995). Volatility structures of forward rates and the dynamics of the term structure. *Mathematical Finance*, *5*(1), 55–72.

Schumann G. W. (2016). *Trolle-Schwartz HJM interest rate model*. M.Sc. Thesis University of Cape Town.

Trolle, A. B., & Schwartz, E. S. (2009). A general stochastic volatility model for the pricing of interest rate derivatives. *Review of Financial Studies*, *22*(5), 2007–2057.

12

The Libor Market Model

12.1 Introduction and Objectives

In the preceding chapters we considered different term structure models, for instance, the Gaussian short rate models or models for the instantaneous forward rate. All the approaches have in common that a non-observable quantity such as the short rate is modelled. There is yet another class of models which are used to model market observable rates such as Libor rates (Sandmann and Sondermann 1997; Jamshidian 1997 or Brace et al. 1997) and propose a stochastic evolution for such rates. The models are called Libor Market models or, respectively, Swap Market models depending which type of rates are considered.

In the following we consider the Libor Market model and give an overview of the dynamic and we show how to enhance the model by adding a local, respectively, a stochastic volatility component. Since the exposition here is only meant as an overview, the details can be found in the cited references.

Finally, we highlight the connection between Libor Market and Swap Market models and discuss this modelling approach in the aftermath of the financial crisis. From Kienitz (2014) we know that the basis between Libor rates of different tenors, the *Money Market basis*, as well as the basis between Libor rates of the same tenors but for different currencies, the *Cross Currency basis*, are non-constant and should even be assumed to be stochastic.

© The Author(s) 2017

J. Kienitz and P. Caspers, *Interest Rate Derivatives Explained: Volume 2*,
Financial Engineering Explained, DOI 10.1057/978-1-137-36019-9_12

12.2 Market Models

So far we considered models where the modelled quantities are non-observable —for instance, the short rate $r(t)$. The concept of a *market model* is to choose some market observable quantities and directly specify their dynamic. In Brace et al. (1997), Sandmann and Sondermann (1997) and Jamshidian (1997), the authors prescribed a dynamic to the evolution of forward Libor rates. We covered FRA in Kienitz (2014). For a given notional N at time T_{i-1} a rate f_i is fixed and at a later time T_i the interest with regard to fixed rate f_i is paid. The total amount is $N \cdot f_i \cdot \tau_i$. The quantity τ_i is the fraction of a year between the dates T_{i-1} and T_i. Today's fair value of a FRA struck at strike level K would be calculated by $P(t, T_i)(f_i - K)\tau_i$.

Here we face the difficulty that usually the curves for discounting and calculating forward rates are different, see Kienitz (Kienitz (2014)). We already considered how to account for this by possibly using a stochastic basis in Chap. 8 Sect. 8.4. However, we shortly summarize the approach followed by Mercurio (2009).

12.3 Libor Dynamics

For the Libor Market Model (LMM), we choose to model Forward Libor rates. To this end we fix a tenor structure

$$\mathcal{T}_x := \{0 = T_0, T_1, \ldots, T_N\}, \quad x = 1\text{M}, 3\text{M}, 6\text{M}, 12\text{M}.$$

Now, let us specify the quantities we are going to model in detail. We define

$$L_i^x(t) := L_i^x(t, T_{i-1}, T_i) := \frac{1}{\tau_x(T_{i-1}, T_i)} \left(\frac{P^x(t, T_i)}{P^x(t, T_{i-1})} - 1 \right). \tag{12.1}$$

Again, in (12.1) the x indicates if we are modelling the 1M, 3M, 6M or 12M Libor rates. Now, we have two possibilities for specifying the stochastic movement of the Libor rate: either we can directly specify the process or we can rely on the stochastic differential equation formulation.

First, to lighten notation we drop the dependence on x and denote by $L = (L_1, L_2, \ldots, L_N)^T$ the vector of forward Libor rates. For this vector, we consider the dynamics

$$\frac{dL(t)}{L(t)} = \mu(L(t), t)dt + \Sigma(t, L(t))dW(t). \tag{12.2}$$

This dynamics consists of a drift $\mu()$ which we are specifying below, a diagonal matrix $\Sigma = diag(\sigma_1(t), \ldots, \sigma_m(t))$ and a correlated m-factor Brownian motion, $m \leq N$. The $m \times m$ correlation matrix is $\rho = (\rho_{ij})_{1 \leq i,j \leq m}$. To clarify things, we observe that each Libor rate L_i is given by

$$\frac{dL_i(t)}{L_i(t)} = \mu_i(L(t), t)dt + \sum_{i=n}^{m} \sigma_i(t, L(t))dW_i(t). \tag{12.3}$$

The correlation matrix is hidden in the motion $W = (W_n, \ldots, W_m)$. The evolution of the Libor rates can be alternatively specified by considering the stochastic movement directly. This leads to consider

$$L_i(t) = L_i(0) \exp\left(\int_0^t \mu_i(L(u), u) - \frac{\sigma_i(u, L(u))^2}{2} du + \int_0^t \sigma_i(u, L(u))dW(u)\right). \tag{12.4}$$

In fact (12.4) is the solution of the Eq. (12.2) in the sense of Itô-calculus.

The above formulation is not rigorous since we have not specified the measure we are considering. Choosing a specific measure and by the general 'change of measure' technique the drift is determined. Now, we wish to consider different measures by especially focussing on the choices relevant for practical applications. If we allow that each forward Libor rate is a martingale with respect to the zero bond P_{T_i} paying one unit of currency at T_i, we observe that (12.3) is

$$\frac{dL_i(t)}{L_i(t)} = \sum_{i=n}^{m} \sigma_i(t, L(t))dW_i(t).$$

For applications it is necessary to consider the Libor dynamics with respect to one common measure for all rates. For instance, let us consider a financial derivative with a payoff that is built from using different Libor forward rates. To be able to calculate the expected value we have to specify a pricing measure and, then, consider the dynamics of the forward Libor rates with respect to this pricing measure. To this end we first show how to compute the necessary drift adjustments applying the general change of measure method, see for instance Kienitz (2014). If we have $\mathcal{T}$ and $\tilde{\mathcal{T}}$ with $\mathcal{T} \subset \tilde{\mathcal{T}}$ and we wish to evolve the forward curves $[T_0, \tilde{T}_M]$, $[T_1, \tilde{T}_M]$,…$[T_N, \tilde{T}_M]$ into the future. To this end we have adjust the drift accordingly. The forward rate dynamics are as follows:

(i) The case $i < N$

$$dL_i(t) = -\sum_{j=i+1}^{N} \frac{\tau_j \lambda_i \cdot \lambda_j L_i L_j}{1 + \tau_j L_j} + \lambda_i \cdot dW(t)$$

(ii) The case $i = N$

$$dL_i(t) = L_i \lambda_i \cdot dW(t)$$

(iii) The case $i > N$

$$dL_i(t) = \sum_{j=N+1}^{i} \frac{\tau_j \lambda_i \lambda_j L_i L_j}{1 + \tau_j L_j} + \lambda_i \cdot dW(t)$$

This means we fix the measure corresponding to the zero bond maturing in T_N and adjust the drifts for $L_1, L_2, \ldots, L_{N-1}$ according to (i), L_N according to (ii) and $L_{N+1}, \ldots, L_{M-1}$ according to (iii). Two numeraires are most important for interest rate modelling. The first is the *Terminal Measure* and, the second, the *Spot Measure*. We suppose that we simulate the Libor dynamics up to some final maturity T_N.

Let us shortly comment on two possible formulations of the Libor Market model. In fact this is only a notational difference. On the one hand we might specify a *factor loading* formulation by considering λ_i to be d-dimensional vectors, $\lambda_i = (\lambda_{i,1}, \ldots, \lambda_{i-d})^\top$. This structure specifies the volatility and the correlation structure. To see how this formulation and, on the other hand, the σ, ρ formulation are related we let $\sigma_i(t) = |\lambda_i|(t)$ with $|\cdot|$ being the vector norm and e_i a unit basis of $\mathbb{R}^d$ such that $e_i e_j = \rho_{ij}$. Now, starting with σ and ρ and choosing the γ_i vectors accordingly gives the factor loading formulation again.

12.3.1 Spot and Terminal Measure

Take the rolling spot measure which is obtained by investing the money at the current forward rate for the next period until maturity. Then, the drift for the i-th Forward Rate is given by Eq. (12.5)

$$\mu_i(t) = \sum_{j=\eta(t)}^{i} \frac{\tau_j L_j}{1 + \tau_j L_j} \lambda_j \cdot \lambda_n. \tag{12.5}$$

The drift for $L_i(t)$ is given using the σ, ρ formulation by (12.6)

$$\mu_{\text{Spot}}(L(t), t) = \sigma_i(t) L_i(t) \sum_{j=\beta(t)}^{i} \frac{\tau_j \rho_{ji} \sigma_j(t) L_j(t)}{1 + \tau_j L_j(t)} dt. \tag{12.6}$$

In (12.5) we dropped the dependence of the loading factor on simulation time, that is the second index. Furthermore, we used the vector notation here and denoted

$$\eta(t) := \sup\{i : t \leq T_i \in \mathcal{T}\} \tag{12.7}$$

The quantity defined by (12.7) gives the index of the first Libor rates of the still alive Libors. We could also take the dynamics in the terminal measure. To this end we consider the dates $\{T_0, T_1, \ldots, T_N\}$. The terminal measure is associated to the zero bond which pays 1 at T_N.

$$dL_i = \sum_{j=i+1}^{N-1} \frac{\tau_i L_i L_j \lambda_i \cdot \lambda_j}{1 + \tau_j L_i} dt + L_i \lambda_i \cdot dW(t) \tag{12.8}$$

and again in the σ, ρ formulation we have (12.9)

$$\mu_{\text{Terminal}} = -\sigma_i(t) L_i(t) \sum_{j=i+1}^{N} \frac{\tau_j \rho_{ij} \sigma_j(t) L_j(t)}{1 + \tau_j L_j(t)} \tag{12.9}$$

Again, this dynamic is given explicitly by

$$\begin{aligned} dL_i(t) = \sum_{j=i+1}^{N-1} & \frac{\tau_i L_i L_j (\lambda_{i,k}^{(1)} \lambda_{j,k}^{(1)} + \lambda_{i,k}^{(1)} \lambda_{j,k}^{(2)})}{1 + \tau_j L_i(t)} dt \\ & + L_i \left(\lambda_{i,k}^{(1)} dW_1(t) + \lambda_{i,k}^{(2)} dW_2(t) \right) \end{aligned}$$

12.3.2 Discretization

The above formulae include the fraction of a year τ_i and in practice you never should use a constant approximation! This can lead to erroneous results and, thus, to a substantial pricing error.
Once we know the computation of the drift and diffusion part of the model we can use a discretization to simulate paths corresponding to the model dynamic. We only consider the example of an Euler scheme together with a constant volatility function. We fix a tenor structure

$$0 = T_1 < \cdots < T_m < T_{m+1}, \qquad \tau_j := T_{j+1} - T_j,\ j = 1, \ldots, m$$

Let $(\sigma_1, \ldots, \sigma_m) \in \mathbb{R}_+^m$ be a vector of constant volatilities and denote by $\sigma \in \mathbb{R}^{m\times m}$ the corresponding diagonal matrix. Define the drift to be the function

$$\begin{aligned}\tilde{\mu} : \mathbb{R}^m \times \mathbb{R}^m &\to \mathbb{R}^m \\ (y, \sigma) &\mapsto \tilde{\mu}(y, \sigma),\end{aligned}$$

where

$$\tilde{\mu}_i(y, \sigma) := \sigma_i \sum_{j=\eta(t)}^{i} \frac{\sigma_j \tau_j \tilde{y}_j}{1 + \tau_j y_j}.$$

The $\mathbb{R}^m$-valued diffusion described by the SDE (12.10) with a m-dimensional Brownian Motion $W(t)$

$$d\tilde{L}(t) = \tilde{\mu}(\tilde{L}(t), \sigma) + \sigma dW(t) \tag{12.10}$$

is called *Libor Market Model*. Applying the Euler Scheme to the logarithms of the $\tilde{L}_i(t)$, one obtains the following approximation to (12.11). For any $1 \le n \le m - 1$

$$\begin{aligned}\forall 1 \le i \le n : L_i(n+1) &:= L_i(n), \\ n+1 \le i \le m : L_i(n+1) &:= L_i(n) \exp\left((\mu_i(n) - \frac{1}{2}\sigma_i^2)\tau_n + \sqrt{\tau_n}\sigma_i Z(n+1) \right), \\ \mu_i(n) &:= \sigma_i \sum_{j=n+1}^{i} \frac{\tau_j L_j(n) \sigma_j}{1 + \tau_j L_j(n)}.\end{aligned} \tag{12.11}$$

These equations can also be expressed by

$$L(n+1) = L_n(L(n), \sigma),$$

where $L_n : \mathbb{R}^m \times \mathbb{R}_+^m \to \mathbb{R}^m$ is a suitable map. Consequently (12.11) is an evolution equation for the initial Libor curve that produces realizations of future values of the Libor rates. If one defines $\eta(j) := \tilde{\eta}(T_j) = T_{j+1}$, it is intuitively clear that one can think of $L_i(n)$ as an approximation to $\tilde{L}_i(T_n)$. We use this representation for generating paths for derivatives pricing or for exposure simulation.

Of course there are much more sophisticated approaches to simulate trajectories for Libor market models. Furthermore, the introduced model is not capable to model the market observed smile. To this end the basic model has to be combined with a local volatility or a stochastic volatility model as considered in Chap. 6 or 7.

12.4 Modelling Volatility

After specifying the dynamic of the model and being able to consider the dynamic with respect to different measures, we now focus on modelling the stochastic movement by specifying the volatility structure. This means we have to determine the matrix $\Sigma(t)$ from Sect. (12.3) and the correlation structure of the Brownian motion $W(t)$.

First, we consider two different methods to further detail the Libor dynamics. We already used one specific way when expressing the Libor dynamics using (12.3). We used the Libor volatilities $\sigma_i(t)$, $i = 1, \ldots, n$ and assign a correlation structure implicitly by assuming that $W(t)$ is a correlated Brownian motion. Now, we assume that ρ is the $m \times m$ correlation matrix. Then, there exists a $m \times n$ matrix B such that

$$\rho = BB^\top. \tag{12.12}$$

with

$$b_{ik} = \frac{\sigma_{ik}}{\sqrt{\sum_{k=1}^{m} \sigma_{ik}^2}}, \qquad \sigma_{ik} := v_i \alpha_{ik} \tag{12.13}$$

The quantities v_i and α_{ik} in (12.13) are called the variance of the k-th factor score and the eigenvector, respectively, the *factor loading*.
Thus, if $Z(t)$ is an uncorrelated Brownian motion, then $W := BZ$ is a Brownian motion with correlation structure given by ρ. But this means we can write (12.3) using the matrix $B = (b_{ik})_{1 \le i \le N, 1 \le k \le m}$ and we find

$$\frac{dL_i(t)}{L_i(t)} = \mu_i(L(t), t)dt + \sigma_i(t) \sum_{k=1}^{m} b_{ik}(t) dZ_k(t). \tag{12.14}$$

The main modelling work is now to specify the volatility and the correlation structure. For instance, for practical purposes we often rely on a constant correlation structure, thus, $b_{ik}(t) = b_{ik}$. In the sequel of this section, we consider different approaches to model the volatility.

Often a deterministic function $\sigma(t)$ is a good choice for the parametrization of the deterministic volatility. For our setting, we consider for the i-th Libor rate the function

$$\sigma_i(t) = (((T - t)b + a) \exp(-(T - t)c) + d)\, 1_{t<T} \tag{12.15}$$

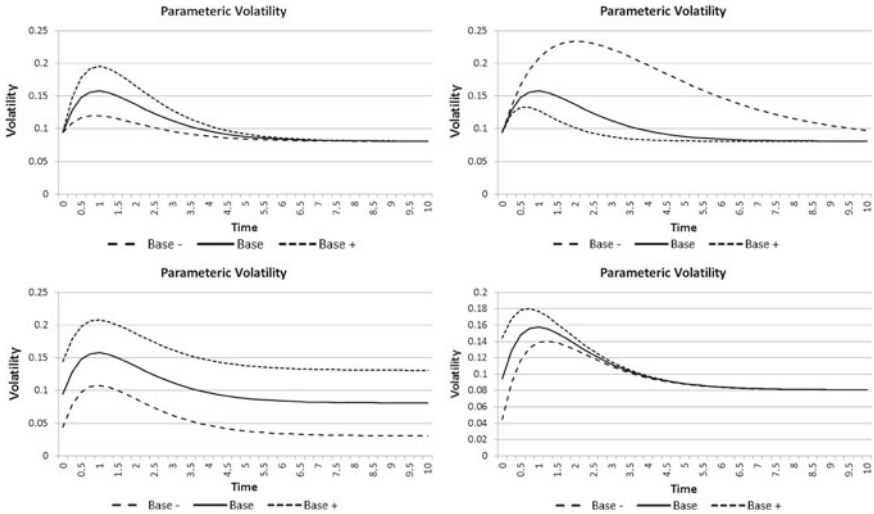

Fig. 12.1 Base parameters: $a = 0.0134$, $b = 0.1908$, $c = 0.9746$ and $d = 0.0808$

The caplet volatility is the integral over a given time interval $[T_i, T_{i+1}]$. That is

$$\int_{T_i}^{T_{i+1}} \sigma_i(s)ds$$

Eventually, we multiply $\sigma_i(t)$ by a constant c_i to exactly match the observed caplet volatility. Then, the volatility is given by $\bar{\sigma}_i(t) = c_i\sigma_i(t)$. The rationale for choosing this kind of volatility is that the four-parametric form is capable of modelling many different term structures. This includes the hump-shaped structure or monotonically decreasing structures of the implied caplet volatility.

Figure 12.1 illustrates the effects of the parameters in the representation of (12.15). For instance, b controls the size of the hump and c controls the location of the hump. Parameters d and a determine the initial volatility and the behaviour on the short end, respectively.

12.5 Modelling Co-movement

After having specified the volatilities, namely the matrix Σ in (12.2) we now consider choosing the matrix ρ from (12.12). It is possible to unite the volatility and the correlation structure by considering the *covariance* structure. If $C = (c_{ij})_{1\leq i,j\leq m}$ is the instantaneous covariance structure and $\sigma_i(t)$, $i = 1, \ldots, m$ are the volatilities and $\rho = (\rho_{ij})_{1\leq i,j\leq m}$ is the correlation matrix, the quantities

are related by

$$c_{ij}(t) = \sigma_i(t)\sigma_j(t)\rho_{ij}(t). \tag{12.16}$$

Many authors use either the covariance or the volatility/correlation notation.

Now, that we have specified how the variance of the Libor rates can be modelled, we consider the co-movement of the rates. For pricing a single caplet and, thus, a cap it is not necessary to specify the co-movement of the rates. This is essential when we wish to model and price financial contracts that depend on multiple Libor rates at the same time. One such example is a European Swaption. The Swap Rate can be seen as a weighted sum of Libor Rates, see Kienitz (2014), Brigo and Mercurio (2006), Andersen and Piterbarg (2010) or other books on interest rates. In the sequel, we consider methods to model this co-movement.

12.5.1 Non-parametric

In general a correlation matrix $\rho = (\rho_{ij})$ is a positive definite symmetric matrix. In principle each entry of the correlation matrix can be treated as a free parameter. This means we have to specify all the correlation coefficients between all forward rates that we model over all time steps. This can be done by specifying all the hedging instruments we would like to apply and, then, run an optimization. This approach is however not feasible. Since in the interest rate market there is practically no hedge against levels of rate correlation. Especially after the market volume in structure interest rate products drained after August 2007. This means hedging against correlation cannot be done and this means that calibrating a market model to calibrate correlation is flawed. To this end we should assume a reasonable structure for correlation that can be controlled using some free variables. This is the parametric approach to correlation modelling considered in the next subsection.

12.5.2 Parametric/Parsimonious

Instead of a numerical calibration of a constant correlation structure, applying a parsimonious approach is beneficial. To this end, a 1–5 parameter form for the correlation matrix ρ was proposed. Proceeding this way, we can allow for the correlation of two adjacent forward rates to gradually decrease as calendar time moves into the future.

In Rebonato (2004) different parametric correlation matrices are considered. The simplest form is given by (12.17).

$$\rho_{j,i} = \exp(-\beta|j-i|) \tag{12.17}$$

To give the rationale of this representation, we take the Libor rate $L_i(t)$. We assume that the evolution of the yield curve is driven by different risk factors. For instance, the PCA analysis, see Kienitz (2014), shows that at least there are three of such factors. If we consider Libor rates $L_{i-1}(t)$ or $L_{i+1}(t)$ it should be intuitive clear that their movement is highly correlated to $L_i(t)$. Thus, if $L_i(t)$ increases it is likely that $L_{i-1}(t)$ and $L_{i+1}(t)$ increase. But if we now choose some Libor rate $L_{i+20}(t)$ we expect that this correlation is not that significant since $L_{i+20}(t)$ is calculated from a different part of the yield curve. Thus, the correlation should deteriorate. This effect is modelled by (12.17). It assumes that this deterioration is exponential with rate $-\beta$. Examples are shown in Fig. 12.2.

For pricing applications this is not sufficient. It can only be thought of as a qualitative model. To be able to fit the model to the market, it is necessary to consider more flexible structures with two or more parameters. We could take correlation structures suggested by Schoenmakers (2005). Take for instance

$$\rho_{j,i} = (1-\eta)\exp(-\beta|\tau_j^\gamma - \tau_i^\gamma|) + \eta, \quad \eta \in [-1, 1] \tag{12.18}$$

as a two-parameter structure or a three-parameter structure (12.19)

$$\begin{aligned}\rho_{j,i} = \exp\Big[&-\frac{|j-i|}{n-1} \\ &\Big(-\ln\Big(\beta_3 + \beta_1 \frac{j^2+i^2+ji-3nj-3ni+3j+3i+2n^2-n-4}{(n-2)(n-3)}\Big) \\ &-\beta_2 \frac{j^2+i^2+ji-nj-ni-3j-3i+3n+2}{(n-2)(n-3)}\Big)\Big]\end{aligned} \tag{12.19}$$

The formula (12.19) leads to a correlation matrix if $3\beta_1 \geq \beta_2$ and $\beta_1 + \beta_2 \leq -\ln(\beta_3)$ hold. And the quantity ρ_{ij} is only defined for numbers of rates larger than 3.

Using these parameter structures, we get much more flexibility and a reasonable fit to market quotes can be achieved. Figure 12.3 shows the possible shapes for the correlation.

For considering quoted prices from the CMS or even the CMS Spread market, it is necessary to be even more flexible. Considering the most flexible one so far, (12.19), we observe that there is a hidden dependency present since

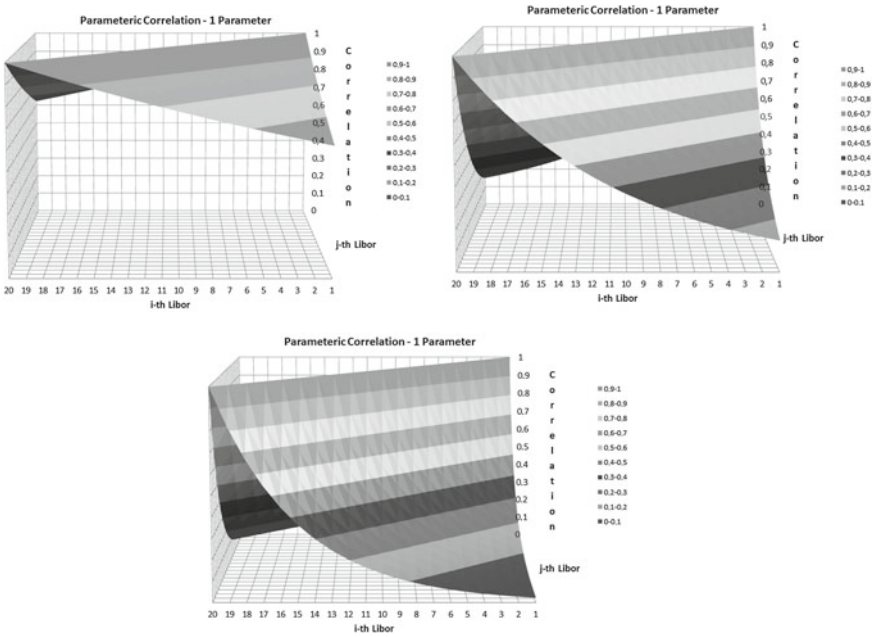

Fig. 12.2 Different possible shapes of the correlation structure (12.17)

the last row is always inverse proportional to the first one. This means it is not possible to control the short time and the long time of the correlation independently. In particular we wish to further decouple the co-movement of the short dated Libor rate with the long dated ones. To this end Lutz (2010) proposed the following parametric structure:

$$\rho_{j,i} = \beta_1 + (1-\beta_2)\Big(\exp(-\beta_3(j^{\beta_2} + i^{\beta_2})) + \frac{\theta_{j,i}}{\sqrt{\theta_{j,j}\theta_{i,i}}}\sqrt{(1-\exp(-2\beta_3 j^{\beta_2}))(1-\exp(-2\beta_3 i^{\beta_2}))}\Big) \tag{12.20}$$

with

$$\theta_{j,i} := \begin{cases} 1 & ; \min(j,i) = 0 \\ \min(j,i) & ; \min(j,i) > 0 \text{ and } \xi_i\xi_j = 1 \\ \frac{(\xi_j\xi_i)^{\min(j,i)}-1}{1-1/(\xi_j\xi_i)} & ; \min(j,i) > 0 \text{ and } \xi_i\xi_j \neq 1 \end{cases}$$

and

$$\xi_j = \exp\left(-\frac{1}{j}\left(\frac{j-1}{n-2}\beta_4 + \frac{n-1-j}{n-2}\beta_5\right)\right)$$

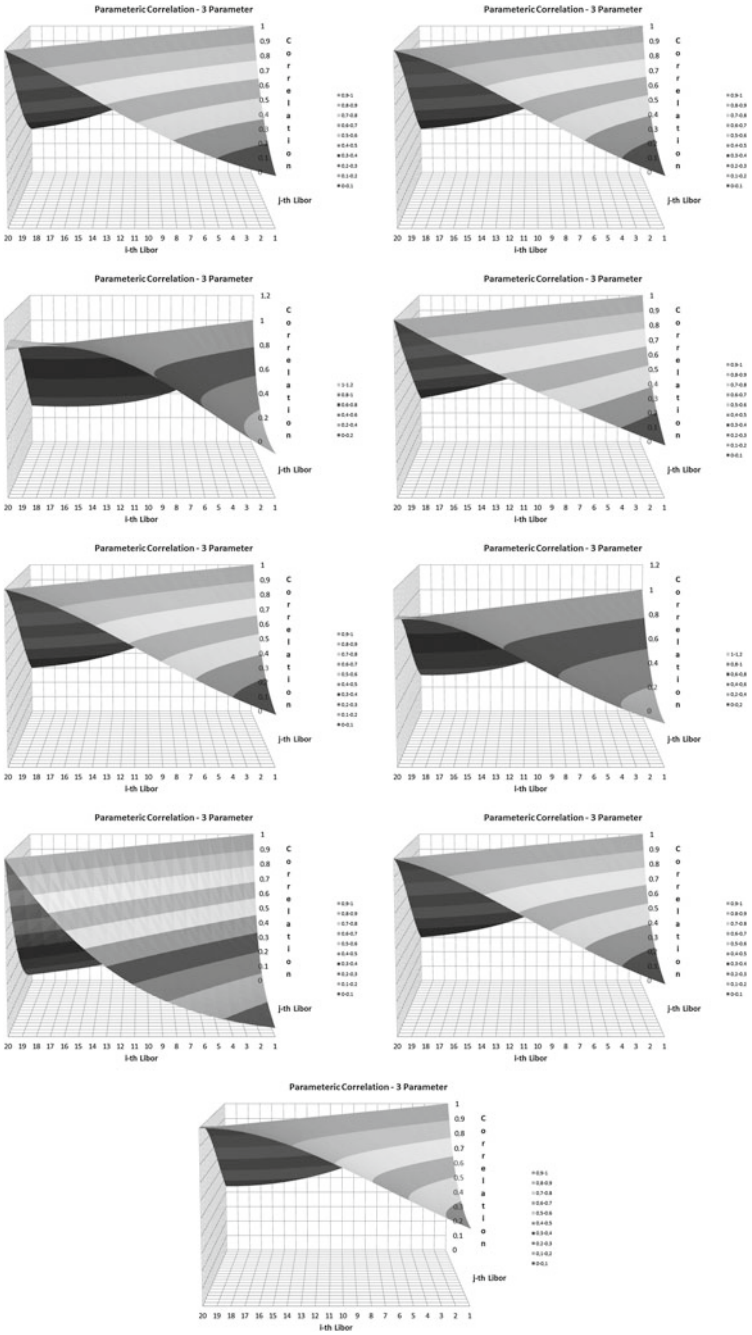

Fig. 12.3 A possible parametrization of the correlation matrix for (12.19)

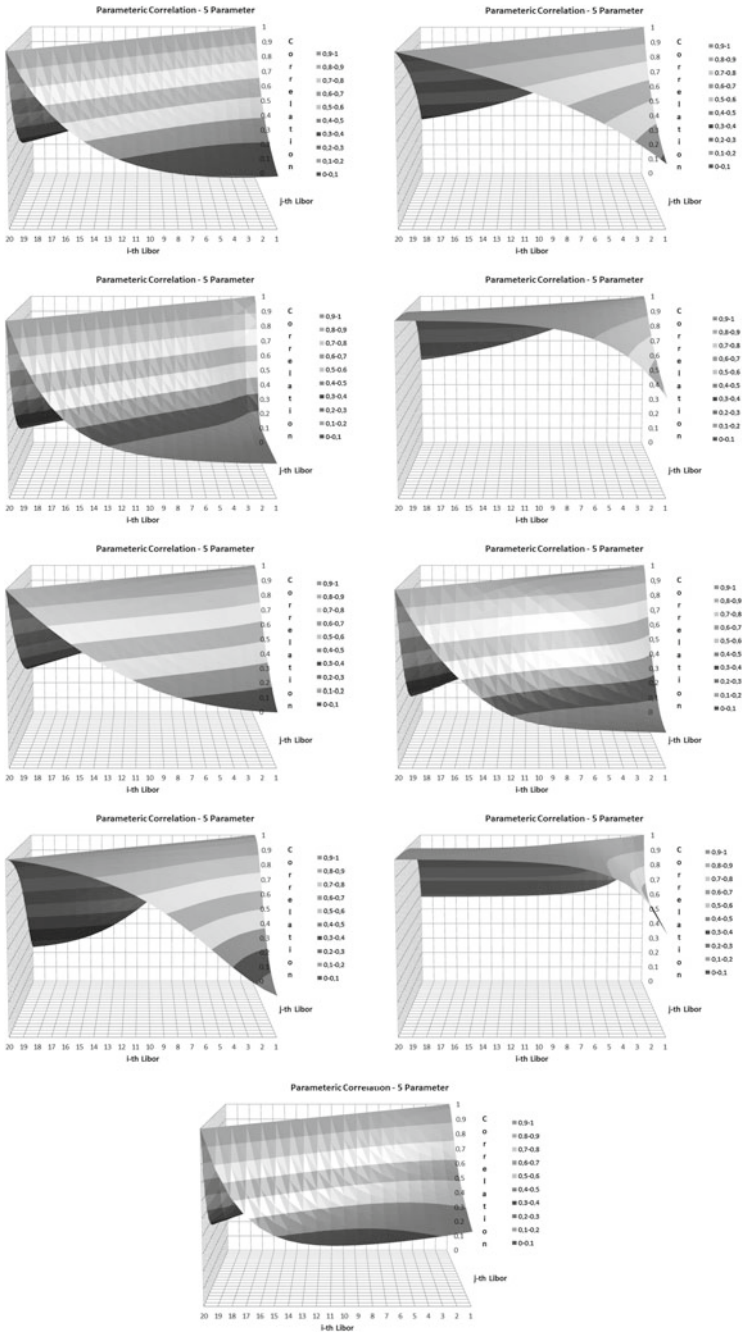

Fig. 12.4 Different possible shapes of the correlation structure. We have chosen the parameter sets given in Table 12.1

Table 12.1 Parameter sets for illustrating different shapes of the correlation matrix

Parameter	1	2	3	4	5	6	7	8	9
β_1	0.2	0.2	0.2	0.2	0.2	0.2	0.2	0.2	0.2
β_2	1	1	3	1	1	1.5	2.2	0.5	1
β_3	0.1	0.1	0.01	0.1	0.1	0.1	0.006	0.8	0.06
β_4	−3.7	0	−5.6	10	−1.7	−3.4	0.95	3	−7
β_5	−0.3	0	1	4.5	3.7	8.3	3.6	−0.2	2

Figure 12.4 illustrates the flexibility of (12.20).

For the implementation it is most relevant to be able to compute the integrated volatilities, respectively, covariances. Using parametric correlation structures this is often possible. For instance for the structure (12.17) and the parametric form of the volatility (12.15), we give the integrated covariance as an analytic expression. This means that we have to integrate the instantaneous covariance structure which leads to (12.21).

$$\mathrm{COV}_{ij} = \int \rho_{ij}\sigma_i(t)\sigma_j(t)dt \tag{12.21}$$

Since the correlation matrix ρ does not depend on time and denoting $\tau_k := t - t_k$, we find an analytic expression for the covariance

$$\begin{aligned}\mathrm{COV}_{\mathrm{ij}} = \exp\Big(&- \beta|\tau_i - \tau_j|c_i c_j \frac{1}{4c^3} \\ &\Big(4ac^2 d(e^{c\tau_i} + e^{\tau_j}) + 4c^3 d^2 t - 4bcdee^{c\tau_i}(c\tau_i - 1) \\ &-4bcdee^{c\tau_j}(c\tau_j - 1) + e^{c(\tau_i+\tau_j)}\Big(2a^2c^2 \\ &+2abc(1 - c(\tau_i + \tau_j))\Big) + b^2(1 + 2c^2\tau_i\tau_j - c(\tau_i + \tau_j))\Big)\Big)\end{aligned}$$

12.5.3 Factor Reduction

Since in practice the valuation has to be done on portfolio level as well as on the trade level it is of utmost importance to use a model which is stable and its implementation leads to results which can be calculated reasonably fast. To this end some practitioners argue that it is advisable to reduce the number of factors. In our setting of (12.10) this means that the number of driving Brownian motions has less factors than there are modelled rates, that is $m < n$. Sometimes it is suggested to take $m = 2$ or $m = 3$.

In this case, the full covariance matrix $C \in \mathbb{R}^{N\times N}$ is to be replaced by a matrix $B \in \mathbb{R}^{N\times m}$. This matrix has to satisfy

$$\sum_{k=1}^{m} b_{jk}^2 = c_{jj}.$$

This is necessary to retain the calibration of the caplets which solely depend on the volatilities of the single Libor rates. In practice when choosing a parametric volatility, a rescaling is used to multiply each of the integrated parametric volatilities by a factor. The rescaling is given by

$$b_{jk} \to a_{jk}\sqrt{\frac{c_{jj}}{\sum_{l=1}^{m} b_{jl}^2}}$$

What are the advantages, respectively, disadvantages of this approach? When working with a market model taking less driving Brownian motions than there are modelled rates the less terms appear in the corresponding quantities for drift and covariance calculations. However, given the complexity of current markets, the disadvantages may outweigh this. First, factor reduction prohibits term structure of instantaneous volatility or the ability to take long time steps in a numerical simulation or both. Second, we might destroy the given correlation structure.

Let us summarize what factor reduction means. When we reduce the number of factors the variances of the individual rates are still correct. This is even the case if we reduce the number of factors to one. But the effective covariances differ from the specified ones. If we allow for a term structure of volatility, or loading coefficients b_{jk}, factor reduction disables taking time steps longer than the used time discretization. For instance, assume piecewise constant instantaneous loading coefficients for two factors of four forward rates over a first semi-annual time step. The most severe fact is nevertheless that by decreasing the number of factors we in fact move from a market model to a factor model. Using fewer factors than discrete forward rates means a destruction of either the term structure of instantaneous volatility of FRAs, or the correlation structure of the FRAs or both. Simultaneous calibration to market instruments of different nature such as caplets and swaptions—which are the natural calibration instruments—becomes practically impossible. Finally, from a computational perspective, there is no noticeable speed gain unless you have significantly fewer than $m = 4$ factors but this could decrease the calibration flexibility or almost completely lose it.

12.6 Interpolation

Not all products can be described by the aid of canonical forward rates alone. In practice, a Libor Market model implementation has to cope with many intermediate cashflows, with settlement delays, fixing conventions, and many other idiosyncracies of the interest rates markets.
A flexible Forward Rate Market model may have to handle stub discount factors that cover only part of the associated discrete forward rate's accrual period. It is difficult to construct non-canonical discount factors from a given set of discrete forward rates in a completely arbitrage-free manner. However, in practice, it is usually sufficient to choose an approximate interpolation rule such that the residual error is well below the levels where arbitrage could be detected.
It is also important to remember that the numerical evaluation of any complex deal with a Libor market model is ultimately still subject to inevitable errors resulting from the calculation scheme.
In this context it may not be surprising that the following discount factor interpolation approach is accurate for practical purposes.
Our base structure for the spanning forward rates is again $\tilde{\mathcal{T}}$, see Fig. 12.5.

For further ease of notation, we consider the interval indicator given by

$$i[s] := \max(i | s \leq \tilde{T}_i)$$

and the modified accrual factor

$$a[s] := \tilde{T}_{i[s]+1} - s$$

Let us furthermore define the discrete interest rate for the accrual period from time s to the next grid point time $\tilde{T}_{i[s]+1}$. We call this forward rate $F[s](t) := F(t, \tilde{T}_{i[s]}, \tilde{T}_{i[s]+1})$. A forward discount factor, thus, decomposes into

$$P[s, e](t) = \frac{P(t, \tilde{T}_e)}{P(t, \tilde{T}_s)} = \frac{1 + a[e]F[e](t)}{1 + a[s]F[s](t)} \prod_{j=i[s]+1}^{i[e]+1} \frac{1}{1 + \tau_j L_j(t)}$$

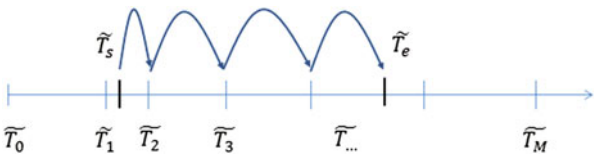

Fig. 12.5 Illustration of tenor structures and Forward Rates

For practical purposes it is feasible to consider the freezed version of the forward, that means we transfer the shape of the spot forward curve to the simulated curve in the future. This is done by multiplication with a factor γ. This concept is realized using Eq. (12.22)

$$F[s](t) = \underbrace{\frac{F[s](0)}{L_{i[s]}(0)}}_{\gamma[s]} L_{i[s]}(t) \tag{12.22}$$

The factor $\gamma[s]$ can be written as

$$\gamma[s] = \frac{\left(\frac{P(0,s)}{P(0,\tilde{T}_{i[s]+1})} - 1\right)/a[s]}{L_{i[s]}(0)} \tag{12.23}$$

In this way, taking (12.23), we essentially approximate the yield curve dynamics in between grid times by a one-factor model. More advanced approaches to interpolation construct a one-factor model allowing for a stochastic correction factor γ. This is not the scope of the current exposition.

12.7 Libor Market and Swap Market Models

One of the biggest markets is the swap market. There are many derivatives with swap rates as the underlying. The way practitioners have chosen to apply market models in a swap market context is to start with a Libor Market model and, then, consider the distribution of the swap rates. It turns out that the dynamics of the swap rates is a bit different from the dynamics of the Libor rates if the latter are assumed to follow a Libor Market model. Nevertheless, a model using the same dynamics for the swap rate is a good approximation. The corresponding parameters for the volatilities can be computed using the model parameters from the Libor model. This means we essentially use a Libor Market model to approximate a Swap Market model.
To shed further light on this approach we take a Libor Market model as considered in Sect. 12.4. We take co-terminal swap rates S_{in}, $i = 1, \ldots, n-1$. These rates are defined by (12.24)

$$S_{in}(t) = \frac{\sum_{j=i+1}^{n} P(t, T_j)\tau_{j-1}L_{j-1}}{\sum_{j=i+1}^{n} P(t, T_j)\tau_{j-1}} = \frac{A_i(t)}{B_i(t)} \tag{12.24}$$

with

$$A_i(t) =; \quad B_i(t) =$$

We wish to use a Black76-type formula for swaptions with an adjusted volatility. To this end we calculate the covariance structure of the portfolio of Libor rates given by (12.24):

$$\begin{aligned}
\mathbf{COV}_{ij}^{\text{Swap}} &= \mathbf{COV}\left(\frac{dS_i}{S_i}, \frac{dS_j}{S_j}\right)/dt \\
&= \sum_{k=0,l=0}^{n-1,n-1} \frac{\frac{\partial S_i}{L_i}\frac{\partial S_j}{L_l}}{S_i S_j} L_k L_l \mathbf{COV}\left(\frac{dL_k}{L_k}\frac{dL_l}{L_l}\right)/dt \\
&= \sum_{k=0,l=0}^{n-1,n-1} \frac{\partial S_i}{\partial L_k}\frac{L_k}{S_i}\mathbf{COV}_{kl}^{\text{L}}\frac{L_l}{S_j}\frac{\partial S_j}{\partial L_l}
\end{aligned}$$

Thus, if we define a linear transformation T by

$$(T_{ik})_{ik} = \left(\frac{\partial S_i}{L_k}\frac{L_k}{S_i}\right)_{ik}$$

it is possible to determine the mapping transforming the covariance matrix for the Libor forward rates to the swap rates using T.

$$\mathbf{COV}^{\text{Swap}} = T\mathbf{COV}^{\text{L}}T^{\top}$$

In the case where the fixed and floating payments occur simultaneously and they are paid with the same frequency it is possible to find a simple formula. We have for $i, k < n$:

$$\frac{\partial P(0, T_i)}{\partial L_k} = -P(0, T_i)\frac{\tau_k}{1 + \tau_k L_k} 1_{\{k \le i\}}$$

and we calculate the partial derivatives:

$$\frac{\partial S_i}{\partial L_k} = \left(\frac{P(0, T_{k+1})\tau_{k-1}}{B_i} - \frac{\tau_k}{1 + L_k\tau_k}\frac{A_k}{B_i} + \frac{\tau_k}{1 + L_k\tau_k}\frac{A_i B_k}{B_i^2}\right) 1_{\{k \ge i\}}$$

Using the assumption above, we have for T

$$T_{ik} = \left(\underbrace{\frac{P(0,T_k)L_k\tau_k}{A_i}}_{\text{Constant Weight Approx}} + \underbrace{\frac{(A_iB_k - A_kB_i)K_k\tau_k}{A_iB_i(1+L_k\tau_k)}}_{\text{Shape Correction}} \right) 1_{\{k \geq i\}}$$

The shape correction can more explicitly be written as follows:

$$\frac{(A_iB_k - A_kB_i)L_k\tau_k}{A_iB_i(1+L_k\tau_k)} = \frac{\tau_k L_k}{A_iB_i(1+\tau_k L_k)} \times \sum_{l=i+1}^{k} \sum_{m=k+1}^{n} P(0,T_l)P(0,T_m)\tau_{l-1}\tau_{m-1}(L_{l-1} - L_{m-1})$$

This means for a (nearly) flat curve $(L_l - L_k)$ vanishes! Using the results involving constant weights as well as shape correction, we find an approximation of a Black-type swaption volatility

$$\sigma^2_{\text{Swaption}}(t,T) = \sum_{\substack{k=i+1 \\ l=i+1}}^{n} T_{i-1,k-1}(0) \frac{\int_t^T \sigma_{k-1}(s)\sigma_{l-1}(s)\rho_{kl}(s)ds}{T-t} T_{i-1,l-1}(0)$$

We use this volatility to calibrate the parameters Θ as well to swaption volatility quotes. For non-homogenous float/fixed schedule, all partial derivatives have to be calculated individually. But still leading to a transformation rule $T\text{COV}^{\text{L}}T^{\top}$.

12.8 Extensions

The basic Libor Market Model as the Black76 model cannot match market observed structures. One shortcoming is that this model is not capable to model the skew/smile that we considered in Kienitz (2014). Furthermore, the model is based on a Geometric Brownian Motion approach and, thus, the appearing probability distributions are log normal. This excludes negative forward Libor rates. In the early days of Libor modelling, the feature of non-negative rates was a desirable one but the current market practice is different.
In the following we list some extensions of the Libor Market Model which can be applied to model negative rates and enhance the model such that it is

possible to account for skews/smiles for interest rate markets. Since this is only an overview and a summary, we give relevant references for further research.
A commonly used extension in the context of Libor Market Models is to apply the following dynamic:

$$\frac{dL_i(t) + d_i}{L(t) + d_i} = \mu_i(L(t), t)dt + \sigma_i(t)dW_i(t), \quad d_i > 0. \tag{12.25}$$

The displaced diffusion, respectively, shifted log-normal model is introduced in Kienitz (2014). This extension was used in the early days of Libor Market Models to be able to fit the observed skew for the ATM strike. Today this approach is mainly used for modelling negative forward Libor rates.
Another possible extension is to consider the dynamic

$$dL_i(t) = \mu_i(L(t), t)dt + \sigma_i(t)(L(t) + d_i)^{\beta_i}dW_i(t), \quad d_i > 0. \tag{12.26}$$

This is a combination of CEV dynamic and a shifted log-normal one. The CEV component allows for introducing skew and at the same time considers negative rates.
More sophisticated Libor Market Models combine the CEV/DD dynamic with one or more components of a stochastic volatility models. One common approach is to combine the dynamic of the Libor Market model with a Heston stochastic volatility model in a way that the dynamic is considered under the Spot measure, (12.27). Thus, the stochastic volatility is spread among all Libor rates to the same extent. We take

$$dL_i(t) = \mu_i(L(t), t)dt + \sigma_i(t)(L(t) + d_i)^{\beta_i}dW_i(t) \tag{12.27}$$

$$dV(t) = \kappa(\theta - V(t))dt + \sqrt{V(t)}dZ(t)$$

$$\langle W_i(t), Z(t)\rangle = 0 \tag{12.28}$$

Since the interest rates even for major currencies are at very low levels or even negative, we find the situation that the market quotes are all around 0. But many banks still keep trades from times when the prevailing level of rates was much higher. This makes it difficult to model the skew/smile in a way that the derivatives based on high strikes are reasonably valued. Models such as (12.27) cannot produce enough convexity to lift the right wing of the smile up again. One solution would be to consider not only one stochastic volatility component, see Piterbarg (2005), but one for each modelled rate.

12.9 Multi-tenor LMM and Stochastic Basis

To incorporate the multi-curve setting into our pricing methodology, we consider the following approach based on deterministic basis spreads: For the multi-curve setting, we consider a curve of basis spreads given as a discount curve, that is

$$BS(0,T) = \exp(-r_{BS}(T)T) \tag{12.29}$$

Then, to calculate the Forward Rate corresponding to the basis curve BS as defined by (12.29) and a given OIS curve P at time t corresponding to the period $T, T+\Delta T$, we consider

$$L(t,T,T+\Delta T) = \frac{1}{\Delta T}\left(\frac{P(t,T)BS(0,t+T)}{P(t,T+\Delta T)BS(0,t+T+\Delta T)} - 1\right).$$

Yet, there is the need to model a stochastic basis. We follow the approach taken by Mercurio (2009). In this set-up, we fix a period for the Forward rates. This could be 1M, 3M, 6M or 12M for instance. As pointed out, the discounting curve depends on the CSA but the standard is to use the OIS curve for that purpose. See Kienitz (2014). Assume a tenor structure corresponding to the forward rate period given $\mathcal{T} = \{T_0, T_1, T_2, \ldots, T_N\}$. We consider the FRA rate L_k for the interval $[T_{k-1}, T_k]$ which is

$$L_{nM,k}(t) := \mathbb{E}_t^{OIS,T_k}[L(T_{k-1},T_k)] \tag{12.30}$$

The quantity appearing in Eq. (12.30) is nothing but the conditional expectation of the Libor rates with period nM with respect to the T_k-Fwd measure but corresponding to the Zero Coupon Bond for the OIS curve. Now to set up the Libor Market model we consider the forward rates L_k determined by considering the OIS curve and the ones defined by (12.30). We now consider the definition of the basis already defined in Chap. 8 Sect. 8.4:

$$S_{nM,k}(t) = L_{nM,k}(t) - F_k(t).$$

The dynamic assigned to the nM-Forward rates is given by

$$\begin{aligned} dF_{nM,k}(t) &= f_k(t, T_{nM,k}(t))g_k(V(t)) \\ &\quad \left[\sum_{j=\beta(t)}^{k} \frac{\tau_{nM,j}\rho_{nM,j}f_j(t, F_{nM,j}(t))g_j(V(t))}{1+\tau_{nM,j}F_{nM,j}(t)}dt + dZ_k(t)\right] \\ dV(t) &= a(t,V(t))dt + b(t,V(t))dW(t) \end{aligned}$$

This is a very general dynamic with function f_k, g_k, a and b and the stochastic variance extension allows to model the skew/smile to some extent. While the general formulation is theoretically appealing, it is not applicable in practice and the modeller has to switch to more simple models by suitably choosing the functions. In Mercurio (2010) it is shown that for a suitable parametrization the basic instruments, that are Caplets, Floorlets and Swaptions can be valued using expressions similar to the standard Libor Market model. To this end we could either use the general machinery reviewed in Chap. 8 but let us follow the lines of thought from Mercurio (2010) here. Define the Libor Market model as follows:

$$\begin{aligned} dF_{nM,k}(t) &= \sigma_{nM,k} V(t) \left[\frac{1}{\tau_{nM,k}} + F_{nM,k} \right] dZ_k(t) \\ dV(t) &= -\nu V(t)^2 \sum_{j=\beta(t)}^{i_k} \sigma_{nM,j} \rho_{nM,j} dt + \nu V(t) dW_{nM,k}(t) \\ V(0) &= 1 \end{aligned}$$

and the spread by

$$dM(t) = \sigma M(t) dZ(t). \tag{12.31}$$

This setting allows to consistently specifying a Libor Market model for each period 1, 3, 6 and 12M. However, the model parameters need to be specified. This is not an easy task since the market does not quote options on the basis spreads nor can the volatilities for non-standard forward rate tenors be derived from market data. The modeller may rely on other approaches. For instance, historical analysis using time series can be applied. The parameter ν corresponds to the SABR volatility of volatility and there is a correlation ρ between the driving Brownian motions of the forwards and the volatility. For ease of application, the values $\sigma_{nM,l}$ are deterministic functions or even constants. The spot correlations $\rho_{nM,k}$ are constant. The chosen set-up leads to a Libor model with a SABR-type stochastic volatility. With this modelling assumption, we find that the Caplet and the Swaption formulae can be obtained in closed form with just a one-dimensional integration. For the details, we refer to Mercurio (2009, 2010).

12.10 Summary and Conclusions

In this section, we considered Market Models. As the basic example, we considered the Libor Market model. The basic modelling assumptions are introduced. Especially, we considered how to model volatility and correlation in an

efficient and practical way. Then, we showed how to apply the rates to calculate a full-term structure necessary for pricing or exposure generation. Numerical schemes as well as approximation formulas are given and we finally gave an overview of several methodologies for extending the model to fit observed market features. This includes volatility smiles, fitting to Constant Maturity Swap options data and extending the model to allow for multiple curves.

References

Andersen, L., & Piterbarg, V. (2010). *Interest rate modeling—Volume I: Foundations and Vanilla models*. Atlantic Financial Press.

Brace, A., Gatarek, D., & Musiela, M. (1997). The market model of interest rate dynamics. *Mathematical Finance*, *7*, 127–155.

Brigo, D., & Mercurio, F. (2006). *Interest rate models—Theory and practice* (2nd ed.). Berlin, Heidelberg, New York: Springer.

Jamshidian, F. (1997). LIBOR and swap market models and measures. *Finance and Stochastics*, *1*, 293–330.

Kienitz, J. (2014). *Interest rate derivatives explained: Volume 1 products and markets*. Palgrave McMillan.

Lutz, M. (2010). *Extracting correlations from the market: New correlation parametrizations and the calibration of a stochastic volatility LMM to CMS spread options*. SSRN: Preprint.

Mercurio, F. (2009). Modern libor market models: Using different curves for projecting rates and for discounting. *International Journal of Theoretical and Applied Finance*, *13*(1), 113–137.

Mercurio, F. (2010). Libor market models with stochastic basis. *RISK*, *23*.

Piterbarg, V. (2005). Stochastic volatility model with time-dependent skew. *Applied Mathematical Finance*, *12*(2), 147–185.

Rebonato, R. (2004). *Volatility and correlation, (2nd ed)*. Wiley.

Sandmann, K., & Sondermann, D. (1997). A note on the stability of lognormal interest rate models and the pricing of Eurodollar futures. *Mathemtical Finance*, *7*, 119–128.

Schoenmakers, J. (2005). Robust libor modelling and pricing of derivative products. *Hall/CRC financial mathematicss series*

A

Numerical Techniques for Pricing and Exposure Modelling

In this section, we summarize how to apply the Heston model in practice. Actually, the techniques are more widely applicable for instance to other Stochastic Volatility models. To this end, we need to be able to apply the model to price simple European options as well as exotic options and simulate paths. The latter is very important if we wish to use the model for exposure modelling. All the techniques are summarized in Kienitz, J. and Wetterau, D. (2012). Furthermore, source code for Matlab is published. In this section, we can only summarize the techniques and give an overview.

A.1 Numerical Integration

As for the transformation method instead of reviewing all the techniques and methods, we consider one example which can be applied to the Heston model and which is used in practical applications apart from the Heston setting. We consider a method introduced in Lewis, A. (2001). Let v be the payoff and $V(K,T)$ the price of a European option. If $w = x + iy$ denotes a complex number, it is possible to express the price by (A.1)

$$V(K,T) = \frac{e^{-rT}}{2\pi} \int_{i\mathcal{I}(w)-\infty}^{i\mathcal{I}(w)+\infty} \Phi(-z)\mathcal{F}(v)dz. \tag{A.1}$$

To be able to apply this formula in practice, we need to know the transform $\hat{v}$. Luckily, this is the case for many different European options including European Call and Put options, see Lewis, A. (2001). For instance the price of

© The Editor(s) (if applicable) and The Author(s) 2017

J. Kienitz and P. Caspers, *Interest Rate Derivatives Explained: Volume 2,*
Financial Engineering Explained, DOI 10.1057/978-1-137-36019-9

a European Call option, denoting $k := \log(S/K) + (r-d)T$, we have

$$C(K,T) = S(0)e^{-dT} - \frac{S(0)^{\nu_1}}{K^{\nu_1-1}\pi} e^{-rT} e^{(r-d)T\nu_1} \tag{A.2}$$

$$\int_0^\infty \mathcal{R}\left(e^{iuk} \frac{\Phi(u-i\nu_1)}{u^2 - 2iu\nu_1 + iu - \nu_1(\nu_1+1)}\right). \tag{A.3}$$

For the Heston model, the function Φ is known and given by Chap. 6 (6.11). In Lewis, A. (2001) it is suggested to take $\nu_1 = \frac{1}{2}$ in (A.2) and that this value is a reasonable choice. The formula becomes

$$C(K,T) = S(0)e^{-dT} - \frac{1}{\pi}\sqrt{SK}e^{-(r+d)T/2} \int_0^\infty \mathcal{R}\left(e^{iuk}\Phi\left(u - \frac{i}{2}\right)\frac{1}{u^2+\frac{1}{4}}\right) du.$$

A.1.1 Greeks

It is possible to evaluate Δ and Γ numerically. The use of finite difference methods is possible but there exist semi-analytic formulae which can be evaluated very fast. We have

$$\Delta = 1 - \frac{Ke^{-rT}}{S(0)\pi} \int_0^\infty \frac{\mathcal{R}\left[\left(iu+\frac{1}{2}\right)\exp\left(\left(iu+\frac{1}{2}\right)k\right)\Phi\left(u-\frac{i}{2}\right)\right]}{u^2+\frac{1}{4}} du$$

$$\Gamma = \frac{Ke^{-rT}}{S(0)^2\pi} \int_0^\infty \mathcal{R}\left[\exp\left(\left(iu+\frac{1}{2}\right)k\right)\Phi\left(u-\frac{i}{2}\right)\right] du.$$

A.2 Fourier Transformation

Another method for tackling the integration problem is to apply a technique called Fourier Transform. This approach is first considered in Carr, P. and Madan, D. (1999). To illustrate the method, we denote $x_T := \log(S_T)$ the log asset price at time T, $k := \log(K)$ the logarithm of the strike, $f(\cdot|x)$ the risk neutral density at maturity T with logarithmic spot value x. The price of a European Call option is then given by

$$C(K,T) = \int_k^\infty e^{-rT}\left(e^y - e^k\right) f(y|x)dy. \tag{A.4}$$

A problem might arise here since for a given maturity T the integrand is not integrable since

$$C(K,T) \to S(0) \text{ as } K \to 0(\text{ or } k \to -\infty). \tag{A.5}$$

To assure integrability, we need to introduce a parameter $\alpha \in \mathbb{R}$. This parameter is called *dampening parameter*. We consider a modified Call price or damped Call price $c(k,T)$:

$$c(k,T) := e^{\alpha k} C(k,T). \tag{A.6}$$

To illustrate the dampening on the payoff, we consider Fig. A.1. We consider the payoff without dampening which corresponds to $\alpha = 0$ and for different values of α. It has been proven that an optimal value for choosing α can be computed, see for instance Kienitz, J. and Wetterau, D. (2012).

The dampened integrand is now integrable. If for $\alpha > 0$ the expectation $\mathbb{E}[S_T^{\alpha+1}] < \infty$, then $\varphi_T(0)$ is finite since $\varphi(v) = \int_{-\infty}^{\infty} e^{ivk} c(k,T)dk$. To have a finite value for $v = 0$, we choose α such that $\varphi(-(\alpha+1)i)$ is finite which is equivalent to assigning an upper bound on the dampening factor. The integral

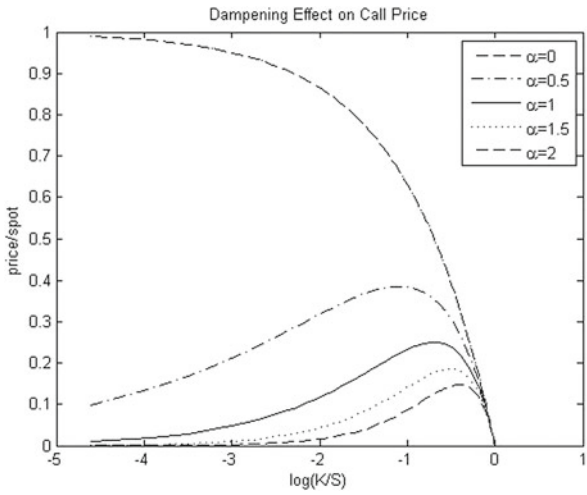

Fig. A.1 Effect of dampening on a payoff for a call option $\log(S/K) = 0, 0.01, \ldots, 2$ and $\alpha = 0, 0.5, 1, 1.5, 2$

expression for φ can be evaluated in case of a European Call option and we get

$$\varphi_{\text{Call}}(v) = \frac{e^{-rT}\varphi(v-(\alpha+1)i)}{\alpha^2+\alpha-v^2+i(2\alpha+1)v}. \tag{A.7}$$

In Carr, P. and Madan, D. (1999) it is shown that the Call price can be evaluated numerically by approximating the integral in terms of a sum by applying the trapezoidal integration rule and fixing a numerical grid such that $\eta > 0$ we set $b = \frac{N\lambda}{2}$ and use $v_j = \eta j, j = 0, \ldots, N-1$; $k_u = -b+\lambda u$, $u = 0, \ldots, N-1$. This leads to

$$C(k_u, T) \approx \frac{e^{-\alpha k_u}}{\pi} \sum_{j=0}^{N-1} e^{-i\lambda\eta j u} e^{i\left(\frac{N\lambda}{2} v_j\right)} \varphi_{\text{Call}}(v_j)\eta. \tag{A.8}$$

The latter is directly accessible for applying the Fast Fourier Transform comes into play to compute sums of the form: The same methodology can be applied to European Put options by choosing

$$\varphi_{\text{Put}}(u) = \frac{\varphi_{\text{Call}}(u-(-\alpha+1)i)}{\alpha^2-\alpha-u^2+i(-2\alpha+1)u}.$$

A variation of the method is to use Call and Puts at the same time with regard to their moneyness. In this case, we have

$$z_T(k) = \begin{cases} (e^k - e^y)1_{\{y<k,k<0\}} & \text{if } k < \log(S(0)) \\ (e^y - e^k)1_{\{y>k,k>0\}} & \text{if } k > \log(S(0)) \end{cases}.$$

If $U(K, T)$ denote the corresponding option price, then, we can apply (A.9) for approximating it.

$$U(k_u, T) \approx \frac{1}{2\pi \sinh(\alpha k_u)} \sum_{j=0}^{N-1} e^{-i\frac{2\pi}{N}ju} \underbrace{e^{ibv_j}\gamma(v_j)\frac{\eta}{3}(3+(-1)^{j+1}-\delta_j)}_{=:x_j}. \tag{A.9}$$

A.2.1 Greeks

To calculate Δ and Γ, we find by differentiation with respect to the spot price $S(0)$:

$$\Delta = \frac{\exp(-k\alpha - (r-d)T)}{S(0)\pi} \int_0^\infty \frac{e^{iuk}(iu + (\alpha+1))\varphi(u - (\alpha+1))}{\alpha^2 + \alpha - u^2 + (2\alpha+1)iu} du. \tag{A.10}$$

For Γ a similar formula can be derived.

$$\Gamma = \frac{\exp(-\alpha \log(K) - (r-d)T)}{S(0)^2\pi} \int_0^\infty e^{iu\log(K)} \varphi(u - (\alpha+1)i) du. \tag{A.11}$$

A.3 Finite Difference Techniques

We consider a classic valuation technique in this section. The pricing methodology is based on the connection of Stochastic processes and Partial Differential Equations. We aim to apply discretization to model the partial differential operator. Below we give a brief overview of this technique.

A.3.1 Finite Differences

First, for a function $f : \mathbb{R} \to \mathbb{R}$ let us consider the derivative and its discrete approximations. We consider x_{i-1}, x_i, x_{i+1} with $x_{i-1} < x_i < x_{i+1}$ and the Taylor expansions

$$\begin{aligned} f(x_{i-1}) &= f(x_i) - \frac{\partial f}{\partial x} h + \frac{1}{2}\frac{\partial^2 f}{\partial x^2} + O(h^3) \\ f(x_{i+1}) &= f(x_i) - \frac{\partial f}{\partial x} h + \frac{1}{2}\frac{\partial^2 f}{\partial x^2} + O(h^3) \end{aligned}$$

This, firstly, subtraction leads to a second-order accurate approximation of the first derivative, (A.12)

$$\frac{\partial f}{\partial x} = \frac{f(x_{i+1}) - f(x_{i-1})}{2h} + O(h^2) \tag{A.12}$$

and, secondly, by adding the terms an approximation for the second derivative is obtained, (A.13)

$$\frac{\partial^2 f}{\partial x^2} = \frac{f(x_{i+1}) - 2f(x_i) + f(x_{i-1})}{h^2} + O(h^2). \tag{A.13}$$

Now, we fix a grid with a space and a time dimension $\mathcal{S} \times \mathcal{T}$. The space dimension can be of any order d which means that $\mathcal{S} \subset \mathbb{R}^d$. In practice, however, the method we are going to consider is only applied up to $d = 1, \ldots, 5$ dimensions. Let us take for illustration the case $d = 1$ and $\mathcal{S} = \{x_0, x_1, \ldots, x_M\}$. For the function f, we consider the values taken at these points. Then, $F = (f(x_0), \ldots, f(x_M))^\top$ is an m-dimensional vector. We consider the approximations to the derivatives (A.12) and (A.13) for each entry.

A.3.2 Finite Difference Schemes

For illustration purposes, we assume a equidistant grid in space and in time. This means that the consecutive differences $x_m - x_{m-1}$ are independent of m and we can denote them by δ_x. The same holds true for the time dimension and we use δ_t to denote the differences.

Now, we need to introduce a bit more notation. To this end let U_m^n denote the approximate value of f taken at the gird point (x_m, t_n)

$$U_m^n = f(x_m, t_n) + O(\delta_t) + \sum_{j=1}^{M} O(\delta_x)$$

We base our considerations on Strickwerda J. C. (2004), Duffy, D. (2006), Domingo T., Randall C., (2000) or Mitchell A, Griffiths D. (1980). Our aim is to illustrate and describe the basic concepts but we cannot present a formal account of the theory here. Therefore, we advise that the interested reader should consult the references.

A.3.2.1 Inner Scheme

The idea is to use the above to find a numerical approximation to the solution of the following Partial Differential Equation.

$$L - r = 0, \tag{A.14}$$

where L is a second-order differential operator. In general, we consider

$$\frac{U^n - U^{n-1}}{\delta_t} + \theta L_\delta U^{n-1} + (1-\theta) L_\delta U^n = 0.$$

This is known as the θ scheme

- **The Explicit Scheme**, $\theta = 0$, the Explicit Scheme is given by choosing $\theta = 0$

$$U_m^{n-1} = (1 - 2b\nu - rk)U_m^n b\nu(1+\alpha)U_{m+1}^n + b\nu(1-\alpha)U_{m-1}^n$$

  with $\nu = k/h^2$ and $\alpha = a/(2b)h$.
- **The Implicit Scheme**, $\theta = 1$, the Implicit Scheme corresponds to the case $\theta = 1$ and is given by

$$(1 + 2b\nu - rk)U_m^{n-1} - b\nu(1+\alpha)U_{m+1}^{n-1} + b\nu(\alpha - 1)U_{m-1}^{n-1} = U_m^n$$

- **The Mixed Scheme**, $0 < \theta < 1$, we have a Mixed Scheme if $0 < \theta < 1$. A special case, $\theta = 1/2$, is known as the Crank-Nicolson Scheme.

A.3.2.2 Boundary Conditions

Each of the finite difference schemes from above can be solved using the values on the grid and the equations which are determined by the discrete finite difference operator. In general this leads to a linear equation. For such equations, there are efficient numerical techniques available. However, we have to truncate the domain since we cannot work with infinitely large or small numbers. The largest and the smallest values of the grid are the boundary points. To be able to solve the equations arising in the finite difference approach, we need to specify what happens at the boundaries. Otherwise we were not able to find a unique solutions.

In numerical analysis practitioners consider two different kinds of boundary conditions

- Numerical boundary conditions
- Analytical boundary conditions
  - Dirichlet boundaries
  - Neumann boundaries
  - Robin boundaries.

For a treatment of boundary conditions and their application, we point to Duffy, D. (2006) and Mitchell A, Griffiths D. (1980).

A.3.3 Consistency/Stability/Convergence

Since we are interested in finding a numerical approximation to the solution of Eq. (A.14), we need to establish the notion of convergence and we wish to find conditions when convergence is guaranteed.

Before we are able to state the main Theorem, we have to define stability and consistency. If we apply a discretization to a continuous quantity there is an error. This error is called the truncation error. The local truncation error at grid point (t_n, x_m) for a finite difference scheme is defined as the residuum to the exact solution. We call it $\tau_{k,h}(t_n, x_m)$. A numerical scheme is called consistent if for $k, h \to 0$ we find that the local truncation error vanishes, that is $\tau_{k,h}(t_n, x_m) \to 0$.

For stability there are many different definitions. One common is the von-Neumann stability. This notion of stability is based on the Fourier transform. In a von-Neumann stability analysis, one considers the transforms at consecutive time points and relates the transforms via an amplification factor. This factor depends on the grid specifics. A finite difference scheme is called stable (von-Neumann stable) if there are constants which can be used to find a linear bound on the absolute value of the amplification factor.

The main result is the fact that a consistent finite difference scheme for a partial differential equation, for which the initial value problem is well posed, is convergent if and only if it is stable.

In general, there are two ways by which this setting is applied in financial engineering. First, we start with current spot price and try to find the density at maturity. Or we know the payoff at maturity and wish to determine today's price. The first case is known to solve for the density whereas the second is the case of solving for the price.

A.3.4 Solving for the Density

Figure A.2 illustrates the setting. We need to specify the boundary conditions and use the finite difference method to evolve the density given today to the one prevailing at maturity. In most situations, the today's density is simply the Dirac density at the current observed forward. To propagate the density to the final time point we apply a numerical scheme. For instance, this was illustrated when we considered the SABR model in Chap. 7. The density at

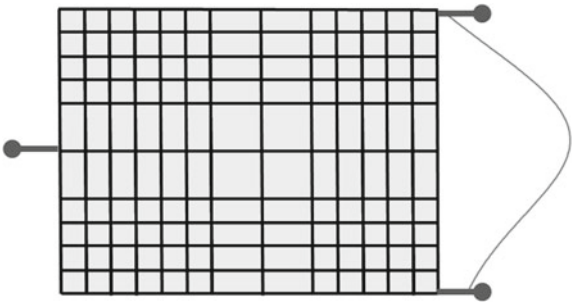

Fig. A.2 Density via the forward method

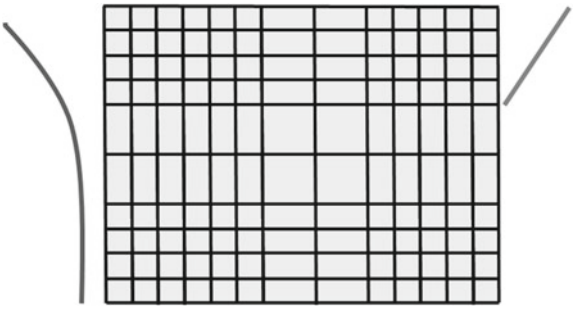

Fig. A.3 Price via the backward method

maturity is then used to numerically integrate the payoff we need to evaluate. In the literature this method is known as the Forward Method. We saw an example of this method in Chap. 7.

A.3.5 Solving for the Price

If we consider the pricing equation for the value of the derivative we take a different path. Now, we do know the payoff at maturity. This is simply the payoff function. After specifying the boundary conditions, we have to work backwards in time and get the value function at time 0. Then, we can directly use the function to interpolate the price of the derivative. Figure A.3 illustrates this approach. We call it the Backward Method.

A.4 Monte Carlo Simulation

In this section we consider the Monte Carlo Simulation. This methodology is based on probabilistic and analytic concepts and can be universally applied. Especially for high dimensional problems such as exposure simulation where

many risk factors have to be modelled this is the method of choice. We give an introduction to the technique starting with random numbers and distributions. This lies at the heart of the method. For many applications, this is not enough and we need to evolve certain quantities like rates into the future. This evolution is governed by a stochastic dynamic. Thus, the numerical method has to make sure that it is appropriate to approximate this dynamic. To this end, we consider paths and schemes that can be applied in this case. Now, having the paths it is possible to evaluate any payoff along a path. Doing the evaluation for each path, collecting the results and averaging leads to an estimator. This estimator comes together with an estimate of the goodness of the estimator. Namely we construct an interval in which the true value lies with a certain probability. This is the confidence interval.

Monte Carlo Simulation has its name from the famous Monaco city Monte Carlo with all the casinos and gambling opportunities. The first systematic introduction is due to John von Neumann when working on the atomic bomb but nowadays this method is widely applied in many disciplines.

The main concept of the method is that we conduct a random experiment which produces a number and record it. Then, this experiment is repeated n-times. From the recorded results we take the average and take this value as our outcome. For the experiment, we can for instance take a mechanism that produces realizations of a risk factor which is then used to calculate a price for a financial instrument. The method is theoretically justified by the so-called *Law of Large Numbers*. Thus, the technique of Monte Carlo Simulation uses concepts from Probability Theory and Analysis to derive estimates. If we know the stochastic dynamic and the problem in terms of a payoff the main algorithm is as follows:

- Specify a time grid for simulation $\mathcal{T} := \{t_0, t_1, \ldots, t_M\}$ with $\delta_i := t_i - t_{i-1}$
- Evolve the quantities under consideration from t_{i-1} to the next grid point t_i
  - Generate independent uniformly distributed random numbers $(u_1, \ldots, u_N) \in [0, 1]^N$
  - Transform these random numbers into numbers of a given distribution, $(d_1, \ldots, d_N)$
  - Follow the numerical scheme using the random numbers $S(t_{i-1}) \to S(t_i)$
- Calculate the value of the payoff for each path
- Calculate the sample mean and the sample variance.

Let us consider each step in a bit more detail. We already did the first step by defining the time grid $\mathcal{T}$.

A.4.1 Random Numbers

A.4.1.1 Uniformly Distributed Randoms

First, we consider random number generation. The task here is to be able to run a random number generation on a computer. For this task there are many libraries which provide such methods. In general, these methods allow to uniformly sample a number in the interval [0, 1]. For instance in Excel this is the function Random(). In this situation we write $U \sim \mathcal{U}(0, 1)$.

A.4.1.2 Multiple Dimensions

Theoretically, it is easy to generate uniformly distributed random numbers in several dimensions. If we wish to sample a d-dimensional vector of $U(0, 1)$ distributed random numbers, we could simply generate $u_i \sim U(0, 1), i = 1, \ldots, d$ and take the vector $u = (u_1, \ldots, u_d)^\top$. In practice, we need to be sure that the random number generator we use is capable of handling the number of dimensions. For a practical simulation exercise, we need to generate $Nt \times NSim \times d$ independent uniformly distributed random numbers. This means taking $Nt = 240$, $NSim = 1.000.000$ and $d = 40$ we need to be able to generate 9.600.000.000 uniforms.

A.4.1.3 Transforming to a Given Distribution

The models we considered in this book involve more complicated distributions than the uniform distribution on [0, 1]. Of utmost important is the Normal Distribution or Gaussian Distribution. If available we suggest to use what is known as the Inverse Method. To this end let $F : \mathbb{R} \to [0, 1]$ be the cumulative distribution, for instance

$$F(x) = \frac{1}{\sqrt{2\pi}} \int_{-\infty}^{x} e^{-\frac{1}{2}u^2} du.$$

Now, the Inverse Method calculates a realization n from a random variable having cumulative distribution function F by

$$n := F^{-1}(u) = \inf\{x : F(x) \geq u\}, \quad u \sim U(0, 1). \tag{A.15}$$

To this end we need a number generated from the uniform distribution on [0, 1] and an efficient algorithm for determining F^{-1}. In the case of the

Standard Normal distribution such methods exist, see Moro, B. (1995) or Acklam, P.J. (2001). Since for $X = F^{-1}(U)$ we have

$$P(X \leq x) = P(F^{-1}(U) \leq x) = P(U \leq F(x)) = F(x)$$

the Inverse Method indeed produces realizations of random variable that has cumulative distribution function F. Other methods for tackling the problem of transforming to given distributions are considered in Glasserman, P. (2004).

A.4.1.4 Multiple Dimensions

So far we have only considered one-dimensional problems, respectively, multi-dimensional problems for $U \sim U([0,1]^d)$. Now, we wish to consider the multi-dimensional Gaussian distribution with Covariance structure Σ. This matrix is given by

$$\Sigma = \begin{pmatrix} c_{11} & \dots & c_{1d} \\ \vdots & \ddots & \vdots \\ c_{d1} & \dots & c_{dd} \end{pmatrix} = DRD$$

with D being a diagonal matrix with entries $(\sigma_1, \dots, \sigma_d)$ being the standard deviations and R being the $d \times d$ correlation matrix.

A.4.1.5 The Cholesky Decomposition

One way to transforming realizations of a d-dimensional Standard Gaussian distribution, $N(0,1)$ to one which has mean vector x and covariance matrix σ, $N(x, \Sigma)$ is to apply the Cholesky decomposition. For other techniques we refer to Glasserman, P. (2004) or Jäckel, P. (2002). First, we notice that if X is distributed with respect to $\mathcal{N}(0,1)$ and $x \in \mathbb{R}$ and $\sigma \in \mathbb{R}^+$, then, $x + \sigma X$ is distributed according to $\mathcal{N}(x, \sigma^2)$. This means it would be possible to adjust the mean and the variance if we do this operation per dimension. This means also that we need to be able to generate a realization of a random vector X of Gaussian variates with a given correlation matrix.
To illustrate how this is possible we simply consider the two dimensional case. To this end let Z_1 and Z_2 be two realizations of independent Standard Gaussian distributed variables. To obtain two realization which are correlated with correlation $\rho \in [0,1]$ we set $\tilde{Z}_1 := Z_1$ and $\tilde{Z}_2 := \rho Z_1 + \sqrt{1-\rho^2} Z_2$. For general correlation matrices R, it is possible to find a lower diagonal matrix,

the Cholesky decomposition

$$L := \begin{pmatrix} 1 & 0 & 0 & \dots 0 \\ \rho & 1 & 0 & \dots 0 \\ \vdots & \vdots & \ddots & \vdots \; 0 \\ \rho_{1d} & \rho_{2d} & \dots\dots & 1 \end{pmatrix}$$

such that

$$R = LL^T.$$

If $Z = (Z_1, \dots, Z_d)$ is a Standard Gaussian distributed vector, then, LZ is a Gaussian distributed vector with correlation matrix R.

A.4.2 Path Simulation

After discussing how to obtain realizations of random numbers with respect to a given distribution, we now consider recipes for evolving a path corresponding to a prescribed dynamic

$$dS = \mu(t, S)dt + \sigma(t, S)dW(t), \quad t \in [t_0, T] \tag{A.16}$$

The dynamic (A.16) can equivalently written in integral notation

$$S(t) = S(t_0) + \int_{t_0}^{t} \mu(u, S(u))du + \int_{t_0}^{t} \sigma(u, S(u))dW(u), t \in [t_0, T]. \tag{A.17}$$

For fixed $\omega \in \Omega$ the functions μ (drift) and σ (volatility) of (A.16), respectively, (A.17) are given by

$$\mu : [t_0, T] \times \mathbb{R} \to \mathbb{R}, \quad \sigma : [t_0, T] \times \mathbb{R} \to \mathbb{R}^+.$$

For an interval $[t_0, T]$, we fix a discretization $\mathcal{T} := \{t_0, t_1, \dots, t_{NT} = T\}$ and denote $\Delta_k := t_k - t_{k-1}$, $k = 1, \dots, NT$ where NT is the number of time steps.

A.4.2.1 The Exact Scheme

Rarely, it is possible to find an exact solution to (A.16), respectively (A.17). For instance if $\sigma(t, S(t)) = \sigma S(t)$ and $\mu(t, S(t)) = rS(t)$ the exact solution

is known.

$$S(t_k) = S(t_{k-1}) \cdot \exp\left(\left(r - \frac{\sigma^2}{2}\right)\Delta_k + \sigma\sqrt{\Delta_k}Z\right), \quad Z \sim \mathcal{N}(0,1).$$

A.4.2.2 The Euler Scheme

The Euler scheme approximates the integrals in (A.17) by simply taking the values of μ and σ at t_{k-1} of an interval $[t_{k-1}, t_k]$ and multiplying with the time step Δ_k, respectively, by $\sqrt{\Delta_k}Z_k$ with $Z_k \sim \mathcal{N}(0,1)$, thus

$$\int_{t_{k-1}}^{t_k} \mu(u, S(u))du \approx \mu(t_{k-1}, S(t_{k-1}))\Delta_k$$
$$\int_{t_{k-1}}^{t_k} \sigma(u, S(u))dW(u) \approx \sigma(t_{k-1}, S(t_{k-1}))\sqrt{\Delta_k}Z_k.$$

The corresponding sample scheme is

$$S(t_k) \approx S(t_{k-1}) + \mu(t_{k-1}, S(t_{k-1}))\Delta_k + \sigma(t_{k-1}, S(t_{k-1}))\sqrt{\Delta_k} \cdot Z_k. \tag{A.18}$$

For the logarithm of $S(t)$, denoted by $X(t) := \log(S(t))$, applying the Euler scheme leads to

$$X(t_k) \approx X(t_{k-1}) + \mu(t_{k-1}, X(t_{k-1}))\Delta_k + \sigma(t_{k-1}, X(t_{k-1}))\sqrt{\Delta_k} \cdot Z_k. \tag{A.19}$$

The latter scheme is called the *log-Euler scheme*.

A.4.2.3 The Predictor-Corrector Scheme

We consider the $\frac{1}{2}$-Predictor-Corrector scheme. This idea can be applied to approximating the drift as well as the volatility component and is relevant for working with Libor Market models.
For this scheme, first, a predictor S_{P} is sampled by the following equation and denoting $Z_k \sim \mathcal{N}(0,1)$:

$$S_{\mathrm{P}}(t_k) := S(t_{k-1}) + \mu(t_{k-1}, S(t_{k-1}))\Delta_k + \sigma(t_{k-1}, S(t_{k-1}))\sqrt{\Delta_k} \cdot Z_k. \tag{A.20}$$

Define $\hat{\mu}(t_1, t_2, x_1, x_2) := \frac{1}{2}(\mu(t_2, x_2) + \mu(t_1, x_1))$ and $\hat{\sigma}(t_1, t_2, x_1, x_2) := \frac{1}{2}(\sigma(t_2, x_2) + \sigma(t_1, x_1))$ Then, the corrector S_C specified by (A.21) is used as the approximation to the dynamics of S. The variates Z are the same as in (A.20). The corrector is given by

$$\begin{aligned} S_C(t_k) := S(t_{k-1}) &+ \hat{\mu}(t_{k-1}, t_k, S(t_{k-1}), S_P(t_k))\Delta_k \\ &+ \hat{\sigma}(t_{k-1}, t_k, S(t_{k-1}), S_P(t_k))\sqrt{\Delta_k} \cdot Z_k. \end{aligned} \tag{A.21}$$

Again, the logarithmic version is called the *log Predictor-Corrector* scheme.

A.4.2.4 The Milstein Scheme

The Milstein scheme is a refinement of the Euler scheme. It approximates the integrals appearing from (A.17). Denoting $Z \sim \mathcal{N}(0, 1)$ the scheme is given by

$$\begin{aligned} &\int_{t_{k-1}}^{t_k} \sigma(u, S(u))dW(u) \\ &\quad \approx \sigma(t_{k-1}, S(t_{k-1}))\sqrt{\Delta_k}Z + \frac{\sigma(t_{k-1}, S(t_{k-1}))'\sigma(t_{k-1}, S(t_{k-1}))}{2}\Delta_k(Z^2 - 1). \end{aligned}$$

This leads to the following numerical scheme, again denoting $Z_k \sim \mathcal{N}(0, 1)$:

$$\begin{aligned} S(t_k) = S(t_{k-1}) &+ \mu(t_{k-1}, S(t_{k-1}))\Delta_k + \sigma(t_{k-1}, S(t_{k-1}))\sqrt{\Delta_k} \cdot Z_k \\ &+ \frac{1}{2}\sigma'(t_{k-1}, S(t_{k-1}))\sigma(t_{k-1}, S(t_{k-1}))\Delta_k(Z_k^2 - 1). \end{aligned} \tag{A.22}$$

The Milstein scheme does not preserve the martingale property. The fourth summand of (A.22) destroys this property.

A.4.3 Averaging and Error Analysis

The first sections were about sampling from a diffusion process. Now, we analyse the calculation of the sample mean and the sample variance. Our aim is to determine the value of an expected value by using the simulated quantities from the last section, and thus, we wish to calculate

$$\Phi = \mathbb{E}[h(X)],$$

where X is a random variable with values in $\mathbb{R}^d$ and h is some Payoff function. We proceed by simulating independent, identically distributed random variables $X_1, \ldots, X_n$, $n \in \mathbb{N}$ which correspond to the quantities we are interested in on each path. Then, we consider

$$\hat{\Phi}_n := \frac{1}{n} \sum_{i=1}^{n} h(X_i). \tag{A.23}$$

By the law of large numbers, we can be sure that $\hat{\Phi}_n \longrightarrow \Phi, \quad n \to \infty$. But how large should n be to be sufficiently close to the true value? To this end we need to specify what we mean by 'sufficiently close'. We consider a confidence interval. Let $0 < \alpha < 1$ and we call it the confidence level, for instance $\alpha = 3\%$. It should be interpreted as the probability such that the true value of Φ lies within a probability of $1 - \alpha$ in the interval $I_\alpha := [L(h(X)), R(h(X))]$, the so-called confidence interval. Thus, the random interval I_α is characterized by

$$\mathbb{P}[I_\alpha] = 1 - \alpha.$$

If we replace $h(X)$ by a realization x of the random variable X I_α becomes a real interval. From Tschebycheffs inequality, we know that for two random variables X and Y with finite variance we have

$$\mathbb{P}\left[|X - Y| \geq k\right] \leq \frac{\mathbb{V}\left[X - Y\right]}{k^2}.$$

Thus, smaller values for $\mathbb{V}$ improve our estimate of Φ but it can only be used to construct very rough confidence intervals and is not of real practical use. We show how the Central Limit Theorem or in fact Slutskys Theorem can be applied to obtain practical and reasonable estimates. Let $z_{1-\alpha/2}$ denote the α-quantile of the $\mathcal{N}(0, 1)$-distribution,

$$\mathcal{N}(-z_{1-\alpha/2} \leq Z \leq z_{1-\alpha/2}) = 1 - \alpha.$$

We find by some algebraic operations:

$$\mathcal{N}\left[\hat{\Phi}_n - z_{1-\alpha/2}\frac{\sigma}{\sqrt{n}} \leq \Phi \leq \hat{\Phi}_n + z_{1-\alpha/2}\frac{\sigma}{\sqrt{n}}\right] \approx 1 - \alpha. \tag{A.24}$$

Therefore, using (A.24) the confidence interval I_α is given by

$$I_\alpha = \left[\hat{\Phi}_n - z_{1-\alpha/2}\frac{\sigma}{\sqrt{n}}, \hat{\Phi}_n + z_{1-\alpha/2}\frac{\sigma}{\sqrt{n}}\right]. \tag{A.25}$$

In general, we do not know the variance σ in (A.25) which is explicitly used to construct I_α. To overcome this difficulty, we replace the variance by its sampled counterpart given by (A.26)

$$\hat{\sigma}_n^2 = \frac{\sum_{i=1}^n \left(h(X_i) - \hat{\Phi}_n\right)^2}{n-1}. \tag{A.26}$$

Then, the confidence interval from (A.25) becomes

$$I_\alpha = \left[\hat{\Phi}_n - z_{1-\alpha/2}\frac{\hat{\sigma}_n}{\sqrt{n}}, \hat{\Phi}_n + z_{1-\alpha/2}\frac{\hat{\sigma}_n}{\sqrt{n}}\right]. \tag{A.27}$$

The advantage of the representation in (A.27) is that it can be determined by using samples. Theoretically, this is justified by Slutsky's theorem based on the central limit theorem. In fact, when using the estimated variance, we find that

$$\frac{\hat{\Phi}_n - \mu}{\hat{\sigma}_n/\sqrt{n}} \sim t_{n-1}$$

has t-distribution with $n-1$ degrees of freedom. According to this fact, we have to replace the quantile $z_{1-\alpha/2}$ by the quantile of this distribution.

$$I_\alpha = \left[\hat{\Phi}_n - t_{n-1,\alpha/2}\frac{\hat{\sigma}_n}{\sqrt{n}}, \hat{\Phi}_n + t_{n-1,\alpha/2}\frac{\hat{\sigma}_n}{\sqrt{n}}\right].$$

But in the sequel we use the normal quantile as a good approximation. I_α covers Φ with probability $1 - \frac{\alpha}{2}$. The total width of the interval is given by

$$\frac{2z_{1-\alpha/2}\hat{\sigma}_n}{\sqrt{n}}.$$

Therefore, the width does depend on α, n and $\hat{\sigma}_n$. Thus, for a fixed α, increasing the number of simulations leads to smaller intervals and therefore to saver estimates of Φ. Since Length($I_\alpha \propto \frac{1}{\sqrt{n}}$), it follows that decreasing the length of I_α by $1/2$ the number of simulations has to be increased by a factor 4. It can be shown that it is the symmetric interval which has the smallest width!

Now, we aim to determine an error criterion used to determine how to stop the simulations. To this end we can consider the absolute error, $\mathcal{E}_a := |\Phi_n - \Phi|$

or the relative error, $\mathcal{E}_r := \left|\frac{\Phi_n - \Phi}{\Phi}\right|$. Given some confidence level $0 < \alpha < 1$ and *error level* $\epsilon > 0$. We say the error criterion is fulfilled if

$$\mathbb{P}[\mathcal{E}_j \leq \epsilon] \leq 1 - \alpha, \quad j = a, r.$$

The goal is to choose the number of simulations such that the estimator lies within I_α whenever the error criterium is fulfilled. In many books the *Standard Error* , ϵ_n, which depends on the number of simulations n is taken as a measure of the quality of the simulation result. It is defined by

$$\epsilon_n := \frac{\hat{\sigma}_n}{\sqrt{n}}. \tag{A.28}$$

Whenever the Standard Error, (A.28), is used as an error measure, it is important to remember that it is only of statistical nature! In practice, however, we do not need to store every value $h(X_i),\ i = 1, \ldots, n$ in order to calculate the new values for $\hat{\Phi}_n$ and $\hat{\sigma}_n$ because they can be updated efficiently since

$$\hat{\Phi}_n = \hat{\Phi}_{n-1} + \frac{h(X_n) - \hat{\Phi}_{n-1}}{n}, \quad \hat{\sigma}_n = \left(\frac{n-2}{n-1}\right)\hat{\sigma}_{n-1}^2 + n\left(\hat{\Phi}_n - \hat{\Phi}_{n-1}\right)^2.$$

A.4.4 Special Purpose Schemes

For many models applied in Quantitative Finance special purpose schemes have to be researched. Either an exact scheme is not available and at the same time standard approximations for instance the Euler scheme are not good enough. Such special purpose schemes include the QE scheme for the Heston model first published in Andersen, L. (2008) or the Chen-Oosterlee-van der Weide scheme for the SABR model Chen et al. (2010).

We wish to give a sampling algorithm for the Heston dynamic since this is very often needed in practice. For instance we considered it in 11. The following pseudo-code essentially is the method given in Andersen, L. (2008): Compute

$$m = \Theta + (V(t) - \Theta)\exp(-\kappa\Delta), \quad s^2 = \frac{V(t)\nu^2 e^{-\kappa\Delta}}{\kappa}\left(1 - e^{-\kappa\Delta}\right) + \frac{\Theta\nu^2}{2\kappa}\left(1 - e^{-\kappa\Delta}\right)^2.$$

For choosing the approximating distribution compute Ψ

$$\Psi = \frac{s^2}{m^2} = \frac{\frac{V(t)\nu^2\exp(-\kappa\Delta)}{\kappa}\frac{(1-\exp(-\kappa\Delta))\Theta\nu^2}{2\kappa}(1 - \exp(-\kappa\Delta))^2}{(\Theta + (V(t) - \Theta)\exp(-\kappa\Delta))^2}$$

Generate $u \sim \mathcal{U}(0, 1)$
Compute $V(t + \Delta)$ by the Switching Rule.
If $\Psi \leq \Psi_C$, then use a non-central χ^2-distribution for approximation. To this end:

- Compute $b^2 = 2\Psi^{-1} - 1 + \sqrt{2/\Psi^{-1}}\sqrt{2\Psi^{-1} - 1} \geq 0$ and $a = \frac{m}{1+b^2}$
- Let z_1 denote a variate of $Z_1 \sim \mathcal{N}(0, 1)$
- Set $V(t + \Delta) = a(b + z_1)^2$.

If $\Psi > \Psi_C$, then use an exponential distribution:

- Set $p = \frac{\Psi-1}{\Psi+1}$
- Set $\beta = \frac{1-p}{m} = \frac{2}{m(\Psi+1)} > 0$
- Set $V(t + \Delta) = \Psi^{-1}(u; p, \beta)$ with

$$\Psi^{-1}(u) = \Psi^{-1}(u; p, \beta) = \begin{cases} 0 & 0 \leq u \leq p \\ \beta^{-1} \log\left(\frac{1-p}{1-u}\right) & p < u \leq 1 \end{cases}.$$

Denoting by z_2 a realization of $Z \sim \mathcal{N}(0, 1)$, we set

$$X(t + \Delta) = X(t) + K_0 + K_1 V(t) + K_2 V(t + \Delta) + \sqrt{K_3 V(t) + K_4 V(t + \Delta)} z_2. \quad \text{(A.29)}$$

Since $K_0, \ldots, K_4$ depend on the time step Δ_i, $i = 1, \ldots, N$ it is only possible to pre-compute these quantities. For a non-equidistant grid with Δ_i, $i = 1, \ldots, N$ we define

$$K_{i0} = -\frac{\rho\kappa\Theta}{\nu}\Delta_i \; ; \; K = \frac{\rho}{\nu}$$
$$K_{i1} = \gamma_1 \Delta_i \left(\frac{\kappa\rho}{\nu} - \frac{1}{2}\right) - K \; ; \; K_{i2} = \gamma_2 \Delta_i \left(\frac{\kappa\rho}{\nu} - \frac{1}{2}\right) + K$$
$$K_{i3} = \gamma_1 \Delta_i (1 - \rho^2) \; ; \; K_{i4} = \gamma_2 \Delta_i (1 - \rho^2)$$

for $j = 1, \ldots, 4$ and $i = 1, \ldots, N$. If the grid is equidistant all the numbers can be pre-computed. Numerous improvements and extensions can be made, see Kienitz, J. and Wetterau, D. (2012), Glasserman, P. (2004) or Jäckel, P. (2002). For instance we consider the Martingale Correction. Here we replace the constant K_0 in equation (A.29) by

$$K_0^* = -\log(M) - \left(K_1 + \frac{1}{2}K_3\right) V_n. \tag{A.30}$$

The constant M is determined explicitly and we have in the first case, namely $\Psi \leq \Psi_c$,

$$M = \frac{\exp\left(\frac{Ab^2a}{1-2Aa}\right)}{\sqrt{1-2Aa}}, \quad A < 1/2a.$$

For the second case it is given by

$$M = p + \frac{\beta(1-p)}{\beta - A}, \quad A < \beta$$

with $A = K_2 + \frac{1}{2}K_4 = \frac{\rho}{\omega}(1 + \kappa\gamma_2\Delta) - \frac{1}{2}\gamma_2\Delta\rho^2$. The martingale correction approach imposes a restriction on the discretization in terms of the correlation and the volatility of variance. For negative correlation, there is no restriction but if $\rho > 0$, then we have to guarantee that $\Delta < \frac{2}{\rho\omega}$. For practical problems this is not a serious restriction. For a numerical test we consider the QE scheme to price European Call options and test is against the test cases of Andersen, L. (2008). The spot price is $S(0) = 100$ and $r = d = 0$. For the model parameters we take (Table A.1):

For the prices corresponding to the strikes $K = 70, 100$ and 140, see Table A.2, we find by semi-analytic methods considered earlier, see Sects. A.1 and A.2.

First, we consider the standard QE scheme and price the European Call options. We display the differences to the option prices from Table A.3.

Table A.1 Model parameters for the numerical tests of the QE scheme

Parameter	Value		
ν	1	0.9	1
κ	0.5	0.3	1
ρ	−0.9	−0.5	−0.3
T	10	15	5
V(0) = θ	0.04	0.04	0.09

Table A.2 Prices for European Call options using the Heston model for strike $K = 70, 100$ and 140 and the test cases

	I	II	III
K=70	35.8498	37.1697	38.7720
K=100	13.0847	16.6492	21.7953
K=140	0.2958	5.1382	9.9831

Table A.3 Relative differences of the Monte Carlo prices for different numbers of time steps using the standard QE scheme and the semi-analytic prices

Steps 1	2	4	8	16	32
K=70					
0.0199	0.0047	0.0015	0.0009	0.0018	0.0003
0.0100	0.0011	0.0003	0.0133	0.0003	0.0022
0.0032	0.0115	0.0011	0.0022	0.0027	0.0107
K = 100					
0.0724	0.0259	0.0071	0.0001	0.0034	0.0005
0.0177	0.0083	0.0021	0.0254	0.0007	0.0047
0.0197	0.0070	0.0016	0.0039	0.0017	0.0208
K=140					
0.2887	0.0289	0.0014	0.0051	0.0133	0.0111
0.0532	0.0105	0.0025	0.0562	0.0006	0.0097
0.0590	0.0019	0.0021	0.0056	0.0022	0.0407

A.5 The Longstaff-Schwartz Method

To compute the value of Bermudan call option, it is not enough to be able to compute the value of cashflows along all Monte Carlo Paths. One also needs to take exercise decisions. This requires the knowledge of the future expectation of the option value, because on an exercise date the Bermudan right is exercised if

1. the value from exercising the option (that is either the realized cash amount or the underlying exercised into in case of physical settlement) is positive and
2. this value is also greater than the continuation value of the option, that is the value of the option if not exercised on this particular exercise date (but possible on a future date).

In mathematical terms, one needs access to expectations of the option value conditional on the model state $x(t)$ to the exercise time[1] t. Since at the last exercise date there are no future exercise dates, the general task is to estimate a expectation based on simulated path-dependent values $V = V(\omega)$, at time t, conditional on $x(t)$, that is (in rather abstract notation)

$$f(x(t)) = E(V(\omega)|x(t)) \tag{A.31}$$

which then allows to determine the optimal exercise date on each path. Once this date is known, the resulting cashflows can easily be calculated on this path, and thus the contribution of the path to the NPV is known.

Any regression technique can be applied to this problem; most common in finance are linear least squares regression with a basis of polynomial functions or a local regression approach, see Kohler M. (2010) for an overview.

Common improvements using a polynomial function regression include the addition of the payoff function to the basis, or estimating the regression coefficients only on paths being exercised, because only for these the estimate of the continuation value is needed.

Longstaff and Schwartz were the first to apply this to option pricing, see Longstaff, F.A. and Schwartz, E.S. (2001) for the classic paper.

The Feynman-Kac formula recovers the expectation computed in a Monte Carlo simulation as the solution of a certain associated partial differential equation. The original application of the theorem was to compute the solution of partial differential equations as expectation values, but it can also be used in the other direction to express expectations (like derivative prices) as solutions of partial differential equations. Partial differential equations can be solved using several numerical methods including finite difference methods that are the most commonly applied to the partial differential equations occurring in finance.

While the natural direction of solving is forward in a Monte Carlo simulation (one path is simulated starting today and going forward in time), it is backward for the corresponding partial differential pricing equation (starting at the final payoff and going backwards in time until today). Path-dependent products are easily integrated in forward methods, whereas callability is easily integrated in backward methods, but there are techniques both for forward methods to account for callability (like the Longstaff Schwartz regression method) and for backward methods to incorporate path dependency (if this dependency can be eliminated using additional state variables, like the accumulated amount in a

[1] we assume that the exercise value and the option value are given in terms of the numeraire, that is as deflated values, so that they are directly comparable on different t.

TaRN structure).

For more information on this method see Longstaff, F.A. and Schwartz, E.S. (2001), Glasserman, P. (2004), Kienitz, J. and Wetterau, D. (2012).

A.6 Further Considerations

If you wish to dig deeper into the numerical methods, we suggest to take Kienitz, J. and Wetterau, D. (2012) as a starting point. Here you find nearly all techniques not only described but also implemented in Matlab. The code can be downloaded free of charge. From this basis, you may wish to learn more about numerical methods and other programming languages. Then, you could for instance consider reading Duffy, D. and Kienitz, J. (2009) for Monte Carlo methods in C++, Duffy, D. and Germani, A. (2013) for implementation including multi-curves in C# or Duffy, D. J. (2006) for an account of PDE and Finite Difference techniques in C++.
The freely available resources QuantLib (http://www.quantlib.org) and ORE (http://www.opensourcerisk.org) contain further information and implementation of many of the techniques covered in this chapter.

References

Acklam, P. J. (2001). An algorithm for computing the inverse normal cumulative distribution function. *home.online.no/pjacklam/notes/invnorm/*.

Andersen, L. (2008). Simple and efficient simulation of the Heston stochastic volatility model. *Journal Compuational Finance*, *7*, 1–32.

Carr, P., & Madan, D. (1999). Option valuation using the fast Fourier transform. *Journal of Computational Finance*, *2*(4), 61–73.

Chen, B., Oosterlee, C. W., & van der Weide, H. (2010). Efficient unbiased simulation scheme for the SABR stochastic volatility model. *Preprint*.

Domingo T., & Randall C. (2000). *Pricing financial instruments: The finite differnce method*. Wiley.

Duffy, D. (2006). *Finite difference methods in financial engineering*. Wiley.

Duffy, D. J. (2006). *Finite difference methods in financial engineering: A partial differential equation approach*. Wiley. ISBN 0470858826.

Duffy, D., & Germani, A. (2013). *C# for financial markets*. Wiley.

Duffy, D., & Kienitz, J. (2009). *Monte Carlo frameworks—Building customisable and high-performance C++ applications*. Chichester: Wiley.

Glasserman, P. (2004). *Monte Carlo methods in financial engineering*. Berlin: Springer.

Jäckel, P. (2002). *Monte Carlo methods in finance*. Wiley.

Kienitz, J., & Wetterau, D. (2012). *Financial modeling—Theory, implementation and practice (with Matlab source)*. Wiley.

Kohler, M. A. (2010). Review on regression-based Monte Carlo methods for pricing American options. In: L. Devroye, B. Karasoezen, M. Kolher, R. Korn (Eds.) *Recent developments in applied probability and statisitics, physica Heidelberg* (pp. 37–58).

Lewis, A. (2001). A simple option formula for general jump-diffusion and other exponential Lévy processes. *Preprint*. Working Paper. Retrieved from http://www.optioncity.net.

Longstaff, F. A., & Schwartz, E. S. (2001). Valuing American options by simulation: A simple least-squares approach. *The Review of Financial Studies*, *14*(1), 113–147.

Mitchell, A., & Griffiths, D. (1980). *The finite difference method in partial differential equations*. Wiley.

Moro, B. (1995). The full Monte. *RISK*, *8*(2), 57–58.

Strickwerda, J. C. (2004). *Finite differnce schemes and partial differential equations*. Siam.

Index

A
American swaption, 17
Amortizing bond, 28
Asset swap margin, 11

B
Bachelier pricing formula, 73, 76
Basis swap, 54
Behavioural model, 44
Bermudan exercise, 16
Bermudan swaption, 17, 152
Black76 pricing formula, 73, 76

C
Callability, 15
  callable, 15
  puttable, 15
Callable fixed rate bond, 19
Capital deferral option, 42
Capital Value Adjustment (KVA), 58
Central limit theorem, 236
  Slutsky theorem, 236
Cheyette model, 185
Cholesky decomposition, 232
Collateral value adjustment, 58
Confidence interval, 236
Confidence level, 236
Credit spread model, 177
Credit trap, 12
Credit value adjustment (CVA), 57
  recovery, 57
Cross currency basis swap, 54

D
Debit Value Adjustment (DVA), 58
Deterministic basis, 134
Digital option, 48
Displaced diffusion pricing formula, 76
Draw down option, 41
Dynamic Initial Margin (DIM), 58

E
Effective PDE, 95
European swaption, 139, 187
Exposure
  Expected Negative Exposure (ENE/NEE), 58
  Expected Positive Exposure (EPE), 58

© The Editor(s) (if applicable) and The Author(s) 2017
J. Kienitz and P. Caspers, *Interest Rate Derivatives Explained: Volume 2,*
Financial Engineering Explained, DOI 10.1057/978-1-137-36019-9

backward method, 58
Bermudan swaption, 68
callable swap, 68
cross currency swap, 66
effective exposure, 59
Expected Exposure (EE), 58
Expected Future Value (EFV), 58
forward method, 58
interest rate swap, 64
netting set, 59
Potential Future Exposure (PFE), 59

F

Finite difference
consistency, 228
Crank-Nicolson scheme, 227
explicit scheme, 227
forward method, 229
mixed scheme, 227
θ-scheme, 227
stability, 228
truncation error, 228
von-Neumann stability, 228
Finite difference method
boundary condition, 227
Fixed rate bond, 4
Floating rate note, 29
Fourier transform, 222
dampening, 223
fast fourier transform, 224
Free boundary SABR model, 111
integration method, 113
projection, 112
Funding Value Adjustment (FVA), 58

G

Gaussian distribution, 231
Gaussian short rate model, 140
Vasicek model, 140

H

Hedging, 22
Heston model, 77
absorbing boundary, 77
characteristic function, 79
correlation, 77
displaced Heston model, 84
Feller condition, 77
long term variance, 77
mean reversion, 77
reflecting boundary, 77
time dependent parameters, 84
volatility of variance, 77
HJM, 184
Cheyette model, 185
Trolle and Schwartz model, 188

I

Implied volatility, 74
implied Bachelier volatility, 88
implied Black–Scholes volatility, 87
Interest rate swap, 7
fixed versus float, 7
Inter-temporal correlation, 21
Inverse floater, 31
Inverse method, 231

L

LGM, 148
numeraire, 148
Libor market model, 197
CEV local volatility, 216
co-movement, 205
displaced local volatility, 216
European swaption, 205
factor reduction, 211
flexible correlation, 207
libor dynamics, 198
multi-tenor libor market model, 217
non-parametric correlation, 205

parametric correlation, 206
parametric volatility, 203
simple correlation, 206
simulation, 201
spot measure, 200
stochastic basis, 217
stochastic volatility, 216
Swap rate dynamics, 213
terminal measure, 201
volatility, 203
zero rate interpolation, 212
Local volatility, 74
local volatility function, 74

M
Marginal Value Adjustment (MVA), 58
Monte Carlo simulation, 229
confidence interval, 236
multiple dimensions, 231
normal distribution, 231
path simulation, 233
regression, 242
standard error, 238
uniform distribution, 230

N
Normal distribution, 231
Numerical integration, 222
Numerical scheme
Euler scheme, 233
exact scheme, 233
Milstein scheme, 235
Predictor-Corrector scheme, 234
QE scheme, 238

O
Option adjusted spread, 176

P
Partial Differential Equation, 226
PIK option, 42

R
Range accural, 50

S
SABR model, 87
approximation formula, 89
calibration, 94
CEV exponent, 88
correlation, 88
displaced SABR, 104
effective equation, 95
enhanced approximation, 92
free boundary SABR model, 111
local volatility, 88
mixing, 113
moment conservation, 98
normal SABR, 89
parameters, 90
PDE, 100
volatiltiy of volatility, 88
ZABR, 105
Shadow delta hedging, 75
Short rate models, 126
Affine Short Rate models, 157
Cox Ingersoll Ross model, 157
Gaussian short rate model, 140
G2++, 162
Hybrid IR-IR-FX Model, 166
LGM model, 147
mean reversion, 178
multiple factors, 161
stochastic basis, 169
stochastic volatility, 168
Snowball, 49
Standard error, 238
Stochastic basis, 131

Structured finance, 39
Structured floating rate coupons, 53
Survival probability, 178
Swaptions
  Bermudan, 153
  co-terminal, 153
  European swaption, 153

T
Target redemption note (TaRN), 45
  CMS, 47
  Ibor, 47
Tenor basis swap, 54
Tenor option, 43
Term structure
  deterministic basis, 134
  stochastic basis, 131
Term structure models
  discrete forward rate, 129
  instantaneous forward rate, 129
  market model, 129
  short rate, 127
Trolle and Schwartz model, 188

V
Value Adjustment (xVA), 58
Volatility
  true volatility models, 131, 169
  unspanned volatility models, 131, 169
Volatility backbone, 75
Volatility note, 52

Z
ZABR, 105
  diffusion condition, 106
  local volatility, 107
  one step scheme, 109
Zero coupon bond, 33
Zero coupon bond option, 142
Z-spread, 4